

**MECHANOREGULATION OF
ADIPOGENESIS AND
REPLICATIVE SENESENCE IN
ORBITAL FIBROBLASTS
THROUGH SRC FAMILY KINASES**

Viesturs Eglitis

**This thesis is submitted to
University College London for the
Degree of Doctor in Philosophy in Cell
Biology**

2020

Supervisor – Dr Maryse Bailly
UCL Institute of Ophthalmology
11-43 Bath Street, London, EC1V 9EL

DECLARATION

I, Viesturs Eglitis, confirm that the work presented in this thesis is my own. Where information is derived from other sources, I confirm that this has been indicated in the thesis.

January 2020

ABSTRACT

Graves orbitopathy is an autoimmune disorder; a complication encountered 40-50% of Graves disease patients. The initiation of the disease is caused by circulating antibodies recognising the thyroid-stimulating hormone receptor, expressed on the surface of orbital fibroblasts. Antibody attachment recruits immune cells initiating a localised immune response which is amplified during the disease. The chronic inflammation causes a phenotypical change in orbital fibroblasts, leading to increased hyaluronan synthesis, adipogenesis and subsequent orbital tissue scarring. Currently, therapeutic options to treat Graves orbitopathy are limited.

Using a 3D fibroblast culture model, we previously identified that orbital fibroblasts isolated from patients with Graves orbitopathy spontaneously generate lipid droplets and are more contractile than their healthy counterparts. Both of these phenomena are reduced by PP2, an Src family kinase (SFK) inhibitor. When downregulated, two SFK members Fyn and Src reduced orbital fibroblast contractility. Src knockdown dramatically increased lipid droplet production in 2D and 3D orbital fibroblast cultures while Fyn abolished it. Furthermore, reduction in Src expression decreased mTORc1 protein expression while reduction of Fyn increased AMPK protein expression and activity. We also discovered that spontaneous lipid droplet generation is specific to orbital fibroblasts cultured on collagen gels and substrates with an elastic modulus close to orbital soft tissue. Soft-gel cultures exhibited reduced Fyn, Src and mTORc1 protein expression and increased AMPK protein expression, and activity. We found that orbital fibroblasts when cultured on collagen gels express lysosomal and adipogenic markers which co-localised with lipid droplets. Our findings suggest that spontaneous lipid droplet production in orbital fibroblasts may occur due to impaired mechanosensing and at least partially are of autophagic origin.

Orbital fibroblasts display increased proliferation when cultured on soft substrates and enter a senescence-like state when cultured on stiff

substrates, characterised by β -galactosidase activity. Downregulation of Src and Fyn and activation of AMPK reduced this effect, demonstrating a potential functional overlap between signalling components of spontaneous lipid droplet production and replicative senescence.

Overall our findings suggest that SFK activity is subject to substrate stiffness and contributes to lipid droplet production via mTORc1 and AMPK pathways. Moreover, the generation of lipid droplets is associated with autophagy.

IMPACT STATEMENT

Graves orbitopathy is a debilitating autoimmune disorder. Currently, there are no pharmacological therapies available that target the disease due to a lack of understanding of mechanisms of disease progression. In this thesis, we have identified potential molecular drug targets that can alleviate the pathological lipid production and fibrosis underlying Graves orbitopathy if suitable compounds are developed.

ACKNOWLEDGEMENTS

First and foremost, I would like to thank my supervisor, Dr Maryse Bailly, for her support, advice and professionalism during my PhD. She's been an inspirational presence, teaching me how to think like a scientist, to calm down when research feels overwhelming and giving me the freedom to discover and pursue my own scientific ideas. I would also like to thank my secondary supervisor, Dr Daniel Ezra, for his input and encouragement.

This PhD would not have been possible without the financial backing from Fight for Sight and Moorfields Eye Hospital.

Special thanks to many faculty members, who made my life in the lab so much easier, particularly Claire Cox, Aida Jokubaityte, Diana Serfic Svara, Dr Matt Hayes and Dr Emily Eden. Big thank you to Dr Alexis Haas who introduced and guided me through the PAA hydrogel preparation and Dr I-Hui Yang, who helped me settle in during the start of my degree. I would also like to thank all members of the Equality Challenge/Athena Swan committee for their congeniality and Dr Tim Levine (and also Dr Bailly) for their resilience and effort to make the Institute of Ophthalmology a better place for everyone.

Finally, I would like to thank my sisters and the rest of my sizeable extended family for their everlasting love and support, especially my parents Dagmara and Egils who have always been a source of encouragement, support and inspiration. I would also like to thank my friends who have left London behind but still are in touch.

Last but not least, I would like to thank the person who was anxious with me during the whole three years of ups and downs of my PhD, thank you Kosma. I will be forever grateful for bearing with me when data did not make sense or experiments did not work while also inspiring me to never ever give up and push ahead.

TABLE OF CONTENTS

Declaration	2
Abstract	3
Impact Statement	5
Acknowledgements	6
Table Of Contents	8
Abbreviations	11
List Of Figures.....	13
List Of Tables.....	15
CHAPTER 1 INTRODUCTION	16
1.1 Graves orbitopathy; an orbital complication of Graves disease	16
1.2 Orbital fibroblasts and their role in GO.....	20
1.2.1. Molecular characteristics of GO orbital fibroblasts	20
1.3. Pathogenesis of Graves orbitopathy	25
1.3.1. HA production	25
1.3.2. Adipogenesis	27
1.3.3 Formation, function and dynamics of lipid droplets.....	31
1.3.4. Biogenesis of lipid droplets.....	34
1.3.5 Breakdown of lipid droplets	34
1.3.6. Fibrosis	41
1.4 Cellular mechanotransduction	43
1.4.1 Biological role of mechanotransduction	43
1.5 SRC family kinases; structure and function.....	48
1.6 Cellular senescence in orbital fibroblasts.....	55
1.7 Aims and objectives	60
CHAPTER 2 MATERIALS AND METHODS.....	62
Orbital Soft Tissue	62
Fibroblast Expansion	62
Primary cell culture	63
Three-dimensional (3D) cell culture.....	63
3D Cell Contractility Assay	64
Cell Mechanotransduction Assays.....	64
<i>On collagen gels.....</i>	64
<i>On Cytosoft® and Matrigen Softwell® plate wells</i>	65
<i>On PAA/bisAA-coated coverslips</i>	65
Oil-Red-O staining	66
siRNA knock-down.....	67
Cell lysate preparation and Western Blotting	68
<i>Protein extraction</i>	68
<i>Western blot</i>	69

Immunofluorescence.....	70
LD540 lipid droplet staining	71
Senescence-associated β -galactose activity assay.....	71
Inhibitors and activators	73
Orbital fibroblast immortalisation	75
Statistics	76
CHAPTER 3 SFK ROLE IN LIPID DROPLET GENERATION AND CONTRACTILITY	77
3.1 Introduction	77
3.2 Results.....	81
3.2.1 GD patient-derived orbital fibroblasts generate more lipid droplets than healthy controls.....	81
3.3.2. CO and HO cells differ in FYN/SRC expression but not in SRC activity.....	84
3.3.3. SRC knock-down increases the number of lipid droplet positive cells while FYN and CSK knock-downs abolish it	87
3.3.4. FYN may modulate spontaneous lipid droplet generation through regulating AMPK activity	89
3.3.5. SRC suppresses lipid droplet generation through maintaining Akt/mTORC activity	91
3.3.6. SRC and FYN are necessary for orbital fibroblast contractility.....	93
3.4. Discussion.....	95
3.4.1 Role of SFKs in lipid droplet generation and contractility.....	95
3.4.2 Pathways regulated by SRC and FYN	96
3.4.1. Limitations of the study and future work.....	97
3.4.2 Conclusion	98
CHAPTER 4 MECHANOREGULATION OF SFKS	99
4.1 Introduction	99
4.1.1. 3D culture or substrate rigidity; what promotes lipid droplet production?.....	99
4.1.2 Signalling pathways involved in lipid droplet production	100
4.1.3 Autophagic degradation of lipid droplets	102
4.2. Results.....	103
4.2.1 Orbital fibroblasts in 3D cultures do not increase adipogenic gene expression	103
4.2.2. Lipid droplet generation depends on substrate rigidity.....	105
4.2.3. Mechanosensitive lipid droplet generation is unique to orbital fibroblasts ...	111
4.2.4. Src and Fyn protein function on soft substrates the same as in 3D cultures	114
4.2.5. Src and Fyn protein expression is lost in response to decreased substrate stiffness.	118
4.2.6 Orbital fibroblasts increase AMPK activity and autophagy marker expression on soft substrates	120
4.2.7 AMPK and mTORc1 regulated lipid droplet generation	124
4.2.8 AMPK and mTORc1 regulate orbital fibroblast contractility	129

4.2.9. PLIN2 localisation to lipid droplets requires AMPK.....	131
4.2.10. Disruption of autophagosome maturation prevents lipid droplet formation	134
4.2.11 Lysosomal marker Cathepsin D localises with lipid droplets	137
4.3 Discussion	139
4.3.1 Canonical adipogenesis is not the cause of lipid droplet generation	139
4.3.2. Lipid droplet generation in orbital fibroblasts responds to substrate stiffness	140
4.3.3. AMPK and mTORc1 are downstream effectors of lipid droplet generation..	144
4.3.4 AMPK and mTORc1 activity influences orbital fibroblasts contractility	148
4.4 Conclusions	148
CHAPTER 5 REPLICATIVE SENESCENCE IN ORBITAL FIBROBLASTS.....	150
5.1 Introduction.....	150
5.1.1. Replicative senescence.....	150
5.1.2 Biological markers of senescence	151
5.2 Results.....	152
5.2.1 Cell proliferation is increased on soft substrates	152
5.2.2. β -galactosidase activity is reduced in cells cultured on softer substrates....	157
5.2.3. Reduction of Fyn and Src protein decreases β -galactosidase activity	161
5.2.4 ROCK kinase and mTORc1 inhibition reduces the β -galactosidase activity.	163
5.2.5. PTPN22 and CSK reduction decrease β -galactosidase activity.....	165
5.2.6. AMPK activation decreases cellular senescence	168
5.2.7 Human tenon fibroblasts do not display β -galactosidase activity on stiff substrates.....	170
5.2.7 Immortalised orbital fibroblasts display senescence markers when cultured on plastic.....	172
5.3 Discussion	174
5.3.1 Orbital fibroblast proliferation is slower on stiff substrates	174
5.3.2 Stiff substrate orbital fibroblasts show senescence-associated β -galactosidase activity.....	175
5.3.3. SFK and PTPN22 downregulation reduces the β -galactosidase activity.....	177
5.3.4. AMPK and mTORC1 regulate cellular senescence.....	178
5.3.5 Immortalised cells enter senescence if cultured on rigid substrates.....	180
5.4 Conclusion	181
CHAPTER 6 DISCUSSION AND FUTURE DIRECTIONS	182
6.1 Role of SRC family kinases in contractility and lipid droplet generation	184
6.2 Mechanonsensitive lipid droplet production.....	186
6.3 Mechanosensing-associated senescence.....	189
6. 4 Experimental limitations	193
6. 5 Concluding remarks	194
7. Bibliography	195

ABBREVIATIONS

AFM	Atomic force microscopy
Akt	Protein Kinase B, PKB
AMPK	5'-AMP-activated protein kinase
AP2	Adaptor protein complex 2
C/EBPβ	CCAAT/enhancer-binding protein β
CEBPα	CCAAT/enhancer-binding protein alpha
Chk	Csk homologous kinase
Csk	carboxyterminal Src kinase
DAG	Diacylglycerols
DNL	De novo lipogenesis
ECM	Extracellular matrix
ER	Endoplasmic reticulum
FA	Focal adhesion
FAK	Focal adhesion kinase
FAS	Fas Cell Surface Death Receptor
Fyn	Tyrosine-protein kinase Fyn
GAGs	Glycosaminoglycans
GD	Graves disease
GLUT4	Glucose transporter 4
GO	Graves orbitopathy
HA	Hyaluronic acid
HAS	Hyaluronan synthase
HIV	Human immunodeficiency virus
HSL	Hormone-sensitive lipase
IGF-1R	Insulin-like growth factor 1
IL16	Interleukin 16
IL6	Interleukin 6
IL8	Interleukin 8
LD	Lipid droplets
LKB1	Liver kinase B1
MAG	Monoacylglycerols
MAPK	Mitogen-activated protein kinase
MMP	Membrane metalloproteases
MSCs	Mesenchymal Stem Cells
mTORC1	Mammalian target of rapamycin complex 1
OF	Orbital fibroblasts
PDGF	Platelet-derived growth factor
PGHS-2	Prostaglandin endoperoxide H synthase-2
PI3K	phosphatidylinositol 3-kinase
PKA	protein kinase A
PLIN	Adipocyte differentiation-related protein
PPARγ	Peroxisome proliferator-activated receptor gamma

Pref-1	Preadipocyte factor-1
PTPN22	phosphotyrosine phosphatase N22; Lyp
Rac1	Ras-related C3 botulinum toxin substrate 1
RANTES	Chemokine ligand 5, CCL5
ROCK	Rho-associated protein kinase
SA β-gal	Senescence-associated β -galactosidase
SASP	Senescence-associated secretory phenotype
SFK	Src family kinase
SH2	Src homology domain 2
SH3	Src homology domain 3
Src	Proto-oncogene tyrosine-protein kinase Src
SREBP1	Sterol regulatory element-binding transcription factor 1
TAG	Triacylglycerols
TGFβ	Transforming growth factor beta
Thy1	Thy-1 Membrane Glycoprotein, CD90
TSHR	Thyroid-stimulating hormone receptor
UGDH	UDP-Glucose 6-Dehydrogenase
ULK1	Serine/threonine-protein kinase ULK1
Vav	Proto-oncogene vav

LIST OF FIGURES

Figure 1.1 Clinical Manifestations Of Graves Orbitopathy.	17
Figure 1.2 Molecular Mechanism Of Go Initiation.	24
Figure 1.3 Overview Of Ppar γ Pathway For Adipogenesis.	26
Figure 1.4 Basic Structure Of Lipid Droplets (Onal Et Al, 2017)	30
Figure 1.5. Neutral Lipid Synthesis, Lipid Droplet (Ld) Formation And Growth.	33
Figure 1.6. Lipolysis Of Lipid Droplets.	35
Figure 1.7 The Three Types Of Autophagy.	37
Figure 1. 8 Lipid Droplet Breakdown By Lipophagy.	39
Figure 1. 9 Generalized Model Of Wound Healing And Scarring Versus Pathological Fibrosis.	40
Figure 1. 10. Immunopathogenesis Of Go, Highlighting The Role Of Counterplay In	
Figure 1. 11. Application Of Force To A Cell.	44
Figure 1.12. Effect Of Substrate Stiffness On Stress Fibres	45
Figure 1. 13. Src And Fak Co-Localise At Integrin Adhesion Sites	
Figure 1. 14. Src Protein-Tyrosine Kinase Structure	49
Figure 1. 15. General Structural Schematic Of The Src Family Kinases In Their Inactive And Active Configurations.	51
Figure 1. 16. Ampk Structure And Activation	53
Figure 1. 17. Ampk Inhibits Mtorc1.	54
Figure 1. 18. Phenotypic Alterations Associated With Senescence Initiation, Early Senescence, And Late Phases Of Senescence	55
Figure 1. 19. Functions Of SASP	57
Figure 3.1 Go Orbital Fibroblasts Are More Prone To Develop Lipid Droplets Compared To Control Cell Lines From Healthy Patients	80
Figure 3. 2. Sfk Inhibition Reduces The Amount Of Lipid Droplets Generated In 3d.	83
Figure 3. 3. Ho Fibroblasts Express More Fyn Protein, Co – More Src	85
Figure 3. 4. Active Src Localises To Focal Adhesions And Focal Contacts In Orbital Fibroblasts	86
Figure 3. 5. Src Knock- Down Significantly Increases The Amount Of Lipid Droplets In 2d And 3d Cultures While Fyn And Csk Knock-Downs Reduce It.	88
Figure 3. 6. Fyn Downregulation Causes Activation Of Ampk-Associated Pathways	90
Figure 3. 7 Src Knock-Down Downregulates Mtorc/Akt Protein Expression.	92
Figure 3. 8 Src And Fyn Ko Reduces Orbital Fibroblast Contractility.	94
Figure 4. 1 3d Cultured Orbital Fibroblasts Do Not Exhibit Increased Adipogenic Markers.	104
Figure 4. 2 Ho Retain Lipid Droplet Generating Potency When Cultured On Stiffer Substrates.	106
Figure 4. 3 Lipid Droplet Generation Depends On Mechanical Substrate Stiffness Not Protein Coating	107
Figure 4. 4 Orbital Fibroblasts Generate Lipid Droplets When Cultured On Substrates Whose Stiffness Is Within The In Vivo Physiological Range	109
Figure 4. 5 Mechanosensitive Lipid Droplet Generation Is Specific To Orbital Fibroblasts	113
Figure 4. 6 Fyn Knock-Down Effect Is Lost In Cells Cultured On Soft Substrates.	116
Figure 4. 7 Src Knock-Down Increases Lipid Droplet Generation On Stiffer Substrates.	117
Figure 4. 8 Orbital Fibroblasts Lose Sfk, Ptpn22 And Mtorc Expression When Cultured On Softer Substrates	119
Figure 4. 9 Soft Substrate Culturing Increases Ampk Activity And Expression Of Autophagy Markers.	121
Figure 4. 10 Lc3b Expression And Co-Localisation With Lipid Droplets Increases With Increased Ampk Activity.	122
Figure 4. 11 Py418 Src Re-Locates To Perinuclear Space And Co-Localises With Lipid Droplets In Orbital Fibroblasts Cultured On Soft Substrates.	123

Figure 4. 12 Ampk And Mtorc Activity Alter Lipid Generation And Morphology In Orbital Fibroblasts	127
Figure 4. 13 Phospho-Ampk Localises To Lipid Droplets In Soft Gel Cultures.	128
Figure 4. 14 Mtorc1 And Ampk Inhibition Reduce Orbital Fibroblast Contractility.	130
Figure 4. 15 Plin2 Localised To Lipid Droplets In Cells Cultured On Soft Substrates	132
Figure 4. 16 Ampk Activity Is Necessary For Plin2 Localisation To Lipid Droplets.	133
Figure 4. 17 Autophagosome Inhibition Abolishes Mechanosensitive Lipid Droplet Formation	135
Figure 4. 18 Blocking Autophagosome Acidification Reduces Lipid Droplet Generation On Soft Substrates	136
Figure 4. 19 Lysosomal Marker Cathepsin D Localises To Lipid Droplets But Does Not Co-Localise With All Lipid Droplet Positive For Plin2	138
Figure 5. 1 Cell Proliferation Increases With Substrate Softness.	154
Figure 5. 2. Cell Proliferation Increases On Soft Collagen Gels.	155
Figure 5. 3 B-Galactosidase Activity Increases On Cells Cultured On Rigid Substrates	156
Figure 5. 4 Senescence Markers Are Absent In Orbital Fibroblasts Cultured On Soft Matrices	158
Figure 5. 5 Senescence Marker P16ink4a Leaves The Nucleus When Cultured On Soft Substrates.	159
Figure 5. 6 Src And Fyn Knock-Downs Decrease Senescence In Orbital Fibroblasts	162
Figure 5. 7. B-Galactosidase Activity Is Reduced With Rock And Mtorc1 Inhibition.	164
Figure 5. 8 Ptpn22 Knock-Down Reduces B-Galactosidase Activity In Orbital Fibroblasts.	166
Figure 5. 9 Both Ptpn22 Inhibition And Csk Downregulation Decreases B-Galactosidase Activity	167
Figure 5.10 Ampk Decreases B-Galactosidase Activity	169
Figure 5. 11 Tenon Fibroblasts Display Significantly Lower B-Galactosidase Activity On Rigid Substrates Than Co Cells.	171
Figure 5.12. Cell Immortalisation Does Not Prevent Substrate Rigidity-Associated Senescence	173
Figure 6. 1. Model Of Lipid Droplet Production	183
Figure 6. 2. Substrate Stiffness Regulates Replicative Senescence Through Sfks	192

LIST OF TABLES

Table 2. 1 Orbital Fibroblast Donor Information	62
Table 2. 2 Reagent Volumes For E Moduli Used	66
Table 2. 3 Sirnas Used In Knock-Down Experiments	67
Table 2. 4 Antibodies Used In Wb And If Experiments	70
Table 2. 5 qRT-PCR Primers	72

CHAPTER 1 INTRODUCTION

1.1 Graves orbitopathy; an orbital complication of Graves disease

Graves disease was initially characterised in 1835 by Robert J. Graves who described a patient with gout and an enlarged thyroid gland. The modern medical view is that Graves disease (GD) is an autoimmune thyroid disorder caused by circulating thyroid-stimulating antibodies. These provoke a localised immune reaction and cause the thyroid gland to become overreactive (Maheshwari & Weis, 2012). GD affects around 2-3% of the world population and has no ethnic predisposition. It occurs in all age groups but more frequently diagnosed in young and middle-aged women. Despite having approximately 3500 patients diagnosed with GD annually in the UK, it is still classified as a rare disease. 1.2% of the US population suffers from GD with women having a 3.5% risk to develop the disease during their lifetime while the risk in men is seven times lower, 0.5% (McLeod, Caturegli, Cooper, Matos, & Hutfless, 2014). Graves Orbitopathy (GO, also known as Graves Ophthalmopathy and Thyroid-associated orbitopathy) manifests in 40 – 50% of all GD patients. It is characterised by prolonged soft orbital tissue inflammation resulting in retrobulbar adipose tissue expansion. During the active stage of the disease, patients develop proptosis (Figure 1A) due to increasingly expanding orbital tissue volume which is flanked by eye socket, pushing the eye outwards. Proptosis causes eyelid retraction

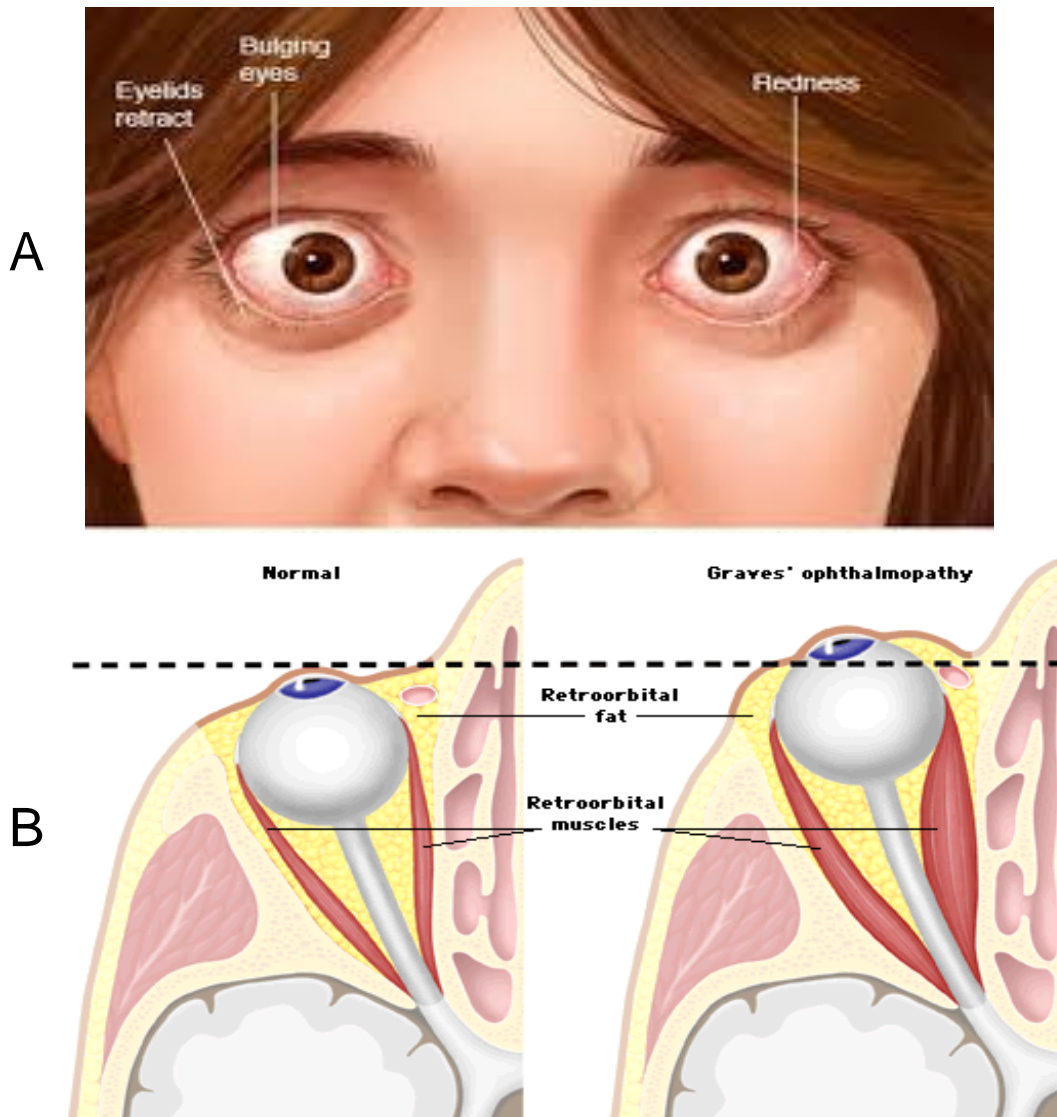


Figure 1.1 Clinical manifestations of Graves Orbitopathy.

A. External symptoms of GO are eyelid retraction, proptosis (bulging eyes) and redness due to inflammation.

B. External symptoms are caused by retroorbital fatty tissue expansion, caused by prolonged inflammation. Tissue expansion presses onto the eye and retroorbital muscles, limiting their movement (from <http://www.aboutcancer.com/graves.htm>).

and limits eyelid ability to cover and moisturise the eye making it prone to dryness. Tissue expansion also limits eye muscle movement (Figure 1B) causing diplopia (double vision). Prolonged inflammation locally depletes immune cells which halts the inflammatory process (inactive or “burn-out” phase) leaving behind accumulated scar tissue. Without surgical

intervention the physical complications of GO to remain (Bahn, 2003). Therapeutic options to treat GO are scarce. Due to the limited understanding of the molecular disease mechanisms, pharmacological interventions target disease symptoms. Severe GO cases are treated with high-dose glucocorticosteroidal, anti-inflammatory drugs and radiation therapy (Burch & Cooper, 2015). Orbital decompression surgery (removal or sculpting of the orbital bone and removal of scar- and orbital fatty tissue) alleviates proptosis. ~2.6% of patients undergoing orbital decompression surgery require repeated intervention due to disease recurrence (Fichter, Guthoff, & Schittkowski, 2012; Zhang-Nunes et al., 2015).

Potential development of GD is strongly associated with genetics; siblings have a 30% higher chance of developing GD. Studies performed in monozygotic twins increase the probability of GD to 79% if detected in one of the twins (Davies, Ando, Lin, Tomer, & Latif, 2005; Płoski, Szymański, & Bednarczuk, 2011). Numerous candidate genes and their single nucleotide polymorphisms (SNPs) have been linked to the development of GD. Human leukocyte antigen (HLA) protein complex family presents antigens on external cellular surface to prompt immune T cell responses and have been linked to the loss of immune tolerance to thyroid-stimulating hormone receptor (TSHR). Protein tyrosine phosphatase-22 (PTPN22) is involved in limiting the adaptive response to antigen by dephosphorylating and inactivating T cell receptor (TCR) associated kinases and their substrates. PTPN22 physically associates with the Csk kinase, an important suppressor of the Src family kinases that mediate TCR signalling and focal contact

formation in fibroblasts. PTPN22 polymorphisms have been demonstrated to have a clinical significance in GD and other autoimmune disorders with PTPN22 R620W mutant disrupting the interaction of PTPN22 and Csk and causing a reduced inactivating phosphorylation of SFK and inactivation of TCR. Polymorphisms in Cluster of differentiation 40 (CD40) and TSHR have a demonstrated association in genome-wide associated studies however exact molecular mechanisms of SNP caused alteration in protein activity have not yet been established.

Environmental factors can also contribute to GD incidence; a strong clinical correlation between GD and smoking has also been shown increased risks of disease relapse (Ferrari, Fallahi, Antonelli, & Benvenga, 2017; Ferrari et al., 2017). Prior medical history of infectious disease increases the likelihood of developing GD. Human T-cell lymphotropic virus-1, herpes simplex virus, rubella, mumps virus, Epstein–Barr virus, enterovirus in HT, retroviruses (human T-cell lymphotropic virus-1, human foamy virus or human immunodeficiency virus (HIV), and Simian virus 40) have been shown to trigger GD (Desailloud & Hober, 2009). Finally, Vitamin D deficiency and impaired molecular binding to thyroid receptors have been attributed to GD. Vitamin D modulates the activity of immune cells. Vitamin D hypovitaminosis or gene polymorphisms affecting its receptors binding affinity has been shown to facilitate GD manifestation (Ferrari et al., 2017).

1.2 Orbital fibroblasts and their role in GO

1.2.1. Molecular characteristics of GO orbital fibroblasts

Fibroblasts are spindle-shaped cells with a flat nucleus found in the extracellular matrix surrounding organs. They inhabit multicellular environments, usually located close to the epithelium or endothelium (Molecular Biology of the Cell, 4th edition, 2002). In laboratory conditions, fibroblasts are cultured on plastic, but in-vivo fibroblasts reside embedded in the ECM, subject to a much softer mechanistic environment than conventional cell cultures (Yeung et al., 2005). Fibroblasts are the primary source of ECM proteins, which play key roles in determining cell phenotype and function. The main functions of fibroblasts are to (a) maintain tissue homeostasis; (b) regulate tissue contraction in response to injury or inflammation; (iii) regulate immune responses; (iv) maintain cell-cell interactions (Darby & Hewitson, 2007). Tissue remodelling is achieved through three mechanisms of modifying ECM structure: ECM production – secretion of ECM components (collagens, fibronectin, laminin); ECM degradation using metalloproteases (MMPs) expressed on the external membrane; ECM biophysical modification by exerting a mechanical pull onto collagenous fibres of ECM (Mester et al., 2016). Fibroblasts also secrete growth factors allowing autocrine and paracrine interactions with the local cell population to maintain tissue homeostasis (Yun et al., 2010). Fibroblasts also play a crucial role in the post-injury immune response by recruiting macrophages, neutrophils and lymphocytes if an adaptive immune response occurs, to the site of tissue damage. Immune cells

undergo apoptosis or phagocytosis once the inflammation has resolved. During chronic inflammation, however, immune response causes “overactivation” of fibroblasts resulting in fibrosis and scarring (Wynn & Ramalingam, 2012).

Orbital fibroblasts (OFs) undertake the characteristic functions of fibroblasts, but phenotypically are composed of a heterogeneous population of cells, expressing a variety of molecular surface markers, separating them from fibroblasts populations across the body and even within the orbital tissue (Dik, Virakul, & van Steensel, 2016). OFs along with the fibrous and adipose tissue, the optic nerve, the sclera and episclera, the peripheral nerve cellular elements, and the osteocytes and cartilaginous elements are are thought to be derived from the neural crest. Compared to other fibroblasts which are largely of mesenchymal origin, OFs have shown to express distinctive molecular markers which can be partly attributed to GO pathology. OF surface expression of thyroid-stimulating hormone receptor (TSHR) and insulin-like growth factor 1 receptor (IGF-1R) are autoantigens involved in triggering the disease (Latif, Morshed, Zaidi, & Davies, 2009). GO orbital fibroblasts also are shown to retain surface markers encountered on mesenchymal stem cells (MSCs) despite being derived from the neural crest (Brandau et al., 2015b; Kozdon, Fitchett, Rose, Ezra, & Bailly, 2015). Smith et al. show that an OF subpopulation expresses CD34, a surface marker associated with fibrocytes and regarded as non-MSC-like, however, these findings have not been reproduced by other groups (Smith et al., 2011). Previous data from the Bailly group show that GO, patient-derived

OFs retain an MSC-like differentiation ability and under specific conditions can be driven to differentiate into myogenic, neuronal, osteogenic and chondrogenic lineage cells, not only retaining a similar surface marker profile but also MSC-like pluripotency. Here, a small subpopulation of CD34+ cells was also detected (Kozdon, Fitchett, Rose, Ezra, & Bailly, 2015). GO fibroblasts have been shown to exhibit increased contractility and adipogenesis where OFs undergo *spontaneous* adipogenesis when embedded in 3D cultures *without* chemical induction or increased glucose uptake. Furthermore, contractility and adipogenesis are regarded as mutually exclusive processes, yet in 3D cultured orbital fibroblasts, these appear to be concurrent. Moreover, OFs isolated from GO patients appear to be more adipogenic than their healthy counterparts when incubated with an adipogenic differentiation mix. An adipogenic effect without chemical induction appears in collagen-embedded GO OFs further amplified by mechanical pressure-induced stress. (He Li et al., 2014). OF adipogenic potential is attributed to another subpopulation of cells expressing Thy-1 (or CD90); Thy-1(+) cells have been shown to have a myofibroblastic predisposition while Thy-1(-) negative fibroblasts differentiate into adipocyte-like cells (Brandau et al., 2015a; Kozdon et al., 2015). This phenomenon can be explained by a dual proposed function of Thy-1 implicating it as a mechanotransduction regulator. Thy-1 is proposed to induce integrin clustering on the same cell and facilitate a conformational change from the active extended state to a bent. closed state limiting integrin binding to the ECM proteins and reducing downstream pathway

activity. Thy-1 can also interact with integrins of other cells, facilitating cell-cell contacts maintaining integrins of the partner cell in an open conformation. In both of these models Thy-1 reduces Src activity.

Li et al. demonstrate that GO fibroblasts sorted by Thy-1 surface expression indeed exhibit different levels of spontaneous adipogenesis; Thy-1 low population was significantly more adipogenic than Thy-1 high. In respect to contractility, GO fibroblasts groups with Thy-1 high-low surface expression did not show any significant difference (He Li et al., 2014). Thy1

The widespread assumption about the onset of GD is the loss of immune tolerance towards the TSHR and subsequent synthesis of circulating anti-TSHR antibodies that bind TSHR expressed on the surface of GO fibroblasts. The evolutionary reason as to why TSHR is expressed in OFs is still unknown, but the OF TSHR presence appears to higher in OFs isolated from GO patients. TSHR expression is particularly high in the CD34+ subpopulation fibrocytes (Garritty & Bahn, 2006). While recruitment of the anti-TSHR antibody is thought to be the main initiator of GO, insulin-like growth factor receptor 1 (IGF-1R) has also been implicated in triggering GO but is not targeted by a specialised anti-IGF-1R antibody (Figure 1.2). Anti-TSHR antibodies recognising different epitopes of TSHR have been shown to attenuate its activity and can not only induce receptor activity but also block it or cleave the TSHR (S. A. Morshed & Davies, 2015; Syed A. Morshed, Ando, Latif, & Davies, 2010). It has been shown that a cross-talk between the TSHR and IGF-1R takes place, implying that the IgG recognises both molecular targets and possibly clusters them, causing a

signalling link (Krieger et al., 2016; Smith, 2015; Smith, Hegedüs, & Douglas, 2012).

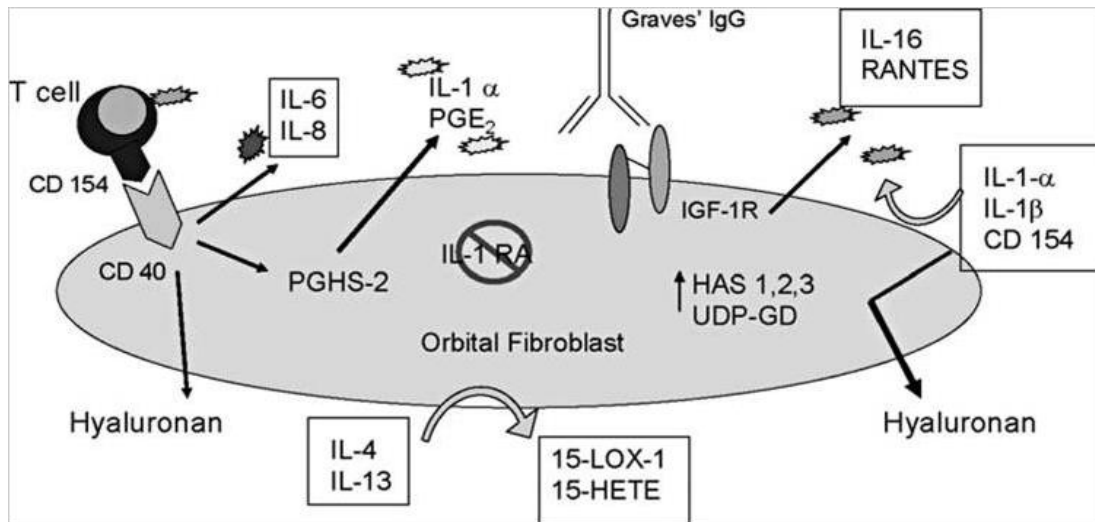


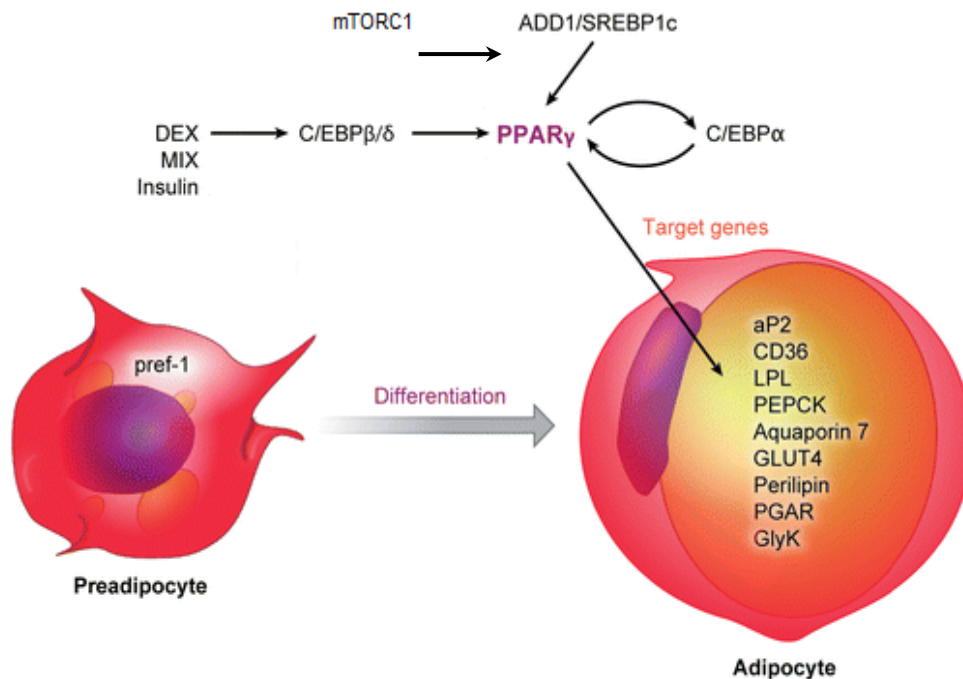
Figure 1.2 Molecular mechanism of GO initiation.

GO-IgGs (anti-TSHR and anti-IGF 1R) bind corresponding surface receptors on OFs. Immune cell recruitment and infiltration follows triggering hyaluronan synthesis activation, cytokine release, further immune cell recruitment and adipogenesis (Smith et al, 2015).

1.3. Pathogenesis of Graves orbitopathy

1.3.1. HA production

The symptoms of GO can be explained mechanically by an increase in the volume of tissue found within the confines of the bony orbit. This change results from both an accumulation of hydrated hyaluronan in the orbital muscles and connective tissues and an expansion of the adipose tissues within the orbit. The active stage of GO is thought to be initiated by the binding of anti-TSHR and anti-IGF 1R to OF (Figure 1.2) which recruits CD4+ T cells and macrophages to the orbital lumen by secreting cytokines RANTES and IL16. Recruitment of T cells further amplifies the inflammatory response by signalling a further release of proinflammatory cytokines (such as IL-1 α , IL-1 β , and IL-6) and expression of CD40L on OF surface, further recruiting more CD4+ T cells. Cytokines, in turn, activate pro-inflammatory genes such as those encoding prostaglandin endoperoxide H synthase-2 (PGHS-2), IL-6, IL-8, hyaluronan synthase (HAS), and UDP glucose dehydrogenase (UGDH). HAS can be activated through growth factor signalling (PDGF) and proinflammatory cytokines (TGF- β and IL-1 β). In GO fibroblasts HAS activation has been proposed to occur due to the increased presence of inflammatory cytokines (TGF- β , IL-1 β). Binding of anti-TSHR antibodies to TSHR expressed on GO fibroblasts has been shown to activate HAS and increased HA synthesis via cAMP signalling, suggesting that inflammatory cytokines and autoimmune antibodies collectively increase HA production in GO cells (Suzuki et al., 2003; Van Zeijl et al., 2011). Excretion of hyaluronates (HA) and other glycosaminoglycans




 Tontonoz P, Spiegelman BM. 2008. Annu. Rev. Biochem. 77:289–312.

Figure 1.3 Overview of PPAR γ pathway for adipogenesis.

PPAR γ is a key player of adipogenesis regulation and is at the core of an adipogenic signalling cascade with CEBP α . A variety of signalling pathways lie upstream of PPAR γ , including CEBP β/δ and Akt/mTORC1/SREBP1. Pre1 is a pre-adipocyte marker, lost during differentiation. Activation of PPAR leads to terminal adipocyte differentiation and expression of numerous adipogenic markers; CD36 is a membrane fatty acid import protein, GLUT4 is a glucose importer, activated during increased blood glucose levels, Perilipin (and its isoforms) is a lipid droplet scaffolding protein, preventing tryglyceride breakdown. Adapted from Tontonoz & Spiegelman, 2008.

(GAGs) into the orbital lumen is a major contributor to the orbital tissue volume expansion (Garrity & Bahn, 2006; Krieger, Neumann, Place, Marcus-Samuels, & Gershengorn, 2015). Biologically, GAGs retain water by providing hydrogen bonding donors to water molecules through their polysaccharide side chains. Secretion of GAGs into the ECM and water retention causes enormous volume expansion and is also proposed to destabilise the ECM mechanistic environment, thus altering the cell-ECM

attachment dynamics and mechanosensing (Pomin & Mulloy, 2018). Flanked by the bony orbit, HA accumulation partly contributes to proptosis and impaired orbital muscle function. Importantly, only OF isolated from GO patients appear to be susceptible to GO autoantibody induced HAS activation; OF from healthy patients and dermal fibroblasts did not secrete HA when exposed to anti-TSHR antibodies (Smith & Hoa, 2004).

1.3.2. Adipogenesis

Adipose tissue is a metabolically dynamic organ that is the primary site of storage for excess energy but it serves as an endocrine organ capable of synthesizing a number of biologically active compounds that regulate metabolic homeostasis. In mammals, adipose tissue differentiates into two separate types; white- (WAT) and brown adipose tissue (BAT). BAT specialises in heat production is almost absent in adult humans but is found at birth. It stores energy in lipid form, but more regularly produces heat by oxidizing fatty acids within the adipocyte, rather than supplying free fatty acids for use by other cell types. BAT cells possess an increased quantity of mitochondria which causes the tissues' brown appearance. The prevalence and function of WAT in adults is much broader; WAT serves as a thermal insulator, a shock-absorbing barrier and an energy storage compartment. It can also be viewed as the largest secretory organ releasing cytokines (IL-6), cell proliferation regulators (IGF-1), appetite regulators (Leptin) and others. An intermediate type of fat cells, beige adipocytes have been discovered relatively recently and can be found within WAT. These are seen as a transitioning cell type between WAT and BAT, and their

occurrence is thought to be stimulated by energy intensive metabolic processes like exercise and stress. While orbital fat is largely seen as a WAT depot, recent evidence suggests that GO associated, prolonged inflammation could cause “browning”, development of beige adipocytes. Evidence suggests that TSHR activation on its own also contributes to the early activation of adipogenesis in OF and TSHR surface expression has a positive correlation with lipid droplet production in MSCs. In orbital fibroblasts TSHR activation favours beige/brown adipocyte development but limits cell response to PPAR γ and WAT development (Draman et al., 2017; L. Zhang et al., 2006).

Prolonged orbital tissue inflammation triggers adipogenesis in OFs. Canonically, adipogenesis is mostly defined as the process by which preadipocytes get differentiated into adipocytes, restricted to cells of MSC lineage, including fibroblasts. The biological function of adipogenesis is lipid storage in the form of triglycerides that accumulate into lipid droplets as intracellular storage compartments (Figure 1.3). Adipogenic differentiation requires initial activation of CCAAT/enhancer-binding protein β (C/EBP β), which subsequently activates Peroxisome proliferator-activated receptor gamma (PPAR γ) and C/EBP α . An alternative mechanism of PPAR γ activation is through sterol responsive element binding protein 1 (SREBP1) which is subject to molecular target of rapamycin complex 1 (mTORC1) activity (Bost, Aouadi, Caron, & Binétruy, 2005; Cai, Dong, & Liu, 2016; Niemelä, Miettinen, Sarkanen, & Ashammakhi, 2008). PPAR γ is the master regulator of adipogenesis which becomes activated during increased blood

plasma glucose concentration and presence of free fatty acids. While PPAR γ primarily is expressed in adipose tissue, its effects also extend to increased cellular glucose uptake in the liver and pancreatic tissue. PPAR γ indirectly stimulates glucose breakdown (glycolysis) and *de novo* lipid synthesis (or *de novo* lipogenesis (DNL)) and also promotes clonal expansion of pre-adipocytes (Madsen, Petersen, & Kristiansen, 2005). Adipogenic differentiation in OF can be chemically induced with thiazolidinediones (rosiglitazone, anti-diabetic agent), an PPAR γ agonist (Durand, Ambinder, Blankson, & Forman, 2012). The adipogenic effect of thiazolidinediones in GO is also observed clinically; type 2 diabetes patients treated with pioglitazone develop or experience exacerbated TAO symptoms and demonstrate increased PPAR γ expression (Starkey et al., 2003).

Enhanced, chemically-induced adipogenesis was reported in GO orbital fibroblasts with an increased expression of PPAR γ and other adipogenic markers (Kumar, Coenen, Scherer, & Bahn, 2004) but exact mechanisms showing how autoimmune inflammation triggers adipogenesis are still not understood. Furthermore, PPAR γ has been shown to possess anti-inflammatory properties by limiting macrophage activation, which appears to be contradictory to widely seen macrophage immune cell infiltration into the orbital tissue (Pascual et al., 2007). However, increased OF hyperplasia has been observed in GO which is consistent with PPAR γ activity. Inhibition of PPAR γ with thalidomide in GO OFs has shown a significant reduction in adipogenesis but did not reduce OF hyperplasia indicating that increased

cellular proliferation can occur via PPAR γ independent means (C. Zhang et al., 2012). The consensus regarding the PPAR γ role in adipogenic GO pathogenesis is clear while reports of its involvement in OF hyperplasia and inflammation suppression are contradictory.

The Bailly lab has previously demonstrated that GO orbital fibroblasts cultivated in 3D show increased the production of lipid droplets without increased glucose uptake or chemical induction. Lipid droplet appearance without expression of characteristic markers or presence of chemical inducers indicates a previously unseen mechanism of lipid droplet production. The production of lipid droplets in this model was decreased in 3D cultured incubated with Src-family kinase inhibitor PP2. PP2 presence also reduced GO contractility (He Li et al., 2014).

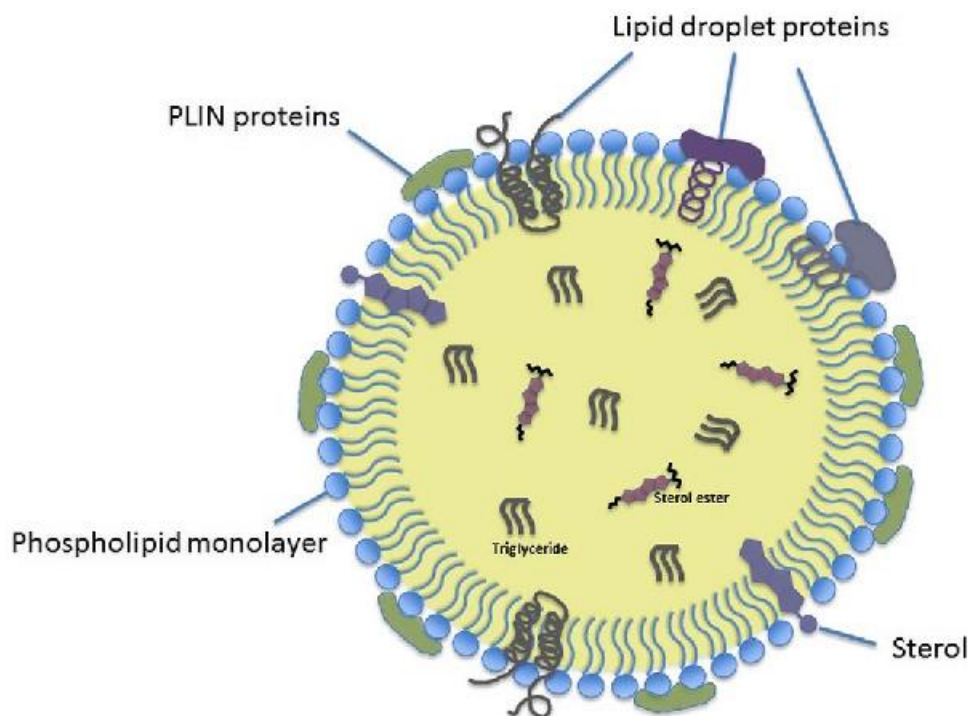


Figure 1.4 Basic structure of lipid droplets (Onal et al, 2017)

1.3.3 Formation, function and dynamics of lipid droplets

The storage of lipids is a universal feature of cells and organisms, which evolved as a mechanism that allowed survival by buffering energy fluctuations. Within cells, lipids are stored in specialized organelles called lipid droplets (LD). All LD share the same structure (Figure 1.4) – a hydrophobic oil core of the storage lipids, which mainly comprise triacylglycerols (TAG) and sterol esters, is shielded by a phospholipid monolayer that contains specific proteins (Onal, Kutlu, Gozuacik, & Dokmeci Emre, 2017).

LD surface proteins are regulating homeostasis and intracellular interactions of LDs. Membrane surface of LD is composed of several structural and functional proteins. In mammalian LDs, predominant proteins are the members of the PLIN protein family, adipocyte differentiation-related protein PLIN2 (ADRP; adipophilin), and PLIN3 (tail-interacting protein of 47 kDa, TIP47) proteins. PLIN proteins (PLIN 1 – 5) share sequence similarity and the ability to bind intracellular LDs, suggesting that they derived from a common ancestral gene (Bickel, Tansey, & Welte, 2009). The most studied member of LD surface proteins is PLIN2 that regulates the access of lipases to neutral lipids in the core of LDs, hence controlling lipid homeostasis. PLIN2 knock-down experiments in mice show that reduced PLIN expression increases lipolysis and limits lipid accumulation.

LDs also host many other proteins-related to lipid homeostasis (Tansey et al., 2001). These proteins can be classified according to their functions, including lipid biogenesis (long-chain fatty acid CoA ligases, lanosterol

synthase, squalene epoxidase), maintenance of intracellular lipid metabolism (long-chain fatty acid CoA ligases) and lipid degradation (patatin-like phospholipase domain-containing protein 2 (PNPLA2, HSL, ATGL) (Welte, 2007). Signalling-related proteins are classes of proteins that accumulate on the surface of LDs. Major signalling proteins such as mitogen-activated protein kinase (MAPK), phosphatidylinositol 3-kinase (PI3K) and Src- family kinases have been shown to localize on LD surfaces (Yu et al., 1998; Yu, Cassara, & Weller, 2000). Caveolins are a group of proteins that specifically form a coat by making invaginations and surrounding cellular membranes called caveolae. Caveolin-1 and caveolin-2 proteins were shown to be present on the surface of LDs co-localising with SFK Fyn (Blouin et al., 2010; Smart et al., 1999).

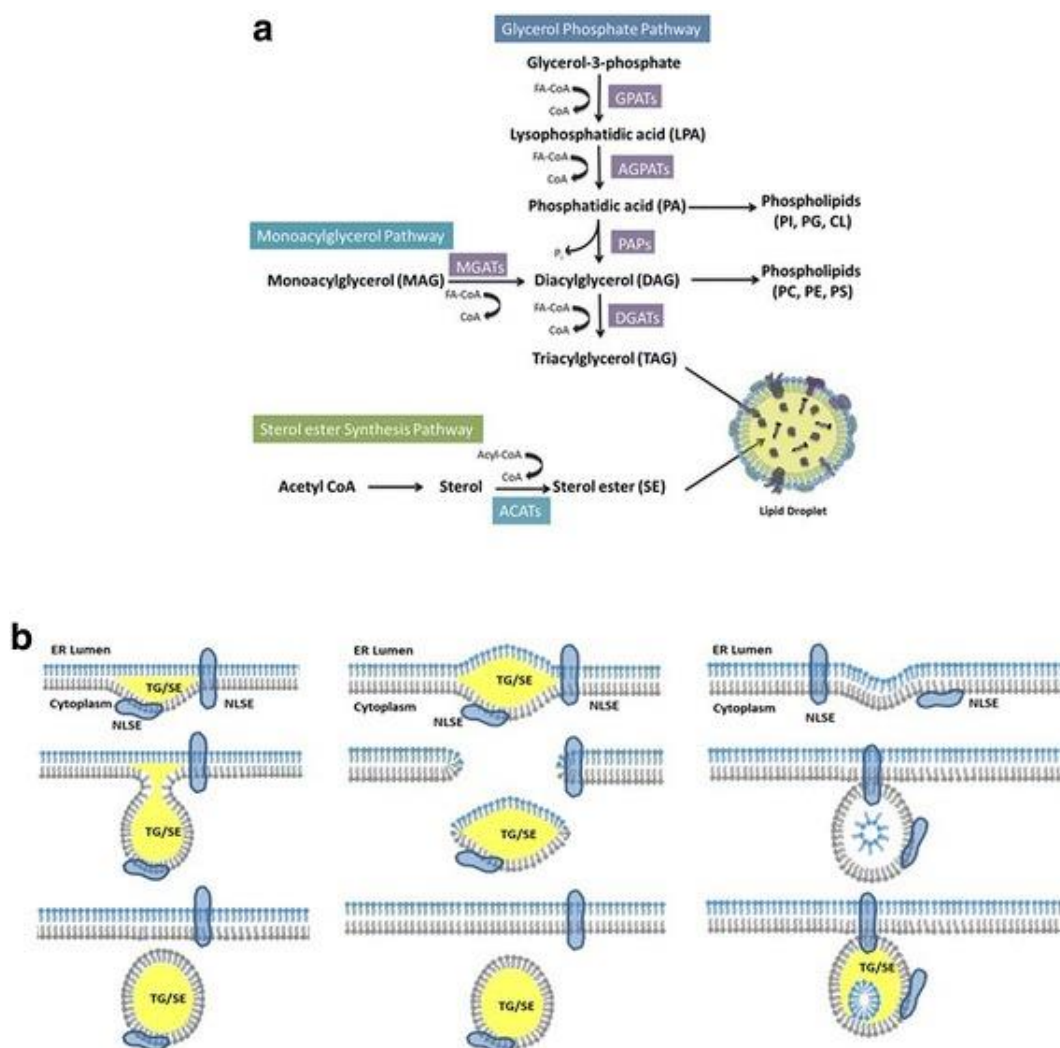


Figure 1.5. Neutral Lipid Synthesis, Lipid Droplet (LD) Formation and Growth.

A. Metabolic pathway of triglyceride (TG) and sterol ester (SE) synthesis dependent on glycolysis.

B LD Formation from Endoplasmic Reticulum (ER) by Neutral Lipid Synthesis Enzymes (NLSE). Left panel shows budding model of LDs from ER; middle panel shows bicelle formation model of LDs originating from ER; right panel shows hatching model of LDs from ER (Onal et al, 2017)

1.3.4. Biogenesis of lipid droplets

LD biogenesis is stimulated by the rise of intracellular FA levels. To prevent lipotoxicity, free fatty acids are converted into neutral lipids and stored in cytosolic LDs. LDs are mainly synthesised de novo but can also be made by fission of already existing LDs. Mammalian LD biogenesis occurs within the ER phospholipid bilayer in separate steps involving neutral lipid synthesis, neutral lipid accumulation and droplet formation. An increased volume of neutral lipid between the ER exceeds the ability to accommodate the insoluble lipids, and LDs are thought to be pushed from the ER bilayer (Figure 1.5). Several imaging studies confirm a strong localisation of lipid droplets on the surface of the ER. Once LDs are synthesized, they keep expanding because of the excessive amount of FA in cells and reach an upper threshold. The size of LDs varies within a wide range (0.4–100 μm) in different cell types (S. Zhang et al., 2016). Even in the same cell, the diameter of LDs may differ under pathological conditions. (H. Yang, Galea, Sytnyk, & Crossley, 2012).

1.3.5 Breakdown of lipid droplets

LDs break down mostly by lipolysis, however, recent discoveries that showed a molecular connection between lipolysis and autophagy mechanisms. Lipolysis is the hydrolysis of ester bonds between long-chain FAs and glycerol backbone in TAGs (Figure 1.6). During the initial stages of lipolysis, protein kinase A (PKA) phosphorylates PLIN and leads to its proteasomal degradation. This results in the release of ATGL activator protein CGI-58, which then initiates TAG breakdown via activated ATGL

(Gruber et al., 2010; Schweiger et al., 2006). ATGL selectively catalyzes the first step of TAG hydrolysis to generate diacylglycerols (DAGs) and free FAs (Zimmermann et al., 2004). The second step of lipolysis depends on the activation of hormone-sensitive lipase (HSL), which hydrolyses the first and the second step of lipolysis. HSL hydrolyzes DAGs and produces monoacylglycerol (MAG) and FAs (Zimmermann et al., 2004). Under starvation, products of lipolysis are secreted from the adipose tissue into the bloodstream and are then used for β -oxidation and energy production.

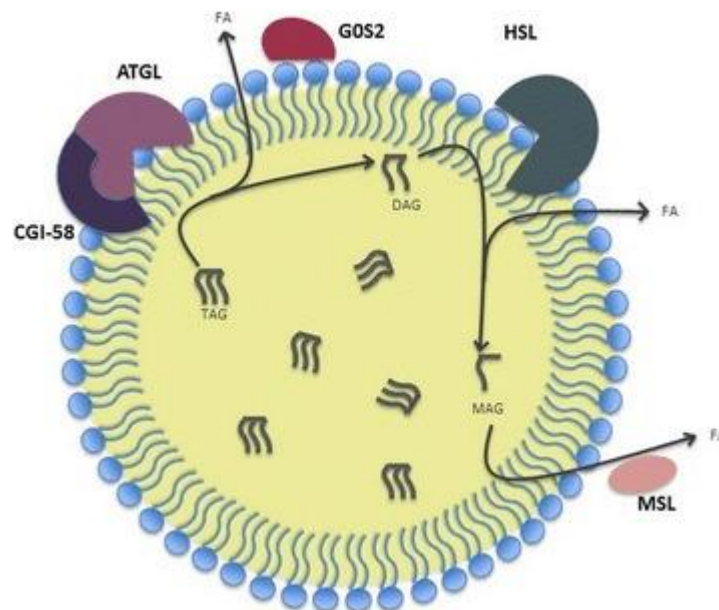


Figure 1.6. Lipolysis of Lipid Droplets.

Lipolysis is initiated by PKA phosphorylation of PLIN. HSL or ATGL is recruited to the phosphorylation sites and degrades PLIN. This allows degradations of TAGs and release of DAGs and FFAs. HSL further breaks down DAGs and releases more FFAs (Onal et al, 2017)

Autophagy, the literal meaning of which is 'self-eating', can be induced by starvation to supply a variety of substrates for ATP generation. Autophagy also serves as a catabolic pathway to recycle excessive or damaged intracellular organelles such as mitochondria. Largely through these two general functions, autophagy regulates a number of essential cellular processes including development and differentiation, immunity, apoptosis and ageing (Jaishy & Abel, 2016). Three forms of autophagy have been defined: macroautophagy, chaperone-mediated autophagy (CMA) and microautophagy (Figure 1.7). In macroautophagy (the most physiologically important of the three in terms of the quantity of degradation) cytosolic organelles and protein complexes are sequestered in a double-membrane vesicle, the autophagosome (Zaffagnini & Martens, 2016). Autophagosomes fuse with lysosomes to form an autolysosome, in which the cargo of the autophagosome mixes with the hydrolytic enzymes of the lysosome for degradation and release into the cytoplasm for reuse. In microautophagy, organelles or proteins are taken up within an invagination of the lysosomal membrane for breakdown (W. Li, Li, & Bao, 2012). Rather than targeting cellular organelles, CMA instead removes individual proteins with a specific peptide motif recognized by the chaperone protein Hsc70 (70 kDa heat shock protein). The chaperone–protein complex translocates to the lysosome, where it binds to lysosome-associated membrane protein 2A (LAMP-2A) for protein internalization and degradation (Massey, Zhang, & Cuervo, 2006).

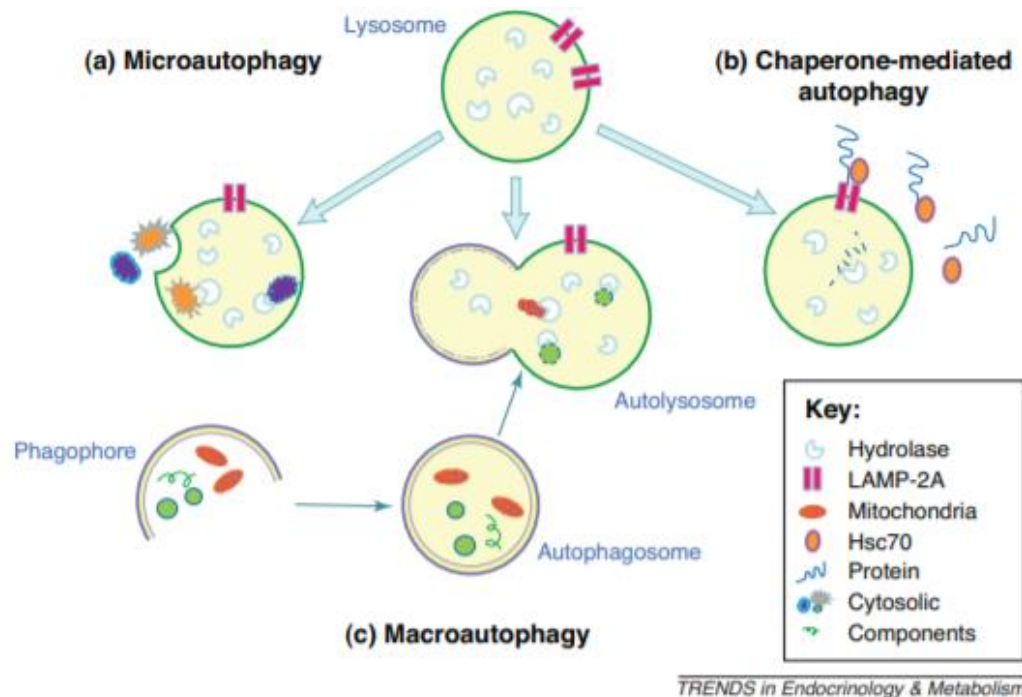


Figure 1.7 The three types of autophagy.

All three pathways result in the degradation of cytosolic components by lysosomal hydrolytic enzymes.

A. In microautophagy, an invagination of the lysosomal membrane allows internalization of cytosolic components such as organelles and proteins for degradation by hydrolases. **B.** CMA is specific for the removal of cytosolic proteins with a pentapeptide motif recognized by the chaperone protein Hsc70. Binding of this complex to the lysosomal LAMP-2A receptor leads to protein internalization and degradation. **C.** Macroautophagy begins with the formation of a double membrane to form a structure termed a phagophore. The membrane elongates to sequester cellular elements, including organelles and proteins, within an autophagosome. The autophagosome traffics to a lysosome for fusion of the two into an autolysosome. The cargo of the autophagosome mixes with the hydrolytic enzymes of the lysosome for degradation (Dong et al, 2011).

Lipophagy is a type of autophagy in which LDs are sequestered in autophagosomes for delivery to lysosomes for degradation (Figure 1.8) (Jaishy & Abel, 2016). Under cellular stress or starvation conditions, LDs are mobilised to sustain metabolic needs of cells. In imaging experiments, lipid droplets can be seen localising within autophagosomes and lysosomes. Inhibition of lipophagy by Atg5 knock-down in 3T3-L1 fibroblasts blocked the LD formation and resultant TG accumulation that occurs with the chemically induced differentiation of these cells into white adipocytes (Singh et al., 2009). A similar effect occurred in Atg5(-) MEFs induced to differentiate into adipocytes. In 3T3-L1 cells, the effect of a loss of autophagy on LDs was secondary to a failure of the cells to differentiate into white adipocytes. Cells lacking autophagy failed to increase crucial inducers of adipocyte differentiation, such as CEBP α and PPAR γ . As a result, the cells lacked terminal markers of white adipocyte differentiation including FAS, AP2 and GLUT4. Thus, LDs were decreased from a lack of LD biogenesis secondary to a primary failure in adipocyte differentiation due to disrupted autophagy (Y. Zhang et al., 2009). Autophagy can also supply building drops for lipid droplet development. Recent evidence demonstrates that autophagy can increase LD formation and size in starving murine embryonic fibroblasts (MEFs), this effect was abolished in Atg5 knock-down cells. Similar observations were made in experiments treating starving MEFs with bafilomycin A1 (Rambold, Cohen, & Lippincott-Schwartz, 2015).

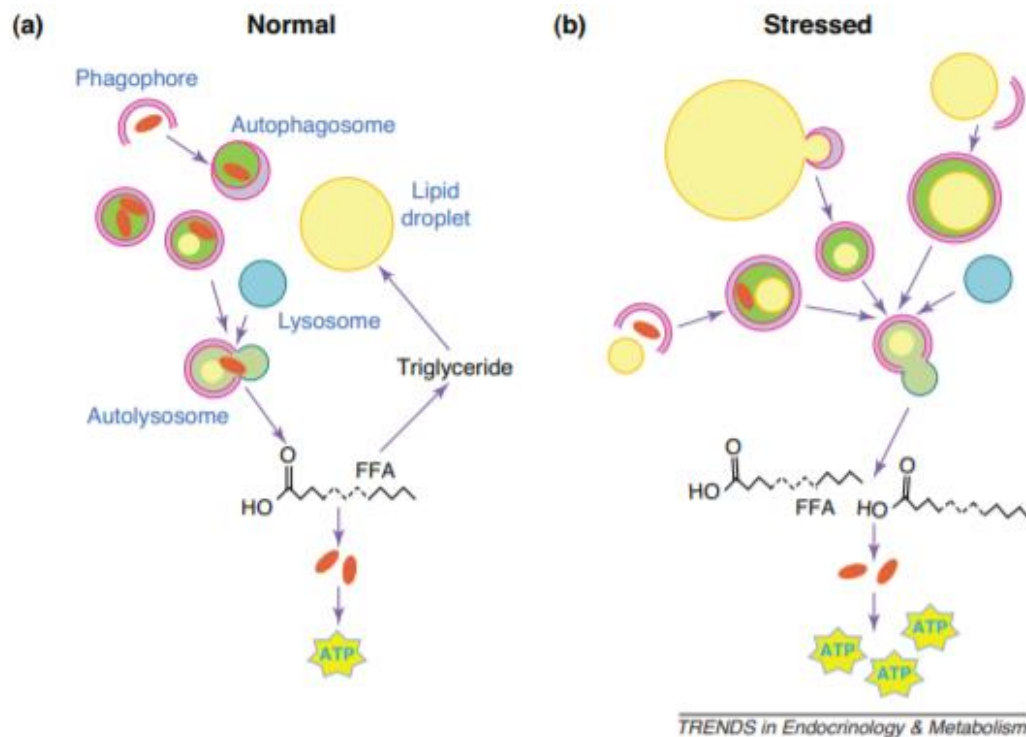


Figure 1. 8 Lipid droplet breakdown by lipophagy.

A. In the normal state, during times of sufficient nutrient supply, LDs are sequestered by autophagosomes and delivered to lysosomes for the degradation of TGs to FFAs. FFAs might contribute in a minor way to energy generation through mitochondrial β -oxidation to produce ATP or be re-esterified back into TGs for continued storage. Under these conditions, the minority of autophagosomes contain lipid, which is usually in combination with other cytosolic components.

B. When the cell is stressed either by nutrient deprivation or an excess of lipids, LD breakdown by this lysosomal pathway is increased. More autophagosomes contain lipid, often in the absence of other cargo. The increase in autophagy generates more FFAs, which are utilized to generate ATP (Dong et al, 2011).

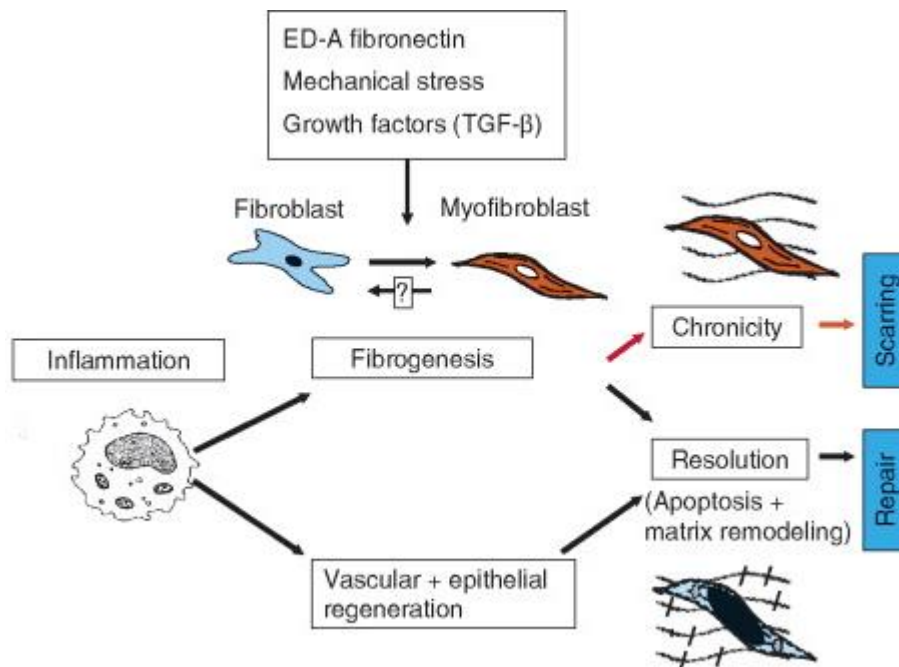


Figure 1. 9 Generalized model of wound healing and scarring versus pathological fibrosis.

Acute inflammation post-injury recruits innate immune cells (macrophages and neutrophils), promotes vascular and epithelial regeneration, and matrix remodelling. Once wound healing is complete, inflammation is resolved and immune cells undergo apoptosis. Chronic inflammation caused by an autoimmune reaction or persistent, repeated injury continuously recruits more immune cells which release fibroblast stimulating growth factors (TGF α , TGF β , PDGF) resulting in fibroblast over-activity. Increasing mechanical stress prompts resident fibroblasts to undergo and myofibroblast differentiation characterised by the formation of actin stress fibres, maturation of focal adhesions and fibronectin expression (a splice variant of fibronectin). Further TGF β secretion causes myofibroblasts to develop thicker stress fibres, rigid focal adhesions and expression of α -smooth actin (α SMA). Cumulative effect of phenotypical change is the remodelling of ECM and sedimentation of fibrillar collagen forming scar tissue Darby et al, 2007.

1.3.6. Fibrosis

Fibrosis is the overgrowth, hardening, and scarring of various tissues accompanied by excess deposition of ECM components. Fibrosis is the result of chronic inflammatory reactions induced by persistent infections, autoimmune reactions, allergic responses, chemical insults, radiation, and tissue injury. As opposed to acute wound healing, tissue fibrosis occurs due to persistent localised injury caused by long-term inflammation (Figure 1.9). Although fibrosis can manifest in many tissue types, orbital tissue scarring directly affects the function of the eye and has a serious negative effect on the patients' quality of life.

As described before, GO TSHR, and IGF-1R autoantibodies recruit immune cells to the orbital tissue. In the early inflammation, the majority of cells are T lymphocytes CD4+ and CD8+, and B lymphocytes are only occasionally seen. Macrophage influx is increased in the early disease and less so in late disease (Wakelkamp, Bakker, Baldeschi, Wiersinga, & Prummel, 2003). The inflammatory cells, T and B lymphocytes, and macrophages as well as mast cells infiltrating the orbit interact with orbital fibroblasts and amplify inflammatory/autoimmune reaction (Figure 1.10). Macrophages have been shown as key players in promoting the fibrotic phenotype of GO fibroblasts (I.-H. Yang, Rose, Ezra, & Bailly, 2019). When under prolonged exposure to TGF- β released by the immune cells, Thy-1+ fibroblasts differentiate into myofibroblasts with Rac1/ROCK- activated stress fibres that promote local tissue remodelling in GO (Mester et al., 2016). GO fibroblasts demonstrate

increased contractility in 3D cultures, pointing towards a more fibrotic phenotype than cells from healthy donors (He Li et al., 2014).

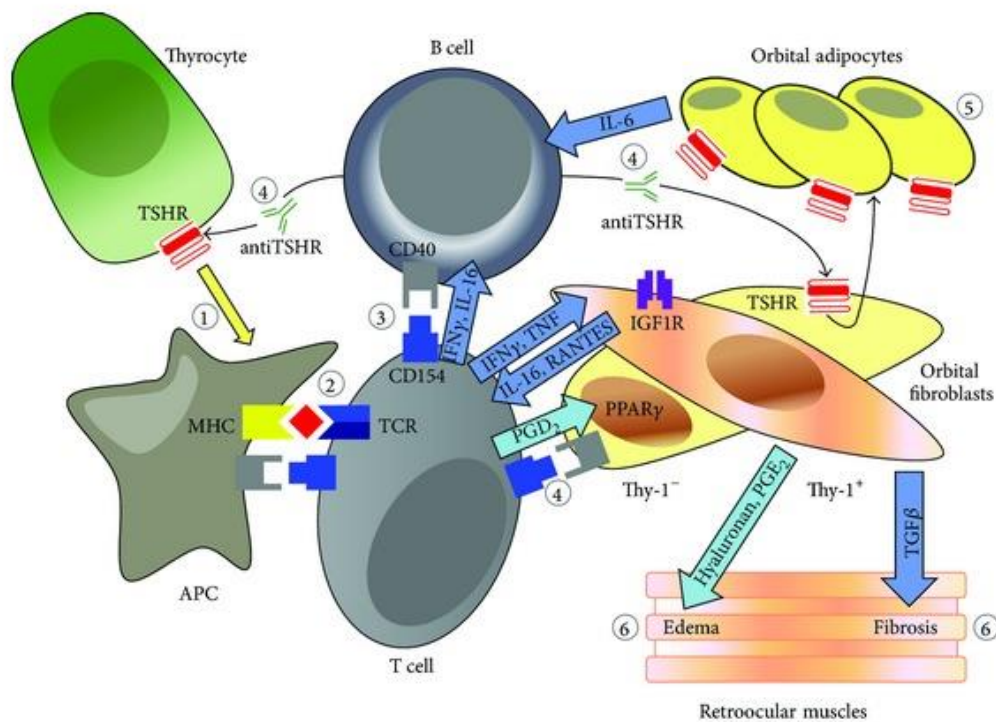


Figure 1. 10. Immunopathogenesis of GO, highlighting the role of counterplay in the orbit between adipocytes, orbital fibroblast, and immunocompetent cells . Przemyslaw Pawlowski et al. 2014

While not previously shown to act in orbital tissue fibrosis, mTORc1 has been implicated in pulmonary fibrosis where it could be subject to TGF-β mediated activation (Woodcock et al., 2019) and may particularly contribute to excessive collagen synthesis during fibrosis (Woodcock et al., 2015). Moreover, mTORc1 has been implicated in cell contractility in skeletal (Hornberger, 2011; Parkington, Siebert, LeBrasseur, & Fielding, 2003) and cardiac (Sciarretta, Volpe, & Sadoshima, 2014) myocytes. Excessive collagen sedimentation contributes to ECM remodelling (Herrera, Henke, & Bitterman, 2018), implicating mTORc1 in fibrosis progression.

1.4 Cellular mechanotransduction

1.4.1 Biological role of mechanotransduction

Mechanotransduction is the translation of external mechanical stimuli into intracellular biochemical and biological processes that can change gene expression, cell behaviour and differentiation (Ingber, 2006). The translation of the changes is mediated mainly by the actin with less pronounced input from microtubules and intermediate filaments. Increasing matrix stiffness leads to activation of integrin signalling and subsequent focal adhesion maturation, stress fibre formation and increased actomyosin contractility. External mechanical forces range from forces such as gravity and exercise-induced stresses on the skeletal muscle and bone to tissue-specific forces such as the shear stress of blood circulation across endothelium to the expansion and contraction of vessels from blood pressure, and to microscopic forces that occur when contracting cells exert pull on surrounding extracellular matrix (ECM) and on each other (Figure 11 A) (Salvi & DeMali, 2018b). In orbital fibroblasts, the main sensor component involved in mechanotransduction is the focal adhesions (FA) coupled to integrins, which in turn transfer the mechanistic change occurring in the ECM. FA are connected on the cytoplasmic face by the actin cytoskeleton and on the extracellular face by the ECM (Figure 11 B). An intracellular generated force leads to stress in the focal adhesion because an equal and opposite reactive force arises in the ECM. Studies demonstrate that when the ECM is soft cytoskeletal tension and stress at adhesions do

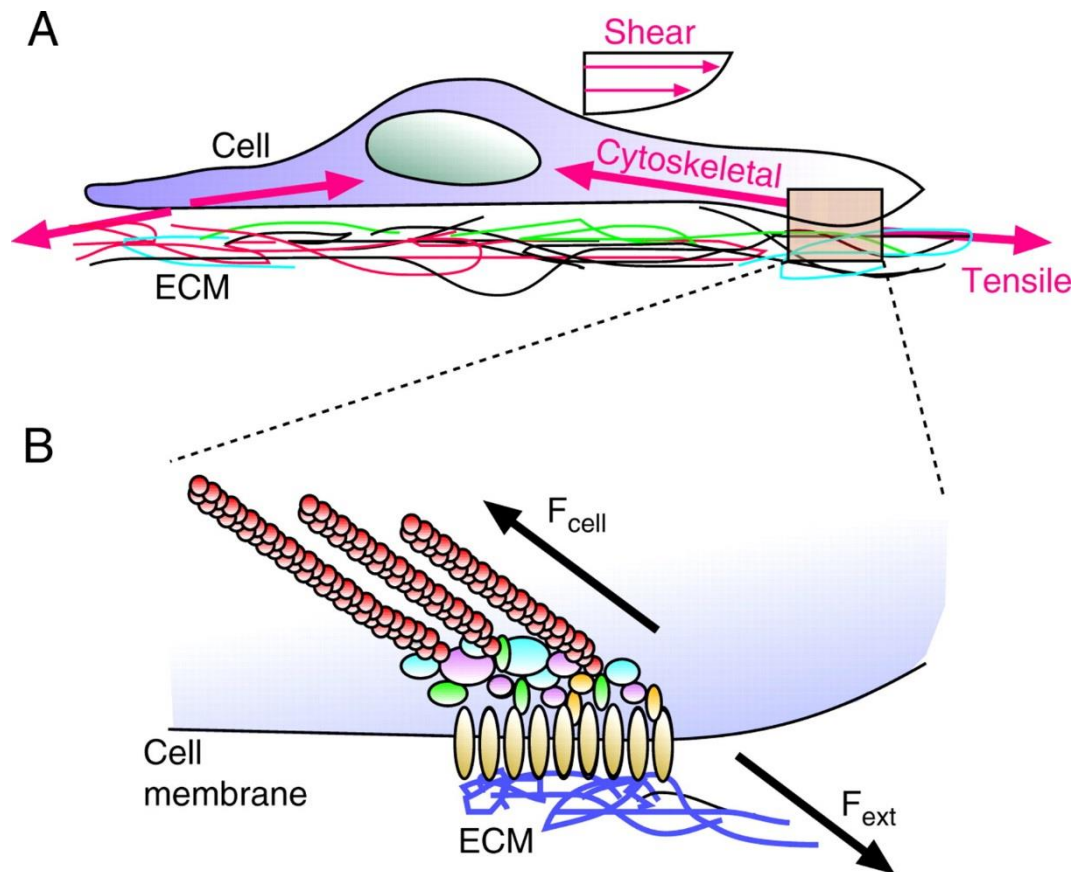


Figure 1. 11. Application of force to a cell.

A. Cells can be exposed to multiple types of forces, such as shear forces through fluid flow over the cell, tensile forces acting through the ECM, and cytoskeletally generated contractile forces. Depicted is a single cell attached to a complex ECM (illustrated as a multicolored fabric).

B. Close-up of a focal adhesion showing the balance of external and internal forces (F_{ext} and F_{cell} , respectively) in driving stress at a mechanosensor. Depicted are actin stress fibers (red) anchored into focal adhesions (multicolored array of proteins) that bind to the ECM (blue) through integrins (brown) (Chen, 2008).

not develop and focal adhesions fail to mature. Conversely, an increased force through the ECM results in stress at the focal adhesion only when the actin cytoskeleton provides an opposite traction force that balances the applied force (Albiges-Rizo, Destaing, Fourcade, Planus, & Block, 2009) . Atomic force microscopy (AFM) of fibroblasts cultured on collagen matrices with mechanical stiffness up to 40 kPa can internally balance out the substrate tension up to 20 kPa (Solon, Levental, Sengupta, Georges, & Janmey, 2007).

In the presence of strong adhesion against a substrate, actin filaments will form stress fibres that are tethered at the FAs. Some cell types that are grown on stiff substrates, such as plastic or glass, display thick stress fibres, whereas these structures are absent or very thin in the same cells grown on flexible substrates. Furthermore, both stress fibres and focal adhesions are aligned along a central cell axis when cells are grown on a stiff matrix, whereas, on a compliant, flexible matrix, focal adhesions are smaller and stress fibres are poorly aligned.

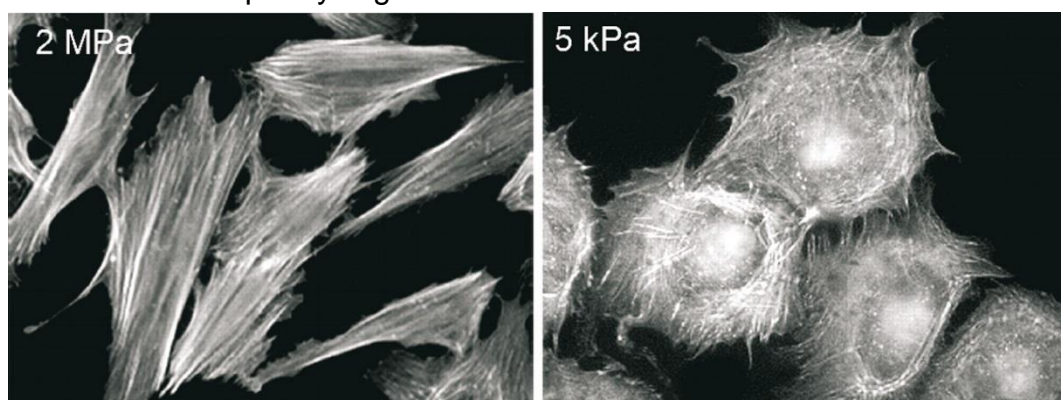


Figure 1.12. Effect of substrate stiffness on stress fibres. (Tojkander et al., 2012)

Stress fibres are more prominent in cells that are grown on rigid than on soft substrates (Figure 1.12). Shown are fibroblasts that have been plated on substrates with various stiffness that are made of poly(dimethylsiloxane). As shown in the picture on the left, cells grown on a stiff (2 MPa) substrate display thick and well-aligned stress fibres. By contrast, as shown in the right image, cells cultured on a compliant (5 kPa) substrate display thinner and poorly oriented stress fibres. Images are from (Prager-Khoutorsky et al., 2011).

Multiple protein-protein interactions have been defined at focal adhesions. Because most proteins have several potential interacting partners, this allows the cell an opportunity to construct various signalling complexes leading to diverse behaviours. Tyrosine phosphorylation is one of the key

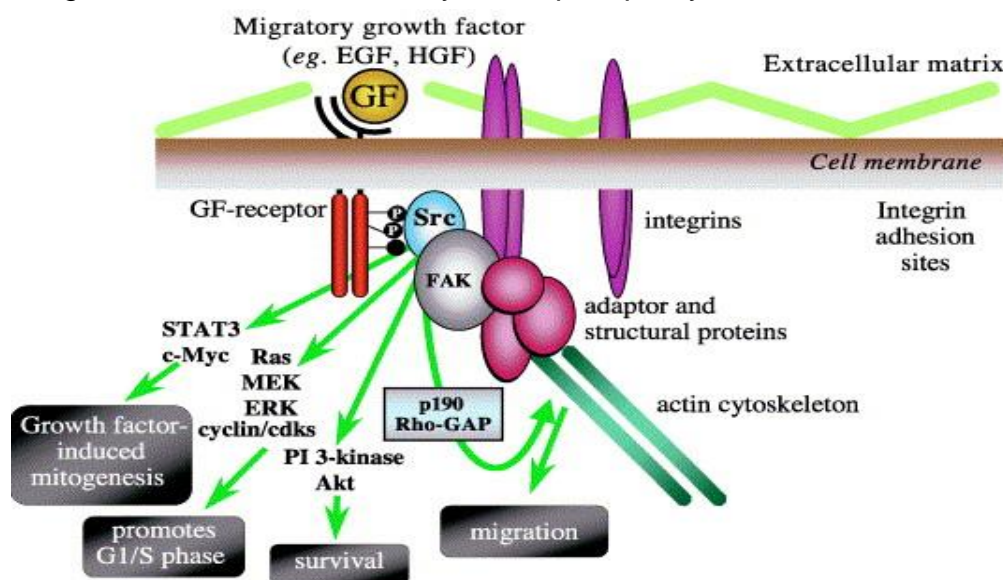


Figure 1. 13. Src and FAK co-localise at integrin adhesion sites in fibroblasts and cooperates with growth factor (GF) receptors, such as EGF and PDGF to induce signalling pathways that control diverse aspects of cell behaviour, including growth, survival and migration (Frame, 2002).

signalling events occurring at focal adhesions and involves recruitment of proteins such as FAK, vinculin, and paxillin to focal adhesions preceding significant tyrosine phosphorylation. This suggests that phosphorylation of these molecules and subsequent signalling occur primarily at focal complexes and adhesions. Tyrosine phosphorylation at the focal adhesion creates docking sites for the binding of Src homology domain 2-containing proteins (SH2) and regulates the subsequent activation of additional kinases and phosphatases. Two of the major kinases found in focal adhesions are Focal Adhesion Kinase (FAK) and Src, which bind to different partners to regulate focal adhesion dynamics and cell behaviour. To bind Src, FAK is autophosphorylated at Y397 which is thought to be triggered by the clustering of integrins attached to the ECM. Once this event occurs, Src phosphorylates FAK at additional phosphorylation sites to recruit other FA proteins.

Understanding how FAs are formed and mature in 3D cultures and on soft mechanical substrates is poorly understood. The limited evidence available shows that while fibroblasts form focal adhesions on the 3D cell-derived matrix, these adhesions differ from the focal adhesions formed by fibroblasts cultured on coverslips. Evidence suggests that in 3D and on flexible substrates FAs have diminished FAK active phosphorylation. The increased rigidity of the material causes the focal adhesions to resemble those observed in 2D cultures on rigid substrates (Cukierman, Pankov, 2001).

While in 2D it has been demonstrated that Src or related kinase recruitment is crucial to FA function (L. Li, Okura, & Imamoto, 2002), no such evidence is shown in regard to 3D cultures.

1.5 SRC family kinases; structure and function

Src and Src family protein kinases (SFK) participate in many cellular processes including apoptosis, cell proliferation, cell migration, cytoskeletal rearrangement, differentiation, development, the immune response, nervous system function, and transcription (Roskoski, 2015a). The Src protein-tyrosine kinases comprise a family of eleven related proteins that are divided into three groups (I–III) (Manning et al., 2002). The four closely related group I kinases include Fgr, Fyn, Src, and Yes; the four group II enzymes include Blk, Hck, Lck, and Lyn. Group III enzymes are distantly related to these two groups and include Brk, Frk, and Srm. Src, Fyn, and Yes are expressed in all cell types while Blk, Fgr, Hck, Lck, and Lyn are found primarily in hematopoietic cells (Roskoski, 2004). Of the group III enzymes, Srm is found in keratinocytes, and Frk occurs primarily in the bladder, brain, breast, colon, and lymphoid cells while Brk occurs mainly in the colon, prostate, and small intestine. Of these, fibroblasts express Src and Fyn, both shown to be required for adipogenesis in 3T3-L1 mouse fibroblasts (Y. Sun et al., 2005). Furthermore, adipogenesis in 3T3-L1 fibroblasts is decreased when treated with SFK inhibitors (He Li et al.,

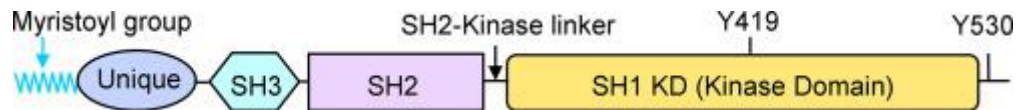


Figure 1. 14. Src protein-tyrosine kinase structure (Roskoski, 2004).

2014). Fyn has been implicated in pulmonary fibrosis where it is proposed to be over-activated in lung fibroblasts due to Thy1-mediated integrin coupling mechanism.

All SFK family members share a similar domain arrangement (Figure 1.14.) (Boggon & Eck, 2004), possessing an N-terminal unique region (50–70 residues) of high variability among the family members, but always encompassing a myristoylation and sometimes a palmitoylation site (Koegl, Zlatkine, Ley, Courtneidge, & Magee, 1994; Resh, 1999), followed by the ~ 50 amino acid Src homology 3 (SH3) domain which directs specific association with proline-rich motifs related to the PXXP consensus (Roskoski, 2004). Next is the ~ 100 amino acid Src homology 2 (SH2) domain, which provides interaction with phosphotyrosine motifs, with SFKs showing the highest affinity for the consensus sequence pYEEI (Koch, Anderson, Moran, Ellis, & Pawson, 1991). The last domain is the kinase (~ 300 residues), or Src homology 1 (SH1), responsible for the enzymatic activity. The activity and substrate targeting of the SFKs are highly regulated through both intra-molecular interactions of the SH3 and SH2 domains and by association with ancillary molecules including activators, inhibitors and substrates. These regulated intra-molecular associations involve several internal recognition motifs, one between the SH2 and kinase domains, which binds its own SH3 domain, and a C-terminal tyrosine that docks with

its own SH2 domain when phosphorylated. In addition, the SFKs possess the classical kinase activation loop (A-loop) with a tyrosine motif, which is phosphorylated in the most active forms (Roskoski, 2015).

The most important regulatory phosphorylation site in human Src is Tyr530. Under basal conditions in vivo, Src is phosphorylated at Tyr530 (Roskoski, 2004), which binds intramolecularly with the Src SH2 domain. SH2 and SH3 from other proteins and binding partners are able to destabilise the intramolecular association that reinforces the dormant form of the enzyme. Tyr530 phosphorylation results from the action of other protein-tyrosine kinases including Csk (carboxyterminal Src kinase) and Csk homologous kinase (Chk). Src undergoes intermolecular autophosphorylation catalyzed by another Src molecule at the activation segment Tyr419, which promotes Src to enter a fully active catalytic state (Figure 1.15).

There is little data available on phosphatases removing the active phosphorylation from SFKs. In recent years, phosphotyrosine phosphatase N22 (PTPN22, formerly known as Lyp) has garnered amounting interest due to its potential involvement in causing autoimmune conditions, including GO (Douroudis et al., 2008). Specific PTPN22 polymorphisms have been linked in an earlier and more frequent onset of GD (Fedetz et al., 2006). PTPN22 polymorphisms are thought to have particular importance; a transitional C-to-T mutation at position 1858 in an exon of the PTPN22 gene results in a single amino acid change of Arg to Trp at codon 620 in exon 14. This R620W amino acid substitution is located in a polyproline motif is thought to

weaken the association between SFKs and PTPN22, impairing the phosphatase ability to deactivate the kinases (Fiorillo et al., 2010).

SFK involvement in adipogenesis and adipogenic differentiation has had some controversy. SRC has been shown necessary in chemically-induced adipogenic differentiation in insulin-sensitive cells; both Src knock-down and chemical inhibition limit or block adipogenesis in 3T3-L1 preadipocytes (Y. Sun et al., 2005). Deficiency of SFKs blocked adipogenesis in subdermal human fibroblast cells. Others report that the inhibition of SFKs by several inhibitors or by exogenous expression of CSK, the differentiation adipocytes and the with SRC expression levels gradually decreasing (Usui, Uno, &

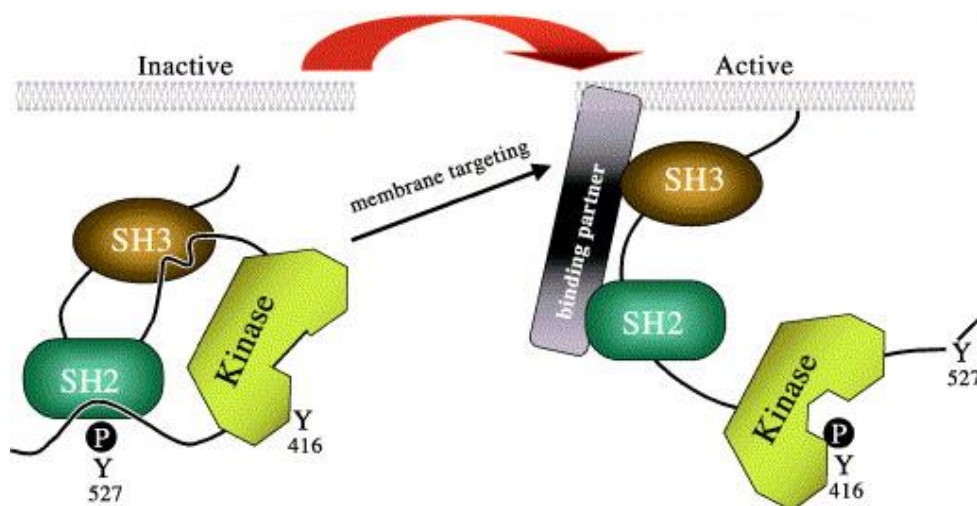


Figure 1. 15. General structural schematic of the Src family kinases in their inactive and active configurations.

Left, the inactive configuration showing the SH2 domain interacting with the phosphorylated C-terminal tyrosine (pY527), the SH3 domain interacting with the SH2-kinase connector which forms a left-handed polyproline type II helix, and the dephosphorylated activation loop (Y416) folded back over the substrate binding site. Right, the active configuration, showing SH2 and SH3 domains released from the intramolecular interactions and available for binding to substrates and regulatory molecules, the C-terminal tyrosine is dephosphorylated (Y527), and the activation loop is phosphorylated (pY416) and is folded away from the substrate binding site and allows the two kinase lobes (N and C) to form a kinase competent catalytic cleft (Boggon and Eck, 2004).

Nishida, 2016). Published results by the Bailly group show that GO orbital fibroblasts are less adipogenic when treated with PP2; when cultured in 3D orbital fibroblasts from GO patients spontaneously generate more lipid droplets than their healthy counterparts (He Li et al., 2014). Mechanistically, it has been shown that disordered actin cytoskeleton dynamics impair FAK/Src and PI3K/AKT signalling, leading to impaired adipogenic differentiation (Caron-Lormier & Berry, 2005).

SFK Fyn has been shown a dual role in regulating both fibrosis and adipogenesis in vitro and animal models. FYN knock-down and inhibition has been shown to decrease the kidney and pulmonary fibrosis (Fiore et al., 2015a; Seo et al., 2016). FYN has been shown to promote adipogenesis through PPAR γ and block lipid break-down, and autophagy by limiting AMP-activated kinase (AMPK) activity (Yamada et al., 2016). Another publication shows that downregulation of FYN caused increased lipid breakdown via AMPK activation in mice, implying that FYN blocks AMPK activity through negative phosphorylation of its activator liver kinase B1 (LKB1) (Woeller et al., 2015).

AMPK is an evolutionarily conserved energy-sensing kinase that is activated by metabolic stress or ATP consumption and that globally promotes catabolic processes (Hardie, 2014). In accordance with that, AMPK could also be linked to the regulation of autophagy (Figure 1.16). It has been suggested that a variety of other non-starvation-related autophagy-inducing stimuli primarily act through the activation of AMPK even under normal energy levels, including mechanotransduction AMPK

has been shown to modulate ECM-integrin attachment in migrating cells, promoting ATP production at the leading edge while facilitating mature FA dismantling at the cell periphery (Salvi & DeMali, 2018a). AMPK is also required for the reorganization of the actin cytoskeleton that supports monocyte adhesion to adhere to endothelial cells. In non-migratory cells, loss of AMPK increases cell adhesion, FA maturation and mechanotransduction (Chang, Huang, Ho, Huang, & Lin, 2012).

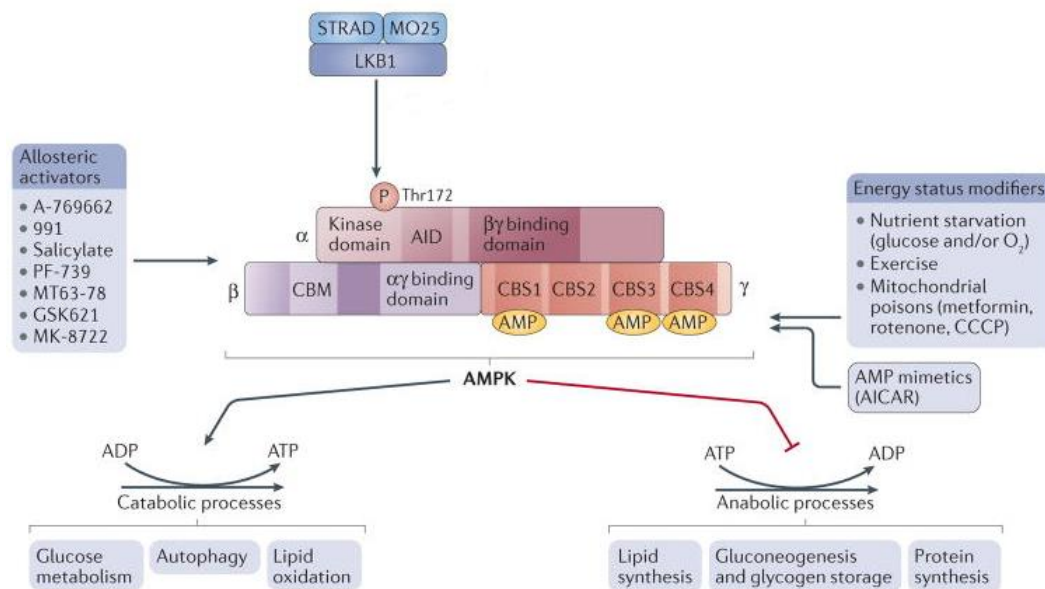


Figure 1. 16. AMPK structure and activation

Domain structure of the AMP-activated protein kinase (AMPK) trimer, showing the α-, β- and γ-subunits with their respective domains. The upstream kinase liver kinase B1 (LKB1) is shown above the AMPK complex. Several factors lead to AMPK activation, such as mitochondrial poisons and oxygen or glucose starvation, as well as exercise. Drugs that activate AMPK include the AMP mimetic AICAR and several small-molecule allosteric activators (listed on the left-hand side). The effect of AMPK activation is to rewire metabolism to decrease anabolic processes (that is, ATP consumption) and increase catabolism (that is, ATP production) to restore a more favourable energy balance by limiting lipid, protein and carbohydrate synthesis and increasing consumption of glucose and fats. AMPK also may activate autophagy by activating UDP-linked kinase 1 (ULK1) and inhibiting mTORC1 (not shown)(Herzig and Shaw, 2017).

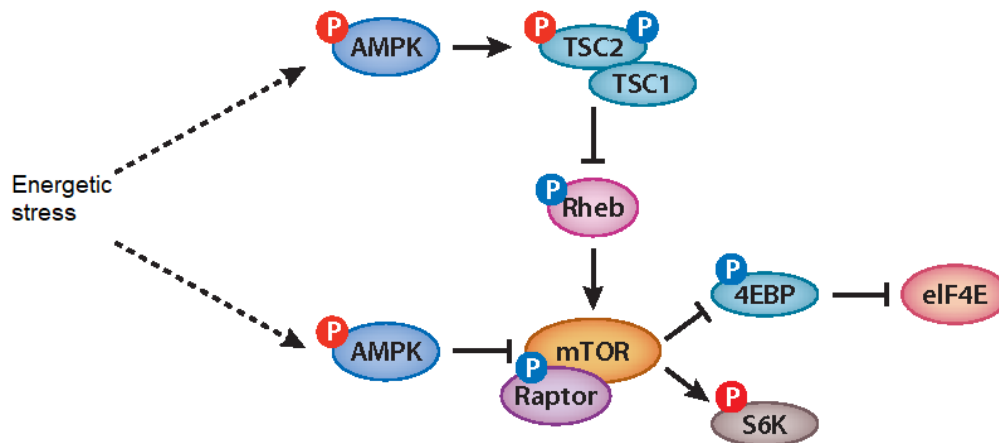


Figure 1. 17. AMPK inhibits mTORC1.

AMP-activated protein kinase (AMPK) inhibits the pathway of the mammalian target of rapamycin complex 1 (mTORC1) in multiple fashions. AMPK can phosphorylate tuberculous sclerosis complex 1/2 (TSC1/2) that blocks the mTORC1 complex assembly by phosphorylating Rheb and by directly blocking mTORC1 activity. Active TORC1 phosphorylate S6K, activating protein synthesis and blocks the activity of translation-inhibiting protein 4EBP (Dunlop & Tee, 2013).

The activation of AMPK inhibits mTOR activity (Figure 1.17) (Dunlop & Tee, 2013). Mammalian target of rapamycin (mTOR) is an evolutionarily conserved serine/threonine-protein kinase that regulates multiple cellular processes such as growth, cell cycle, cell survival, and autophagy. mTOR forms two functional complexes, mTORC1 and mTORC2 (Saxton & Sabatini, 2017). mTORC1 is directly regulated by cellular energy and nutrient status, whereas mTORC2 is not. mTORC1 plays essential roles in the regulation of translation and autophagy and is sensitive to inhibition by rapamycin. mTORC1 activity is promoted by Akt, which in turn is activated by SRC phosphorylation. Inhibition or downregulation of SRC has been shown to disrupt Akt/mTORC1 signalling (Vojtěchová et al., 2008). In the absence of active AMPK, mTORC1 suppresses autophagy. Cellular stress,

low levels of ATP and lack of nutrients activate AMPK, which suppresses mTORC1 (Dunlop & Tee, 2013).

1.6 Cellular senescence in orbital fibroblasts

Under normal conditions cell grow and multiply in a cyclic and tightly regulated manner, the cell cycle. This process is defined by two major phase. DNA duplication occurs during the synthesis (S) phase after which chromosomes segregate and the cells divide during mitosis or M phase. Most cells require much more time to grow and double their mass of proteins and organelles than they require to replicate their DNA and divide. Partly to allow more time for growth, extra gap phases are inserted in most cell cycles—a G1 phase between M phase and S phase and a G2 phase between S phase and mitosis. Thus, the eucaryotic cell cycle is traditionally divided into four sequential phases: G1, S, G2, and M. G1, S, and G2 together are called interphase. In a typical human cell proliferating in culture, interphase might occupy 23 hours of a 24 hour cycle, with 1 hour for M

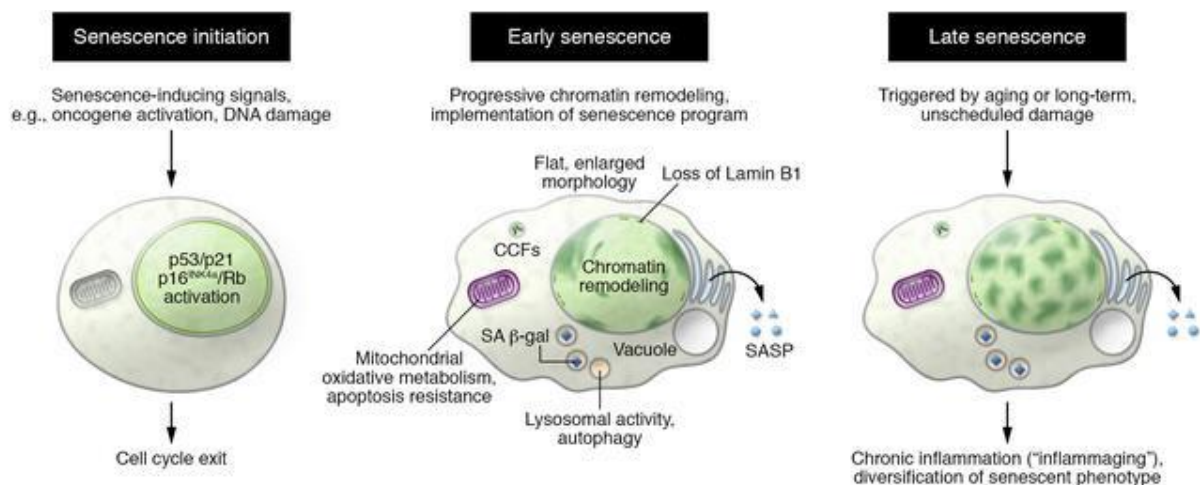


Figure 1. 18. Phenotypic alterations associated with senescence initiation, early senescence, and late phases of senescence (Herranz and Gil, 2018).

phase. Gap phases also provide time for the cell to monitor the internal and external environment to ensure that conditions are suitable and preparations are complete before the cell commits itself to the major upheavals of S phase and mitosis (Molecular Biology of the Cell, 2002.).

Replicative senescence is a highly stable cell cycle arrest occurring in response to different stresses and considered to be irreversible. By forcing a growth arrest, senescence limits the replication of old or damaged cells but also is seen as a major contributor to whole-body ageing. Apart from halting the cell cycle, senescent cells undergo other phenotypic changes such as metabolic reprogramming, chromatin rearrangement, and autophagy modulation. Senescent cells synthesise and excrete a complex combination of factors, collectively referred to as the senescence-associated secretory phenotype (SASP), that alters neighbouring cell behaviour in a paracrine fashion (McHugh & Gil, 2018). Senescence is seen as a stress response that can be induced by a variety of intrinsic and extrinsic signals, including oncogenic activation, oxidative and genotoxic stress, mitochondrial dysfunction, irradiation, or chemotherapeutic agents. Senescent cells undergo morphology changes, chromatin remodelling, and metabolic reprogramming, and secrete a complex mix of mostly proinflammatory factors. The accumulation of senescent cells also drives ageing and age-related diseases, and selectively killing senescent cells significantly improves the healthspan of mice in the context of normal ageing and ameliorates the consequences of age-related disease or cancer therapy. Initial senescence-inducing signals are enough to initiate cell cycle

arrest (Figure 1.17). Then senescent cells gradually remodel their chromatin and start to implement other aspects of the senescence, such as the SASP, to enter into the next step of full senescence. If these senescent cells are not removed by immune clearance, they continue progressing and enter into the third stage or “late senescence,” which can involve adaptation and diversification of the senescent phenotype causing localised inflammation, immune cell recruitment, oncogenic changes in the surrounding tissue but also beneficial effects like fibrosis resolution, and accelerated wound healing (Figure 1.18).

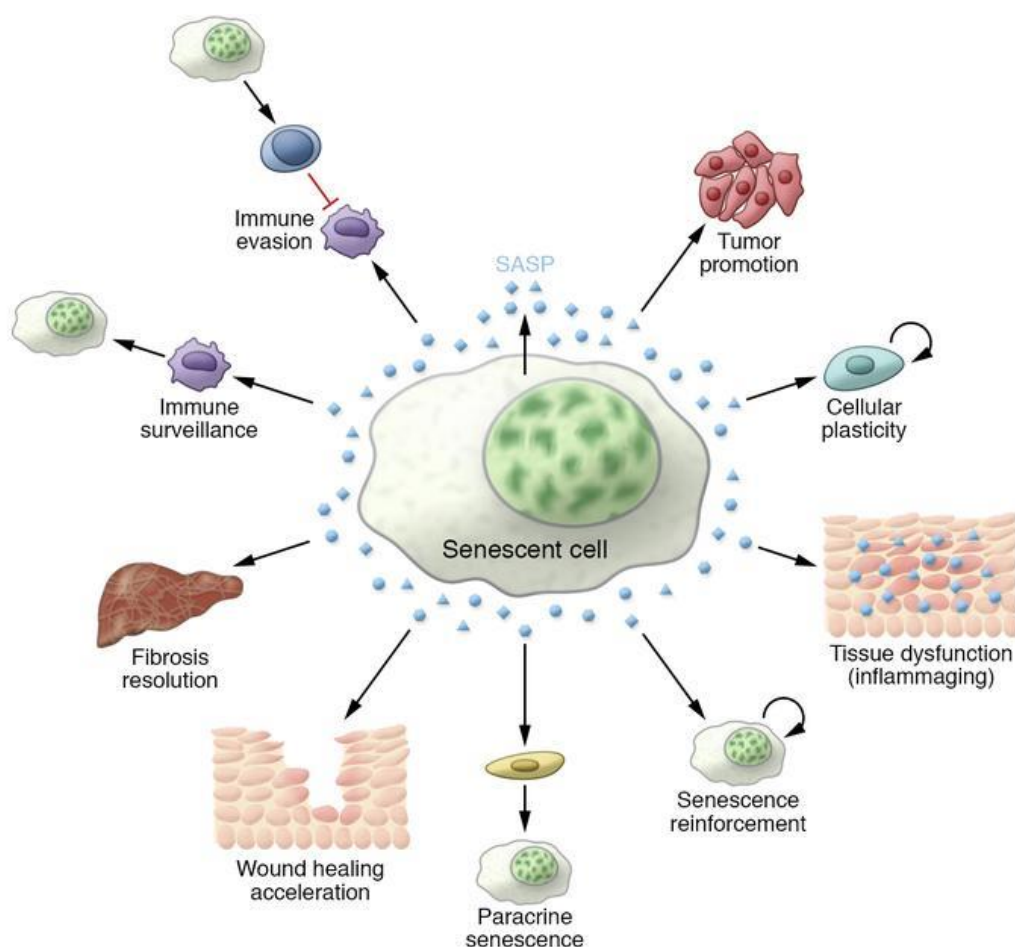


Figure 1. 19. Functions of SASP. (Herranz and Gil, 2018)

The most known senescence marker is senescence-associated β -galactosidase (SA β -gal) activity. This enzymatic activity, which is frequently found in normal cells under physiological conditions (pH 4.0–4.5), is significantly amplified in senescent cells as a result of increased lysosomal content (Childs, Baker, Kirkland, Campisi, & Deursen, 2014). Because of this, histochemical assessment of β -gal activity is possible at pH 6.0 and allows specific identification of senescent cells (Piechota et al., 2016). Since SA β -gal activity is detectable in most senescent settings, it is considered a *de facto* hallmark of senescence.

Recent data identified mTORC1 to promote the SASP and puts it in the centre of pro-senescence signalling. mTORC1 actively suppresses autophagy by phosphorylating ULK1 and, accordingly, inhibition of mTORC1 induces autophagy. Senescent human fibroblasts induced by stress, replicative exhaustion, or oncogene activation, show constitutive mTORC1 activation, which is resistant to serum and amino acid starvation (Antonioli, Torres, Ferretti, de Azevedo PIFinato, & Sertie, 2019; Weichhart, 2018). Cells unable to undergo autophagy cannot clear out cellular debris and are likelier to enter senescence (Kang, Lee, Kim, Choi, & Park, 2011). AMPK is shown to be inactivated in senescent cells, and while its activation protects cells from becoming senescent. Contrary to the established view that senescence is irreversible, senescence can be alleviated by activating AMPK in murine MSCs (Zhan et al., 2018a).

Senescent cells are also shown to reduce cell sensitivity to mechanistic cues (Moujaber et al., 2019). The onset of SASP and release of

proinflammatory cytokines have important consequences for tissue mechanical properties, with remodelling resulting from a combination of immune system activation and the expression of ECM-modifying enzymes such as MMPs (Ruiz-Ojeda, Méndez-Gutiérrez, Aguilera, & Plaza-Díaz, 2019). A recent publication shows that the onset of senescence can be delayed in vitro if cells are cultured on mechanistically softer substrates by promoting a proliferating, adipogenic-like phenotype (Kureel et al., 2019).

1.7 Aims and objectives

Despite a growing understanding of GO disease mechanisms and progression, the current therapies to alleviate symptoms and pathological consequences of the disease scarce. Our earlier research shows that adipogenesis occurs in orbital fibroblasts when cultured in 3D collagen matrices, indicating a new possible mechanism of lipid droplet production in orbital fibroblasts. In this 3D model GO orbital fibroblasts demonstrate not only spontaneous lipid droplet production but also higher contractility than their healthy counterparts. Both of these processes are reduced by PP2, an SFK inhibitor. After analysing available literature and publications, I selected two candidates of SFK: Src is shown to be required for lipid accumulation, and Fyn plays a role in the onset of lung fibrosis while both kinases are implicated in mechanotransduction. The aim of my work is to determine the role of SFK in spontaneous adipogenesis and contractility in GO and investigate associated downstream pathways of these kinases.

Firstly, published data by the Bailly group suggests that non-specific inhibition of SFKs reduces lipid droplet production in 3D-cultured orbital fibroblasts. I will perform separate Src and Fyn siRNA interference experiments to determine if kinases individually affect lipid droplet production. I will also assess the activity of downstream associated pathways (AMPK, mTORc1) and their dependency on Src/Fyn activity.

Secondly, we have shown that spontaneous lipid droplet production occurs in 3D cultures but have previously discounted the mechanical stiffness of collagen matrices and the effect of this parameter on lipid droplet

production. I will assess if lipid droplet production depends on substrate stiffness by using commercially available stiffness models and our own rigidity assays.

Lastly, during my experiments assessing lipid droplet dependency on substrate stiffness, I observed that orbital fibroblasts proliferate faster on soft substrates. I will investigate whether slowed growth on rigid substrates can be attributed to cellular senescence by performing β -galactosidase staining in cultures grown on substrates with different rigidity. I will also assess the senescence marker presence.

CHAPTER 2 MATERIALS AND METHODS

Orbital Soft Tissue

Orbital fat tissue was harvested from patients undergoing orbital decompression surgery from disease and non-disease related surgeries. Informed consent was obtained prior to patient enrolment into the study, approved by the Ethics Committee was granted under the National Research Ethics Service Committee London Bentham (Table 2. 1).

Tenon (HTF) and conjunctival (HCF) fibroblasts were obtained from deceased donors at the Moorfields Eye Hospital under the approved ethics.

Table 2. 1 Orbital fibroblast donor information

Cell line (HO as disease, CO as control)	Age	Gender	Surgical procedure	Tissue source	Disease duration (months)	Cell passages used
HO6	58	F	Orbital decompression	Deep orbit	9	p. 3 to 9
HO8	62	F	Orbital decompression	Deep orbit	28	p. 5 to 9
HO9	54	M	Orbital decompression	Deep orbit	9	p. 5 to 9
HO11	57	F	Orbital decompression	Deep orbit		p. 5 to 9
CO7	33	M	Lacrimal Gland exploration	Deep orbit	n/a	p. 3 to 9
CO12	78	M	Fat prolapse excision	Deep orbit	n/a	p. 4 to 9
CO13	56	M	Fat prolapse excision	Deep orbit	n/a	p. 6 to 9
CO14	65	M	Fat prolapse excision	Deep orbit	n/a	p. 4 to 9

Fibroblast Expansion

Samples from orbital decompression surgery and control samples were used for orbital fibroblasts expansion. The explants were placed in 32 mm tissue culture plates after being dissected and digested in 0.05% collagenase D in PBS under 37°C for 10 -15 minutes. Coverslips were placed on top of the tissue fragments to weight them down and to prevent

floating. Cells were then cultured in Dulbecco's Modified Eagle's Medium (DMEM)(Gibco, Thermofisher Scientific, USA) supplemented with 10% (v/v) heat-shock inactivated foetal calf serum (FBS, Sigma-Aldrich, UK), 100 IU/mL penicillin and 100 µg/mL streptomycin until 90% confluence and then passaged into a T25 tissue culture flask (Corning, NY, USA). Contaminating epithelial and goblet cells were eliminated from the cell tissue culture after the first or second passage. A frozen stock was kept in liquid nitrogen in 10% v/v DMSO in FBS.

Primary cell culture

Cells were defrosted in a warm water bath for 5 min at 37°C and maintained in complete DMEM supplemented as described previously and incubated at 37°C and 5% CO₂ in T75 tissue culture flasks with a medium change after 2 days of defrosting to remove residual DMSO. Medium for each flask was changed weekly. Cultures were assessed for typical fibroblast morphology by phase-contrast microscopy before every experiment. The cells were passaged 1:3 when confluent with trypsin-EDTA detachment (Gibco, Life Technologies, UK).

Three-dimensional (3D) cell culture

3D collagen gel culture environment was established by embedding cells in rat tail collagen type 1 matrix (First Link Ltd., Birmingham, UK) at a final concentration of 1.5 mg/mL. Typically, triplicates gels were made of 600 µL of rat tail collagen, 96 µL of concentrated medium mix (from 700 µL 10x DMEM (Sigma-Aldrich, UK), 70 µL L-glutamine, and 180 µL NaHCO₃

(Gibco, Life Technologies, UK)], titrated with about 56-59 μL of 1M NaOH to reach neutral pH assessed by indicator colour shift from yellow to pink. Cells were counted using a hemocytometer; 5×10^4 cells were aliquoted, centrifuged at 14000 rpm for 5 min; DMEM aspirated and cells resuspended in 60 μL FCS. After reaching neutral pH, cells were added to the collagen mix and briefly mixed by swirling. 150 μL of collagen mix was cast onto MatTek microwell glass dishes (MatTek Corporation, MA, USA), left to coagulate for 10 – 20 min with Complete DMEM added.

3D Cell Contractility Assay

Gels were made in MatTek dishes for contraction assay the same way as described previously. Orbital fibroblasts at a concentration of 0.5×10^5 cells/mL were cast onto MatTek glass microwell plates. The detached gels within the dish microwells were photographed daily for 5 days. Gel area and microwell area in each photo were measured with ImageJ software, and the ratio (gel area vs well area) was calculated to obtain the percentage of contraction. The daily contraction rate expressed in percentage was calculated as $100\% \times (1 - \text{ratio of gel area to microwell area})$ for 1 meaning the equal size of gel area and microwell area at the time when gels were made.

Cell Mechanotransduction Assays

On collagen gels

Rat tail collagen mix was prepared as previously described, and a volume of 210 μL was cast in a 24 well plate to polymerise for 20 min. 1×10^5

cells/mL were cast on top of the gels after polymerization and incubated at 37°C and 5% CO₂ for 3 days.

On Cytosoft® and Matrigen Softwell® plate wells

CytoSoft® and Matrigen Softwell® elastic modulus 6-well (Cytosoft, USA) and 24-well (Softwell, USA) plates are used to culture cells on substrates with various defined rigidities covering a physiological range of 0.2 kPa- 64 kPa. The bottom of each well of plates is covered with biocompatible silicone (CytosoftO or polyacrylamide (Softwell), with a pre-determined and certified elastic modulus (rigidity). The surfaces of the gels were coated with soluble collagen diluted in 1x DPBS (1:20, vol/vol, 0.1 mg/mL) and left in the dark at room temperature for 30 mins, washed 3 times with DPBS and covered in complete DMEM for additional 10 minutes. Each well was seeded with 3 mL of 1×10^5 cells/ml and incubated at 37°C and 5% CO₂ for 3 - 5 days.

On PAA/bisAA-coated coverslips

Protocol adapted from Vitiello, E. et al., 2019. 13 mm and 22 mm circular glass coverslips (Corning, USA) were de-dusted (Fellowes Air Dust Remover, Fellowes, UK) with air and burned in a Bunsen burner flame for 3 sec and left to cool for 10 minutes at room temperature. 13 mm coverslips were covered with bind-silane (Merck, USA) for 3 minutes and washed with ethanol, dried and stored in a Petri dish for later use. 22 mm coverslips were inverted onto a drop of protein coating (0.1 mg/mL soluble or fibrillar collagen, or fibronectin (Sigma Aldrich, UK)) and left in room temperature for 30 min.

After incubation, 22mm coverslips were inverted and washed briefly with PBS.

Table 2. 2 Reagent volumes for E moduli used

E moduli \pm SD (kPa)	40% PAA (mL)	2% bis-AA (mL)	ddPBS / ddH₂O (mL)
40.40 \pm 2.39	2	2.4	5.6
1.00 \pm 0.31	1.25	0.15	8.6

Polyacrylamide (PAA) and bis-acrylamide (bisAA) (Sigma Aldrich, UK) solutions were mixed in a pre-calculated ratio determined post-coating rigidity (Table 2). 1 μ L N,N,N',N'-tetramethylethylenediamine (TEMED, Sigma) and 6 μ L 10% APS (Sigma) was added to PAA/bis-PAA mixes to prior polymerisation, and 25 μ L drop of activated mix was added on each coated 22 mm coverslips. Quickly, silanized 13 mm were added on top of the drops, and gels were let to polymerise for 30 min. After polymerisation, sandwiches were soaked in sterile H₂O for 10 min, and then the gels attached to the top coverslips were detached from the bottom coverslips using a scalpel blade. Gels bound to coverslips were stored at 4° C in sterile H₂O containing 150 mM NaCl and 10 mM Hepes and incubated in culture medium for 30 min at 37° C prior to cell seeding.

Oil-Red-O staining

After 7 days of culture in 3D gel, the medium was removed from wells followed by PBS rinse and 20 minutes of 10% formaldehyde (Sigma-Aldrich, UK) in PBS for fixation. Gels were then detached and washed in distilled water. After 5 minutes of incubation in 60% isopropanol, gels were stained for 2 minutes with freshly filtered Oil-Red-O (ORO) [working solution made

of 3:2 vol/vol dilution of ORO stock (3 mg/mL in 99% isopropanol) and distilled water]. The following rinse with water, gels were then counterstained with hematoxylin (Gill No. 3, Sigma-Aldrich, UK) for 30 seconds, followed by several long washings. Gels were topped with a 50% glycerol in TBS mixture before observing and imaging. The ORO staining was quantified by counting ORO positive cells directly under the microscope (Leica DMIL 20x objective). ORO positive cells were counted as having red-stained lipid droplets within the cytoplasm, regardless of the amounts of lipid droplets within each cell.

At least 100 cells were evaluated randomly from 4~5 fields in each gel. Cell counts were assessed as the number for Oil-Red-O positive cells per all cells counted.

Table 2. 3 siRNAs used in knock-down experiments

Target siRNA (5 nmol)	Sequences (siGENOME SmartPool)
siSRC	CCAAGGGCCUCAACGUGAA CCUCAGGCAUGGCGUACGU CGUCCAAGCCGCAGACUCA GAGAACCUGGUGUGCAAAG
siFYN	CGGAUUGGCCCGAUUGAUA GGACUCAUAUGCAAGAUUG GAAGCCCGCUCCUUGACAA GGAGAGACAGGUUACAUUC
siCSK	GGCCUCCGCCUGGGUCAUG GCCUGUGGGCACUGAACCU GUGGCGGCCAGGAUGAGU GACGGCAUCAUCCAGCCA
siPTPN22	CCCUCCACAUCCUGUACGG UACUCUGUAGCCAACAUC AACACGGACCAAUAACU ACCUCCUCUCCAGAAAGAA

siRNA knock-down

Patient and control fibroblasts were trypsinised, and 8×10^4 cells were precast in 6-well plates 24h prior to administering the siRNA. 280 ng of FYN,

SRC, CSK, PTPN22 and Control Pool siRNA (Table 2. 3) (Dharmacon, LifeSciences, USA). 0.8 uL of each siRNA were incubated in 100 uL of serum-free DMEM with 12 uL HiPerFect (Qiagen, USA) transfection reagent for 5 – 10 min, added to the pre-cast cells and incubated at standard conditions for 72h. siRNAs previously unused by the Bailly group had their minimum effective experimental amount assessed to minimise off-target silencing effects. Due to DNA sequence similarities between Src and Fyn kinases, separate Src and Fyn knock-downs were assessed for both kinases; no off-target WB band reduction was observed. Knock-down efficiency was assessed with Western Blot.

Cell lysate preparation and Western Blotting

Protein extraction

For 2D monolayer culture, cells were trypsinised and cell suspension diluted of PBS to limit the medium protein content in the cell suspension. Cells were centrifuged for 5 min at 1400 rpm and the supernatant aspirated. Then the pellet was resuspended in 120 uL RIPA lysis buffer (150 mM NaCl, 0.1% Triton X-100, 0.1% sodium dodecyl sulphate, 50 mM Tris-HCl pH8.0, 0.5% sodium deoxycholate, protease and phosphatase inhibitors). For 3D collagen gel culture, gels were detached and then digested with 0.05% collagenase-D until completely liquified. Digested gel solution was centrifuged to pellet the cells and pellet were resuspended in RIPA lysis buffer on ice for 5 min. The lysate was centrifuged for 10 min at 1400 rpm.

The supernatant was aliquoted to a new tube and the pellet discarded. After the sample concentration was measured using a BSA assay (ThermoFisher Scientific, UK), each sample was diluted with an equal volume of 2x Tris-Bis Sample Buffer (ThermoFisher Scientific, UK) and denatured at 95°C for 5 mins. Samples were stored at -20°C

Western blot

5 µg of samples were loaded and electrophoresed on 4~12% precast polyacrylamide gels (Novex Bolt™, Invitrogen, Thermo, UK) using SDS-PAGE. Proteins were transferred to PVDF membranes (Thermo, UK), and then membranes were blocked for 1 hour at room temperature in 5% BSA, washed 3 times and probed overnight in 5% BSA or 5% NFDM with a primary antibody (Table 2. 4). Membranes were washed with TBS-T the next day before 1-hour incubation of secondary antibody (Peroxidase-AffiniPure goat anti-mouse or anti-rabbit IgG (H+L), Jackson ImmunoResearch, PA, USA) at room temperature. After another wash with TBS-T, membranes were developed using ECL (ECL PLUS Substrate (Pierce, Thermo, UK) for PPARγ; ECL (Pierce, Thermo, UK) for GAPDH), X-ray film (Fujifilm, Japan) exposure in darkroom and X-ray film developer. For loading control, membranes were washed, stripped with stripping buffer (Thermo Scientific, UK), blocked with 5% milk, and then reprobed with rabbit anti-GAPDH at 1:3000 in 5% milk and secondary antibody (Peroxidase-AffiniPure goat anti-rabbit IgG (H+L), Jackson ImmunoResearch, PA, USA). Films were scanned and analyzed using ImageJ software. Band intensities were normalized to GAPDH.

Table 2. 4 Antibodies used in WB and IF experiments

Antibody	Country of Origin	Host	Method used, dilution (vol/vol)
Anti-AMPK	Cell Signalling, USA	Rabbit	WB (1:1000), IF (1:100)
Anti-CSK	AbCam, USA	Goat	WB (1:1000)
Anti-FYN	BioLegend, USA	Mouse	WB (1:1000)
Anti-GAPDH (loading control)	AbCam, USA	Rabbit	WB (1:3000)
Anti-mTOR	Cell Signalling, USA	Rabbit	WB (1:1000)
Anti-PLIN2	ProteinTech, USA	Rabbit	WB (1:1000), IF (1:100)
Anti-pS73 ACC	Cell Signalling, USA	Rabbit	WB (1:1000)
Anti-pT172 AMPK	Cell Signalling, USA	Rabbit	WB (1:1000), IF (1:100)
Anti-PTPN22	Novus Biologicals, USA	Goat	WB (1:1000),
Anti-pY418 SRC	Invitrogen, USA	Rabbit	WB (1:1000), IF (1:100)
Anti-pY530 Fyn	BioLegend, USA	Rabbit	WB (1:1000)
Anti-SRC	Cell Signalling, USA	Mouse	WB (1:1000), IF (1:100)
Anti-p16INKA	R&D Systems, USA	Goat	WB (1:1000), IF (1:100)
Anti-CathepsinD	AbCam, USA	Goat	IF (1:100)

Immunofluorescence

Coverslips (diameter 13 mm) were prepared by acid washing with 1 M HCl for 3-5 minutes, PBS rinse, 70% ethanol for 1-2 minutes, and PBS rinse before seeding cells overnight. For collagen gel imaging, cells were seeded on gels for 5 days. Cells were fixed with 3.7 % formaldehyde in PBS for 7 min , followed by 0.5 % Triton-X 100 (Sigma-Aldrich, UK) permeabilization for 20 min and 0.1 M Glycine (Sigma-Aldrich, UK) wash for 10 min. After rinse in 1 % BSA in TBS pH 8.0 for 5 min, coverslips were transferred to a humidified dark chamber and plates wrapped in foil where they were blocked and stained with F-actin by Rhodamine-phalloidin (1:20 dilution, Invitrogen, UK) in TBS-1 % BSA-1 % fetal calf serum (FCS) for 20 min at room temperature. The phalloidin/block was removed and replaced with primary antibody (Table 2. 4). After washing, secondary antibody (Alexa Fluor 488-Conjugated AffiniPure anti-Rabbit or Anti-Mouse IgG; Jackson

Immunoresearch Laboratories, PA, USA) at a dilution of 1:50 was used for 1-hour incubation at room temperature followed by 3 washings. Coverslips were later mounted on slides with Fluoroshield mounting medium with DAPI (Abcam, UK). Gels were aspirated, placed on glass slides and covered with a 22x22 coverslip with DAPI, and subsequently sealed. Images were taken by Nikon Eclipse Ti microscope with NIS elements software with 10x Plan Fluor 0.30 objective or with or with Zeiss 710 confocal microscope, 40x or 63x water immersion objectives and Zeiss Zen Black software.

LD540 lipid droplet staining

LD540 is a fluorescent, BODIPY-derived lipid stain with the excitation maximum at 514 nm (Spandl, White, Peychl, & Thiele, 2009). For fluorescence imaging, cells on coverslips and gels were seeded, cultured, fixed and permeabilized as mentioned before. LD540 was diluted in PBS (1:8000 vol/vol) and incubated on cells for 20 min, followed by 3 washes with PBS. Coverslips and gels were mounted on glass slides as before, imaged with Zeiss 710 confocal microscope using 40x and 63x water immersion objectives and Zeiss Zen Black software.

Senescence-associated β -galactose activity assay

SA β -galactosidase activity assay was performed with Senescence Cells Histochemical Staining Kit (CS30010, Sigma Aldrich, UK). Cells had the growth medium aspirated and were washed 3 times with PBS and fixed with a fixation buffer (20% formaldehyde, 2% glutaraldehyde, 70.4 mM Na_2HPO_4 , 14.7 mM KH_2PO_4 , 1.37 M NaCl, and 26.8 mM KCl). After fixation, cells were

washed 3 times with PBS and incubated overnight with the staining solution (400 mM Potassium Ferricyanide, 400 mM Potassium Ferrocyanide, 40 mg/mL X-gal solution and Mili Q water) at 37°C without CO₂ enrichment. Cells were imaged with phase-contrast microscopy (Leica DMIL 20x objective). Total and β -gal-positive cells were counted, and each field of view imaged. The total amount of β -gal signal was assessed with ImageJ.

Quantitative PCR

Total RNA was isolated using the TRIZOL Reagent (Invitrogen, Carlsbad, CA). To quantify TFPI-2 expression levels, equal amounts of cDNA were synthesized using the QuantiTect Reverse Transcription Kit (Qiagen, US). Gene expression was measured using FAM dye-labelled MGB probe and TaqMan PCR Master Mix kit (Thermofisher Scientific, US), and 5 nmol of primers (Thermofisher Scientific, US) (Table 2.5), according to the manufacturer's protocol. GAPDH was used as a reference. qRT-PCR cycle was performed according to manufacturer's instructions.

Data interpretation was performed using the comparative Δ CT method. For each gene, PCR amplifications were performed in triplicate and in three independent RT reactions.

Table 2. 5 qRT-PCR primers

Gene name	TaqMan Gene Expression reference number
FOXO1	Hs00231106_m1
PPARα	Hs00947536_m1
PPARγ	Hs01115513_m1
C/EBPβ	Dr03201503_s1

Inhibitors and activators

SFK inhibition

SRC and FYN inhibition in 3D orbital fibroblast culture were achieved by incubating cells with 10 μ M PP2 (Tocris, UK), a selective SFK inhibitor (Usui et al., 2016) and has been shown to inhibit FYN, SRC and CSK. Final dilution in DMEM prepared from a stock of 10 mM in DMSO, kept at -20°C. Inhibitor concentration was used as described in Li et al., 2014.

mTORC inhibition

Rapamycin (Sigma Aldrich, UK) is a potent mTORC1 inhibitor (D. D. Liu et al., 2016), shown to disrupt protein synthesis, lipogenesis and prevent senescence. Rapamycin was used in mechanotransduction and contractility assays at a final 5 μ M concentration, prepared from a stock of 10 mM in DMSO, kept at -20°C. Final concentration was used as described Chen et al. 2003. Concentrations as high as 20 μ M were assessed with 5 μ M showing no difference in results or toxicity.

mTORC activation

MHY1485 is a mTORC1 activator, shown to prevent autophagosomal and lysosomal fusion, preventing later stages of autophagy (Zhao, Chen, Wang, Ji, & Xie, 2016). Mechanism of mTORC1 activation is unclear. MHY1485 was used in mechanotransduction and contractility assays at a final 5 μ M concentration, prepared from a stock of 10 mM in DMSO, kept at -20°C. Working concentration was used as described in Choi et al., 2012 and matched to the working concentration of rapamycin where applicable.

AMPK inhibition

Dorsomorphin (Tocris, UK) inhibits AMPK through an unknown mechanism, shown to promote mTORC1 activity and autophagy. Dorsomorphin was used at a final 5uM concentration, prepared from a stock of 5 mM in DMSO, kept at -20°C. Working concentration was derived from and used as described in Liu et al., 2014.

AMPK activation

Salicylate (Sigma Aldrich, UK) is the active form of aspirin, shown to activate AMPK by binding its $\beta 1$ subunit and stabilizing the active conformation (O'Brien et al., 2015). Salicylate was used at the final concentration of 5 mM directly diluting it into the cell medium prior to the experiment in contractility and mechanotransduction assays. Working concentration of salicylate was estimated from Hawley et al., 2012.

PTPN22 inhibition

LTV-1 (Calbiochem, UK) is a PTPN22 (Lyp) inhibitor shown to increase T cell activation when inhibiting PTPN22 via an unknown mechanism (Schickel et al., 2016). LTV-1 was used at a final 5uM concentration, prepared from a stock of 5 mM in DMSO, kept at -20°C and wrapped in foil and used in mechanotransduction assays on cells cultured on collagen gels to observe its effects on lipid droplet generation. Inhibitory effect was tested at a range of concentrations starting at 0.5 uM. Maximum inhibitory effect

was found at 5 μ M, higher concentrations showed to increase in effect. Toxicity was not observed.

Autophagy inhibition

Chloroquine (Sigma Aldrich, UK) is an antimalarial drug that has been shown to disrupt autophagy by an unclear mechanism (Mauthe et al., 2018). Chloroquine was used at a final 5 μ M concentration as described Mauthe et al., prepared from a stock of 10 mM in ddH₂O, kept at +4°C. Bafilomycin A1 is a vacuolar H⁺-ATPase disrupting the acidification of autophagosomal lumen and blocking late-stage autophagy (Mauvezin & Neufeld, 2015). Bafilomycin A1 was used at a final concentration of 10 nM, prepared from a 3.2 μ M stock in DMSO as described in Mauvezin et al. 2015. Both compounds were used in mechanotransduction assays to observe their effects on lipid droplet generation.

Orbital fibroblast immortalisation

Orbital fibroblasts were immortalised using SV40 large antigen in a pBABE-puro SV40 LT plasmid. Phoenix cells were used as vector producer cell lines and transfected with the pBABE-puro SV40 LT plasmid using Fugene mix, Fugene:pDNA ratio 3:1. Cells are incubated with the mix for 30 mins at room temperature. After cells are moved to a 5% CO₂ incubator at 37°C and left overnight. Next day, media of Phoenix cells (8 mL) was changed, and CO and HO cells seeded for the next day in 10-cm dishes. The next day 8 mL of Phoenix cell media was taken up and filtered through a 0.45 μ m filter using a syringe. Filtrate used in previously seeded orbital fibroblasts for

direct transfection without cell detachment. Medium on Phoenix cells replaced. The procedure repeated the next day. After transfection fibroblasts are split 1:3 in new Petri dishes. 100 ug/mL hygromycin applied on transfected fibroblasts and negative control for selection. Unsuccessfully transfected cells and the control group should die after 48h.

Statistics

Data are presented as means \pm standard error of the mean (SEM) of the indicative values of experiments (N) and were compared between groups by a two-tailed unpaired Student's t-test. Where more than two groups were compared, a one-way ANOVA statistical analysis test was used. P-values less than 0.05 were considered as statistically significant.

CHAPTER 3 SFK ROLE IN LIPID DROPLET GENERATION AND CONTRACTILITY

3.1 Introduction

Adipogenesis in orbital fibroblasts is a hallmark pathology of GO and may further contribute to disease complication by exerting pressure onto the eye due to tissue volume expansion (Khong, McNab, Ebeling, Craig, & Selva, 2016). We have previously shown that in 3D cultures, both patient (HO) and healthy control (CO) fibroblasts undergo spontaneous lipid droplet generation without chemical induction, while 2D cultures do not show lipid droplets (He Li et al., 2014). *In vivo* fibroblasts reside embedded in ECM, making 3D culturing a more relevant model than 2D culture (Duval et al., 2017). Collagen gels are also a magnitude mechanistically softer than plastic on which cells are seeded in 2D cultures. Therefore, it is likely that cell attachment in 3D and stiffness of substrate are contributors to lipid droplet formation (Hadjipanayi, Mudera, & Brown, 2009; Xie, Bao, Bruekers, & Huck, 2017).

SRC family kinases (SFKs) are a large family of non-receptor tyrosine kinases (RTKs). SFKs consist of 9 highly homologous members (Ingley, 2008). Majority of SFKs are expressed in cells of hematopoietic origin while FYN, SRC and YES are more expressed in fibroblasts. Of these three, FYN and SRC are directly involved in fibroblast integrin-ECM cell adhesion (Playford & Schaller, 2004a). SRC is a widely known integrin attachment regulator, involved in adipogenesis regulation, focal contact formation and

maturation by phosphorylating focal adhesion kinase (FAK) (Caron-Lormier & Berry, 2005). In fibroblasts, SRC is activated by mechanical tension and has been shown to prevent adipogenic differentiation in pre-adipocyte cells (Usui et al., 2016). SRC has been shown to phosphorylate Akt directly, which in turn inhibits the activity of mTORc1 negative regulator TSC 1/2. mTORc1 has been demonstrated to activate SREBP1, a transcription factor initiating lipogenesis (R. Chen et al., 2001a; Vojtechová et al., 2008). The function of FYN is less understood; it is involved in stress fibre regulation by, possibly, assuming the position of SRC at focal adhesions. It has also been implicated in lung fibroblasts attachment regulation in lung fibrosis as a potential pro-fibrotic factor (Fiore et al., 2015b). FYN has also been shown to modulate AMPK activity and blocking lipid catabolism by inactivating LKB1, an AMPK activator showing that activity of FYN directly affects lipid accumulation in cells (Yamada, Pessin, Kurland, Schwartz, & Bastie, 2010). AMPK is activated during cellular low-ATP, low nutrient conditions and blocks lipid synthesis by phosphorylating acetyl-CoA carboxylase and blocking mTORC1 activity (Shaw, 2009).

Both SRC and FYN are negatively regulated by CSK, an SFK-homologous cytoplasmic kinase that phosphorylates SFKs at the C-terminus. Recently, the tyrosine phosphatase PTPN22 (formerly known as Lyp) has been shown to form a functional complex with CSK to inactivate SFKs (Clarke et al., 2018a). PTPN22 may play an important role in autoimmune disorder progression; a mutant version of the phosphatase reduces its association

with SFKs and promotes increased SFK activity which may contribute to GO progression (Fiorillo et al., 2010).

Cell behaviour and signalling are significantly altered in 3D; FAK phosphorylation in 3D cancer cell culture models in comparison to 2D (Riedl et al., 2017b). In comparison to 2D cell cultures on plastic, collagen provides a much softer mechanistic environment (Y. K. Wang et al., 2003) which translates into lower FA adhesion phosphorylation (Wozniak, Modzelewska, Kwong, & Keely, 2004). Whether it influences, SFK activity is currently unknown.

Our lab has previously demonstrated that treatment of CO and HO cells with PP2, a broad spectrum SFK inhibitor, decreases orbital fibroblast contractility and intracellular lipid droplets when cultured in 3D. Here, we aim to demonstrate that SFKs FYN and SRC are involved in spontaneous lipid droplet generation in orbital fibroblasts through modulating the balance between AMPK and mTORC1 activity.

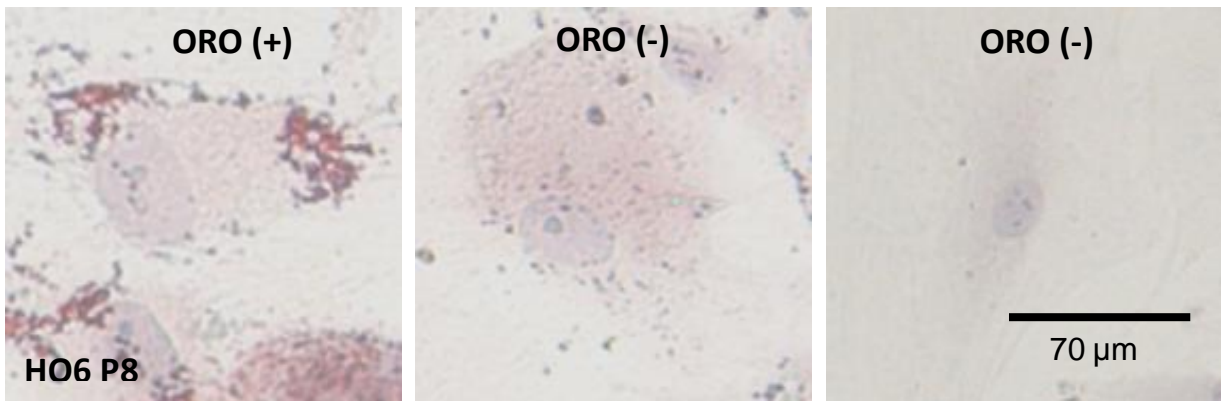
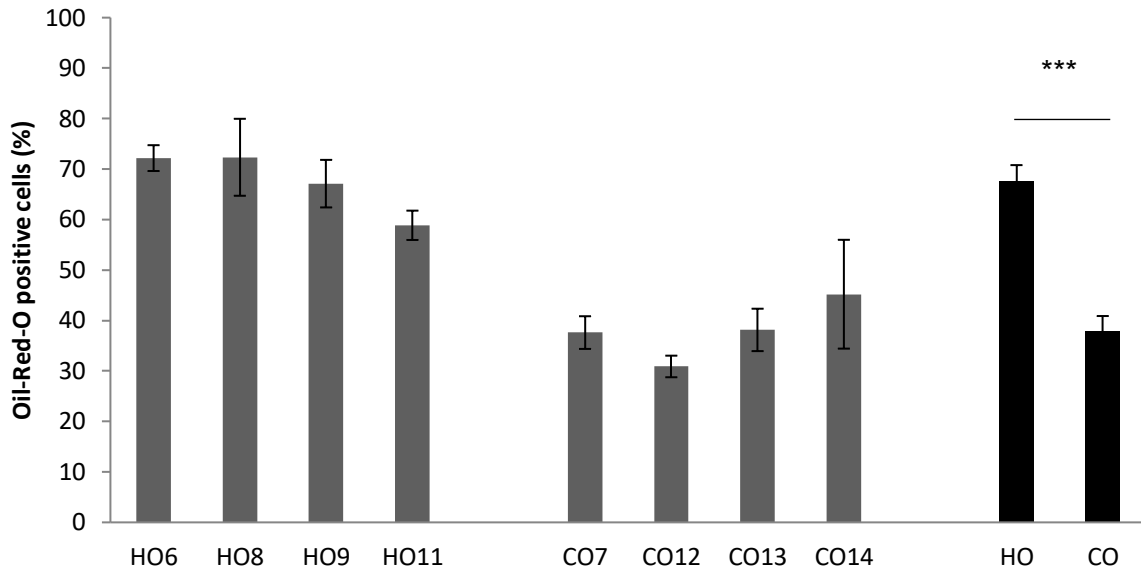


Figure 3. 1 GO orbital fibroblasts are more prone to develop lipid droplets compared to control cell lines from healthy patients

Experiments done by Dr I-Hui Yang. GO (HO) (passage 4 to 7) and control (CO) orbital fibroblasts (passage 4 to 7) were embedded in 1.5 mg/mL collagen matrices for 5 days and stained for neutral lipids with Oil-Red-O. Cells with clear cytoplasmic appearance of lipid droplets were counted as Oil-Red-O positive (ORO(+)) while cells with few or no lipid droplets as negative (ORO(-)). Percentage of positive cells (%ORO+ve) was calculated by ORO+ve vs total amount of cells per field of vision. On average, GO orbital fibroblasts exhibited a significantly higher number of ORO+ve cells than control cell lines (Student's T-Test, $p < 0.001$) (n (replicates) = 3, N (experiments) = 3, ORO+ve cells shown as mean, error bars as SEM).

3.2 Results

3.2.1 GD patient-derived orbital fibroblasts generate more lipid droplets than healthy controls

Primary orbital fibroblast cell lines were obtained and expanded from healthy donors (CO cells) and GO patients undergoing orbital decompression surgery (HO cells) during the active stages of the disease. All CO and HO cells have been derived from posterior orbital tissue. Control cell lines are predominantly of male origin, while disease cell lines were taken from female patients. Disease duration post-diagnosis varies between patients.

Lipid generation is a well-known pathological effect of GO with orbital fibroblasts driven to differentiate into adipocyte-like cells, contributing to increasing intra-orbital pressure, proptosis and limiting eye muscle movement. It has been previously demonstrated that lipid droplets spontaneously appear when cells are cultured in 3D and 2D only when chemically induced.

To confirm whether lipid droplet generation is higher in GO patient cells in 3D, Dr I-Hui Yang cultured both CO and HO in 3D and stained for neutral lipids after five days (Figure 3.1). On average, HO cells were more prone to develop lipid droplets when cultured in collagen gels in comparison to CO cells (Student's T-test, $p < 0.001$). Around 70% of observed HO cells contained ORO-stained neutral lipid droplets, while only 40% of CO cells under the same conditions appeared to be lipid-positive.

Previously published data shows that SFK inhibition decreases the number of lipid droplet positive cells. We confirmed that the same is true for both CO and HO orbital fibroblasts in 3D cultures (Figure 3.2). The number of lipid droplets in 3D cultures was significantly reduced in two representative cell lines (CO7 and HO6) to approximately 10% versus control, showing that both control and diseased cells respond to SFK inhibition equally.

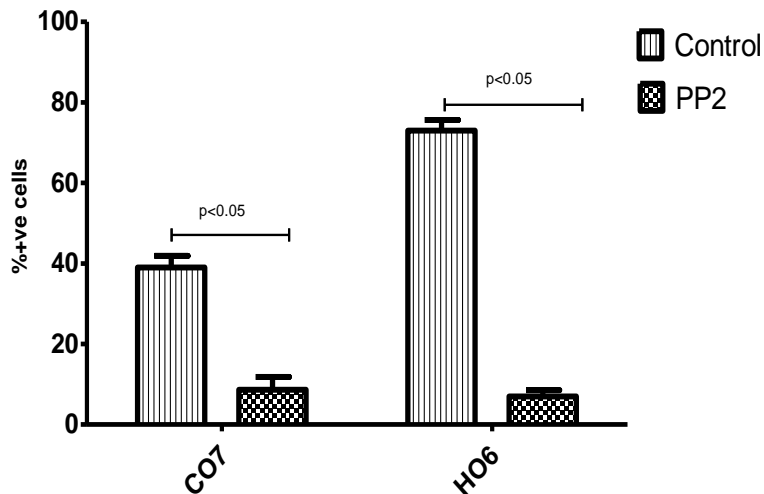
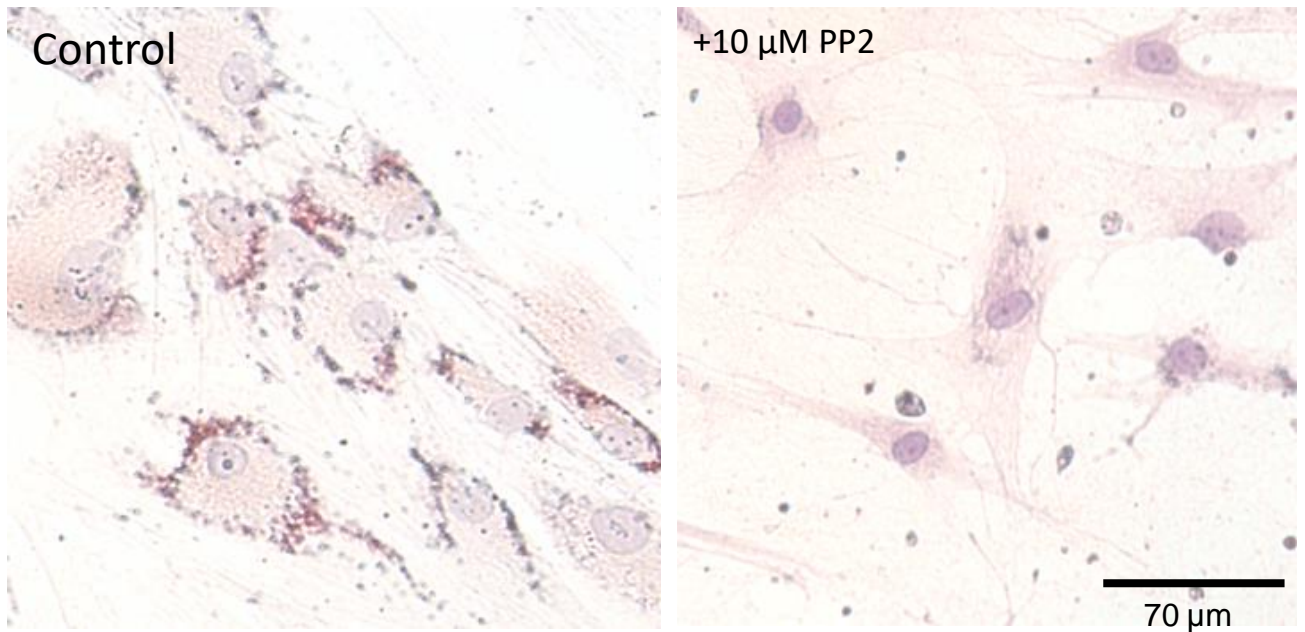


Figure 3. 2. SFK inhibition reduces the amount of lipid droplets generated in 3D.

CO7 (passage 7) and HO6 (passage 6) cells were cultured in 3D in the presence of 10 μ M PP2. Cells with cytoplasmic appearance of lipid droplets were counted as lipid droplet-positive. Cells treated with PP2 exhibited a significantly lesser amount of lipid droplets in comparison to untreated controls (N (experiments) = 3, n (replicates) = 2, ORO+ve cells shown as mean. error bars as SEM).

3.3.2. CO and HO cells differ in FYN/SRC expression but not in SRC activity

We showed confirmed that inhibition of SFKs with PP2 decreases lipid droplet generation in CO and HO cells in 3D cultures. Next, we wanted to determine the amount of SRC and FYN protein present in CO and HO cells and whether the levels of FYN and SRC can be correlated to the lipid droplet generation potential observed in 3D. The total amount of FYN and SRC was assessed by Western Blot (Figure 3.3). Two of the CO cells lines (CO6 and CO7) have lower amounts of FYN while CO12 and CO13 have a high amount, very similar to that of all tested HO cell lines. All HO cells have a comparatively low level of SRC protein. SRC amount in CO12 and CO13 is closer to that of HO cells but noticeably lower than CO6 and CO7. Based on SRC and FYN levels in 2D, CO12 and CO13 appear to have a similar phenotype to HO cells.

We also examined SRC activity by immunofluorescence in CO and HO cells in 2D (Figure 3.4). We were able to confirm that active SRC localised to termini of stress fibres, presumably to focal adhesions. We compared the fluorescent signal intensity with imageJ between CO and HO cells. Relative SRC content in IF experiments is similar to that observed in WB in tested cell lines. While in HO SRC activity appears to be low in both tested cell lines, CO7 displays much higher SRC activity than CO12, which has both SRC and FYN activity levels closer to those of HO cells.

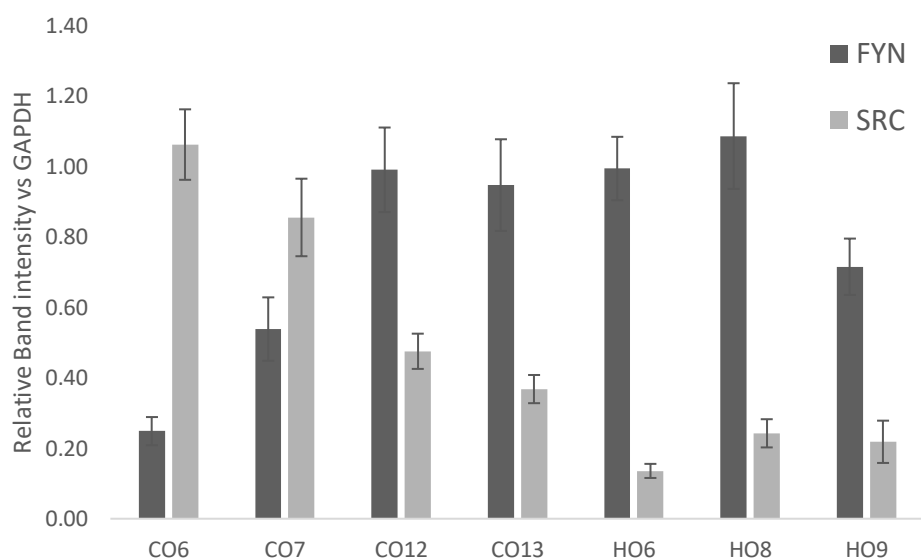
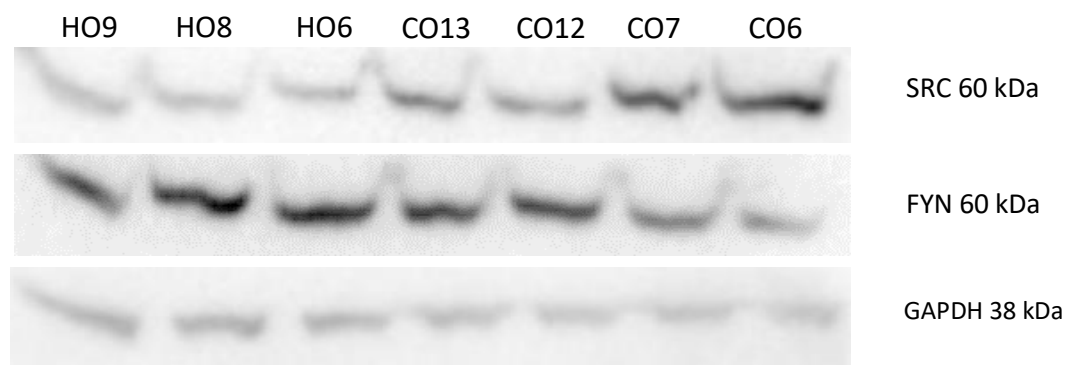


Figure 3. 3. HO fibroblasts express more FYN protein, CO – more SRC

SRC and FYN protein levels were assessed in 2D cultured cell (passages 4 to 9) lysates by WB, and quantified with ImageJ. HO, CO12 and CO13 cells express higher levels of FYN. CO12 and CO13 have FYN levels similar to HO and SRC levels lower than CO6 and CO7 (shown as mean \pm SEM, number of experiments (N) = 3, replicates per experiment (n) = 2).

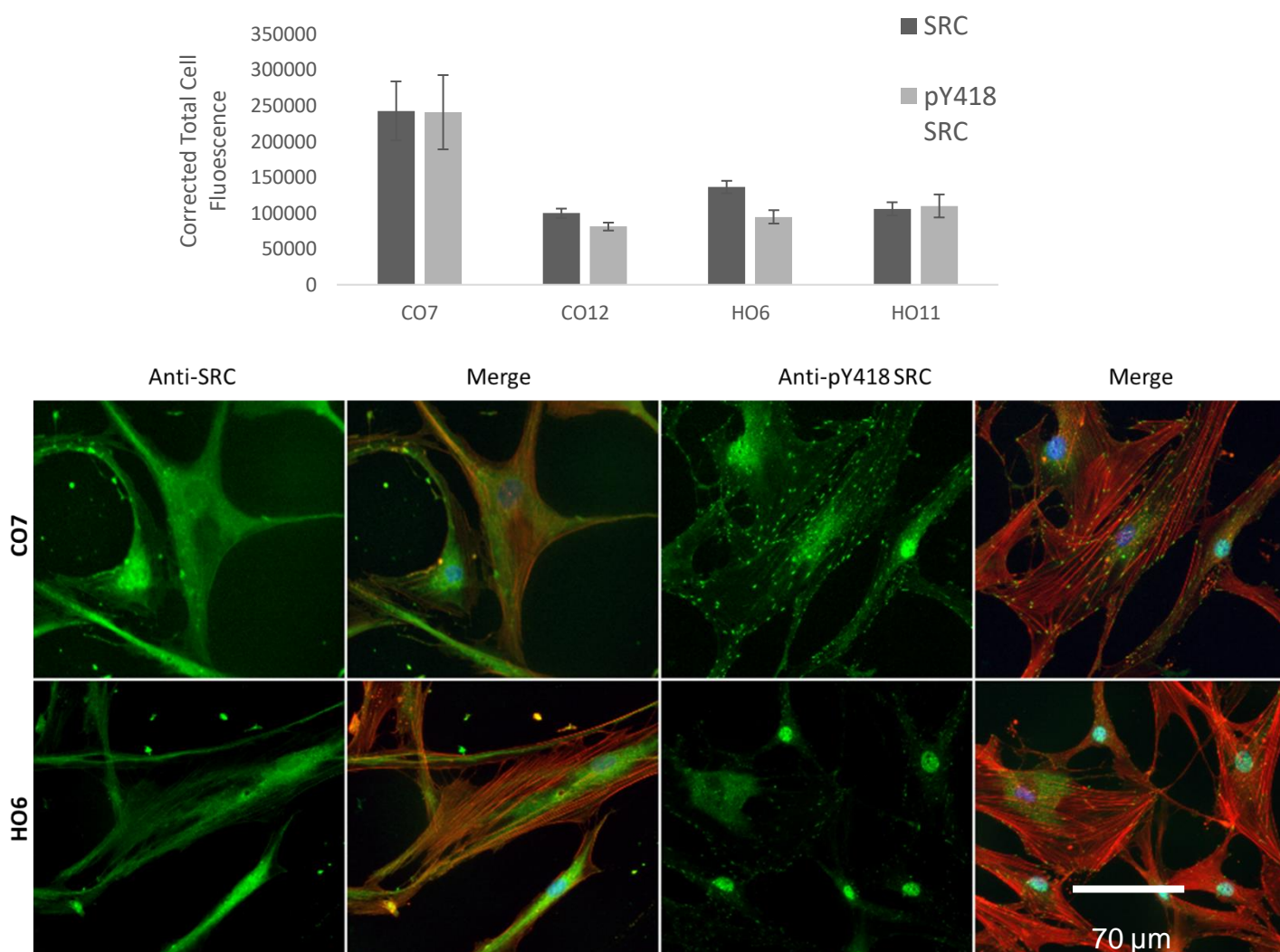
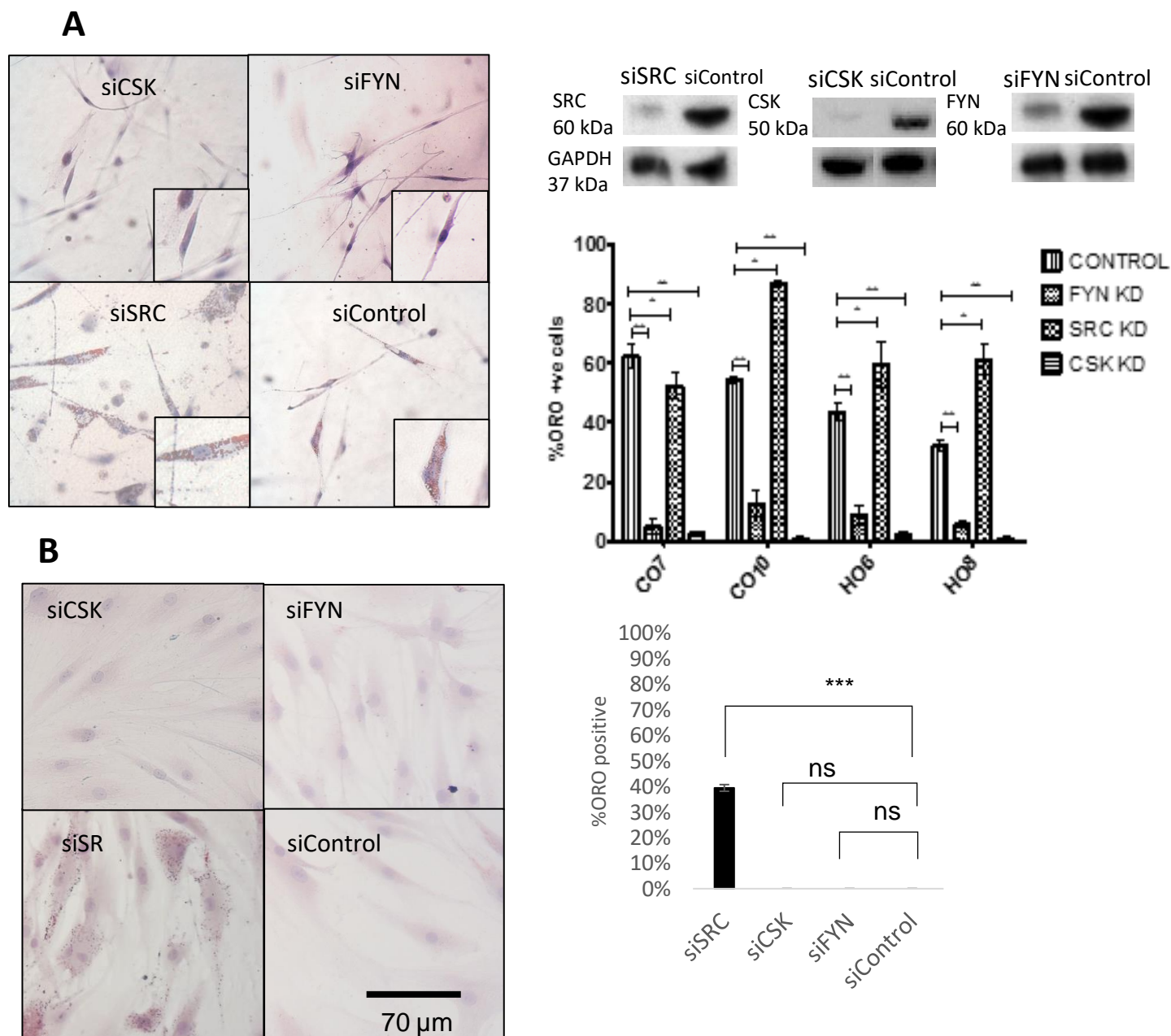


Figure 3. 4. Active SRC localises to focal adhesions and focal contacts in orbital fibroblasts. 2 CO and 2 HO (passages 5-7) cell lines were seeded on glass coverslips overnight, fixed in 3.7% formaldehyde, permeabilised with 0.5% Triton-X stained for active (pY418SRC) and total SRC protein. Samples were imaged with the same exposure time determined from the brightest sample. Corrected Total Cell fluorescence was measured and analysed with ImageJ. (N= 3, n = 2, shown as mean +/- SEM)

3.3.3. SRC knock-down increases the number of lipid droplet positive cells while FYN and CSK knock-downs abolish it

Previously we used PP2 to inhibit all FYN, SRC and CSK activity in 3D cultured orbital fibroblasts and observed an overall decrease in lipid droplet generation. To determine the effect of FYN, SRC and CSK separately, we performed FYN, SRC and CSK knock-downs in 2 CO and 2 HO cells, corresponding a high-SRC/low-FYN phenotype (CO7) and a high-FYN/low-SRC phenotype (HO6) (Figure 3.5). Surprisingly FYN and SRC knock-downs showed opposite effects; SRC down-regulation proved to significantly increase the amount of lipid-positive cells ($p < 0.01$) while FYN downregulation achieved the opposite effect ($p < 0.05-0.01$). CSK knock-down had a similar effect of that of FYN ($p < 0.01$). To assess if a similar effect is present in 2D cultures, we performed an SRC, FYN and CSK knock-down in CO7 cells. SRC downregulation significantly increased the number of lipid-positive cells while CSK and FYN knock-down cells remained completely negative, same as control. SRC knock-down appeared to be noticeably toxic to cells while toxicity was not observed in siFYN, siCSK and siControl cells. We also observed that in all experimental repeats, cells transfected with control pool siRNA showed an inconsistent amount of lipid-positive cells. In previous 3D culture experiments with untransfected cells exhibited a significantly lower lipid positive cell count in CO cells and higher in HO (40% for CO7, 70% for HO8). In knock-down experiments, we saw a positive count increase in CO cells and a decrease in HO cells.



3.3.4. FYN may modulate spontaneous lipid droplet generation through regulating AMPK activity

Previously we observed a significant drop in lipid droplet generation orbital fibroblasts when FYN is downregulated. FYN has been previously implicated in regulating body energy expenditure in mouse models by blocking AMPK activity by phosphorylating LKB1 and regulating adipogenesis via the same mechanism. To determine if AMPK activity is linked to FYN, we downregulated FYN in HO6 cells and determined AMPK and LKB1 activity. LKB1 is a positive regulator of AMPK in adipocytes and fibroblasts while acetyl-CoA carboxylase (ACC1) catalyses a committal step of lipogenesis by converting acetyl-CoA to malonyl-CoA. AMPK is typically activated by low levels of ATP and blocks ACC1 activity by phosphorylating it at Serine-73 to limit lipid synthesis and promotes fat breakdown.

We (Figure 3.6) show that FYN knock-down upregulated LKB1 ($p<0.05$) and AMPK activity ($p<0.05$) further shown by increased ACC1 pS73 phosphorylation ($p<0.05$) consistent with the near-absence of lipid droplets in FYN KO 3D cultures in both CO and HO cells.

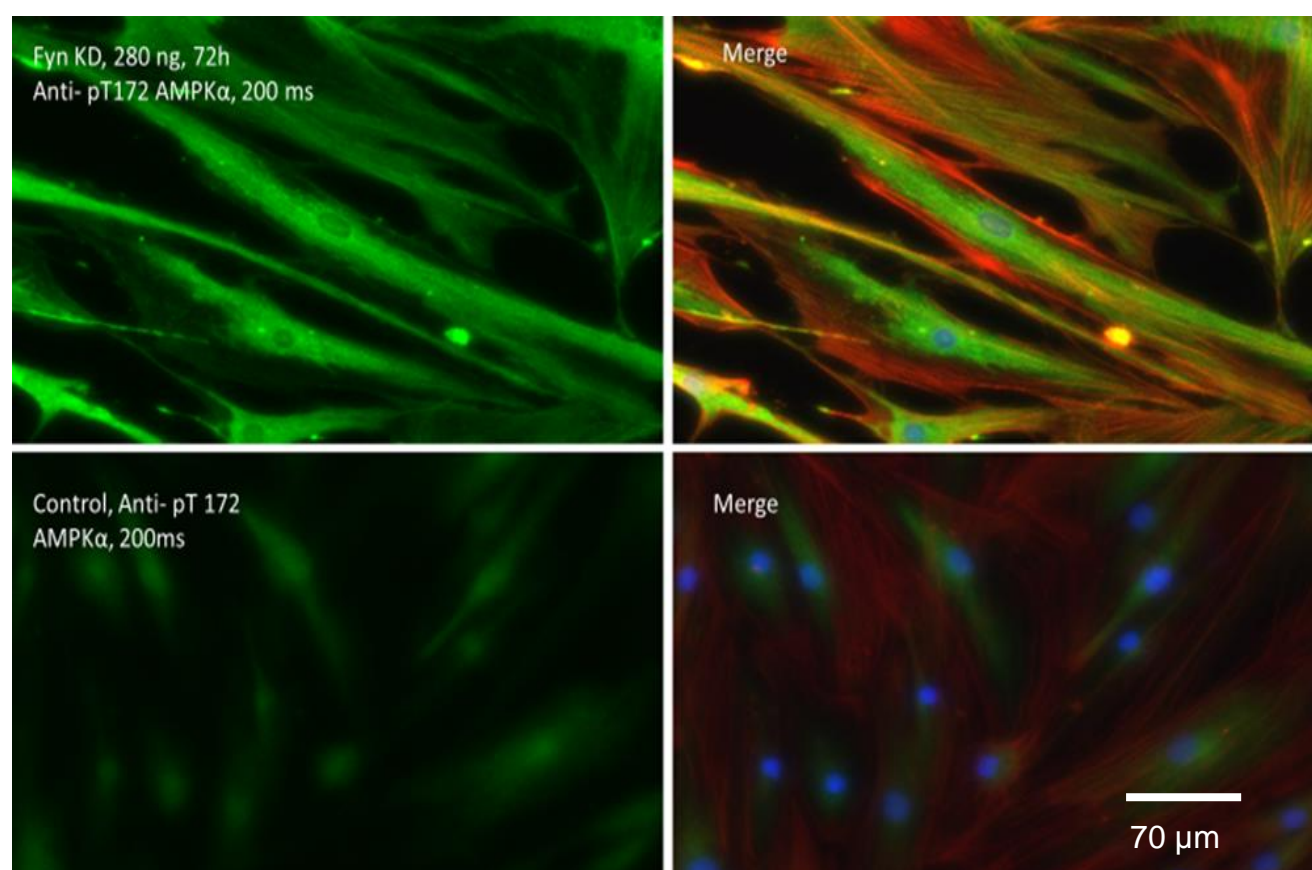
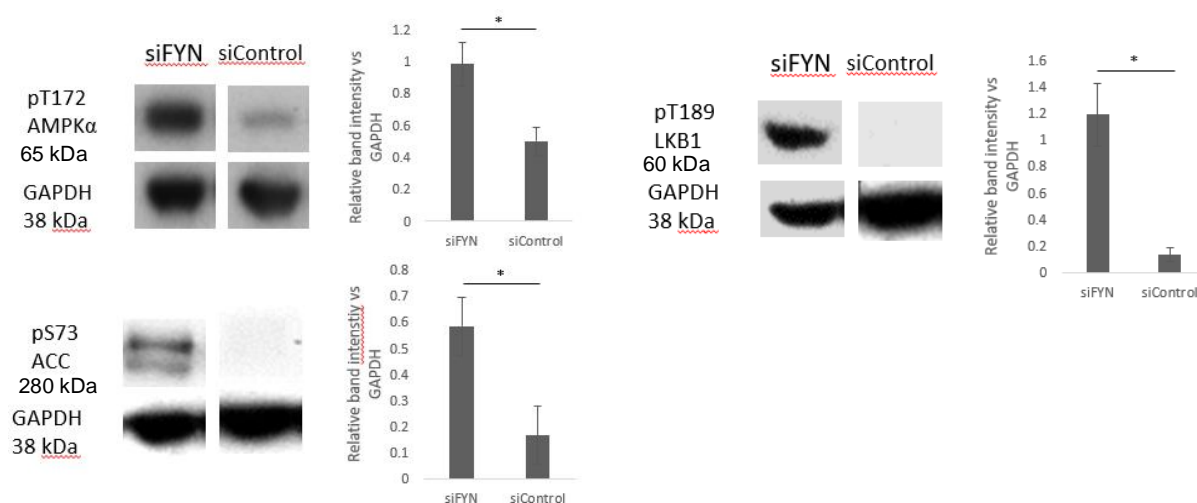


Figure 3.6. FYN downregulation causes activation of AMPK-associated pathways

HO6 orbital fibroblasts were incubated with 280 ng siFYN for 72h, lysed and probed for phosphorylated p172 AMPK, pT189 LKB1 and pS73 ACC1 proteins. pT172 AMPK activity was also assessed by immunofluorescence (shown as mean \pm SEM, N =3, n = 4; statistical significance calculated with Student's T-test, *p<0.05)

3.3.5. SRC suppresses lipid droplet generation through maintaining Akt/mTORC activity

We previously observed that CO and HO fibroblasts generate lipid droplets when cultured in 3D. This effect was further amplified when downregulating SRC, implying that SRC activity suppresses lipid droplet generation. It has been previously shown that SRC positively regulates mTORC1 activity via Akt phosphorylation. Therefore, we wanted to determine whether the Akt/mTORC1 pathway activity can explain the increased amount of lipid droplets.

We performed an SRC knock-down in CO7 cells and assessed mTORC1, Akt and phospho-AKT protein content by WB. Downregulation of SRC (Figure 3.7) significantly decreased Akt ($p < 0.05$), mTORC ($p < 0.001$) protein expression and activity, but as seen in previous experiments also noticeably increased the number of lipid-positive cells. This suggests that SRC and Akt/mTORC1 are negative regulators of lipid droplet formation in 3D cultures.

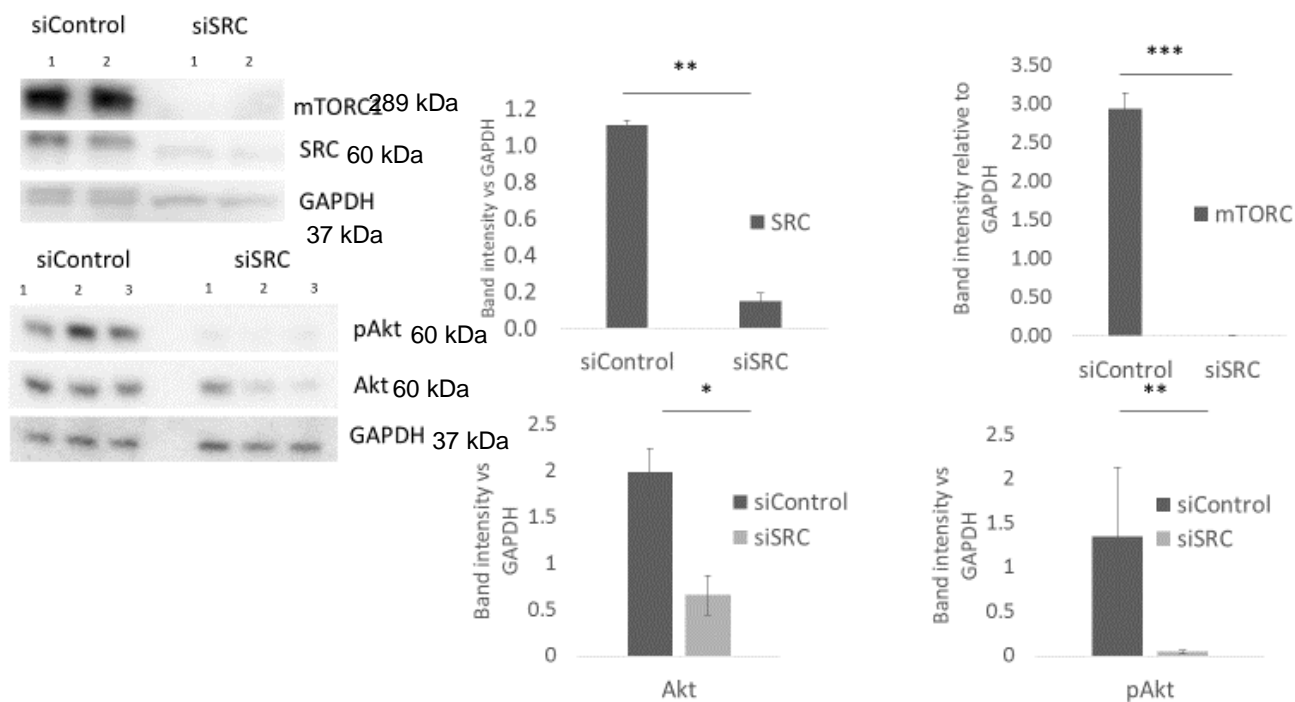


Figure 3.7 SRC knock-down downregulates mTORC/Akt protein expression.

CO7 cells were lysed after incubation with 280 ng SRC or Control siRNA for 72h. SRC, mTORC, Akt and phospho-Akt protein levels were assessed by WB and quantified with ImageJ. SRC KO appears to significantly decrease protein content part of the Akt/mTORC pathway (N = 3, n = 2, shown as mean +/- SEM, Student's T-Test *p < 0.05, **p < 0.01, ***p < 0.001).

3.3.6. SRC and FYN are necessary for orbital fibroblast contractility

We showed that chemical inhibition of SFKs with PP” significantly reduced contractility in orbital fibroblasts. Here, we wanted to investigate whether SRC and FYN contribute to the fibrotic aspects of GO orbital fibroblasts equally. We performed SRC and FYN knock-downs and embedded the cells in collagen matrices in MaTtek dishes. After detaching the gels, we measured gel contraction over five days. Both FYN and SRC KO significantly decrease contractility in CO and HO cells (Figure 3.7) while the difference in contractility between each siRNA treated cell line appears to be minor. HO6 cells exhibit slightly higher contractility than CO7 cells consistent with previously published data while knock-down of FYN and SRC reduces contractility to similar levels in both.

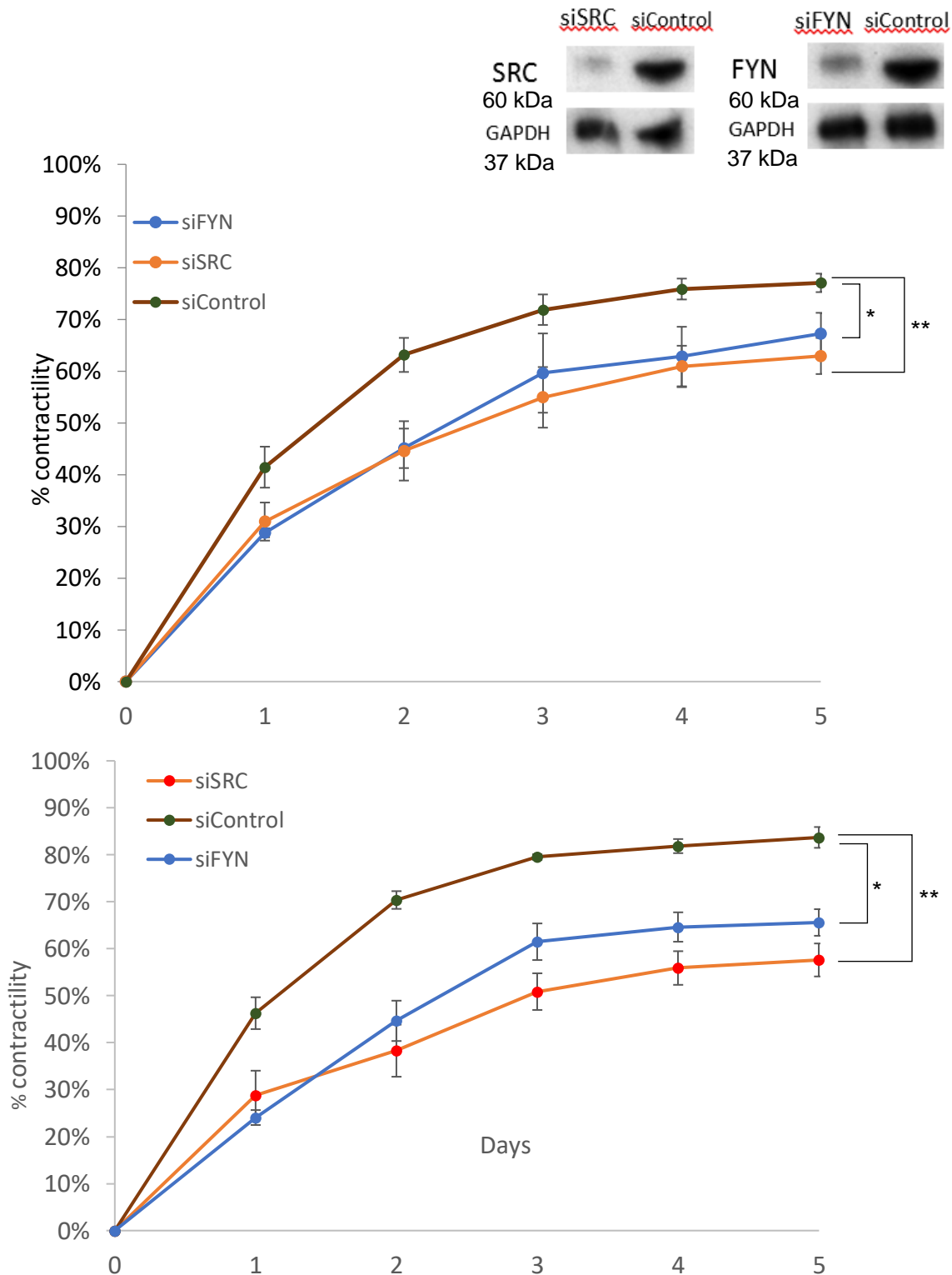


Figure 3.8 SRC and FYN KO reduces orbital fibroblast contractility.

SRC and FYN KO performed as previously. siRNA-treated cells were embedded into collagen gels which were cast in MatTek well plates and detached after polymerisation. Gels were imaged and contractility assessed measured with ImageJ daily over a period of 5 days. KO of FYN and SRC reduce fibroblasts contractility to a similar extent with FYN KO HO6 cells being slightly more contractile than SRC KO (shown as mean \pm SEM, $N = 3$, $n = 3$, Student's T-Test used with terminal gel contraction values on day 5 * $p < 0.05$, ** $p < 0.01$).

3.4. Discussion

3.4.1 Role of SFKs in lipid droplet generation and contractility

We confirmed our previous findings that orbital fibroblasts develop lipid droplets in 3D cultures spontaneous adipogenesis. Lipid droplet development can be disrupted by inhibiting SRC family kinases; chemical inhibition of SFKs causes absence of lipid droplets in 3D cultures while separate knock-down of FYN or SRC promotes opposite phenotypes. FYN KD blocks lipid droplet generation while SRC, in comparison to control cultures, amplifies it. Downregulation of CSK causes a similar effect to that of FYN. Removal of CSK as a negative regulator should increase the activity of both FYN and SRC, that both kinases suppress lipid droplet generation. PP2 acts as an inhibitor of SRC, FYN and CSK, meaning that reducing the activity of FYN, SRC, and their negative regulator also prevents lipid droplets from forming. In line with FYN and SRC knock-down data, it would appear that the balance of FYN and SRC activity is determinant to lipid droplet generation in 3D cultures while chemical inhibition of both kinases and CSK causes loss of lipid droplets. SRC knock-down also caused lipid droplet generation in 2D cultures while FYN and CSK knock-downs showed no significant change. With data from all the mentioned experiments taken together, we can conclude that predominantly SRC activity suppresses lipid droplet generation. While FYN plays a role in lipid droplet removal, its downstream signalling activity may still be dependent on SRC.

SRC and FYN knock-downs reduced contractility in both CO and HO cell lines. Our experiments are consistent with previous publications (He Li et

al., 2014) showing that chemical inhibition of SFKs reduces contractility of orbital fibroblasts. We did not observe a significant difference between SRC and FYN knock-downs. However, untreated (or siControl treated) HO6 cells in our and previously published experiments exhibit higher contractility than CO7. SFK downregulation in both cell lines reduced contractility to the same degree.

3.4.2 Pathways regulated by SRC and FYN

FYN has been previously shown as a negative regulator of AMPK and SRC as a positive regulator of mTORC1 (Majd, Power, Chataway, & Grantham, 2018); however, the two kinases have not been previously described to act within the same model. FYN has been previously shown to be an AMPK suppressor in adipocytes and fibroblasts through inactivating LKB1, an AMPK activator (Yamada et al., 2010). We showed that downregulation of FYN causes increased active LKB1 and AMPK α phosphorylation, and inactivation of ACC1, a well-known downstream target of AMPK. SRC KO decreased Akt phosphorylation and protein expression, and surprisingly also reduced the amount of mTORC1 protein. which is implicated in promoting lipid biogenesis through SREBP1 activation (Cai et al., 2016). Our findings show that SRC KO decreases mTORC expression while increasing lipid droplet generation, suggesting that mTORC activity may suppress lipid droplet development in 3D.

While we were not able to demonstrate SRC activity in 3D cultures, SRC knock-down increased lipid droplet production in both 2D and 3D, suggesting that its activity or expression could be reduced in 3D cultures.

Furthermore, HO cells have both lower SRC activity and protein expression, potentially explaining why GO fibroblasts generate more lipid droplets in 3D.

Thy-1, a surface glycoprotein has been previously reported to regulated Src and Fyn activity, integrin clustering and influence orbital fibroblasts differentiation into adipogenic or myofibroblast phenotypes. Our data (not shown) countered this assumption; the vast majority of GO and HO fibroblasts were Thy1 positive while CO and HO fibroblasts exhibited different contractile and adipogenic properties.

3.4.1. Limitations of the study and future work

Although we were able to assess active SRC localisation with immunofluorescence, an antibody to image active FYN antibody is not yet commercially available. Total FYN antibodies used in WB assays did not show specific fluorescent signals in IF.

We encountered further problems with assessing phospho-SRC and total SRC in 3D cultured cell lysates; 3D samples showed an unusually high band size appearing in the 250 kDa range while such issues were not observed in 2D. This points to incomplete protein separation during lysis and protein denaturation despite the presence of SDS and β -mercaptoethanol in the sample buffer, making it challenging to conclude protein activity in 2D vs 3D.

In FYN and SRC knock-down experiments we observed an unusually high number of lipid droplets in cells transfected with the control siRNA while

control siRNA treatment did not alter the contractile behaviour of the cells used in contractility assays.

We have previously shown that lipid droplet generation appears to be exclusive to 3D cultures and is affected by FYN and SRC activity. However, it is unclear if the cause of lipid droplets lies with cells being cultured in 3D or cell exposure to softer mechanistic environments. Loss of Akt and mTORC1 proteins when downregulating SRC implies that Src/Akt/mTORc1 activity could suppress spontaneous lipid production, which contradicts the assumption of mTORc1 as a promoter of lipogenesis. Previously documented downregulation of the Akt/mTORc1 pathway has been shown to decrease phosphorylation and activity of Akt, and mTORc1 while increasing autophagy marker expression and activity (C. Wang, Zhang, Teng, Zhang, & Li, 2014).

While we assessed the possible off-target effects of Fyn and Src siRNAs, we did not investigate if other members of SFK, expressed in orbital fibroblasts are affected by used siRNAs. It cannot be excluded that Fyn or Src siRNAs produced off-target silencing of other, homologous SFKs.

3.4.2 Conclusion

We demonstrated that SRC and FYN activity is crucial to lipid droplet development in orbital fibroblasts. SRC regulates the activity of Akt and mTORC1 and reduction of SRC activity also reduces the amount of Akt and mTORC1 proteins. FYN knock-down abolishes lipid droplet generation. Downregulation of FYN was shown to increase AMPK phosphorylation which in literature is strongly correlated with lipid droplet break-down.

CHAPTER 4 MECHANOREGULATION OF SFKS

4.1 Introduction

4.1.1. 3D culture or substrate rigidity; what promotes lipid droplet production?

Previous publications by the Bailly group show spontaneous lipid droplet production in 3D cultured orbital fibroblasts, an event that is not encountered in standard 2D culture on plastic (He Li et al., 2014). Molecular mechanisms or biological reasons for this phenomenon are unclear. Previously, we showed that knockdown of Src family kinases significantly affects lipid droplet generation in 3D orbital fibroblasts cultures; Src downregulation increased the number of lipid droplets present while Fyn knock-down nearly abolished it. Numerous other sources report a reduction in Src phosphorylation in 3D cultures and dissociation from focal adhesions accompanied by reduced Akt and mTORc1 activity.

3D collagen matrices have been reported to possess mechanical rigidity lower than 1 kPa (at a collagen concentration ~ 2 mg/mL) by a magnitude less than substrate rigidity on plastic (Cross et al., 2010; Xie et al., 2017; Yeung et al., 2005). In mammary epithelial cells, differentiated structures are formed in a 3D collagen gel only if the gel is floating in media, and not if the gel is left attached to the dish or if the cells are cultured on 2D collagen (Wozniak, Desai, Solski, Der, & Keely, 2003). It is unclear whether lipid droplet generation in 3D appears due to cell position and altered adhesion mechanisms in 3D or placement in a mechanistically gentler and softer

environment, as the substrate tension in soft orbital tissue is around 0.5 kPa (Yoo et al., 2011b). While the majority of literature dealing with 3D cultured fibroblasts report reduced FAK phosphorylation and altered focal adhesion structures, they also attribute substrate softness flexibility as an important component of attachment signalling (Wozniak et al., 2004). Soft matrix is considered an inhibitor of proliferation and a promoter of differentiation in renal tubular cells (W. C. Chen, Lin, & Tang, 2014). Paszek et al. showed that higher extracellular matrix (ECM) stiffness impaired tissue morphogenesis of mammary gland epithelial cells, whereas a decrease in tension alleviated the malignant behaviour of cancer cells (Paszek et al., 2005). Additionally, matrix crosslink-enhanced ECM tension supports tumour development and liver fibrosis (Levental et al., 2009). These data suggest a critical role of ECM stiffness in physiology and pathophysiology. Given that Src regulates FA assembly in orbital fibroblasts in response to substrate rigidity, orbital fibroblast placement on softer mechanistic environments rather than in 3D may play a role in lipid droplet production.

4.1.2 Signalling pathways involved in lipid droplet production

Previously we were able to demonstrate that downregulation of Fyn promotes lipid droplet reduction in 3D while increasing AMPK activity. Src knock-down had an opposite effect, promoting lipid droplet production while reducing Akt and mTORc1 proteins. AMPK and mTORc1 proteins have been shown to have dual roles in lipid production; on one side AMPK is activated in response to low intracellular ATP concentration and signals for lipid reserve breakdown to sustain cellular energy needs (Dunlop & Tee,

2013). Under prolonged periods of starvation, AMPK activates autophagy which may remove cellular lipids through specialised autophagy – lipophagy. AMPK and mechanotransduction relationship is bi-directional; AMPK in softer mechanical environments reduces the surface amount of integrins, internalising and degrading them. AMPK also blocks mTORc1 activity (Huang et al., 2008).

mTORc1 is regulated by Src through Akt phosphorylation and activates lipid and protein synthesis in response to sufficient availability of nutrients (Saxton & Sabatini, 2017; Vojtechová et al., 2008). mTORc1 is upregulated in fibrotic tissue, increasing myofibroblast-like cell population (Lawrence & Nho, 2018; White et al., 2006; Woodcock et al., 2019). Knock-down of mTORc1 in mice impairs adipocyte differentiation and reduces lipid accumulation in cells (Shan et al., 2016). Treatment with rapamycin, a mTORc1 inhibitor reduces fibrosis by limiting fibroblasts proliferation (Hillel & Gelbard, 2015; Molina-Molina et al., 2018). mTORc1 has also been found to respond to increased mechanical load and suggested to act as a FAK regulator (F.-Y. Lee et al., 2017) promoting cell proliferation. Information on mTORc1 expression in soft substrate cultures is scarce. Riedl et al. report that 3D cultured carcinoma cells have relatively lower mTORc1 protein expression (Riedl et al., 2017a), however, another publication demonstrates that in 3D cultured chicken chondrocytes initially lower mTORc1 expression can be increased by applying mechanical tension (Guan, Yang, Yang, Charbonneau, & Chen, 2014). Our data shows that mTORc1 protein is

reduced in Src knock-down cultures accompanied by increased lipid droplet production, hinting that mTORc1 may limit this process.

4.1.3 Autophagic degradation of lipid droplets

Lipophagy is a sub-type of autophagy in which portions of or whole LDs are sequestered alone or with other cytosolic constituents in autophagosomes for delivery to lysosomes for degradation (Jaishy & Abel, 2016). Lipophagy like autophagy is triggered by prolonged lack of nutrients or by excessive production of proteins, or population of damaged intracellular proteins and organelles. Autophagic signalling cascade consists of Atg proteins, while the scaffold of the autophagosome membrane is built of LC3b proteins (Onal et al., 2017). Autophagy can be induced by AMPK and has been shown to be blocked by mTORc1. Autophagy markers have been shown to increase in 3D neuroblastoma cell cultures (Bingel et al., 2017) while in smooth muscle cells autophagy was increased with the application of mechanistic tension (Ulbricht et al., 2013). In different mechanical stiffness environments, autophagy is active while cells adapt to altered tension in their surroundings (King, Veltman, & Insall, 2011) and might be specifically degrading focal adhesion proteins (Kenific, Wittmann, & Debnath, 2016). However, there is little published research available autophagy in fibroblasts in soft and 3D cultures. I

In this chapter, we will investigate how lipid droplet generation in orbital fibroblasts responds to different mechanistic growth conditions and will elucidate the involvement of SFKs.

4.2. Results

4.2.1 Orbital fibroblasts in 3D cultures do not increase adipogenic gene expression

Work previously published by the Bailly lab shows that orbital fibroblasts cultured in 3D collagen matrices spontaneously generate lipid droplets and that orbital fibroblasts obtained from GO patients (HO) are prone to generating more lipid droplets than healthy controls (CO). Dr I-Hui Yang compared adipogenesis marker expression in CO and HO fibroblasts cultured in 3D (Figure 4.1). PPAR α regulates the expression of genes involved in fatty acid beta-oxidation and regulates energy homeostasis. PPAR γ regulates fatty acid storage and glucose metabolism. The genes activated by PPAR γ stimulate lipid uptake and adipogenesis by fat cells. C/EBP β is a marker of early adipogenic differentiation. FOXO1 has anti-adipogenic properties and stimulates myofibroblastic differentiation of fibroblasts. In both CO and HO cells, no statistically significant difference in the expression of markers associated with adipogenesis or adipogenic differentiation. A significant difference was seen in FOXO1 expression in HO cells with FOXO1 expression in 3D cultures being lower than in 2D.

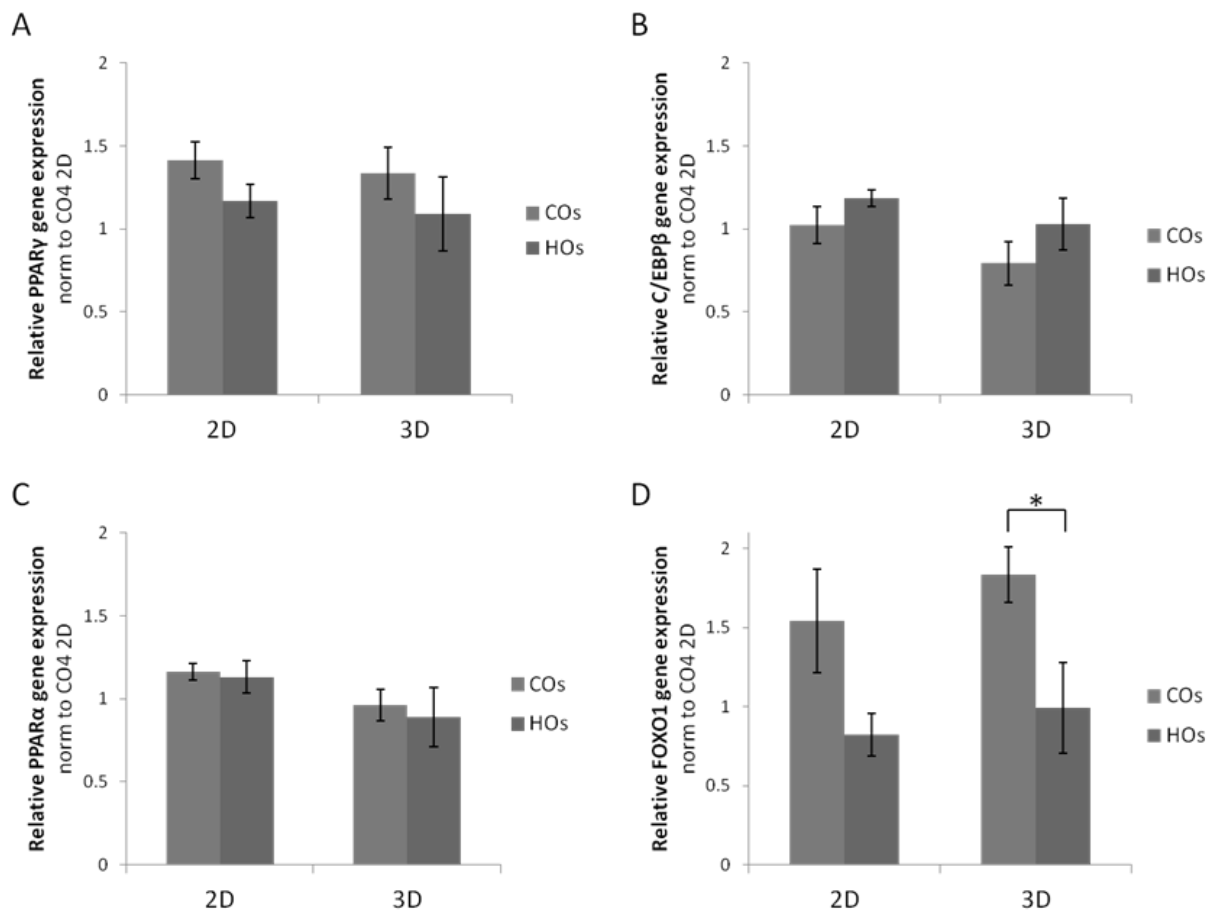


Figure 4. 1 3D cultured orbital fibroblasts do not exhibit increased adipogenic markers.

RNA samples were collected from orbital fibroblasts cultured in 2D and 3D gels for 7 days. Gene expression levels of (A) PPAR γ (B) C/EBP β (C) PPAR α (D) FOXO1 obtained by real-time PCR (qPCR) were normalised to GAPDH and then referred to the mean level of CO4 in 2D. Shown are mean \pm SEM, averaged from 3 control cell lines (COs: CO4, CO6, CO7) and 3 TED cell lines (HOs: HO1, HO2, HO4). (* $p < 0.05$, by t-test; $n \geq 3$).

4.2.2. Lipid droplet generation depends on substrate rigidity

Previously published work by the Bailly lab shows increased lipid droplet production in orbital fibroblasts cultured in 3D collagen matrices. 3D collagen matrix provides orbital fibroblasts not just with the (evident) growth conditions in 3D but also a much softer mechanical environment than plastic or glass, crucial for normal fibroblast differentiation and growth. Here, we aim to investigate whether cell culture in 3D or softer mechanistic environments contribute to lipid droplet generation in orbital fibroblasts and if softer mechanistic substrates may contribute to GO progression. To assess orbital fibroblast ability to generate lipid droplets when cultured on different mechanistic substrates we used polyacrylamide/bisacrylamide-layered (PAA/bisAA) coverslips coated with soluble collagen where PAA/bisAA- formed meshwork determines the approximate mechanistic stiffness (Figure 4.2). We cultured CO and HO fibroblasts on coverslips for 3 days and stained for neutral lipid droplets. We found that droplet generation in control cells is reduced when cells are grown on stiffer substrates as opposed to softer. HO cells appear to retain their ability to produce lipid droplets under stiffer conditions as opposed to CO ($p < 0.001$) while both CO and HO cells produce lipid droplets at 1 kPa without a statistically significant difference. These findings indicate that softer mechanistic conditions and substrates are enough to induce lipid droplet production in both CO and HO orbital fibroblasts. HO fibroblasts appear to be less mechanistically sensitive.

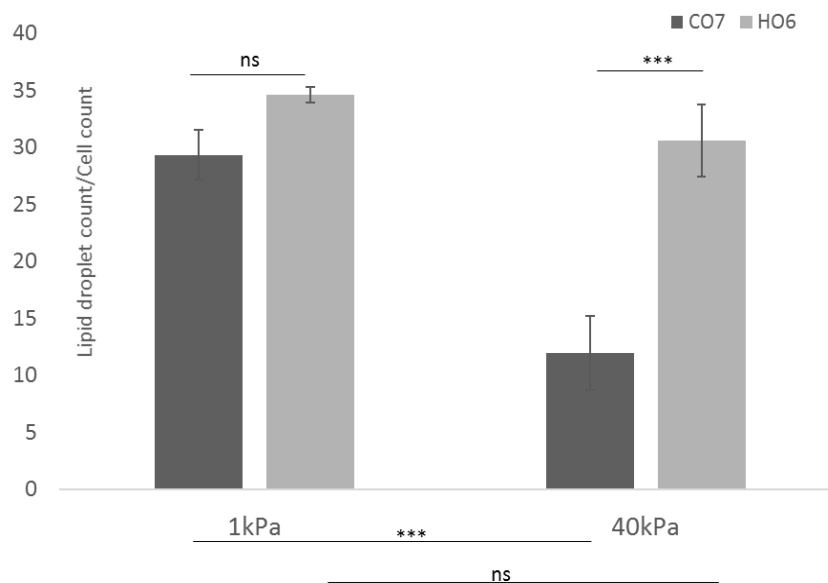
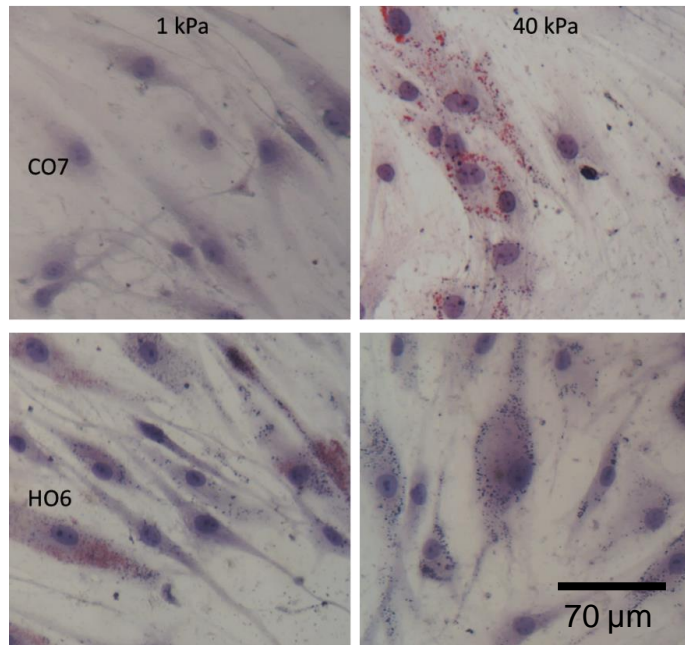


Figure 4. 2 HO retain lipid droplet generating potency when cultured on stiffer substrates.

HO6 and CO7 orbital fibroblasts were cultured on PAA/BisAA layered coverslips with soluble collagen coating (0.1 mg/mL) for 3 days, stained with Oil-Red-O and hematoxylin. Number of lipid droplets per cell were counted using ImageJ. Cells containing lipid droplets were counted as lipid droplet positive (ORO+). Data shown as mean \pm SEM, $n=3$, *** $p < 0.001$.

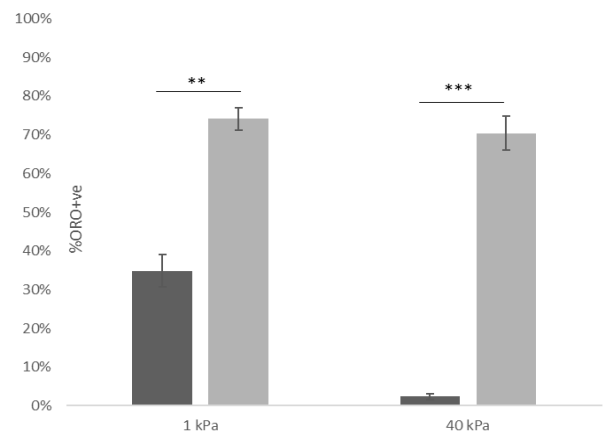
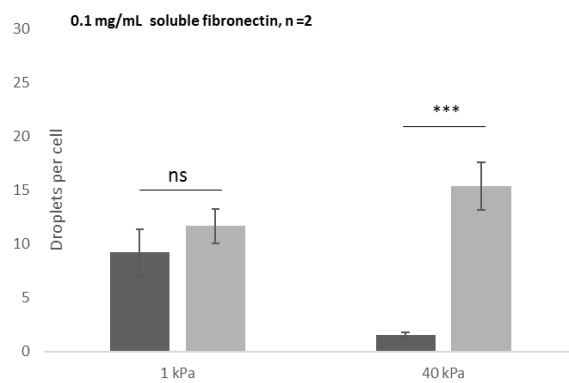
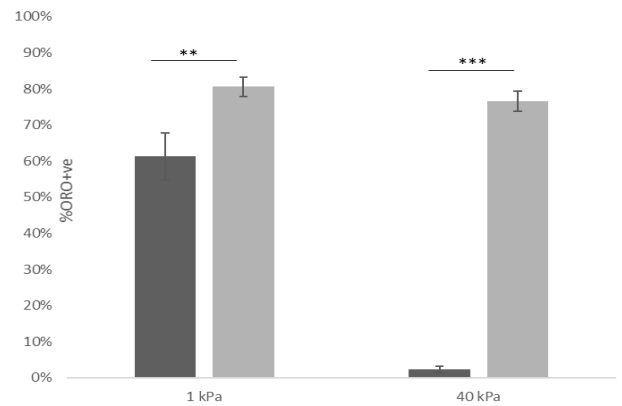
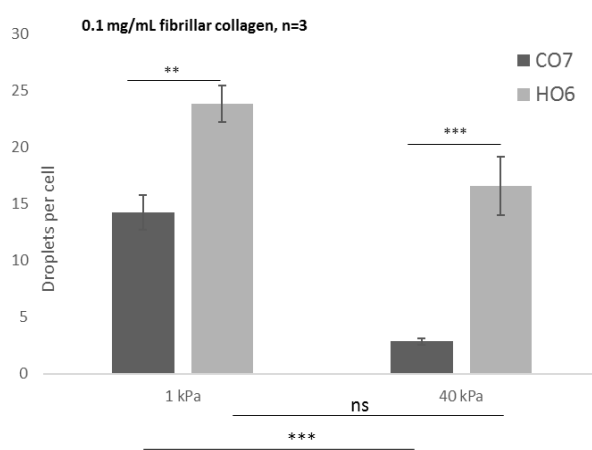
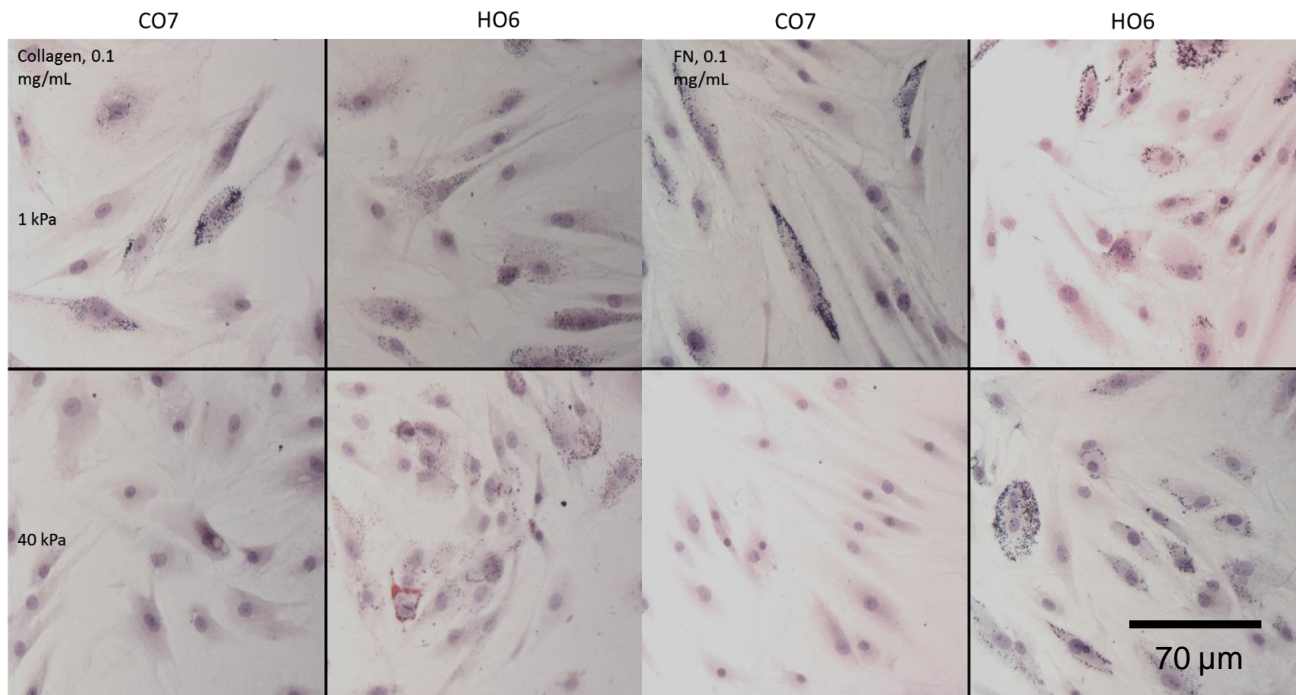


Figure 4. 3 Lipid droplet generation depends on mechanical substrate stiffness not protein coating

HO6 and CO7 orbital fibroblasts were cultured on PAA/BisAA layered coverslips with soluble fibrillar collagen or soluble fibronectin coating (0.1 mg/mL), for 3 days, stained with Oil-Red-O and hemotoxylin. Cells containing lipid droplets were counted as lipid droplet positive (ORO+). Data shown as mean \pm SEM, N = 2-3, n=3, ***p<0.001.

Soluble collagen used in the previous experiment differs in structure to fibrillar collagen which is structurally closer to ECM encountered in the soft tissue of the eye and also has been used in 3D cultures of previous experiments done by the Bailly lab. To determine whether different protein coatings have any influence on lipid droplet generation, we grew cells on PAA/bisAA layered coverslips coated with fibrillar collagen (0.1 mg/mL) and soluble fibronectin (0.1 mg/mL) for 3 days (Figure 4.3). There was no significant difference in the number of lipid droplets generated between CO and HO cells cultured on 1 kPa coverslips coated with fibronectin. HO cells retained their ability to generate lipid droplets at 40 kPa while in CO7, the number of lipid droplets was significantly reduced ($p < 0.001$). HO cells had a larger lipid- positive population ($p < 0.01$) when cultured on fibrillar collagen-coated coverslips and produced more lipid droplets at 1 kPa than CO ($p < 0.01$). Same as with soluble and fibrillar collagen cultures at 40 kPa CO cells produced significantly fewer lipid droplets and fewer lipid-positive cells were seen than in HO cultures ($p < 0.001$). We observed that cells cultured on fibrillar collagen and fibronectin-coated coverslips produce a slightly lower amount of lipid droplets in comparison to soluble collagen-coated coverslips indicating that the chemical composition of the substrate may play a secondary role in lipid droplet generation while mechanical rigidity of the growth environment has a primary role.

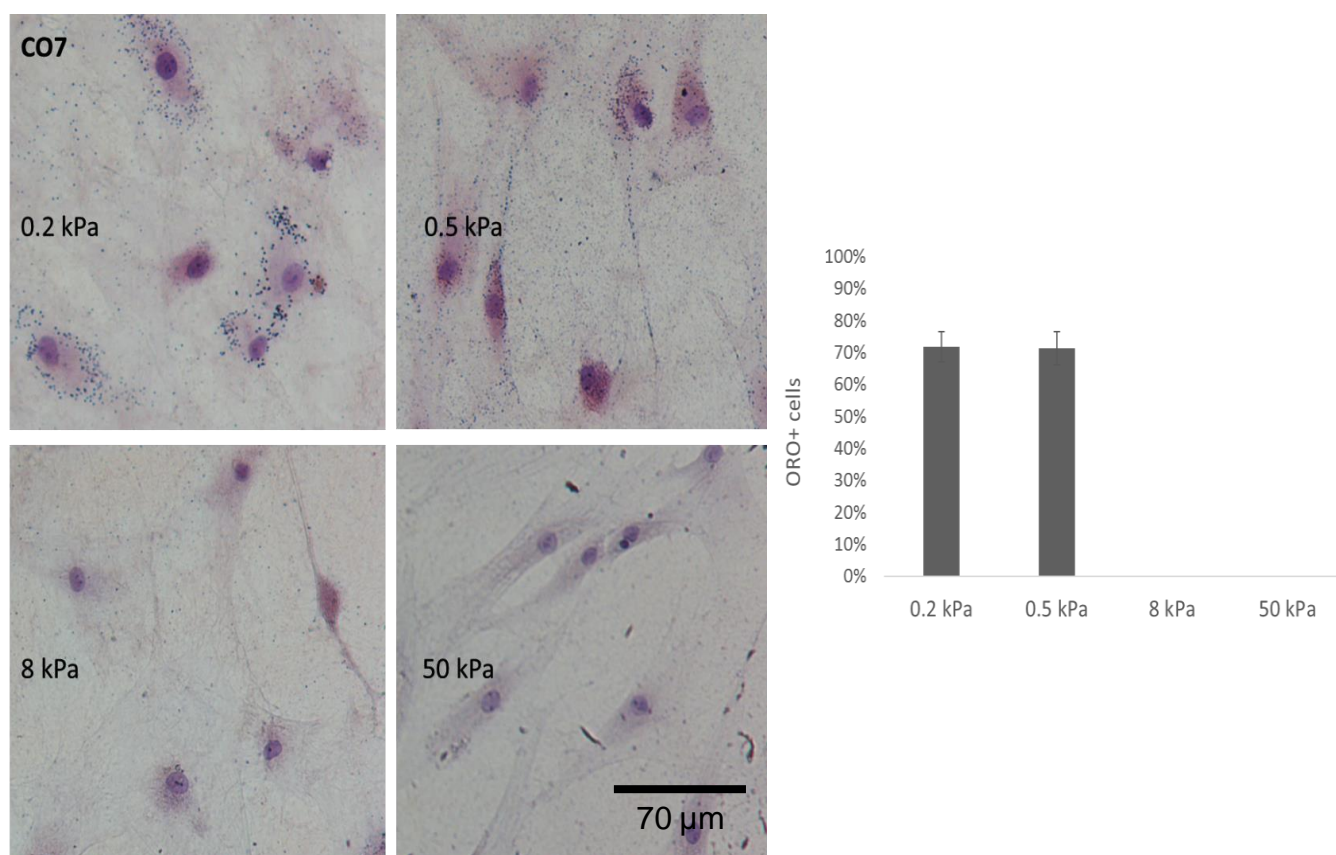


Figure 4. 4 Orbital fibroblasts generate lipid droplets when cultured on substrates whose stiffness is within the in vivo physiological range

Orbital fibroblasts were cultured on Softwell matrigen plates with pre-determined substrate stiffness and coated with 0.1 mg/mL soluble collagen for 3 days, stained with Oil-Red-O and hemotoxylin. Cells with clear cytoplasmic appearance lipid droplets were counted as lipid droplet positive (ORO+) while cells with little to none lipid droplets as negative. GO fibroblasts exhibited an adipogenic phenotype at 0.2 and 0.5 kPa substrate stiffness. Data shown as mean \pm SEM, $N = 2$, $n=2$, *** $p < 0.001$.

Next, we wanted to determine the peak mechanistic stiffness environment within which orbital fibroblasts generate the most lipid droplets. In previous experiments we generated coated coverslips manually, estimating Young's moduli through the concentration and amount of PAA and bisAA as described elsewhere (Tse & Engler, 2010; Vitiello et al., 2019) . To provide a clearer estimate of the stiffness range where orbital fibroblasts generate more lipid droplets; we used commercial Softwell polyacrylamide gels with

certified pre-determined mechanical stiffness. The rigidity of ECM within which orbital fibroblasts reside in vivo has been shown to be around 0.5 kPa. Therefore, we chose this as a test value. We also chose 0.2 kPa, 8 kPa and 50 kPa substrates for control rigidity. After coating the gels with soluble collagen, plating and culturing orbital fibroblasts on them for 3 days, we stained for neutral lipids with oil-red-O and counted cells with a cytoplasmic appearance of lipid droplets (Figure 4.4). We found that orbital fibroblasts generate lipid droplets at equal amounts at 0.2 and 0.5 kPa with no lipid droplets observed at cultured grown on 8 and 50 kPa. The number of lipid droplets generated did not increase at 0.2 kPa. These findings indicate that orbital fibroblasts generate lipid droplets within a mechanical rigidity range corresponding to that of orbital soft tissue.

4.2.3. Mechanosensitive lipid droplet generation is unique to orbital fibroblasts

We were able to show that orbital fibroblasts generate lipid droplets in response to softer substrates. Next, we wanted to determine if such behaviour is observed in fibroblasts from other anatomic origins residing in more rigid mechanistic environments. We chose tenon (HTF) and dermal (SS4) which in vivo reside in ~2 kPa and ~8 kPa respectively (Dulińska-Molak et al., 2014). Collagen gels using 2-3 mg/mL soluble collagen prior to polymerisation possess Young's modulus of <1 kPa (Cross et al., 2010).

We plated orbital fibroblasts (CO, HO), human dermal fibroblasts (SS4) and human tenon fibroblasts (HTF) on top of fibrillar collagen gels of different gel thickness in 24 well plates. In this model, we assume that the stiffness of gel surface decreases with increasing distance from the plastic well bottom (Buxboim, Rajagopal, Brown, & Discher, 2010; Mullen, Vaughan, Billiar, & McNamara, 2015). We used 200 uL collagen (2 mm thickness) and 50 uL collagen (<0.5 mm) and plastic with no collagen as a negative control and cultured cells for 3 days, staining them with Oil-Red-O for neutral lipids (Figure 4.5). All orbital fibroblasts showed an increased amount of lipid droplets (A) and lipid-positive cells (B) in comparison to on-plastic cultures. On 2 mm (200 uL collagen volume) gels HO fibroblasts had more lipid droplets and more lipid droplet positive cells than CO fibroblasts. We also saw an increasing amount of lipid positive cells, especially HO6, on plastic which was previously unseen. One possibility of lipid droplet appearance on

plastic is the increased cell confinement in a smaller well. We have not observed lipid droplet production in HO6 cells when grown in 6 well plates where cells are spread out and less concentrated. Dermal and tenon fibroblasts exhibited almost no lipid droplets, or lipid-positive cells in any of the gel conditions indicated that mechanosensitive lipid droplet generation is orbital fibroblast specific.

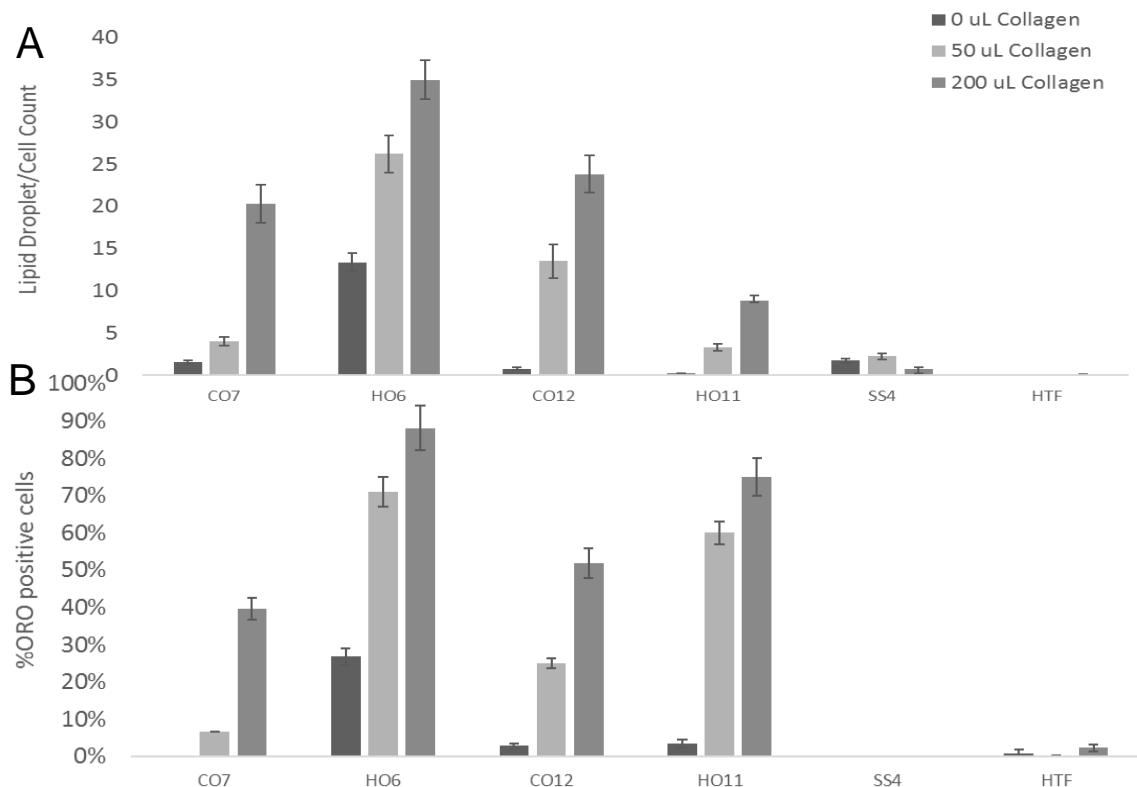
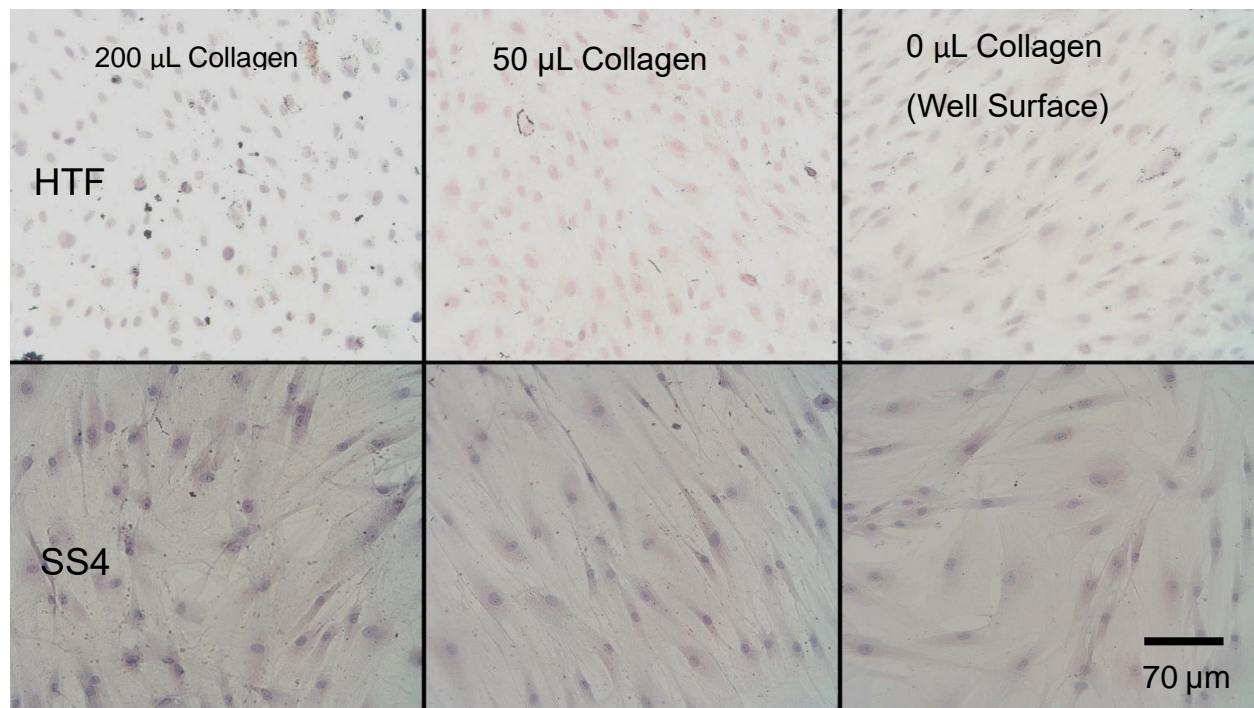


Figure 4. 5 Mechanosensitive lipid droplet generation is specific to orbital fibroblasts

Orbital dermal (SS4) and tenon (HTF) fibroblasts were cultured on plastic and collagen-coated (50 uL, 200 uL) wells for 3 days and stained for neutral lipids with Oil-Red-O. Amount of lipids was assessed with ImageJ and cells with clear cytoplasmic appearance lipid droplets were counted as lipid droplet positive (ORO+) while cells with little to none lipid droplets as negative. Data shown as lipid droplets per cell (A) and percentage of lipid positive cells (B), error bars – SEM, N = 3, n = 3.

4.2.4. Src and Fyn protein function on soft substrates the same as in 3D cultures

Cells cultured in 3D environments have a reduced number of focal adhesions and possess weaker attachment to their substrate. Src and Fyn have been shown to partake in focal adhesion formation with Src having particular importance. PTPN22 has been shown to contribute to various autoimmune illnesses, including GD and is a negative regulator of both Fyn and Src. In previous experiments, we demonstrated that FYN and PTPN22 knock-down in orbital fibroblasts decreases lipid droplet generation in 3D. We wanted to investigate if a similar trend is seen in soft gel cultures. We incubated HO6 orbital fibroblasts with 280 ng of siControl, siFyn, siPTPN22 for 72h and then cultured cells on 50 uL and 200 uL collagen-coated wells on 24 well plate. After 3 days, we stained the cells for neutral lipids with Oil-Red-O. Knock-down verified prior to cell culturing by Western Blot.

We observed that both PTPN22 and FYN knock-downs significantly reduce the number of lipid droplets generated when cultured on 50 uL gels (Figure 4.6). When cultured on 200 uL gels, PTPN22 knock-down produced a significant decline in the number of lipid droplets while FYN KD showed no significant change when compared to siControl treated cells. We compared the amount of FYN protein in lysates from siControl from cells cultured on plastic and on 200 uL collagen gels, and Fyn KD cells, and found that cell-cultured on gels have little Fyn expression when cultured on softer substrates. Using the same model, we assessed the effects of Src downregulation on orbital fibroblasts when cultured on collagen gels (Figure

4.7). We observed again that Src KD increases lipid droplet generation in cells cultured on plastic and also on 50 uL collagen, but no significant change was seen between Src KD and siControl- treated cells on 200 uL gels. These findings show that Src, Fyn and PTPN22 have the same function in cells grown in 3D and on soft substrates.

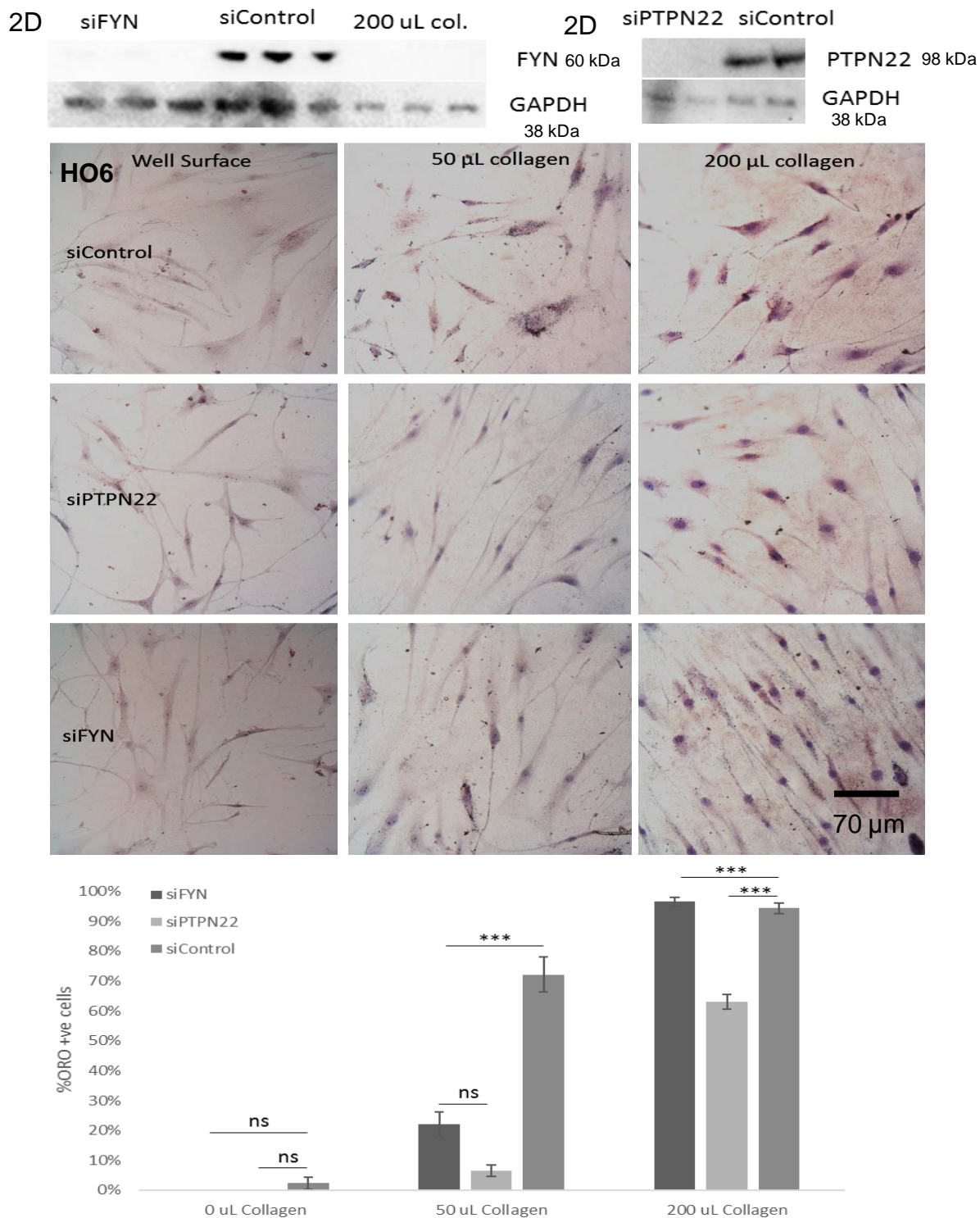


Figure 4. 6 FYN knock-down effect is lost in cells cultured on soft substrates.

CO7 orbital fibroblasts were incubated with 280 ng FYN, PTPN22 or siRNA for 72h and re-seeded on collagen-coated wells (50 uL, 200 uL) for 3 days and stained for neutral lipids. Knock-down verified by WB. Cells with clear cytoplasmic appearance lipid droplets were counted as lipid droplet positive (ORO+) while cells with little to none lipid droplets as negative (data shown as mean %ORO positive cells, +/- SEM, N = 3, n = 3)

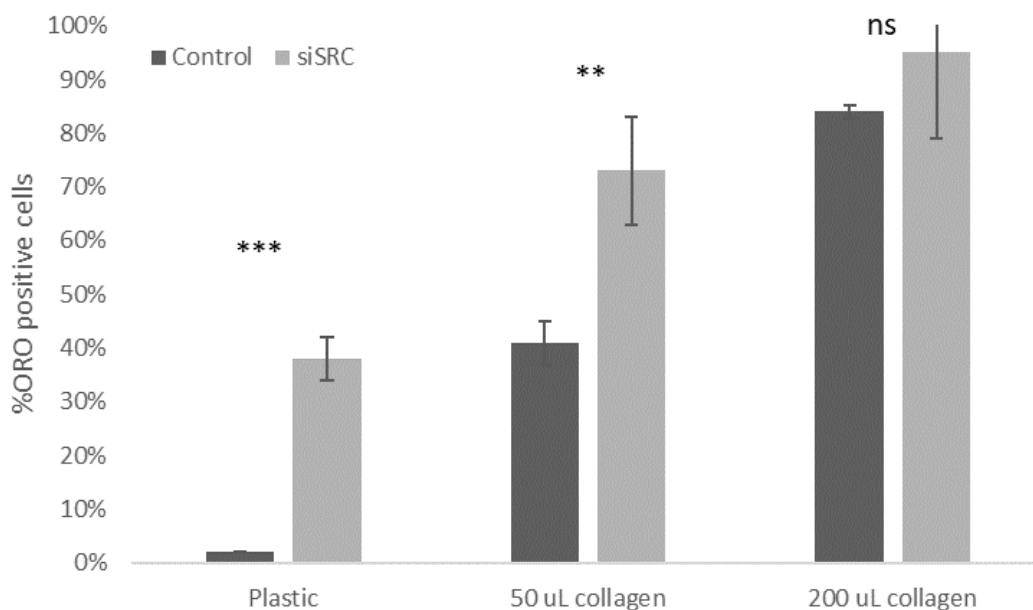
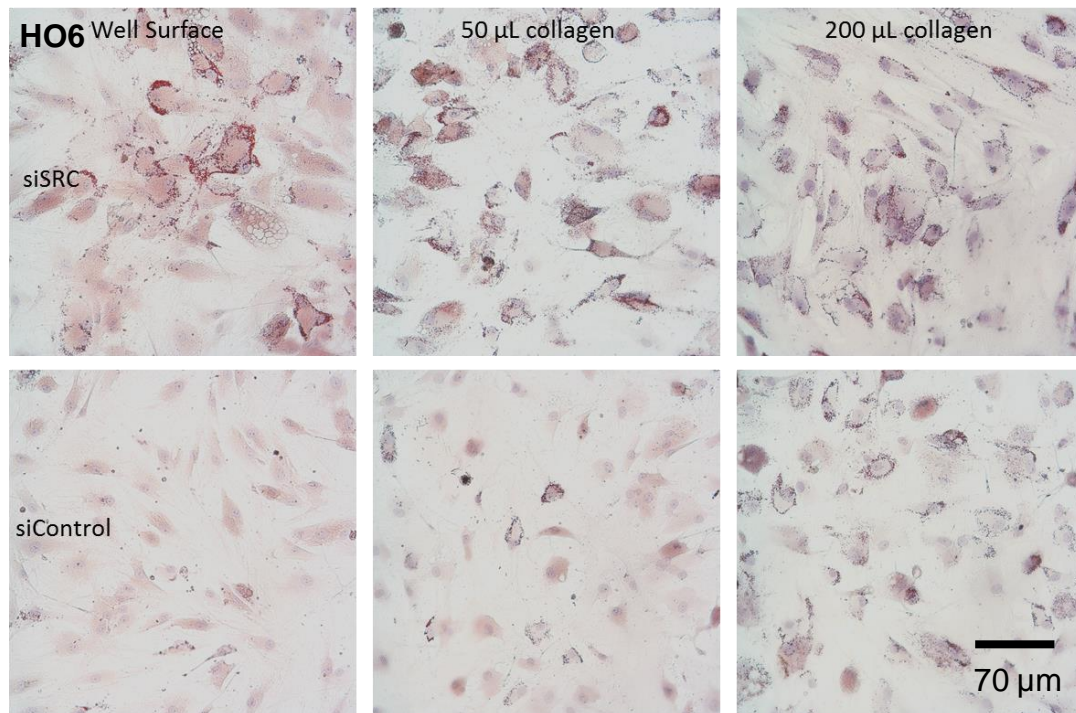


Figure 4. 7 SRC knock-down increases lipid droplet generation on stiffer substrates.

HO6 orbital fibroblasts were incubated with 280 ng SRC and control siRNA for 72h and cultured on collagen-coated wells (50 uL, 200 uL) for 3 days and stained for neutral lipids. Knock-down verified by WB (not shown). Cells with clear cytoplasmic appearance lipid droplets were counted as lipid droplet positive (ORO+) while cells with little to none lipid droplets as negative. Src knock-down increases lipid droplet generation on stiffer substrates while control (data shown as mean %ORO positive cells, +/- SEM, N = 3, n= 3).

4.2.5. Src and Fyn protein expression is lost in response to decreased substrate stiffness.

In previous experiments, we observed that Fyn protein is lost in cells cultured on soft substrates. We investigated if Src, PTPN22, mTORc1 protein quantity is affected by substrate rigidity. We cultured orbital fibroblasts on soluble collagen-coated Cytosoft silicone plates with certified substrate rigidity ranging from 64 kPa to 0.2 kPa and on 50 uL and 200 uL collagen gels. Cells were harvested and lysed on day 3 (Figure 4.8).

In cells cultured on Cytosoft plates (A) Fyn, Src and mTORc1 protein amounts were reduced proportionally to decreasing substrate rigidity. The same trend was observed in cells cultured in collagen gels with orbital fibroblasts cultured on 200 uL (B) gels showing no detectable bands for Fyn, Src or mTORC1.

PTPN22 protein (C) expression is also decreased in gels cultured on soft substrates, indicating that Src, Fyn and their regulatory pathways are downregulated in cells cultured on soft substrates.

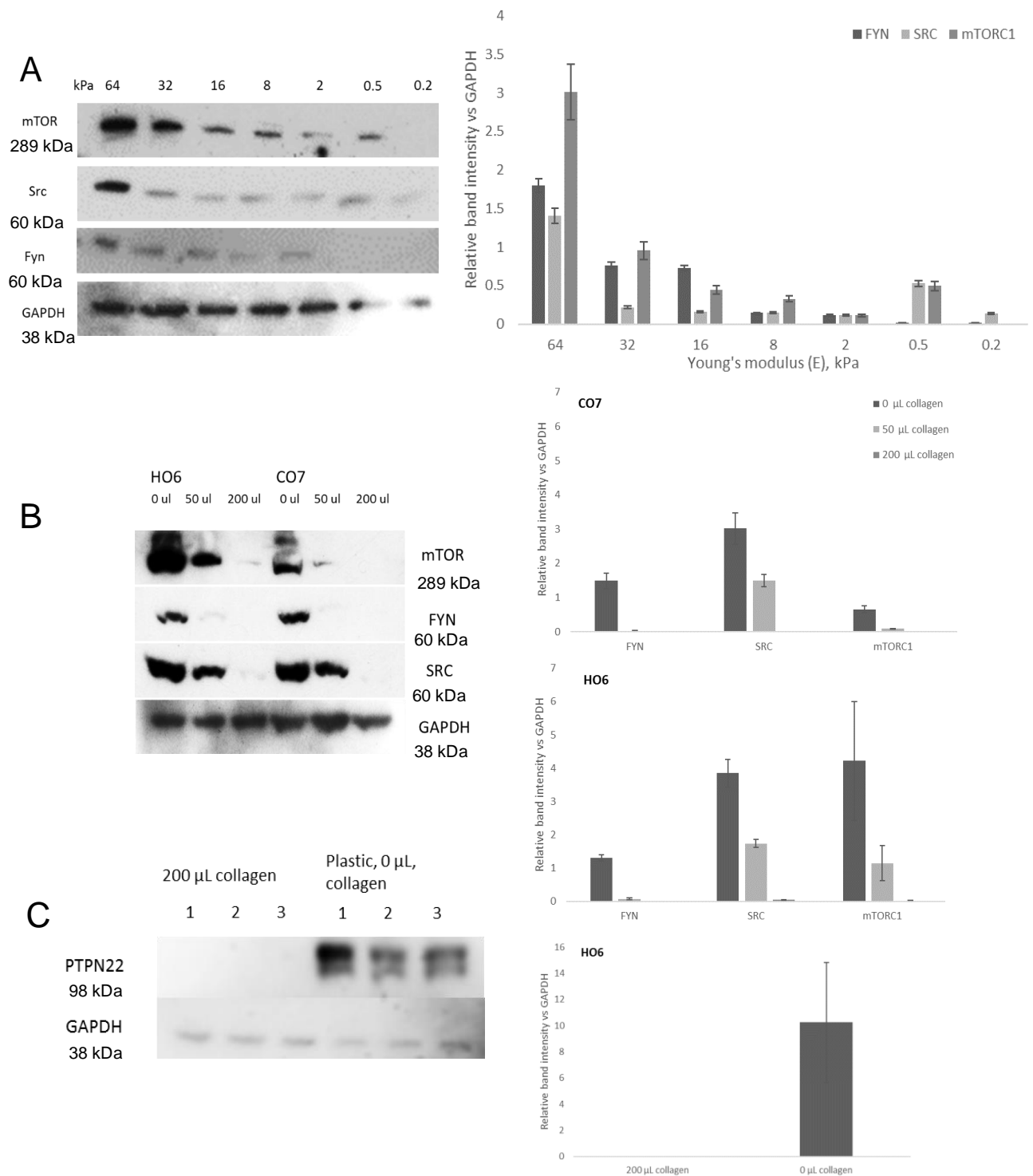


Figure 4. 8 Orbital fibroblasts lose SFK, PTPN22 and mTORC expression when cultured on softer substrates

Representative Western Blot images done with lysates from CO7 orbital fibroblasts. Orbital fibroblasts were cultured on Cytosoft well plates (A) or collagen-coated wells (B, C) for 3 days and then lysed. Protein content assessed by Western blot. Expression of PTPN22, Src, FYN and mTORC is significantly reduced in on stiff substrate cultures. Data shown as mean band intensity, normalised versus GAPDH, +/- SEM, N = 2, n ≥ 2.

4.2.6 Orbital fibroblasts increase AMPK activity and autophagy marker expression on soft substrates

Previously we demonstrated that Fyn knock-down increased AMPK activity. With Fyn downregulated on soft substrates, we wanted to determine if AMPK activity is changed. We probed lysates from standard and soft-cultured orbital fibroblasts for phospho- AMPK and AMPK content (Figure 4.9) (A). AMPK expression and activity are increased in soft- culture cells; however, AMPK active phosphorylation is present only in cells cultured on 200 uL gels. AMPK is a well-known activator of autophagy. Therefore we also investigated if cells cultured on soft substrates show autophagy marker presence. LC3b is a scaffold protein forming autophagosome membranes. We are able to show significant LC3b expression in cells cultured on soft substrates while in standard cultures, LC3b was nearly absent ($p < 0.001$). To confirm whether AMPK activity in orbital fibroblasts increases LC3b activity, we cultured orbital fibroblasts on plastic with added 5 mM salicylate to activate AMPK. Cell lysates from cells incubated with salicylate show an increased LC3b II presence which indicates its incorporation in the autophagosome membrane (Mizushima & Yoshimori, 2007).

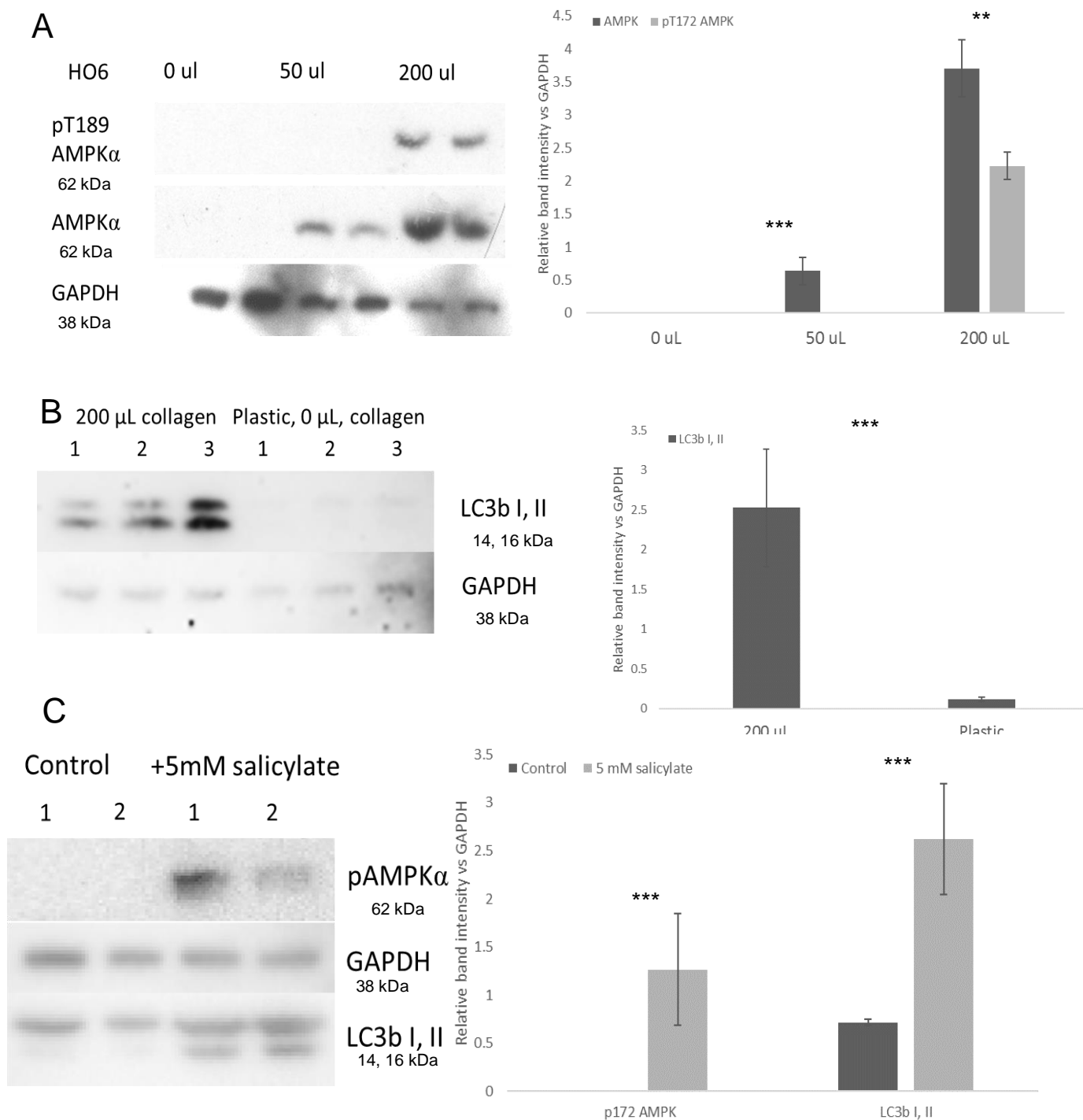


Figure 4. 9 Soft substrate culturing increases AMPK activity and expression of autophagy markers.

Western blot images showing (A) total and phospho- T172 AMPK (B) LC3b I, II in lysates from orbital fibroblasts cultured on collagen gels, (C) phospho- T172 AMPK amount in orbital fibroblasts cultured on plastic with 5 mM salicylate incubation. Cell culture on soft substrates and treatment with salicylate increases autophagy marker expression. Data shown as mean band intensity \pm SEM, N = 2, n = 2-3.

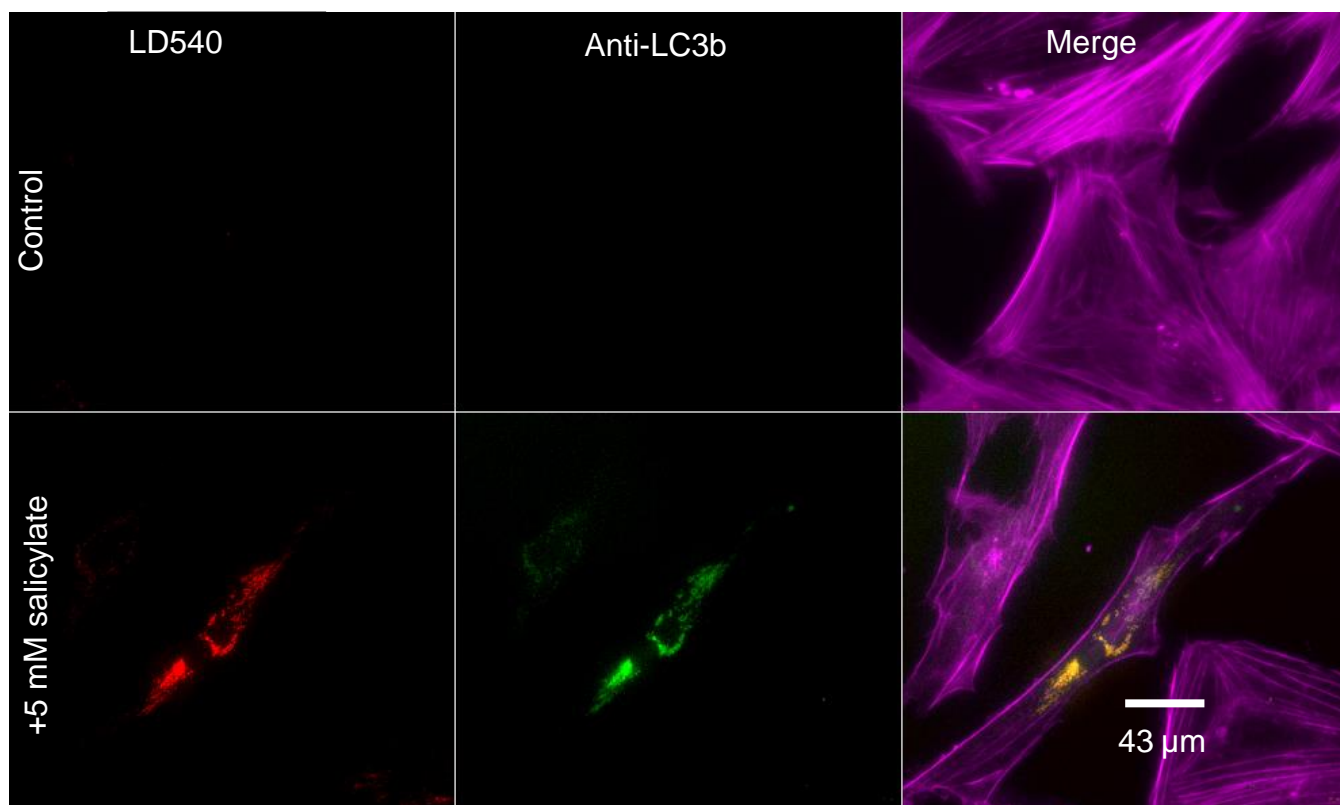


Figure 4. 10 LC3b expression and co-localisation with lipid droplets increases with increased AMPK activity.

Orbital fibroblasts were plated on glass coverslips and incubated with 5mM salicylate for 3 days, fixed and co-stained with LD540 (TRITC) for lipid droplets and with anti-LC3b (Rabbit, Alexa488, FITC). Imaged with fluorescent microscopy. AMPK activation with salicylate increases lipid droplet generation and localises LC3b, an autophagy marker to the lipid droplets.

In order to clarify if LC3b is present in orbital fibroblasts when incubated with sodium salicylate, we stained plated CO7 cells on coverslips and incubated with 5 mM salicylate for 3 days. We performed dual staining of control and salicylate samples with LD540, a fluorescent, BODIPY-derivate lipid stain and with ant-LC3b antibody (Figure 4.10). We were able to show that lipid strongly-colocalise with antibody staining, indicating that lipid droplet might be of autophagosome origin.

Previously we were able to show that active and phosphorylated pY418 SRC localises to the termini of stress fibres when cultured on coverslips.

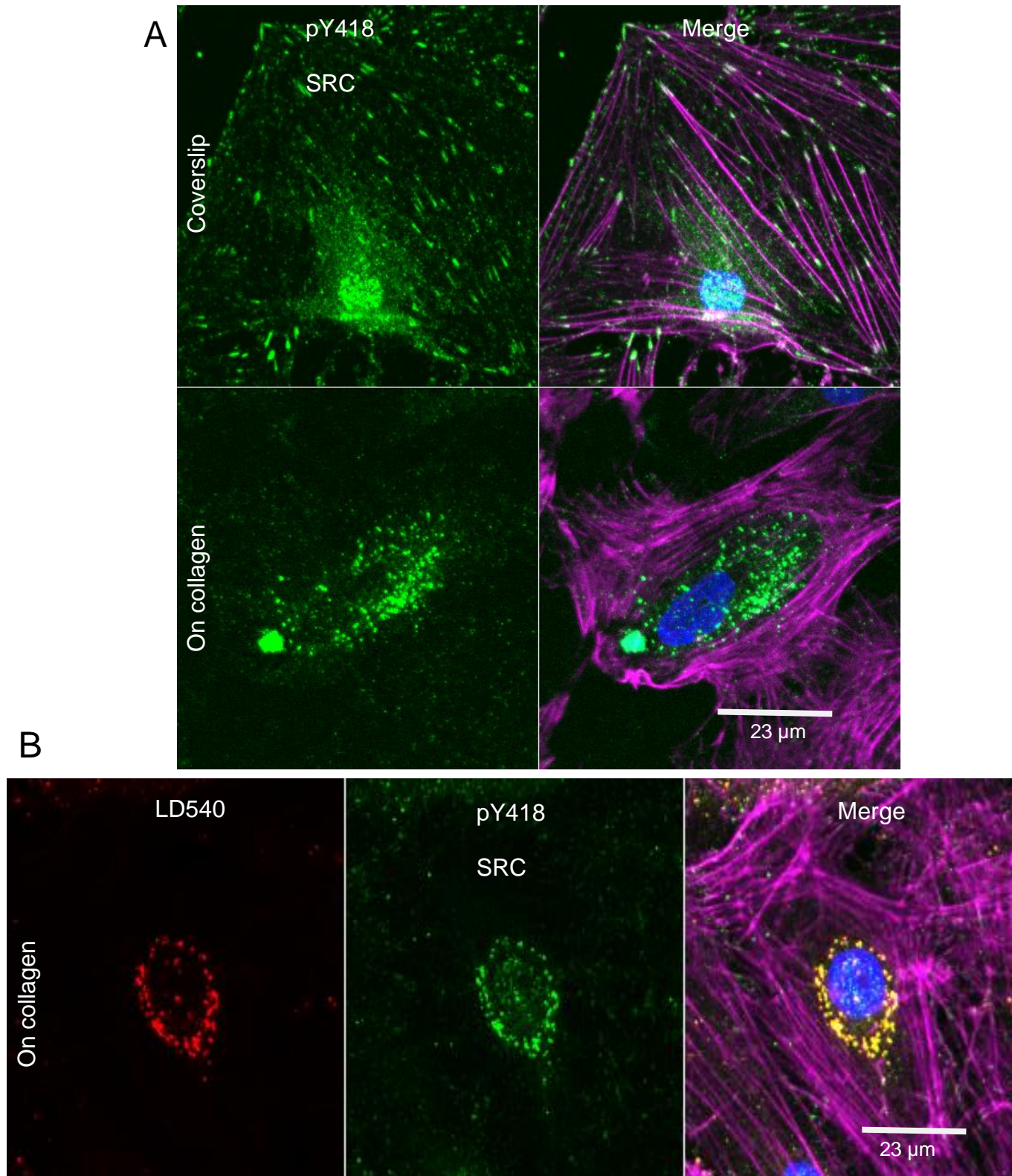


Figure 4 11 pY418 SRC re-locates to perinuclear space and co-localises with lipid droplets in orbital fibroblasts cultured on soft substrates.

CO orbital fibroblasts were seeded on glass coverslips and collagen gels, fixed and stained for (A) active SRC (pY418) and (B) lipid droplets (LD540), and imaged with confocal microscopy, nuclear staining with DAPI (blue), actin fibres stained with rhodamine/Alexa 647 (changed to magenta for clarity).

To investigate if Src is present at stress fibre termini in soft substrate cultures, we plated CO7 fibroblasts on coverslips and collagen gels for 3 days (Figure 4.11), fixed and stained with anti- pY418 Src (A) and additional LD540 (B), imaged with confocal microscopy. On rigid substrates localisation of pY418 Src to stress fibre termini is clearly visible while in cells cultured on soft gels pY418 Src localises to the perinuclear space. We performed immunofluorescent staining for vinculin on both soft and rigid substrates (not shown) where the presence of vinculin at stress fibre termini was clearly present. In soft gel cultures, vinculin was completely absent pY418 Src in soft gel cultures appears to co-localise with lipid vesicles and away from stress fibre termini, indicating its disassociation from focal adhesions. In cells cultured on coverslips, pY418 Src also appears in the nucleus. This effect is reduced when cells are cultured on soft substrates. We have not been able to explain this observation.

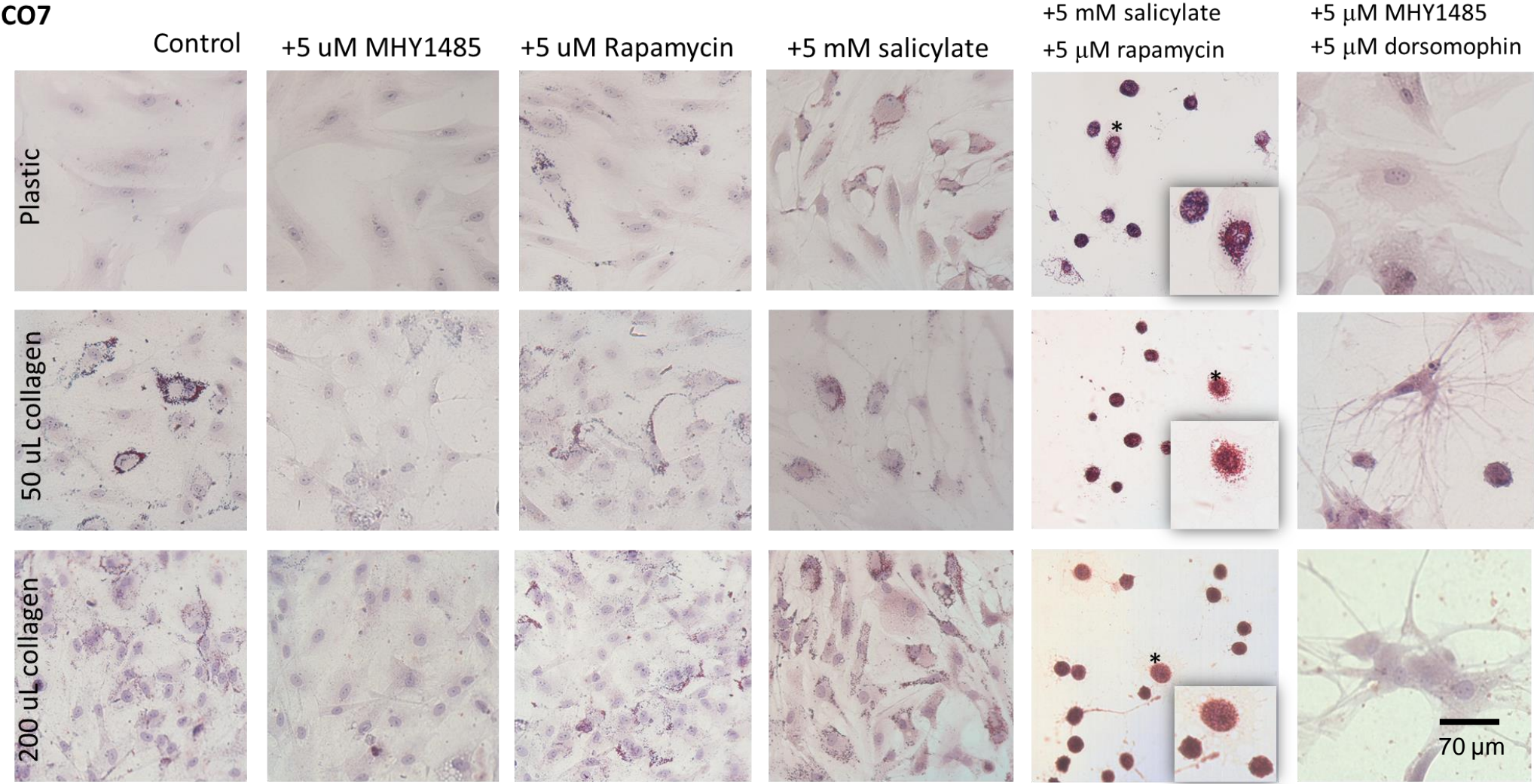
4.2.7 AMPK and mTORc1 regulated lipid droplet generation

Our previous findings suggest that lipid droplet generation is dependent on Src and Fyn activity which is lost when cells are cultured in mechanistically softer environments. Fyn and Src are both implicated in mTORc1 and AMPK regulation which together form a signalling axis regulating lipid breakdown and the onset of autophagy. Therefore we investigated how lipid droplet generation is affected by the altered status of mTORc1 and AMPK.

We cultured CO7 and HO6 orbital fibroblasts on plastic, 50 μ L and 200 μ L collagen gels for 3 days with 5 μ M MHY1485 (mTORc1 activator), 5 μ M rapamycin (mTORc1 inhibitor), 5 mM salicylate (AMPK activator) and 5 μ M

dorsomorphin. AMPK and mTORc1 have been described to regulate each other's activity. We wanted to mimic this signalling process by combining the aforementioned inhibitors and activators in functional pairs with salicylate and rapamycin as AMPK activity promoting and MHY1484 and dorsomorphin as mTORc1 activity fortifying pairs. After 3 days, cells were stained for neutral lipids with Oil-Red-O and counted cells with a cytoplasmic appearance of lipid droplets as ORO positive. In both cell lines, cultures incubated with MHY1485 showed a significantly decreased amount of lipid droplets in all stiffness conditions. Rapamycin incubation increased lipid droplet generation in cells cultured on plastic and on thinner gels while on 200 uL gels caused different outcomes in CO7 and HO6 cells. In soft gel cultures, rapamycin-induced a significant drop in ORO positive CO7 cells while in HO6 cultures, lipid-positive cell count remained similar to control. Interestingly, salicylate increase lipid droplet generation under all rigidity conditions. In cells cultured on plastic, this effect was more pronounced in CO7 cells. Dorsomorphin treatment (not shown) caused an absence of lipid droplets in both cell lines and all conditions.

C07



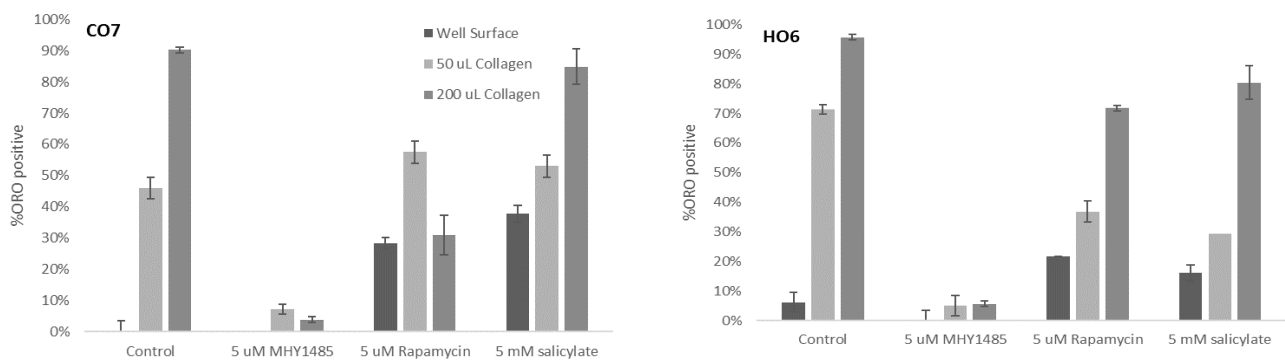


Figure 4. 12 AMPK and mTORC activity alter lipid generation and morphology in orbital fibroblasts

Orbital fibroblasts were cultured on plastic and collagen coated wells and incubated with rapamycin (5 uM), MHY1485 (5 uM), salicylate (5mM), dorsomorphin (5 uM) and combined dorsomorphin/MHY1485 and salicylate/rapamycin for 3 days. Cells were stained for neutral lipids with Oil-Red-O. Cells with clear cytoplasmic appearance lipid droplets were counted as lipid droplet positive (ORO+) while cells with little to no lipid droplets as negative. Orbital fibroblasts generate lipid droplet in response to decreased mechanical stiffness while dermal and tenon fibroblasts remain lipid-negative under all conditions. Data shown as mean percentage of lipid positive cells +/- SEM, N = 3, n = 3.

Combined salicylate/rapamycin and dorsomorphin/MHY1485 treated cultures caused a significant change in cell morphology. Salicylate/rapamycin treatment reduced cell size while still retaining attachment to the substrate. After ORO staining, both CO7 and HO6 cells appeared to filled with lipids. Using a functionally opposite pair of dorsomorphin/MHY1485 caused orbital fibroblasts to become expansive and to generate more protrusions without a noticeable cytoplasmic presence of lipid droplets.

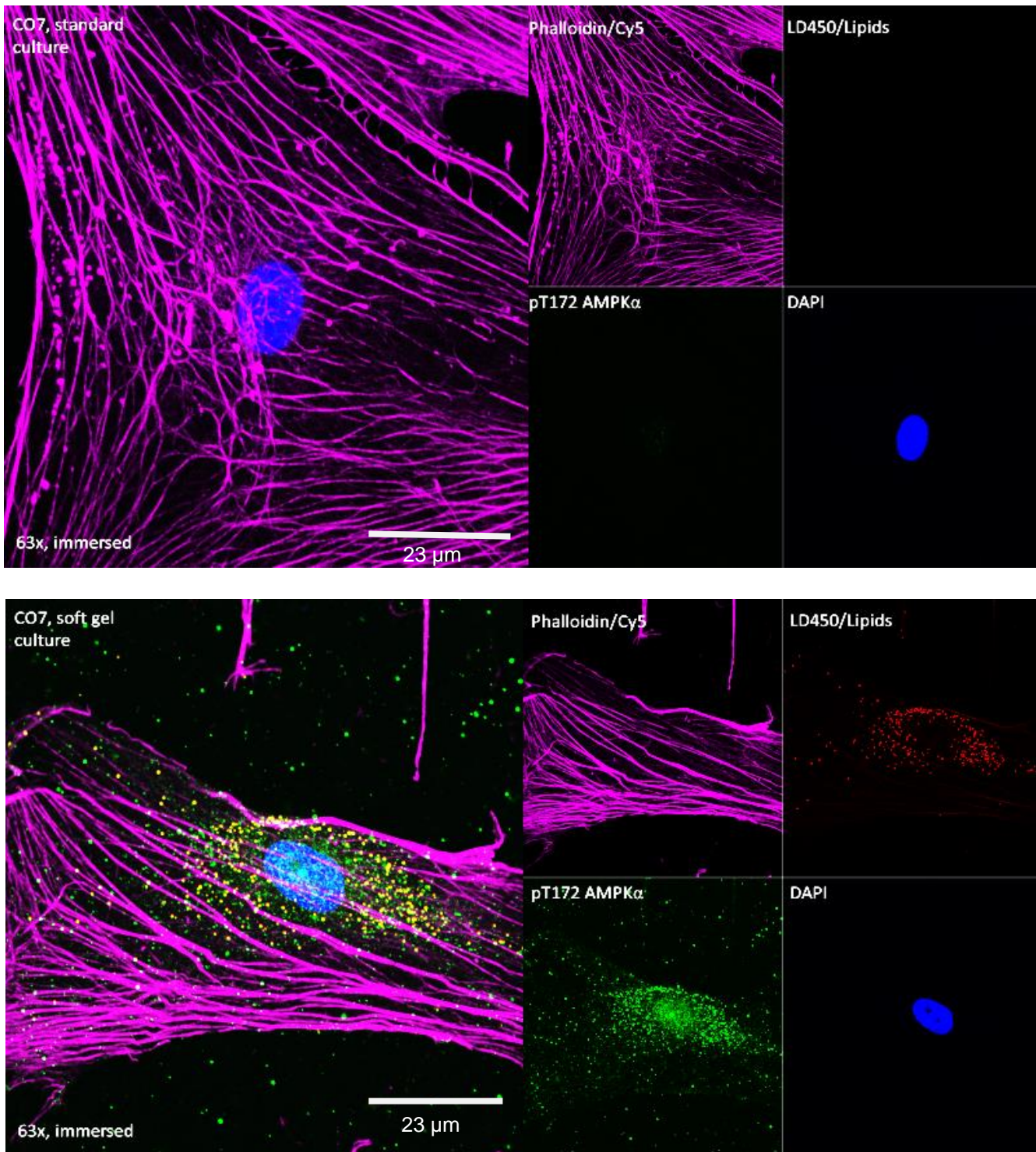


Figure 4. 13 Phospho-AMPK localises to lipid droplets in soft gel cultures.

CO7 orbital fibroblasts were grown on collagen gels for 3 days, fixed and stained for lipid droplets with LD540 (TRITC) and phosphor-AMPK with anti -pT172 AMPK rabbit antibody (FITC). When cultured on rigid (plastic) substrates (top) do not form lipid droplets and have no phospho- AMPK activity. Soft gel cultures show lipid droplet build-up in the cytoplasm to which pAMPK appears to localise to. Imaged with Zeiss 710 confocal microscope.

Literature data suggest that AMPK co-localises with lipid droplet to phosphorylate perilipins, a group of lipid droplet scaffolding proteins which prevent them from breakdown. It has been proposed that AMPK phosphorylates perilipin – 2 (PLIN2) which primes it for degradation. Therefore, we wanted to investigate if AMPK localises to lipid droplets when orbital fibroblasts are cultured on soft substrates. We plated CO7 orbital fibroblasts on glass coverslips and 200 uL collagen gels for 3 days, fixed the cells and stained them with LD540 for lipid droplet presence and with anti-pT172 AMPK (Fig). Cell grown on glass coverslips (Fig 4 13, top) showed no lipid droplets or phospho-AMPK confirming our previous findings. When grown of soft substrates, cells exhibited a cytoplasmic presence of lipid droplets which co-localised with phospho-pT172 AMPK.

4.2.8 AMPK and mTORc1 regulate orbital fibroblast contractility

We assessed orbital fibroblasts contractility in the presence of rapamycin, salicylate and MHY1485. We embedded CO7 and HO6 orbital fibroblasts in collagen gels and imaged gels daily for 5 days assessing gel contractility with ImageJ.

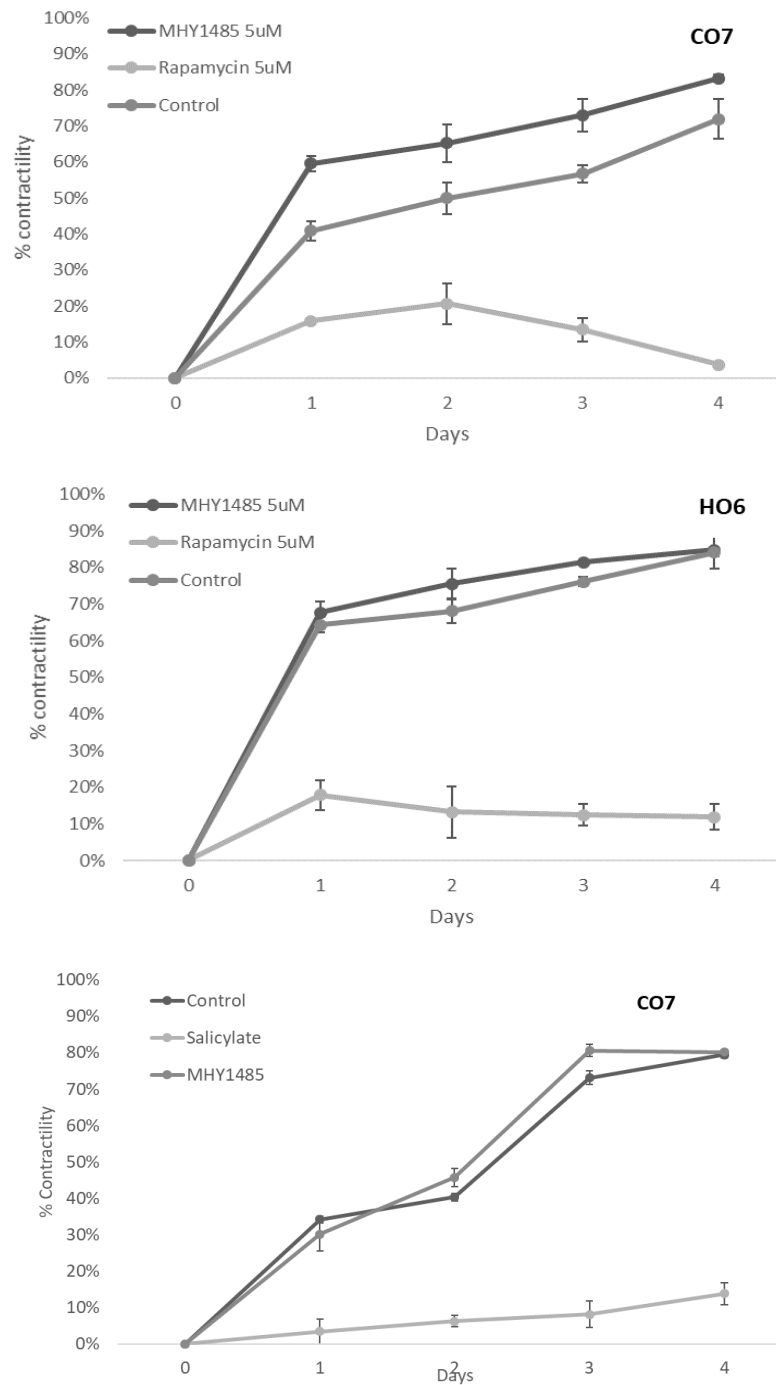


Figure 4. 14 mTORC1 and AMPK inhibition reduce orbital fibroblast contractility.

Orbital fibroblasts were embedded in collagen gels and incubated with 5 uM rapamycin, 5 uM MHY1485 or 5 mM salicylate for 5 days with contractility assessed by daily imaging and assessed by measuring gel size with ImageJ. Cell treatment with rapamycin and salicylate reduces cell contractility significantly. Data shown as gel perimeter reduction over 5 days +/- SEM. N = 2, n =3.

Both CO7 and HO6 cells exhibited much slower contractility when incubated with salicylate and rapamycin. MHY1485 appears to increase the rate of contractility initially but does not increase contractility itself. These findings indicate that AMPK activity decreases fibroblasts contractility while mTORc1 activity is necessary for orbital fibroblasts to contract.

4.2.9. PLIN2 localisation to lipid droplets requires AMPK

In experiments completed by Dr I-Hui Yang, Perilipin-2 (PLIN2) was identified as a marker of lipid droplets encountered in 3D cultured fibroblasts. Her findings show an increase of PLIN2 protein content in CO7 when cultured in 3D, while the difference in HO6 cells was not statistically significant. However, PLIN2 knockdown decreased lipid droplet formation in 3D. We were able to show that when cultured on glass, orbital fibroblasts PLIN2 has a diffuse cytoplasmic appearance. Culturing orbital fibroblasts on soft mediums co-localises lipid droplets with PLIN2. Interestingly, PLIN2 appears to be luminal, inside of the lipid droplets while its nature as a scaffolding protein should localise it to the membrane, i.e., appear around the droplet not inside. Furthermore, when cells in soft cultures were treated with 5 μ M dorsomorphin to inhibit AMPK activity, PLIN2 to its cytoplasmic appearance, similar to our observation of cells cultured on glass coverslips.

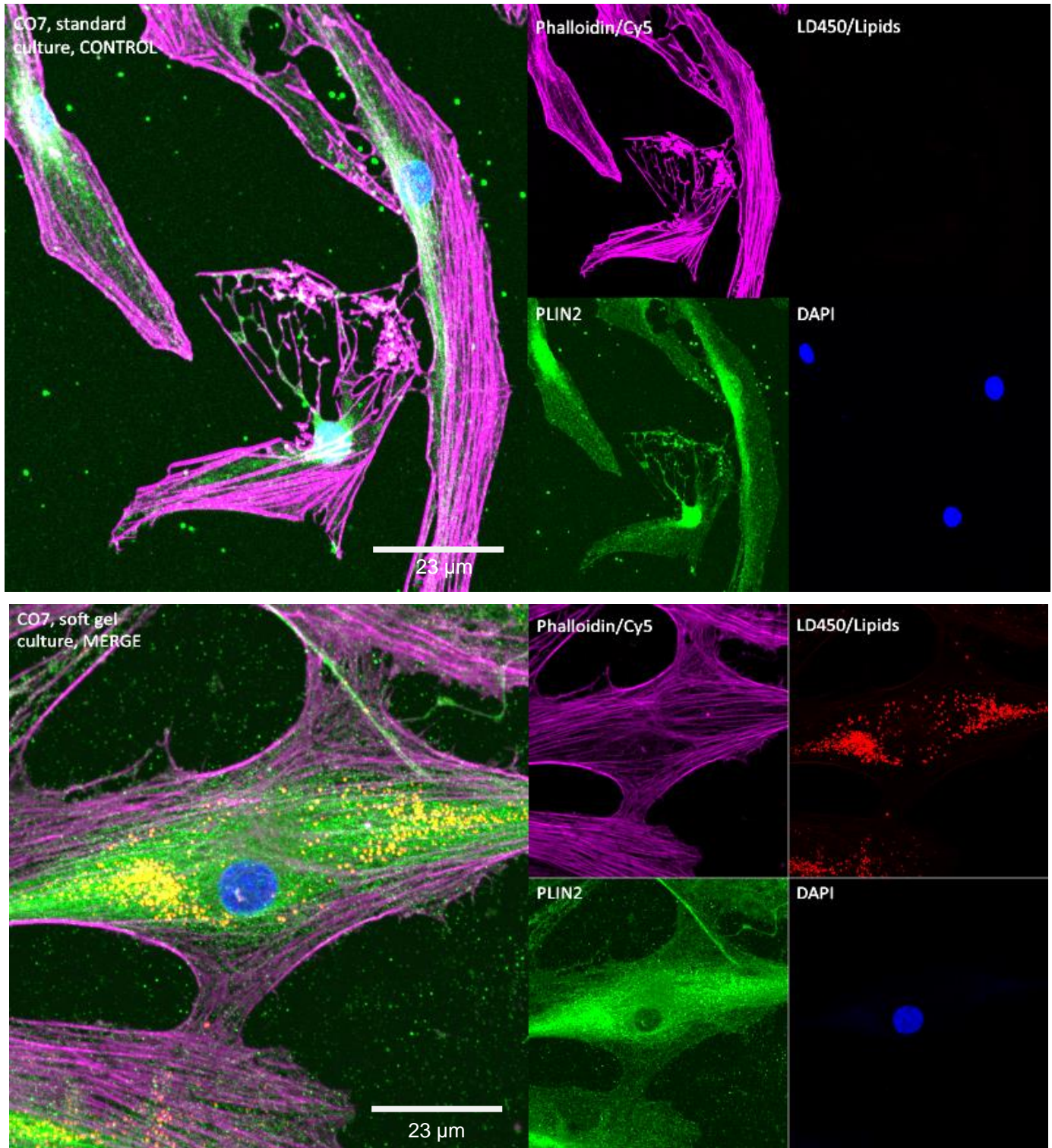


Figure 4. 15 PLIN2 localised to lipid droplets in cells cultured on soft substrates

CO7 orbital fibroblasts were plated on collagen gels and glass coverslips for 3 days. Gels were fixed, compressed and stained with anti-PLIN2 (Rabbit, Alexa488) and LD540 for neutral lipid staining (TRITC) and with rhodamine (magenta) for actin fibres. Imaged with Zeiss 710 confocal microscope. PLIN2 is present in the cytoplasm in both rigid and soft gel cultures but localised if lipid droplets are present.

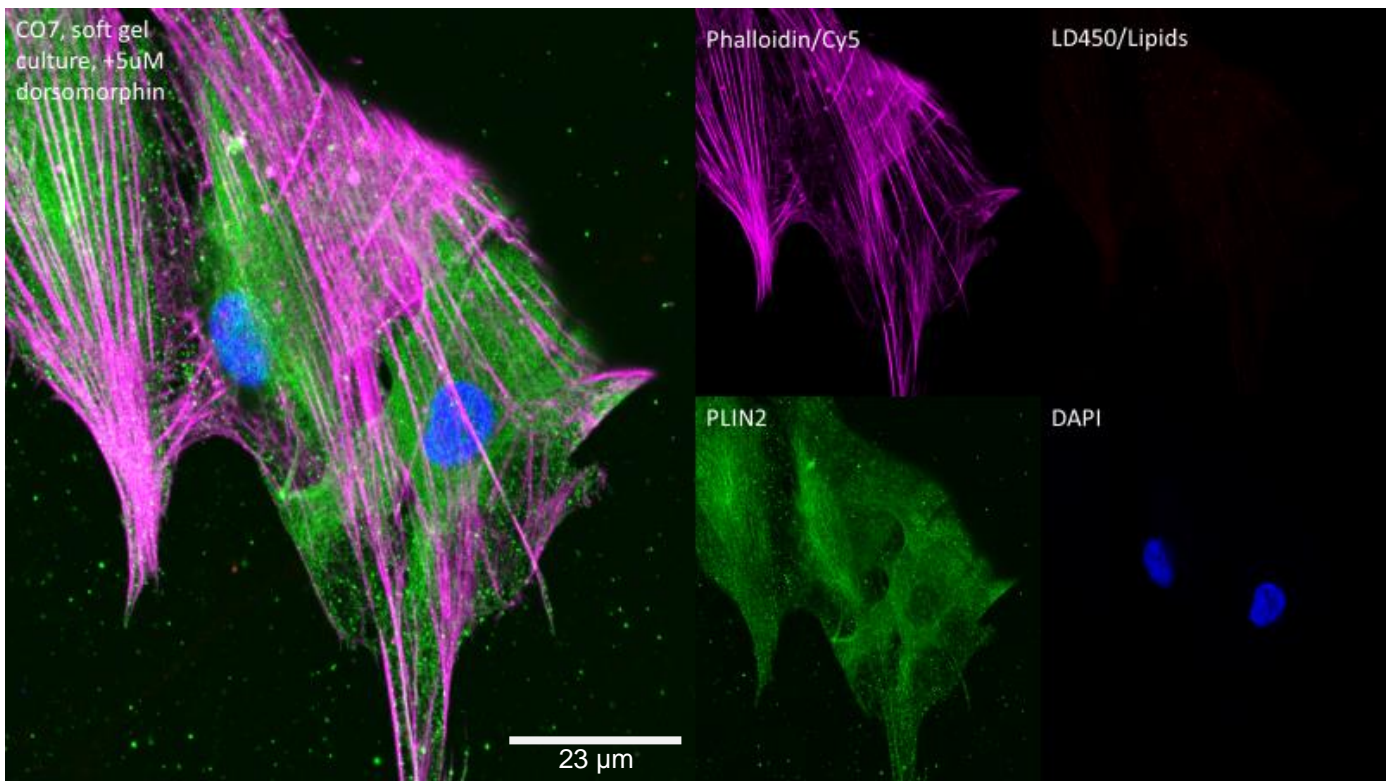


Figure 4. 16 AMPK activity is necessary for PLIN2 localisation to lipid droplets.

CO7 orbital fibroblasts cultured on soft substrates were incubated with 5 uM dorsomorphin for 3 days , fixed and stained for lipid droplets with LD540 and PLIN2 with anti-PLIN2 rabbit antibody. Blocking AMPK activity reduced the amount of lipid droplets present in soft cultures and retaining PLIN2 in the cytoplasm.

4.2.10. Disruption of autophagosome maturation prevents lipid droplet formation

To further elucidate the nature of lipid droplets and their relation to autophagy, we cultured orbital fibroblasts on fibrillar 50 uL and 200 uL collagen gels with standard culture as control treated with 5 mg/mL chloroquine. Chloroquine is used to inhibit autophagy by preventing autophagosome and lysosome fusion, although a concrete mechanism of action has not been shown. Chloroquine-mediated inhibition appears to disrupt lipid droplet formation. However, diffuse ORO staining was still present in cellular cytoplasm, irrespective of stiffness conditions. We repeated the experiment with only 200 uL collagen gels and stained cells with fluorescent lipid dye LD540 additionally using 5 uM MHY1485 as a positive control. In the control cultures, clear cytoplasmic lipid droplets can be seen, while in cells treated with chloroquine lipids are cytoplasmic and delocalised.

To confirm these findings, we used a more potent autophagy inhibitor, bafilomycin A1 which inhibits autophagosome and lysosome specific protons pumps, preventing their acidification at concentrations as low as 5 nM. Orbital fibroblasts treated with 10 nM bafilomycin A1 for 3 days and cultured on 200 uL collagen gels exhibited significantly less lipid droplet positive cells while also reducing the overall amount of cells, indicating toxicity.

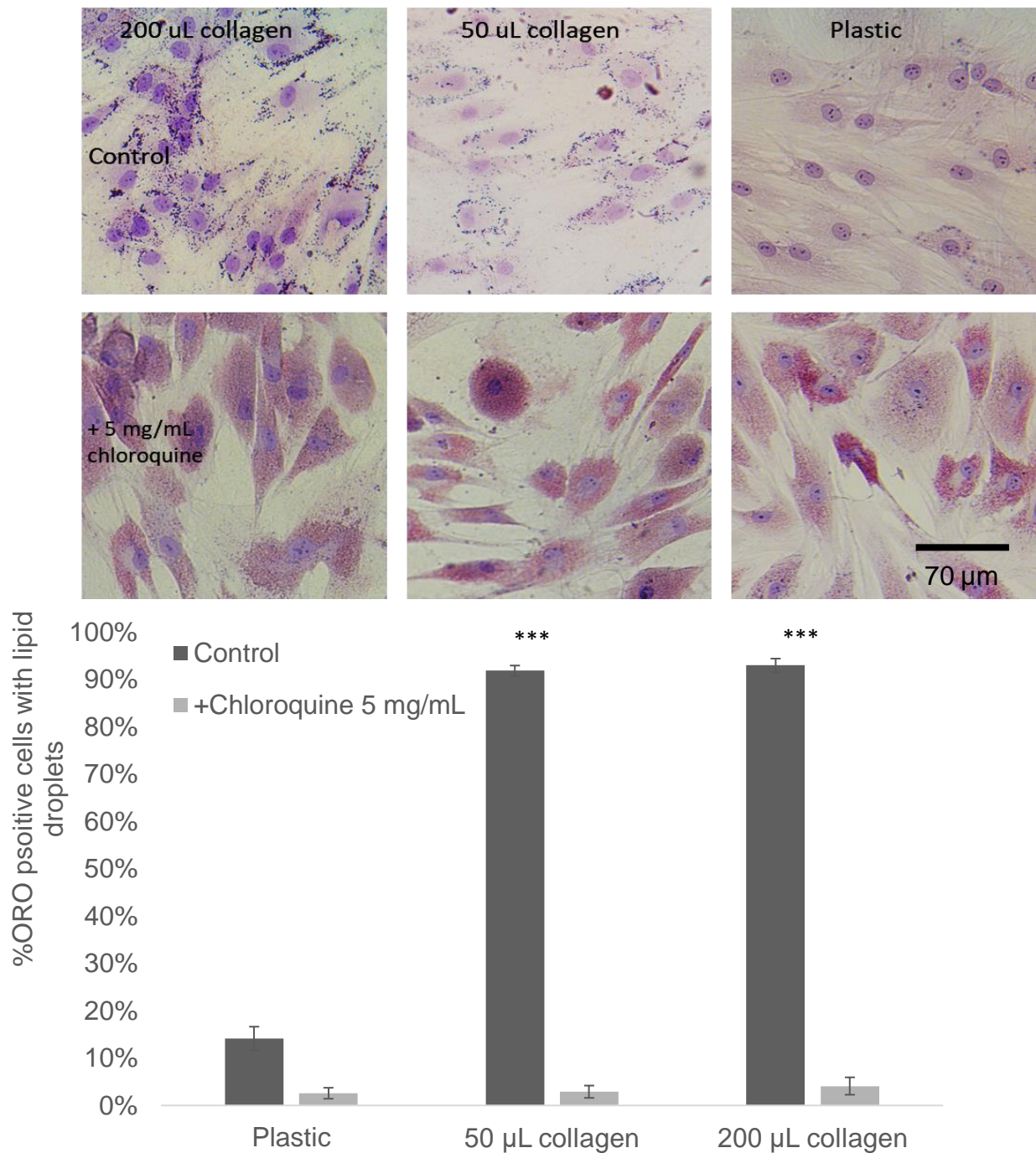


Figure 4. 17 Autophagosome inhibition abolishes mechanosensitive lipid droplet formation

HO6 orbital fibroblasts were cultured on collagen gels with or without 5mg/mL chloroquine for 3 days and stained for neutral lipids with Oil-Red-O. While cells contained positive staining only cells with clear cytoplasmic appearance of lipid droplets were counted as lipid droplet positive (ORO+) while cells with little to no lipid droplets as negative. Data shown as mean lipid droplet count \pm SEM.

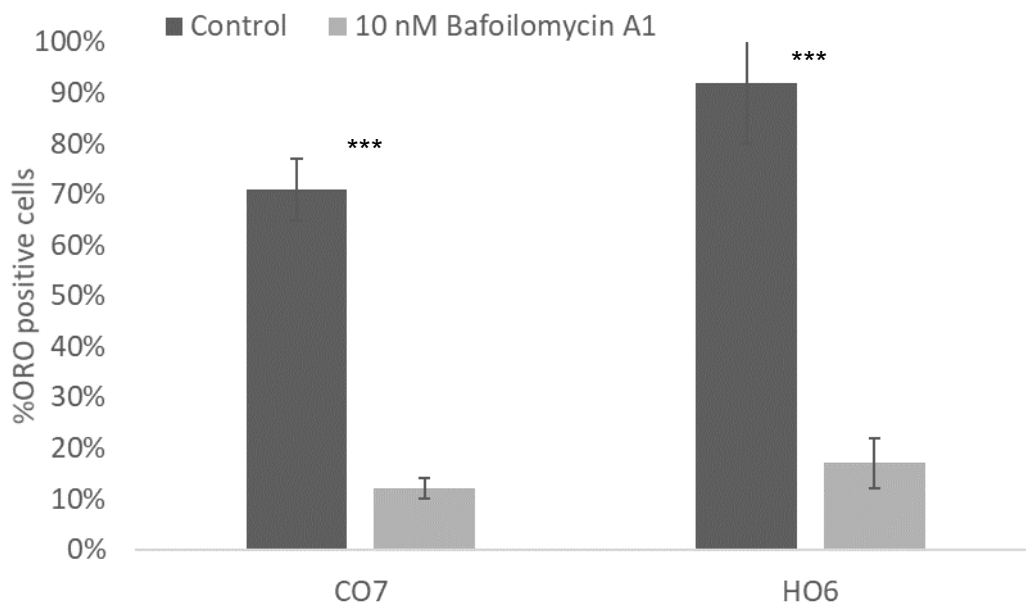
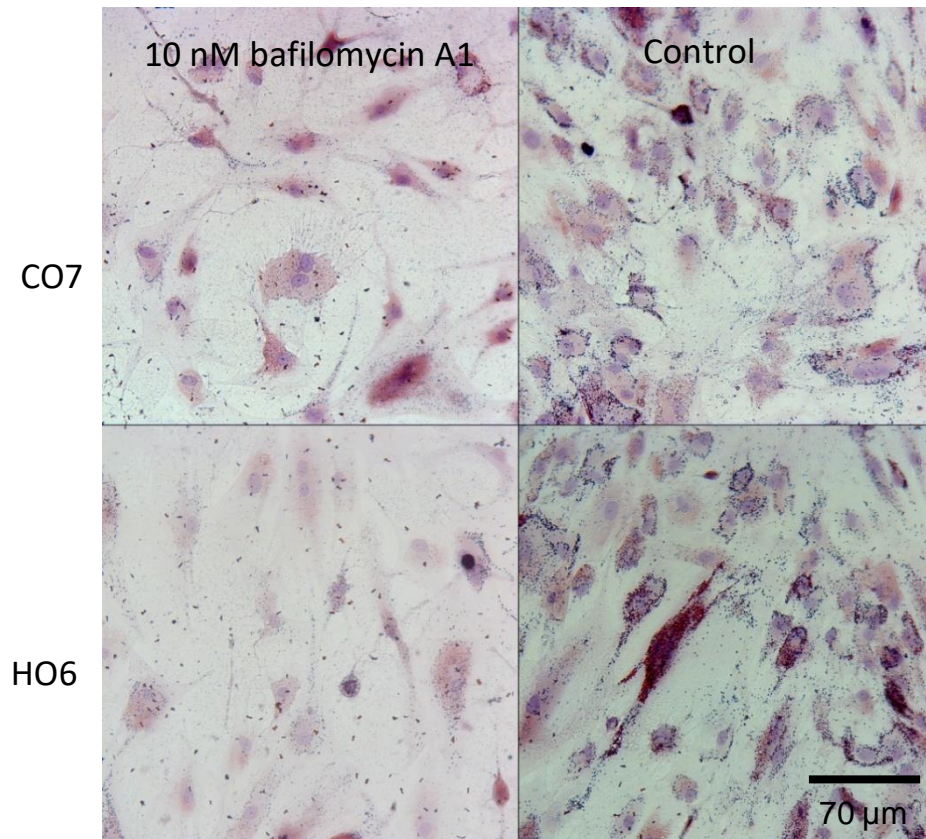


Figure 4. 18 Blocking autophagosome acidification reduces lipid droplet generation on soft substrates

Orbital fibroblasts (CO, HO) were cultured of collagen gels with or without 10 nM bafilomycin A1 for 3 days and stained for (neutral lipids with Oil-Red-O. Cells with clear cytoplasmic appearance of lipid droplets were counted as lipid droplet positive (ORO+) while cells with little to no lipid droplets as negative. Data shown as mean lipid droplet count \pm SEM. Treatment with bafilomycin A1 reduces lipid droplet generation.

4.2.11 Lysosomal marker Cathepsin D localises with lipid droplets

Biologically, the endpoint of autophagosomes as a separate cellular compartment is their fusion with lysosomes where their contents are degraded by pH-dependant hydrolases. If lipid droplets in orbital fibroblasts on soft substrates occur at least partially due to autophagic processes, we would expect some of the visible lipid droplets in soft gel cultures to present lysosomal markers. Cathepsin D is a hydrolase mainly expressed in the lysosomal lumen and is the main protein degrading agent, regarded as a reliable lysosomal marker. We stained soft cultured CO7 orbital fibroblasts with LD540 for neutral lipid staining, with anti-PLIN2 rabbit antibody and anti-Cathepsin D goat antibody. Cathepsin D appears to co-localise with LD540 lipid staining but also is present around the lipid droplets indicating that while some of the lipid droplets are contained within the lysosomes, not all lysosomes contain lipids. PLIN2 also appears to localise with Cathepsin D in PLIN2+ lipids, but not all PLIN2+ droplets appear to contain Cathepsin D and vice versa.

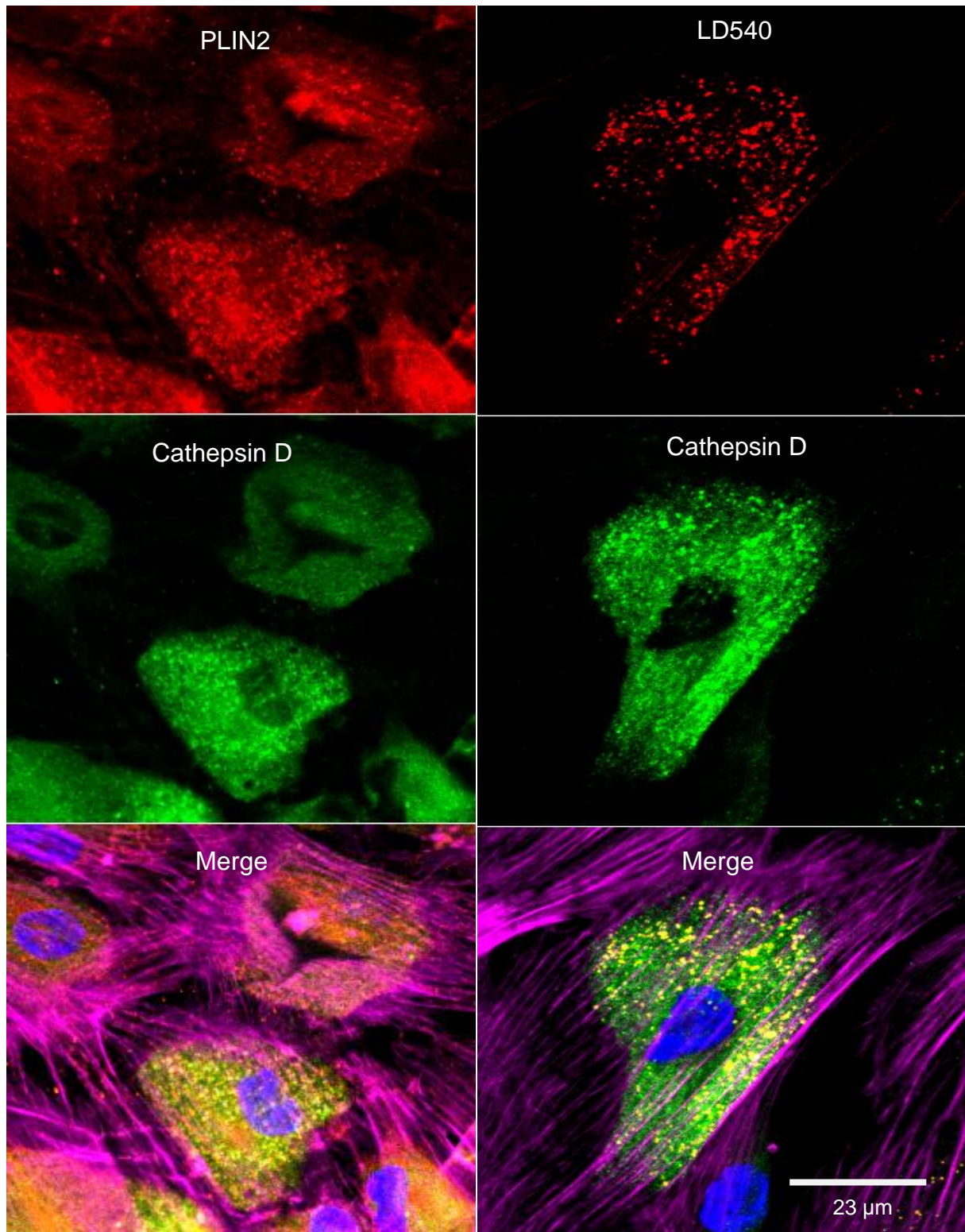


Figure 4. 19 Lysosomal marker cathepsin D localises to lipid droplets but does not co-localise with all lipid droplet positive for PLIN2

Orbital fibroblasts were cultured on collagen gels for 3 days, fixed and compressed, and stained for neutral lipids with LD540 (TRITC), for PLIN2 (TRITC) and cathepsinD (FITC), a lysosomal marker. Imaged with Zeiss 710 confocal microscope.

4.3 Discussion

4.3.1 Canonical adipogenesis is not the cause of lipid droplet generation

The origin of lipids during GO progression is attributed to adipogenic differentiation of orbital fibroblasts characterised by corresponding markers (Smith et al., 2008). Here we identified that spontaneous lipid droplet production might not be related to canonical adipogenesis pathways. 3D-cultured orbital fibroblasts did not show an increase in adipogenic marker expression with PPAR α and PPAR γ to be even lower in 3D cultures despite clearly visible ORO staining. C/EBP β is a transcription factor regulating the expression of both PPAR α and PPAR γ and is reported to be highly expressed in preadipocytes (Kumar et al., 2004). Same as with other adipogenesis markers, we did not observe an increase of C/EBP β in 3D. Furthermore, HO cells expressed a significant increase in FOXO1 in 3D cultures. FOXO1 is a marker for myofibroblastic differentiation (Kurakazu et al., 2019; Vivar et al., 2016) which is regarded as a mutually exclusive process to adipogenic differentiation providing another, indicating that HO fibroblasts cultured in 3D are more inclined to assume a more fibrotic phenotype. Lack of adipogenic marker expression and elevated FOXO1 expression in 3D cultured HO cells together indicate that adipogenic differentiation and adipogenesis through canonical means is an unlikely source of spontaneous lipid droplet production in 3D cultured orbital fibroblasts. Due to the lack of canonical adipogenesis marker expression in 3D, activity of associated pathways (like Pref-1) was not investigated.

4.3.2. Lipid droplet generation in orbital fibroblasts responds to substrate stiffness

As described previously, in 3D cultures GO orbital fibroblasts spontaneously developed more lipid droplets than their healthy counterparts. Here we demonstrate that orbital fibroblasts on soft substrates also spontaneously produce lipid droplets indicating that a soft mechanical environment without 3D is enough to cause this phenomenon. We observed that orbital fibroblasts proliferate significantly faster on soft substrates, investigated further in chapter 5. We found that both CO and HO cells generate lipid droplets at softer 1 kPa while in CO lipid the amount of lipid droplets is decreased at 40 kPa. HO cells, however, retained the same amount of lipid droplets at 40 kPa. When using soluble collagen and fibronectin coatings (0.1 mg/mL) with the same mechanical conditions, we observed a highly similar trend with HO6 cells producing lipid droplets on stiffer substrates. Within the physiological rigidity range of orbital fat, CO fibroblasts generated an increased amount of lipid droplets when cultured on 0.2 and 0.5 kPa gels with no statistical difference in ORO positive cell counts between these conditions. No ORO positive cells were observed at 8 and 40 kPa. This implies that spontaneous adipogenesis can be caused not only by cell placement in 3D but also by soft mechanistic environments. The increased ability of HO6 cells to produce lipid droplets can be explained by a subpopulation of cells with MSC-like phenotype as previously described by the Bailly lab (Kozdon et al., 2015). HO6 could generate lipid droplets at 40

kPa due to their MSC-like characteristics. Kureel et al. demonstrate that hMSC cells retain their stemness and adipogenic differentiation potential when cultured on soft substrates and can sustain this phenotype if subsequently placed on more rigid substrates (Kureel et al., 2019). GO orbital soft tissue have also been shown to have a higher elastic modulus in comparison to healthy tissue (Yoo et al., 2011a). It is possible that due to the disease, HO cells can accommodate higher substrate stiffness than CO cells and continue to produce lipid droplets. Another explanation why HO6 cells generate more droplets is that HO6 fibroblast mechanosensing signalling could be impaired by decreased Src protein expression and activity which we demonstrated earlier.

Earlier we saw that Src knockdown increased lipid droplet production in 3D and 2D on plastic. When cultured on collagen gels, Src knockdown increased lipid droplet production on thinner but not thicker gels. This can be explained by the loss of Src protein expression when orbital fibroblasts are cultured on progressively softer substrates. Interestingly, on soft substrates active Src co-localised with lipid droplets rather than at stress fibre termini indicating that on soft substrates (Figure 4.11.) and appears to be sequestered away from focal adhesions. Focal adhesion marker vinculin was also absent in soft gel cultures while clearly present in orbital fibroblasts cultured on glass coverslips. While Src activity dynamics have not been previously explored in a soft substrate and 3D setting, FA remodelling and change in protein compositions have been described before (Wozniak et al.,

2004), potentially indicating that Src departure from FA in 3D and on soft substrates in 2D could take place.

We also observed Fyn protein reduction in orbital fibroblasts cultured on soft substrates. In 3D cultures, Fyn knockdown caused a near-total absence of lipid droplets while in soft gel cultures, despite the loss of Fyn protein, lipid droplet production is increased in soft gel cultures. This potentially means that Fyn behaves differently in 3D and 2D. Another potential explanation to this discrepancy lies with the activity of Src, which in Fyn knockdown cultures is intact. Src may suppress lipid droplet production in 3D cultures despite Fyn downregulation, indicating that in spontaneous lipid droplet production activity or Src is dominant and suppressive.

Downregulation PTPN22 also decreased lipid droplet production. PTPN22 is thought to deactivate SFKs by removing their active state phosphorylation (Clarke et al., 2018b). In the context of Src activity, reduction of PTPN22 protein expression would fortify the activity of Src and thus reduce lipid droplet production. PTPN22 polymorphisms are thought to play an important role in autoimmune disease progression, including GD (Burn, Svensson, Sanchez-Blanco, Saini, & Cope, 2011). PTPN22 gain-of-function variants have been associated with GD in genome-wide association studies, but a model of a mechanism of action has not been established yet (Zhebrun et al., 2011). Our findings could indicate that in GO PTPN22 gain-of-function variants could contribute to increased SFK activity which would fit a more fibrotic phenotype. While such a notion is interesting, it would require future

experiments to assess the effects of different PTPN22 variants in GO and healthy orbital fibroblasts.

Next, we wanted to assess if spontaneous lipid droplet production occurs in fibroblasts other than orbital. We chose human dermal (SS4) and human tenon (HTF) fibroblasts both of which reside in relatively tenser mechanistic environments; ~2 kPa and ~8 kPa (Dulińska-Molak et al., 2014) respectively. We cultured CO7, HO6, SS4 and HTF on fibrillar collagen matrices of different volumes and thicknesses in a 24 well plate. Thicker gel (200 uL) surface on which the cells were plated was softer than in thin gels (50 uL) or plastic (Buxboim et al., 2010). We observed that CO6 and HO7 cells progressively generate lipid droplets proportional to gel thickness with HO fibroblasts showing the highest number of lipid-positive cells and lipid droplets per cell. SS4 and HTF fibroblasts did not generate lipid droplets in any of the conditions. There is evidence that dermal fibroblasts can be chemically differentiated into adipocytes but are not as predisposed to adipogenic differentiation as which GO cells are (Jääger & Neuman, 2011). There is no documented evidence that dermal and tenon fibroblasts spontaneously generate lipid droplets. Dermal fibroblast inability to generate lipid droplets at mechanical conditions suitable to orbital fibroblasts can be explained by different rigidity environments of both cell types in vivo. Whether HTF can be differentiated into adipocytes is currently unknown. Based on these results, we cannot ascertain that lipid droplet production is specific to orbital fibroblasts. However, it can be assumed that

in a specific mechanistic range (~0.5 kPa) SS4 and HTF fibroblasts will not generate lipid droplets.

4.3.3. AMPK and mTORc1 are downstream effectors of lipid droplet generation

We have previously shown that Src knockdown decreases Akt and mTORc1 protein expression while Fyn knockdown increases AMPK protein expression and activity. When cultured on soft gels, orbital fibroblasts exhibited a decreasing amount of Fyn and Src proteins while, similarly to knockdown experiments, decreased mTORc1 protein expression and increased AMPK protein expression and activity. To clarify the role of AMPK and mTORc1 in lipid droplet production in orbital fibroblasts we cultured CO and HO orbital fibroblasts on 50 uL, 200 uL collagen gels and plastic, and incubated with mTORc1 inhibitor rapamycin, activator MHY1485 (Zhao et al., 2016), AMPK activator salicylate (Hawley et al., 2012) and inhibitor dorsomorphin (X. Liu et al., 2014). We found that CO7 and HO6 fibroblast treatment with rapamycin mTORc1 induces lipid droplet production on plastic while reducing it in CO7 and HO6 cells. mTORc1 seen as a nutrient sensor that promotes protein and lipid synthesis (Laplante & Sabatini, 2009) but also suppresses autophagy (Laplante & Sabatini, 2013) and promotes senescence (Zhan et al., 2018a). mTORc1 inhibition on plastic caused an increase in lipid droplet production, implying that mTORc1 is a negative regulator of this phenomenon and that it is unrelated to nutrient-induced lipogenesis. On soft substrates rapamycin reduced lipid droplet production, especially in HO6 cells. We demonstrated that in soft gel cultures mTORc1

protein amount is diminished in comparison to cells grown on plastic. In later experiments, we demonstrate that soft substrates increase orbital fibroblast proliferation. It would mean that the same concentration of rapamycin acts on a significantly different number of cells and may not be as effective on soft gels in these experiments. Increase of mTORc1 activity with MHY1485 showed a large reduction in lipid droplet production in both CO7 and HO6 cells further fortifying our claim that mTORc1 downregulates spontaneous lipid droplet development.

Salicylate treatment increased lipid droplet production in cells plated on plastic while in 50 and 200 uL cultures ORO positive cell count remained similar to the control group. In the Western Blot experiments, we demonstrated that AMPK is already active in 50 uL and 200 uL cultures and could mean that salicylate does not increase its activity further. Incubation with dorsomorphin completely removed lipid droplet presence in both CO and HO cells in all mechanistic conditions, illustrating that AMPK activity is required for lipid droplet production. Orbital fibroblasts treatment with salicylate. Plastic-cultured orbital fibroblasts treatment with salicylate showed an increased autophagy marker LC3b expression which was also observed with LC3b immunofluorescence staining. LC3b protein expression was also detected in soft gel-cultured orbital fibroblasts.

Dual treatment with functionally coupled inducers and inhibitors showed interesting morphological changes in orbital fibroblasts. We co-incubated CO7 and HO6 cells with rapamycin and salicylate to promote AMPK activity

and observed a significant change in fibroblasts morphology; these cells appeared round and small in comparison to control with cytoplasm completely filled with ORO staining showing that simultaneous increase in AMPK activity and inhibition of mTORc1 leads to even higher lipid droplet accumulation. Co-inhibiting cells with functionally opposite dorsomorphin and MHY1485 yielded cells that were completely lipid-free, spread out and forming more dendritic protrusions.

Taken together, our findings indicate that mTORc1 activity suppresses lipid droplet development while AMPK promotes it through activating autophagy. Lipid droplet co-localisation with autophagy marker LC3b indicates that lipid droplets may be at least partly autophagosomes. Furthermore, AMPK activity is predominant over mTORc1 (Akers, Löffler, Wesselborg, & Stork, 2012), explaining the suppression of mTORc1 in soft substrate cultures and allowing the onset of autophagy. AMPK is proposed to initiate autophagy through Unc-51 Like Autophagy Activating Kinase 1 (ULK1) (Dunlop & Tee, 2013). As a next step, it would be necessary to determine if ULK1 is expressed and active in soft gel-cultured orbital fibroblasts.

Autophagy has been previously implicated in GO with GO fibroblasts expressing and increased amount of autophagy markers with bafilomycin A1 treatment reducing the number of lipid droplets (Yoon, Lee, Chae, & Lee, 2015). We confirmed that mechanosensitive lipid droplet production is sensitive chloroquine (Mauthe et al., 2018) and bafilomycin A1 (Mauvezin & Neufeld, 2015), both shown to disrupt autophagy. Rather than decrease

lipid staining, chloroquine appeared to disperse lipid droplets and retaining some cytoplasmic ORO staining while bafilomycin A1 reduced the overall lipid droplets.

Autophagosomes mature by gradual acidification and eventual fusion with lysosomes. We found that part of the lipid droplet population in fibroblasts cultured on soft substrates stain positive for cathepsin D, a lysosomal marker indicating possible autophagosome maturation.

Active AMPK has been previously reported to localise to lipid droplets to promote their degradation by phosphorylating PLIN2, a lipid droplet scaffold protein protecting from abnormal degradation. AMPK phosphorylation of PLIN2 primes it for removal, exposing lipids for breakdown (Kaushik & Cuervo, 2016). While we observed phosphor-AMPK localisation to lipid droplets, we also observed that AMPK inhibition on soft substrates with dorsomorphin prevents lipid droplet formation while retaining the cytoplasmic presence of PLIN2. These observations potentially imply a dual role of AMPK in orbital fibroblasts; AMPK promotes autophagy but may also be required to breakdown a population of pre-existing PLIN2 positive lipid droplets.

We found a diffuse PLIN2 presence in orbital fibroblasts cultured on stiff substrates. On soft substrates PLIN2 partially localised with lipid staining indicating that some of the lipid droplets are PLIN2-positive. Co-staining with Cathepsin D showed an only partial overlap of both signals indicating a possibility of mixed populations of lipid droplets. Taken together with

autophagy marker expression data, spontaneously generated lipid droplets could be a mixed population of PLIN2-positive lipid droplets at various stages of autophagic degradation.

4.3.4 AMPK and mTORc1 activity influences orbital fibroblasts contractility

In previous experiments, we observed that Fyn and Src knock-down reduces fibroblasts contractility. Published research by the Bailly lab also shows that inhibition of SFKs by PP2 also decreases orbital fibroblast contractility when cultured in 3D. We have shown that Src and Fyn downregulation decreases mTORc1 protein expression and increases AMPK expression. Inhibition of mTORc1 and activation of AMPK with rapamycin and salicylate respectively slowed down CO7 and HO6 cell contraction. mTORc1 has been recently shown as a pro-fibrotic factor in idiopathic pulmonary fibrosis (Woodcock et al., 2015, 2019). Our findings indicate that mTORc1 activity is necessary for orbital fibroblast contractility and that its activity could be suppressed by AMPK also in this context which has been shown to have an anti-fibrotic activity in liver fibrosis (Liang et al., 2017).

4.4 Conclusions

Our findings clarify the nature spontaneous lipid droplet generation in orbital fibroblasts showing that observed lipid droplets might be of autophagous origin. Lipid droplet production may be dependent on the balance of AMPK and mTORc1 activity which in turn can be regulated by SFK and substrate

stiffness. We also were able to show that inhibition of mTORc1 and activation of AMPK significantly reduce orbital fibroblast contractility. Our findings may be important to understand the role of autophagy in GO disease progression, where SFK, mTORc1 and AMPK may serve as potential therapeutic targets for future therapies.

CHAPTER 5 REPLICATIVE SENESENCE IN ORBITAL FIBROBLASTS

5.1 Introduction

5.1.1. Replicative senescence

Replicative senescence is a highly stable cell cycle arrest that takes place in response to different stressors. By causing a growth arrest, senescence limits the replication of old or damaged cells. Besides exiting the cell cycle, senescent cells undergo many other phenotypic alterations such as metabolic reprogramming, chromatin rearrangement, or autophagy (Herranz & Gil, 2018). While initially thought to occur mainly from the accumulation of DNA damage and telomere shortening, senescence has been strongly associated with ageing and cellular mechanotransduction; tissue stiffening occurs with ageing and has been demonstrated to accompany cellular senescence (Phillip, Aifuwa, Walston, & Wirtz, 2015). This connection has also been demonstrated with an opposite approach; onset on senescence was delayed in cells grown on softer substrates that also were more permissive to cell proliferation (Kureel et al., 2019).

Senescent cells show altered morphology including an enlarged size, irregular cell shape, prominent and sometimes multiple nuclei, accumulation of mitochondrial and lysosomal mass and highly prominent stress fibres with many of these phenotypes regulated by mTORC1 in various cell types (Correia-Melo et al., 2016; H. Zhang, Stallock, Ng, Reinhard, & Neufeld, 2000). Furthermore, inhibition of mTORc1 with rapamycin is shown to delay the onset of senescence in MSCs (Antonioli et al., 2019). mTORc1 activity

is closely linked to that of AMPK, and both of these master regulators have been shown to impact senescence in vascular smooth muscle cells (Tan et al., 2016; Zhan et al., 2018a). While SFKs have not been shown to induce cellular senescence, Src is a regulator of mTORc1 in an Akt-dependent and independent manner (R. Chen et al., 2001b; Jiang & Qiu, 2003; Vojtechová et al., 2008) while Fyn limits AMPK activity (Yamada et al., 2016).

5.1.2 Biological markers of senescence

Cells require their cell cycle to be halted prior to the onset of senescence. p16INK4a was discovered as a cdk4-interacting protein that inhibits the catalytic activity of cdk4–cyclin D complexes arresting the cell cycle. p16INK4a expression is low in young replicating or quiescent cells, but high in senescent cells in different cell types (Zindy, Quelle, Roussel, 1997). p16 protein undetectable in immortalised and stem cells (Alcorta, Xiong, 1996). However, more recent discoveries imply that the expression of p16INK4a in senescence may be transient and cell phenotype specific, refuting its role as a core universal senescence marker (Hernandez-Segura et al., 2017).

Senescence-associated β -galactosidase is defined as β -galactosidase activity detectable at pH 6.0 in senescent cells, but the origin of SA- β -gal activity is not precisely known. It has been demonstrated that the enzymatic activity in senescent cells could originate from lysosomal β -D-galactosidase. While SA- β -gal activity is detectable at pH 6.0, the lysosomal β -gal activity requires a lower pH of 4.5. Lysosomal β -galactosidase activity increases in senescent cells due to increased lysosome content, which in

turn allows β -galactosidase activity to be detectable at higher pH levels (Kurz, Decary, Hong, & Erusalimsky, 2000).

Prolonged, chronic inflammation has been shown to contribute to replicative senescence causing vascular remodelling and localised tissue stiffening as an additional effect of fibrosis (Mavrogonatou, Pratsinis, Papadopoulou, Karamanos, & Kletsas, 2019). While ocular fibrosis has been well-established in GO orbital fibroblasts, replicative senescence has not been investigated.

Previously we were able to demonstrate autophagy marker expression in soft-substrate cultured orbital fibroblasts. Starvation-associated autophagy has been shown to protect cells from senescence in rats (Schmitt & Melk, 2017) and is likely induced by AMPK activity (Dunlop & Tee, 2013). Autophagy marker decline has also been observed in ageing rat kidney epithelial cells but can be reversed with rapamycin treatment (Cui et al., 2012). We previously observed that lipid droplet production is sensitive to both rapamycin and AMPK activation with salicylate. Based on these findings, we wanted to determine whether orbital fibroblasts enter a senescence-like state under stiff substrate stiffness conditions as an opposing mechanism to soft substrate cultured cells.

5.2 Results

5.2.1 Cell proliferation is increased on soft substrates

CO and HO orbital fibroblasts were cultured on Cytosoft plates for 3 days.

Cell per each rigidity condition was imaged and counted. We found that in

both CO and HO cultures, the number of cells increases with decreasing substrate rigidity (Figure 5.1A, B). We normalised the cell count from each well against the initial number of cells plated (10000 cells/mL, 2ml per well). Cell count at 0.5 and 0.2 kPa substrate rigidity was 6-fold higher than the initial amount plated and 6-fold higher than the lowest substrate rigidity used (64 kPa) HO cells appear to proliferate slightly faster than CO cells at 0.2 and 0.5 kPa (Figure 5.1C). Previous findings from the Bailly lab show that HO orbital fibroblasts phenotype is closer to that of MSCs. These findings are consistent with previously published data done with a similar model in mesenchymal stem cells ((Kureel et al., 2019). Cell lysates obtained from these cultures show a decreasing mTORc1, Src and Fyn protein content assessed by Western Blot with most of the proteins found in cells cultured at 64 kPa and lowest at 0.2 kPa (Figure 5.1D). We conducted a similar experiment with CO7 and HO6 cells cultured on collagen gels with 50 uL and 200 uL volumes (Figure 5.2). Both CO and HO cells proliferate significantly faster on 200 uL collagen gels with HO6 cell division rate being higher than CO7 (A). Src, Fyn and mTORc1 protein expression are lowest in 200 uL collagen gels (B). Findings from these experiments suggest SFK and mTORc1 downregulation is necessary for senescence onset.

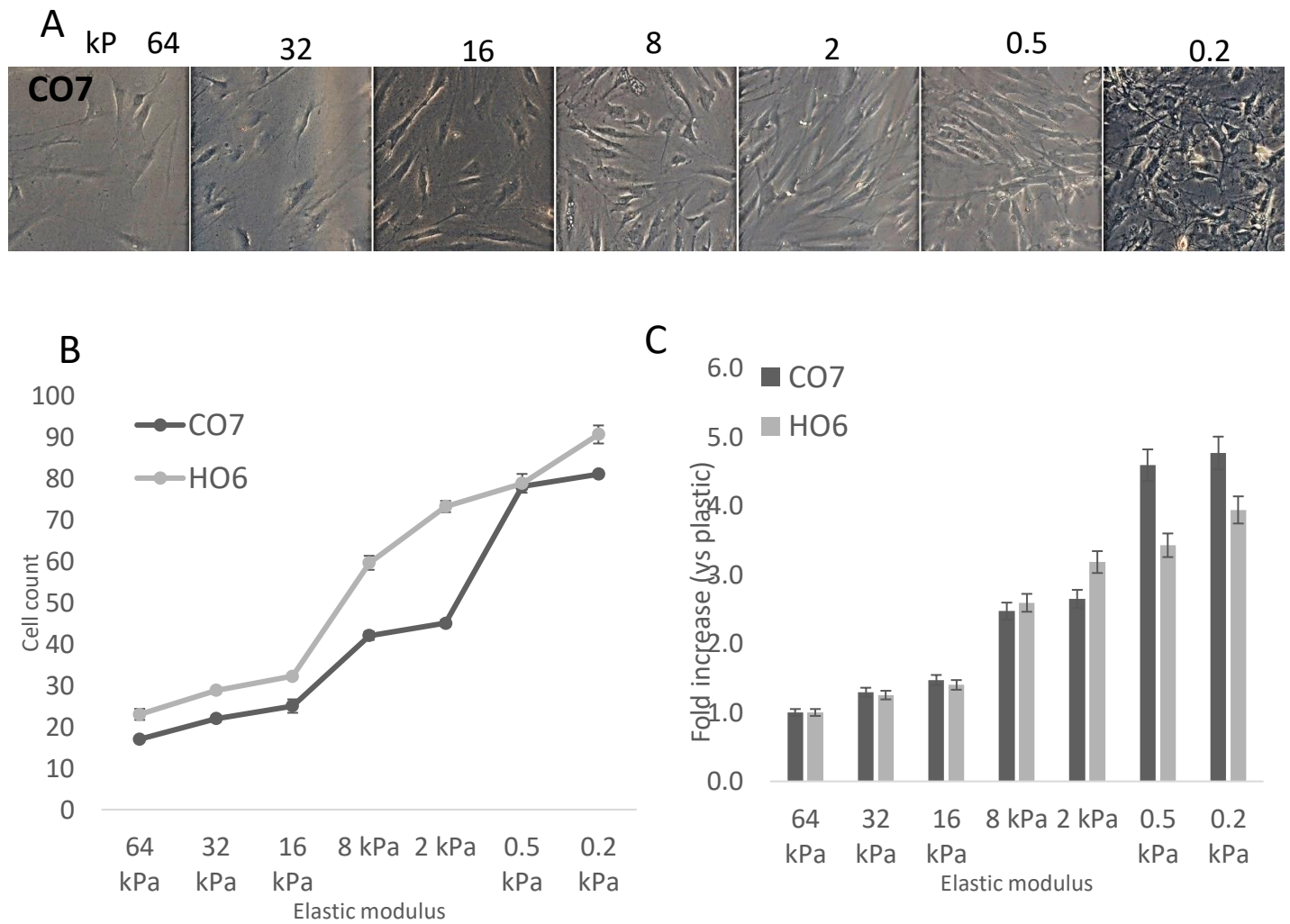


Figure 5. 1 Cell proliferation increases with substrate softness.

CO and HO cells were cast on silicone-coated wells with predetermined mechanical tension, pre-coated with 0.1 mg/mL, incubated for 5 days. Cells were imaged and counted. Cell lysates were taken on day 5. Protein content analysed by WB. Both CO and HO cells show increased proliferation rates on softer substrates. Cells grown at 64 kPa show the lowest cell count while the highest cell count was seen in 0.2 and 0.5 kPa cultures. HO6 cell count was significantly higher than CO7 amongst all Young's modulus values except 0.5 (A,B,C, shown as mean cell count or fold increase \pm SEM, $n = 2$).

A

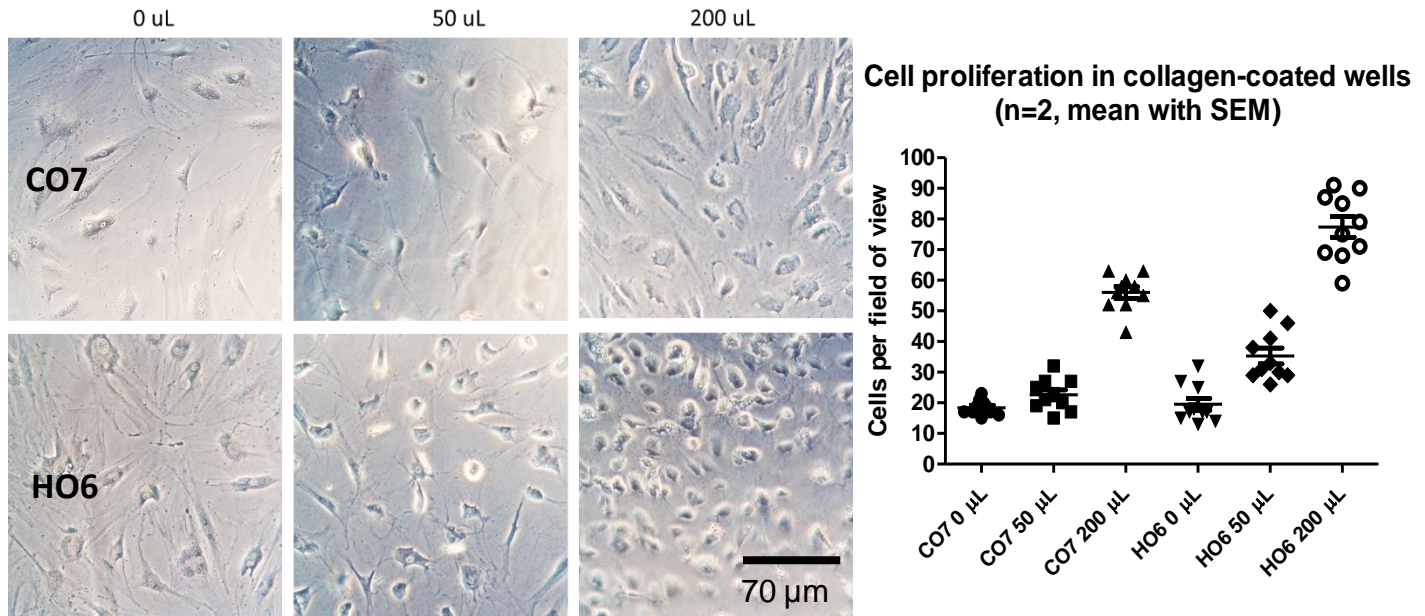


Figure 5. 2. Cell proliferation increases on soft collagen gels.

CO7 and HO6 orbital fibroblasts were grown on collagen gels (50 uL, 200 uL) for 3 days. Cells were imaged and counted, lysed and protein content analysed by WB. Both CO7 and HO6 cells show increased proliferation rates on softer substrates. Cells on thinner gels have a protrusive appearance. (A, shown as mean cells per field of view \pm SEM, n(images) = 5, n (experiments) = 2).

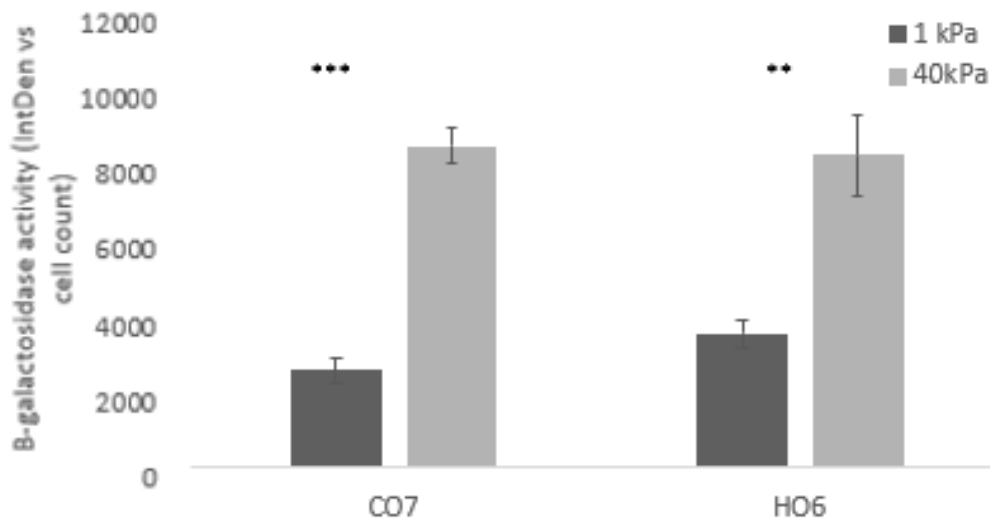
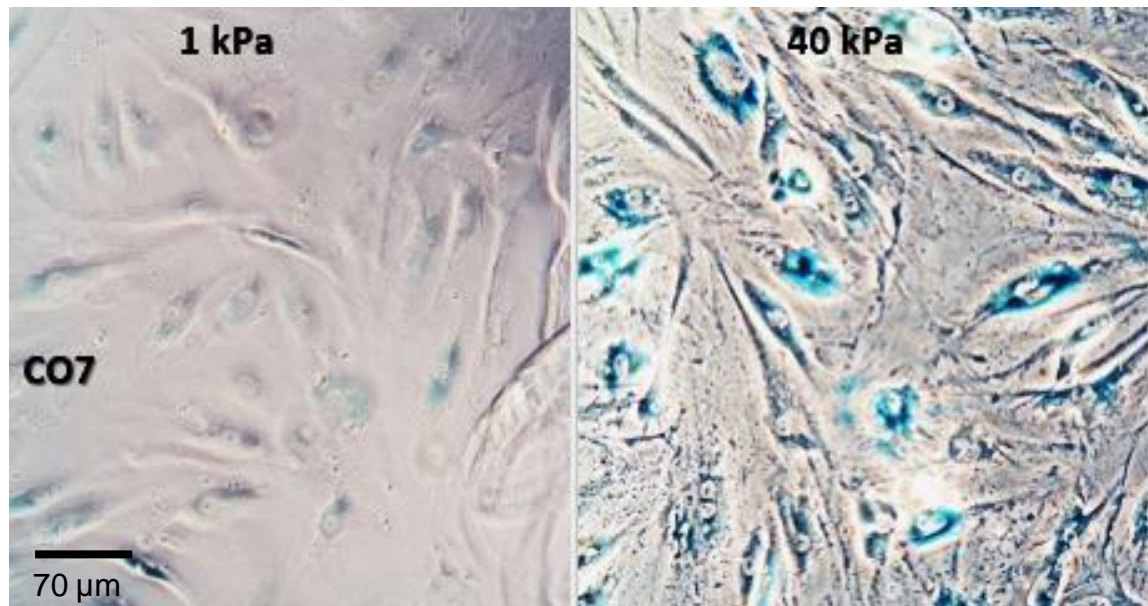


Figure 5. 3 β -galactosidase activity increases on cells cultured on rigid substrates

CO7 and HO6 fibroblasts were cultured on PAA/bisAA layered coverslips with pre-determined Elastic Moduli of 1 and 40 kPa, coated with 0.1 mg/mL polymerised collagen, β -galactosidase activity assay performed after 3 days. Signal intensity assessed with ImageJ. Data shown as mean integrated density per cell count \pm SEM, $n = 2$.

5.2.2. β -galactosidase activity is reduced in cells cultured on softer substrates

To investigate whether orbital fibroblasts enter senescence if grown on a substrate with rigidity outside of the physiologically relevant (<1 kPa) range, we plated CO7, and HO6 orbital fibroblasts on PAA/bisAA layered coverslips with 0.1 mg/mL fibrillar collagen for 3 days. We fixed the cells and performed a β -galactosidase activity assay as an indicator of cellular senescence overnight at CO₂ enrichment-free conditions. We imaged the cells and assessed β -galactosidase staining intensity with ImageJ. We observed a significant difference between 1 kPa and 40 kPa cultured cells (Figure 5.3) in both CO ($p < 0.001$) and HO ($p < 0.01$) cultures. Both CO and HO cells displayed significantly less β -galactosidase staining when cultured at 1 kPa, indicating that cells grown on softer substrates are less senescent. These findings are consistent with research done in MSC models, where cells cultured at their native mechanistic tension displayed little β -galactosidase activity (Kureel et al., 2019).

To confirm these findings, we performed a similar assay on Softwell gels with substrate stiffness conditions at 0.2, 0.5, 8 and 40 kPa. Our findings are in line with the previous experiment; β -galactosidase staining is not present at 0.2 and 0.5 kPa cultured cells. Cells display a slight β -galactosidase signal at 8 kPa while a 40 kPa clear staining is present (Figure 5.4 A).

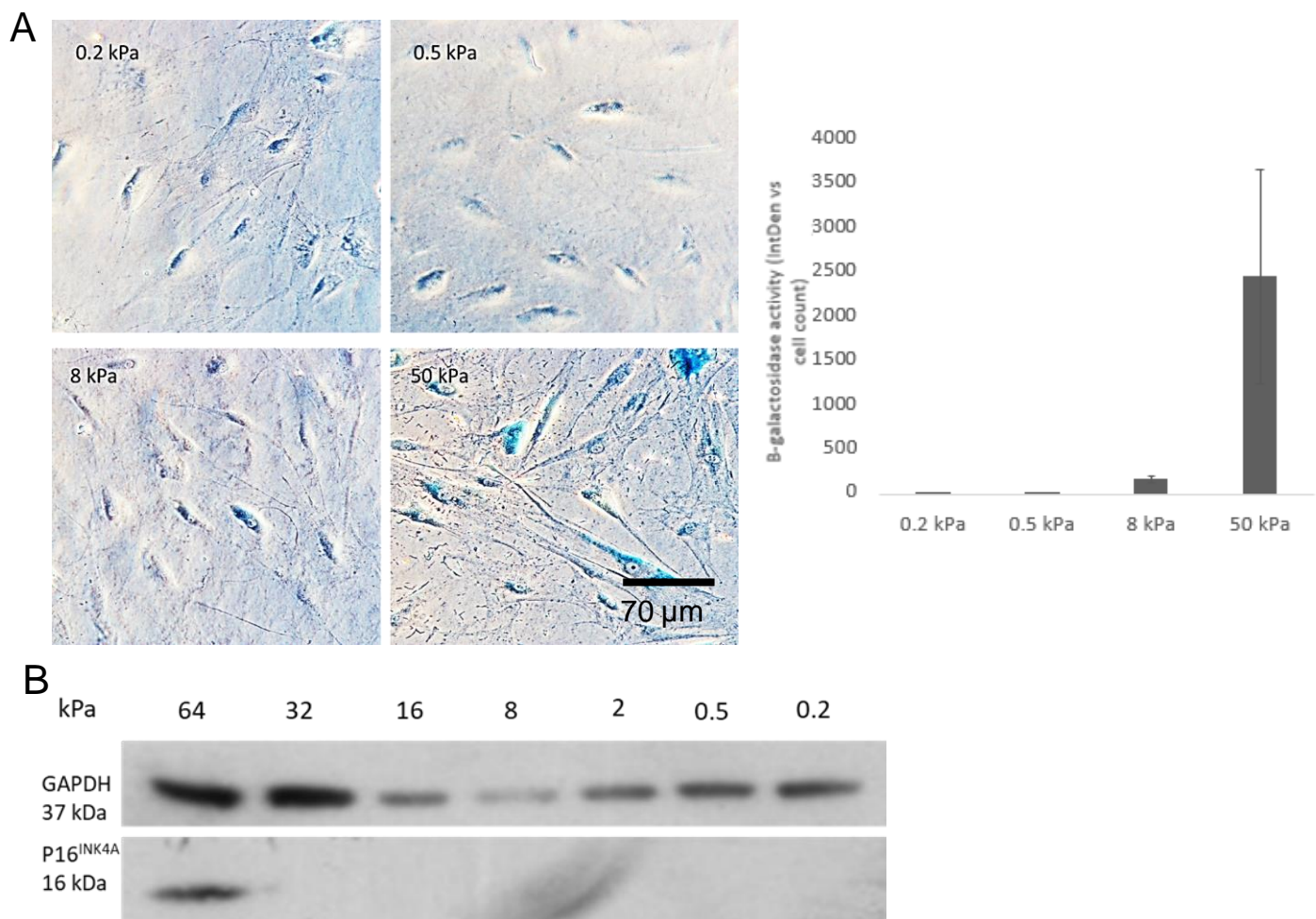


Figure 5. 4 Senescence markers are absent in orbital fibroblasts cultured on soft matrices

CO7 orbital fibroblasts were plated on Softwell gels with pre-determined, certified mechanical rigidity with β -galactosidase activity assay performed after 3 days (A). Signal intensity assessed with ImageJ. Data shown as mean integrated density per cell count \pm SEM, $n = 2$. Lysates from CO7 cells grown on Cytosoft plates were probed for p16INK4A content. P16INK4A was detected at 64 kPa ($n = 1$)(B).

We investigated p16INK4A protein presence in cells cultured on a range of substrates. We could only detect p16INK4A protein in cell lysates obtained from 64 kPa cultures. This is partially in line with β -galactosidase staining; no p16INK4A protein expression was found at a stiffness range closer to 40 kPa where β -galactosidase staining was visible (Figure 5.4 B).

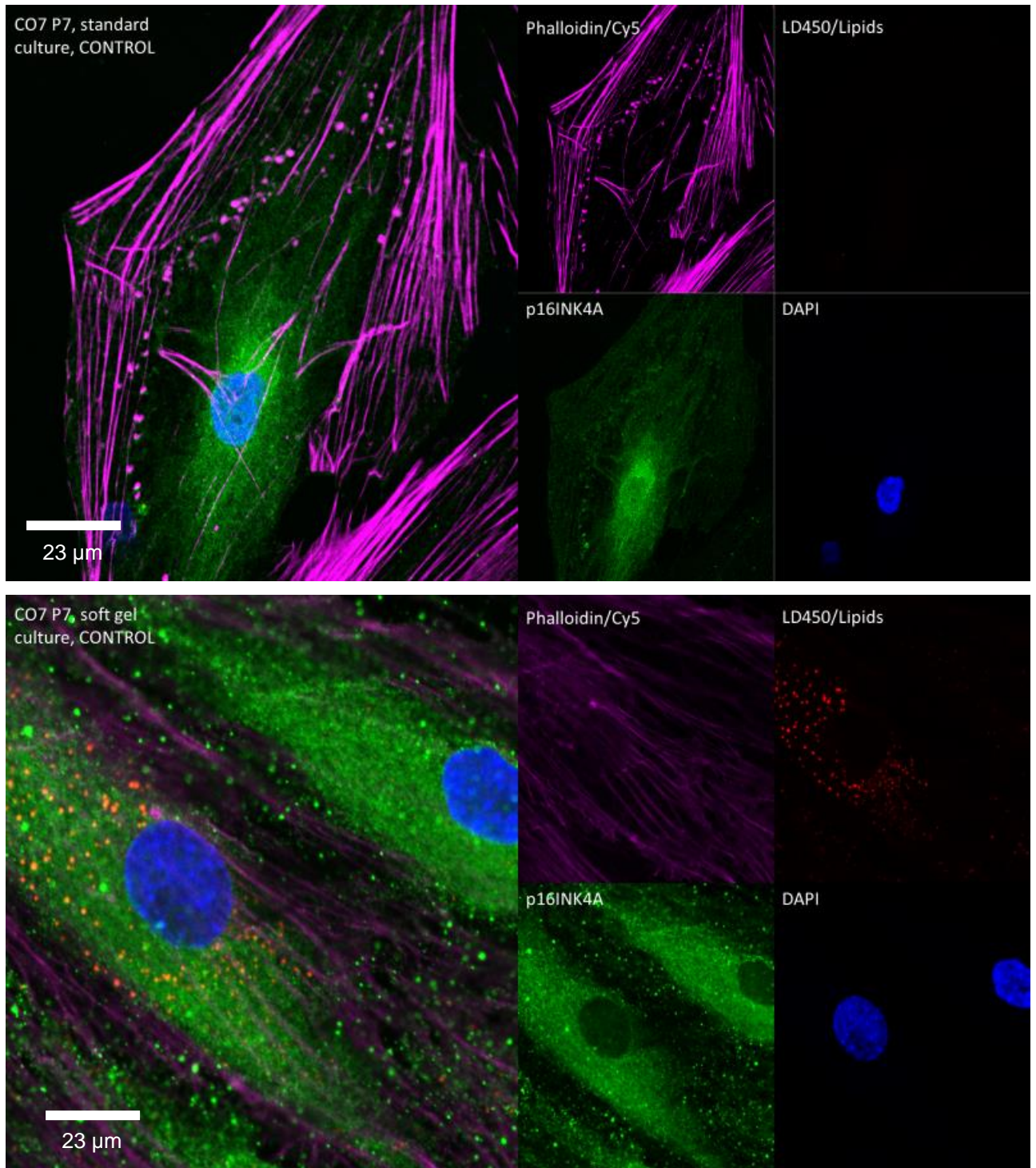


Figure 5. 5 Senescence marker p16INK4A leaves the nucleus when cultured on soft substrates.

CO orbital fibroblasts were plated on glass coverslips and soft collagen gels for 3 days, fixed and stained with anti-P16INK4a rabbit antibody and LD540 for lipid droplet staining. Imaged with Zeiss LSM710 confocal microscope.

Immunostaining of p16INK4A (green) in CO7 fibroblasts on soft substrates (Figure 5.5) and coverslips revealed that the protein is largely absent from cells cultured on soft substrates after 3 days while clearly localising to the nucleus (DAPI) in coverslip-cultured cells. In both stiffness conditions, a strong cytoplasmic presence was seen. We did not observe any specific localisation with lipid droplets (TRITC) or actin fibres (magenta).

5.2.3. Reduction of Fyn and Src protein decreases β -galactosidase activity

In our previous experiments, we were able to show that senescent marker expression and β -galactosidase activity is abolished when cells are plated and grown on softer substrates. This process was accompanied by Src, Fyn and mTORc1 downregulation. Therefore, we wanted to explore if senescence can be reduced by decreasing Fyn and Src expression. We performed a Fyn and Src knock-down with 280 ng siRNA of each, incubated CO and HO fibroblasts for 72h. We fixed and stained the cells with a β -galactosidase activity assay (Figure 5.4). Our findings show that both Src and Fyn downregulation decreases β -galactosidase activity compared to siControl transfected cells. These findings are in line with our previous observations, where both Fyn and Src were downregulated in soft substrate cultures.

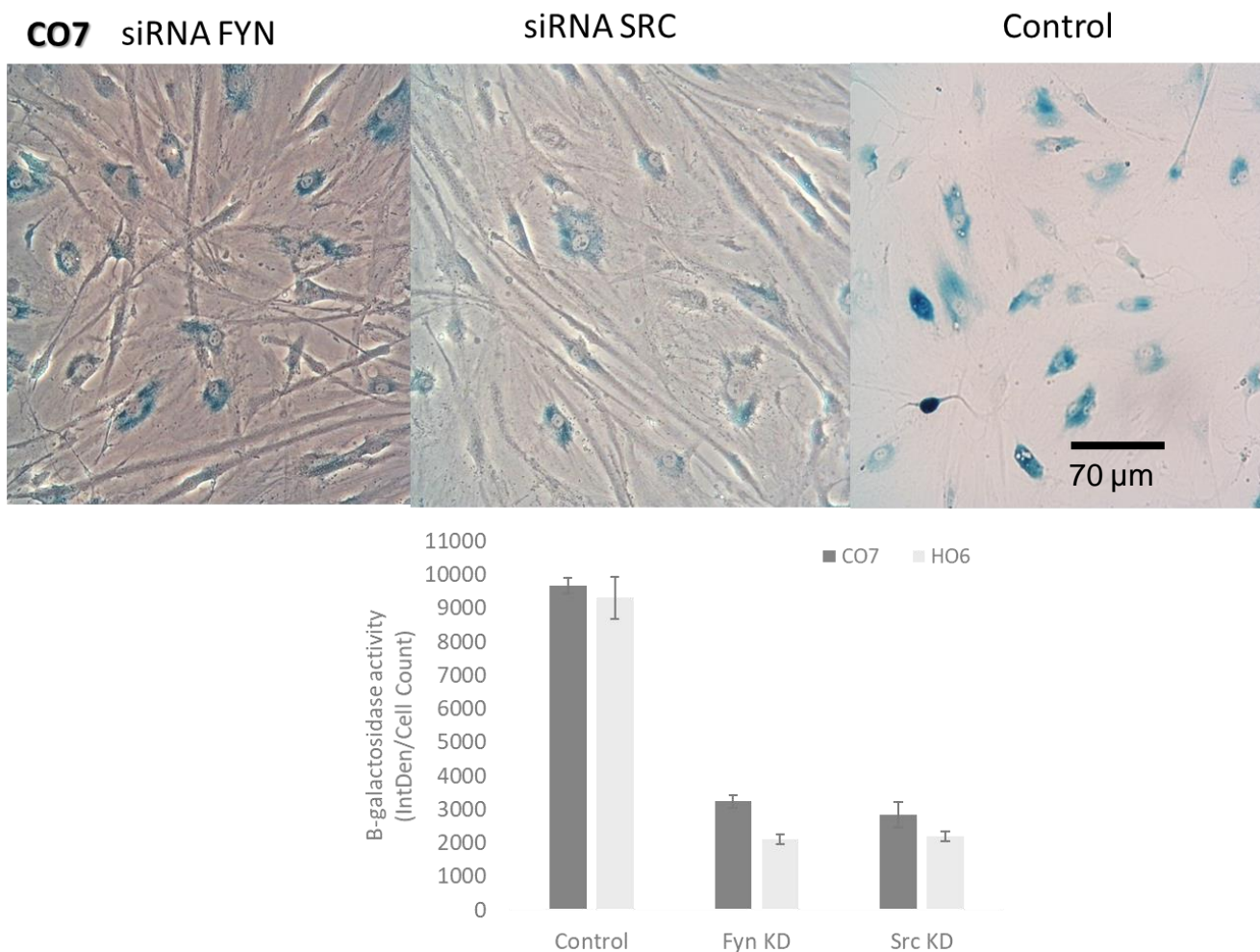


Figure 5. 6 SRC and FYN knock-downs decrease senescence in orbital fibroblasts

CO7 and HO6 orbital fibroblasts were incubated with FYN, SRC and control pool siRNAs for 72h and stained for β -galactosidase activity overnight. Signal intensity assessed with ImageJ. Data shown as mean integrated density per cell count \pm SEM, n = 2.

5.2.4 ROCK kinase and mTORc1 inhibition reduces the β -galactosidase activity

mTORc1 activity is shown to be crucial for the onset of cellular senescence. Our own data shows that mTORc1 is downregulated in cells grown on soft substrates. Next, we wanted to investigate whether mTORc1 inhibition with rapamycin decreases senescence in cells grown on stiff substrates (Figure 5.6). Disruption of Rho-associated kinase (ROCK) activity has been previously shown to reduce cellular senescence, so it was included as a positive control. We plated CO and HO orbital fibroblasts on plastic and collagen gels (50 μ L, 200 μ L) for 3 days with 5 μ M rapamycin and 5 μ M H1152. We then stained the cells for β -galactosidase activity, imaged and analysed with ImageJ. Rapamycin reduced β -galactosidase activity on all stiffnesses in both CO7 and HO6 cells. This effect can be cumulative; in our previous experiments, we provided evidence that mTORc1 is downregulated in cells on soft substrates. The effect of rapamycin treatment was more pronounced in HO6 cells.

With β -galactosidase activity significantly reduced in cells on plastic where mTORc1 expression was previously seen to be the highest, our findings confirm that mTORc1 inhibition reduces senescence. Cell treatment with ROCK inhibitor removed cellular senescence almost completely, which is in line with previously published data (Park et al., 2018).

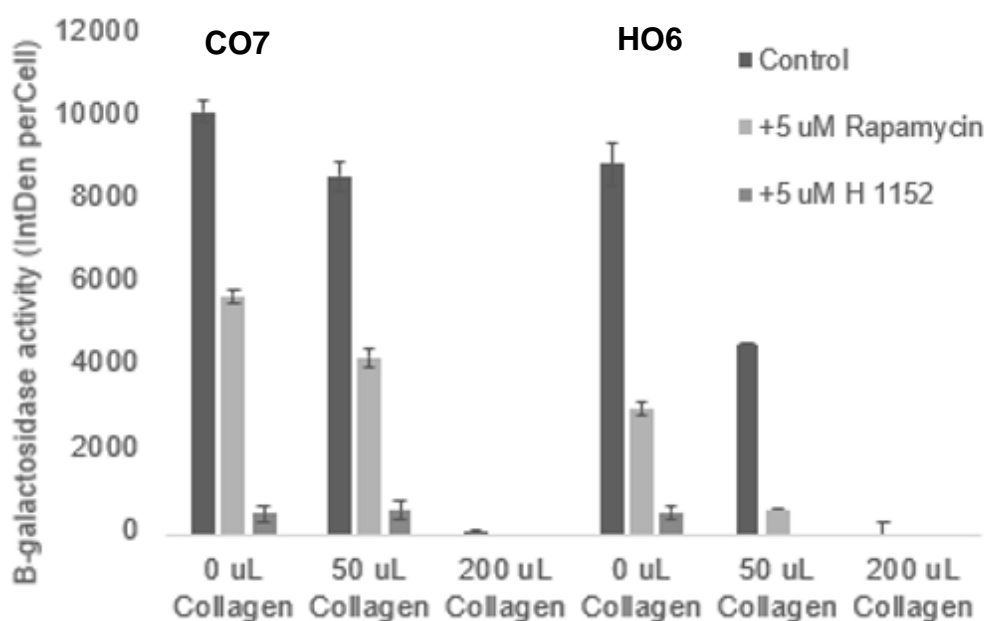
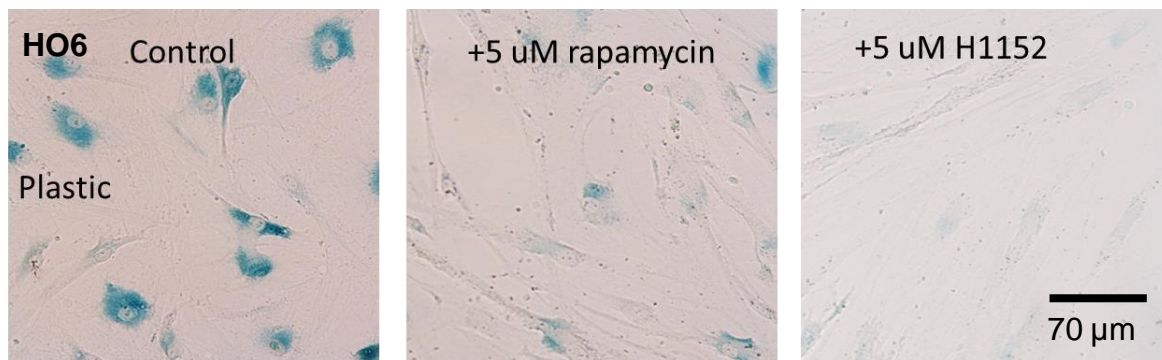


Figure 5. 7. B-galactosidase activity is reduced with ROCK and mTORc1 inhibition.

CO and HO (passages 6, 7) orbital fibroblasts were cultured on plastic and 50 uL, 200 uL collagen gel, incubated with 5 uM rapamycin or 5 uM H1152 (ROCK inhibitor) for 3 days and stained for β -galactosidase activity. Cells in all rigidity conditions displayed reduction in β -galactosidase staining when treated with rapamycin or H1152. Data shown as mean \pm SEM, N(number of experiments) = 3, n(replicates per experiment) = 2.

5.2.5. PTPN22 and CSK reduction decrease β -galactosidase activity

Reduction of Src and Fyn expression on soft substrates and decreased senescence when SFK are downregulated prompted us to investigate whether inhibition and downregulation of SFK negative regulators CSK and PTPN22 would have any effects on β -galactosidase activity. We downregulated PTPN22 and CSK using 280 ng of corresponding siRNAs with CO and HO fibroblasts for 72h. We plated the treated cells on plastic and 50 μ L collagen gels for 3 days and stained for β -galactosidase activity (Figure 5.7.). We also cultured CO cells of plastic with 5 μ M LTV-1, a PTPN22 inhibitor. Both PTPN22 and CSK knock-down cells and those treated with LTV-1 displayed a significant reduction in β -galactosidase activity. This was the opposite of what we expected; reduction of negative regulators of SFK should have increased SFK activity and the intensity of β -galactosidase staining.

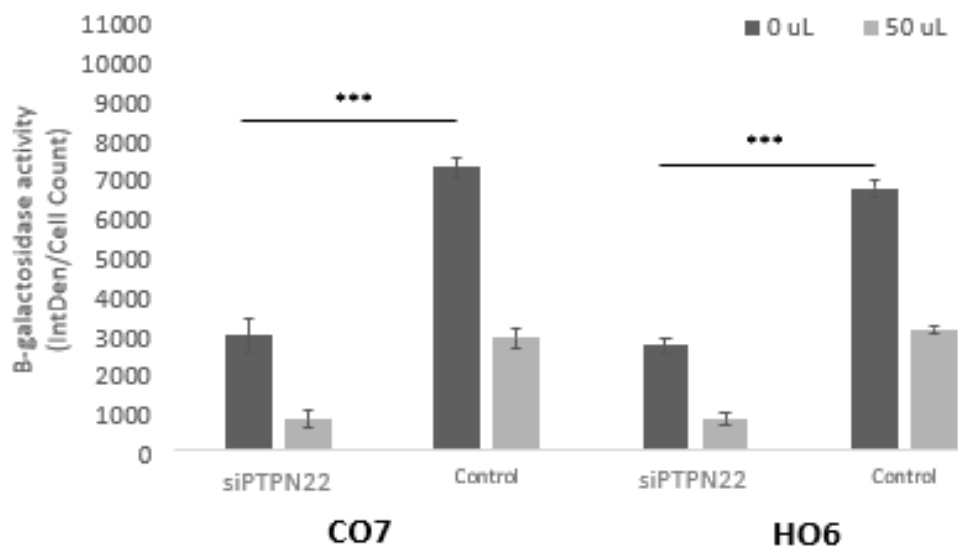
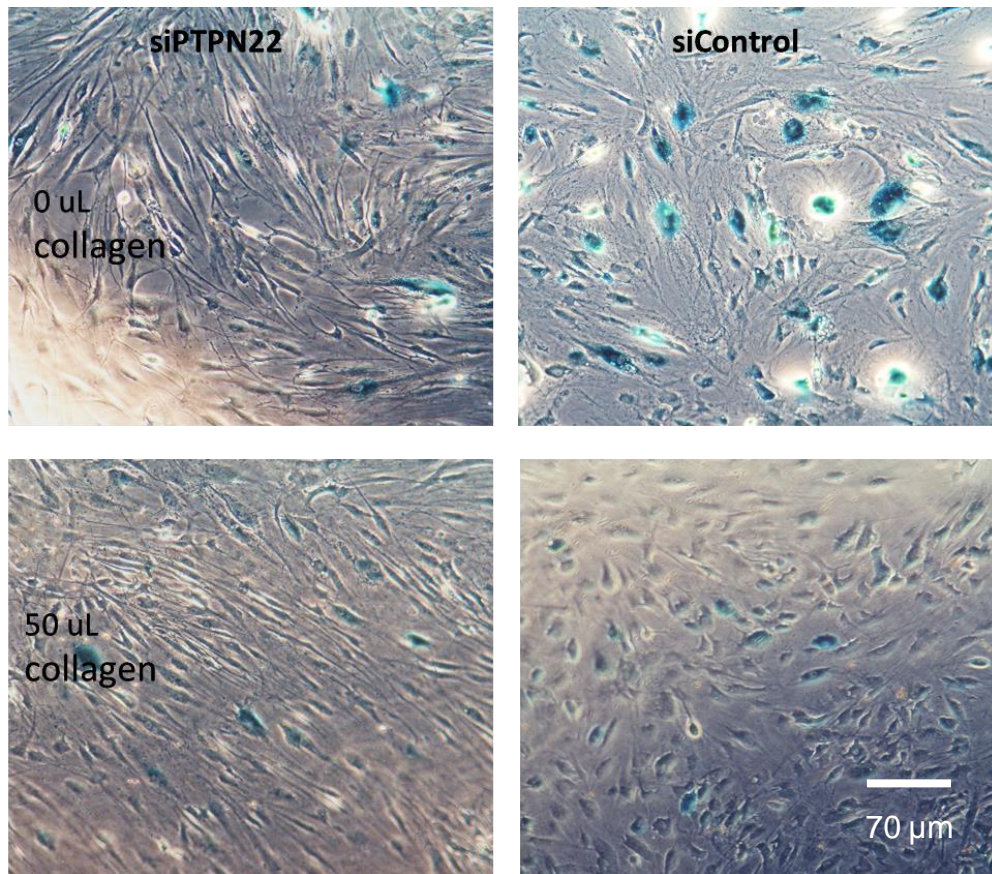


Figure 5. 8 PTPN22 knock-down reduces β -galactosidase activity in orbital fibroblasts.

CO and HO orbital fibroblasts were incubated with 280 ng PTPN22 siRNA for 72h and then plated on plastic or 50 uL collagen gels. After 3 days cells were fixed and stained for β -galactosidase activity. Signal intensity assessed with ImageJ. Data shown as mean integrated density per cell count \pm SEM, N = 2 n = 2, ***p < 0.001

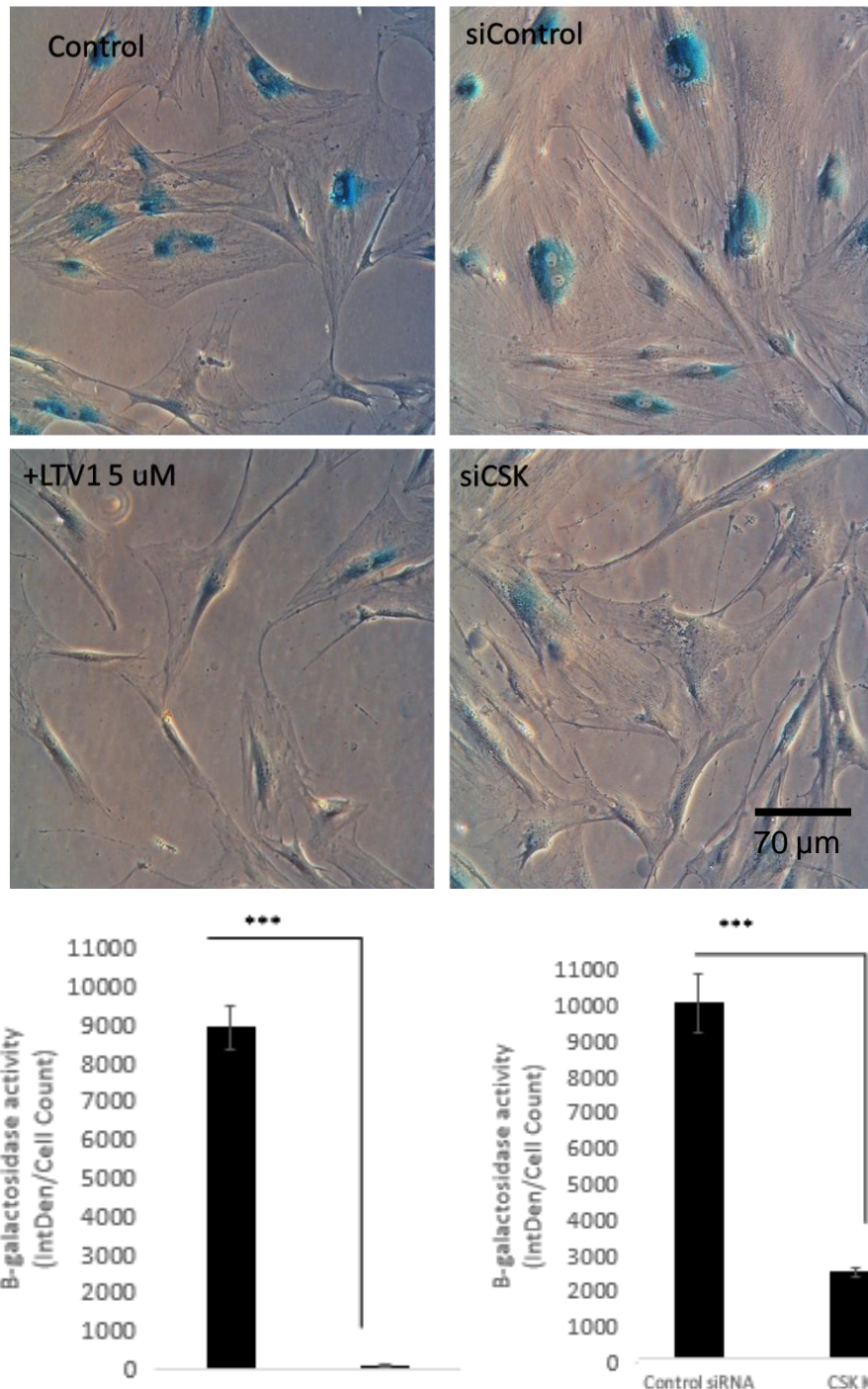


Figure 5. 9 Both PTPN22 inhibition and CSK downregulation decreases β -galactosidase activity

CO orbital fibroblasts were plated (A) treated with LTV-1 (PTPN22 inhibitor) or (B) incubated with 280 ng siCSK for 72h, plated on plastic and after 3 days stained for β -galactosidase activity. Signal intensity assessed with ImageJ. Data shown as mean integrated density per cell count \pm SEM, N = 1, n = 2.

5.2.6. AMPK activation decreases cellular senescence

Our previously conducted experiments show that AMPK activity is increased on soft substrate cultures. In regards to senescence, AMPK has been shown to decrease senescence by limiting mTORc1 activity (Tan et al., 2016; Zhan et al., 2018b). We plated CO7 cells on plastic under standard culture condition and incubated with 5 mM salicylate (AMPK activation), 5 μ M dorsomorphin (AMPK inhibition) and 5 μ M MHY1485 (mTORc1 activation). Our findings show that in cells cultured on plastic AMPK activation (A) significantly reduces in β -galactosidase activity ($p < 0.01$) while cell treatment with dorsomorphin does not cause statistically significant change ($p = 0.06$). We incubated another set of CO7 and HO6 cells with salicylate and lysed after 3 days, assessing P16INK4A protein expression with Western Blot. We observed that salicylate treatment almost completely abolishes p16INK4A expression. Our findings are consistent with literature data showing that AMPK activity indeed has anti-senescent properties. We had expected AMPK inhibition with dorsomorphin to cause a more pronounced increase in β -galactosidase activity. The lack of statistically significant increase can be explained by the cells already being in conditions promoting senescence. In an experiment culturing CO with dorsomorphin on soft substrates (not shown) we were unable to detect any β -galactosidase staining, indicating that AMPK activity is beneficial but not necessary for orbital fibroblasts to remain non-senescent.

A

B

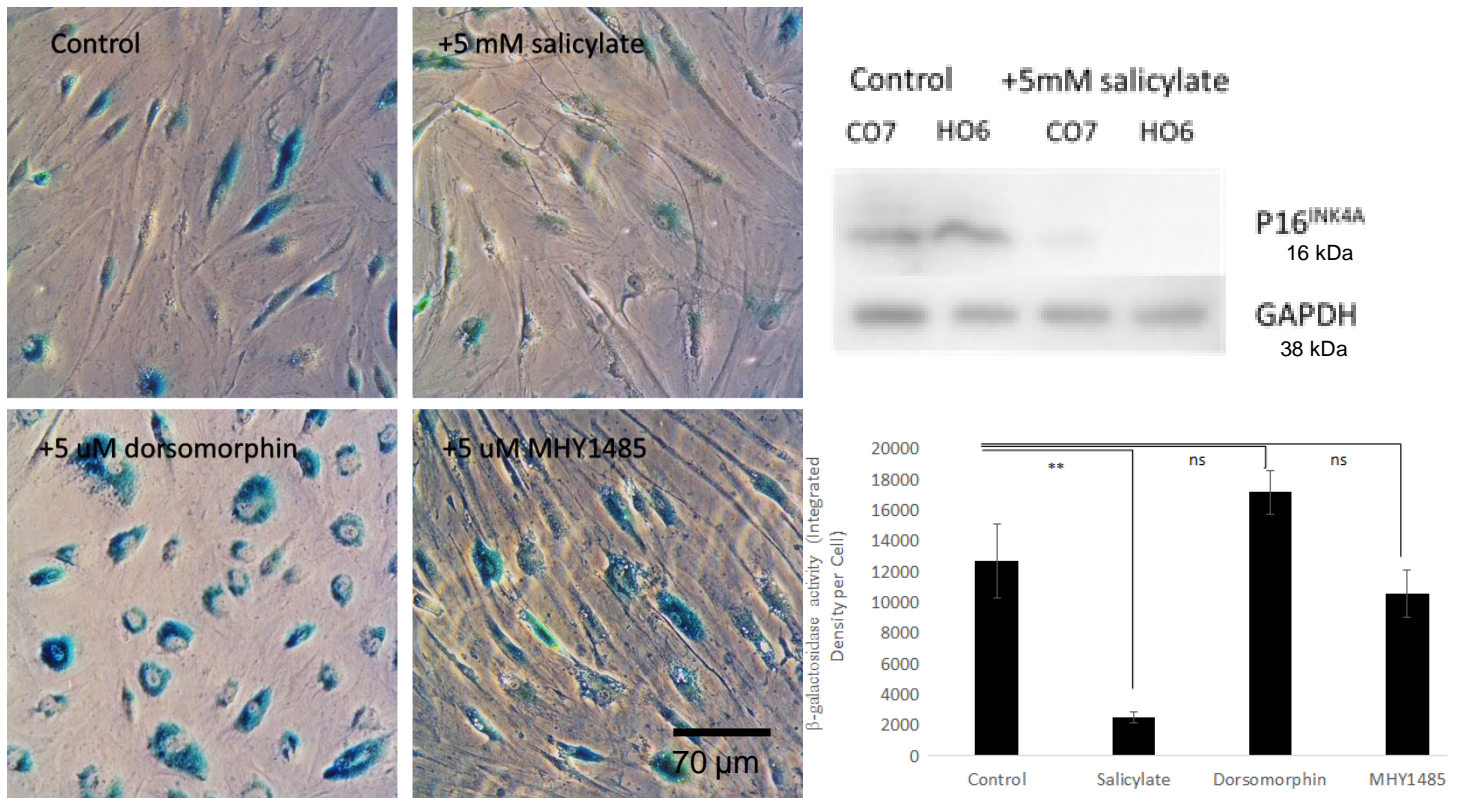


Figure 5.10 AMPK decreases β -galactosidase activity

CO orbital fibroblasts were plated on plastic and incubated with (A) 5 mM salicylate, 5 μ M dorsomorphin or 5 μ M MHY1485 for 3 days, fixed and stained for β -galactosidase activity. Signal intensity assessed with ImageJ. (B) CO and HO cells treated with salicylate for 3 days were lysed and assessed for P16INK4A protein content by Western Blot. Data shown as mean integrated density per cell count \pm SEM, N = 2, n = 2, **p < 0.01.

5.2.7 Human tenon fibroblasts do not display β -galactosidase activity on stiff substrates

We have demonstrated that substrate stiffness promotes cellular senescence in orbital fibroblasts, alleviated by culture on a softer substrate and completely abolished when cells are grown in mechanical conditions close to those native to orbital fibroblasts in vivo. Vav is involved in actin cytoskeleton organisation, and the loss of its activity has been demonstrated to cause cellular senescence (Debidda, Williams, & Zheng, 2006b). Therefore, we wanted to investigate if cellular senescence occurs in fibroblasts residing in stiffer mechanistic environments in vivo. Human tenon fibroblasts (HTF) reside in a mechanical environment with 17 kPa. We plated HTF and CO cells on plastic for 3 days with and without Ehop 16 (a Rac1 inhibitor). We fixed and stained the cells for β -galactosidase activity. Our findings (Figure 5.10) show that tenon fibroblasts exhibit little senescence in comparison to CO7 cells while both cell lines are sensitive to Rac1 inhibition and enter senescence, matching published data. Plastic wells used in cell culturing has a mechanic rigidity of 0.1 GPa, surpassing the substrate rigidity HTF and CO reside in-vivo by multiple magnitudes. Our data suggest that HTF cells are more resilient to cellular senescence when grown on substrates much denser than their native environment.

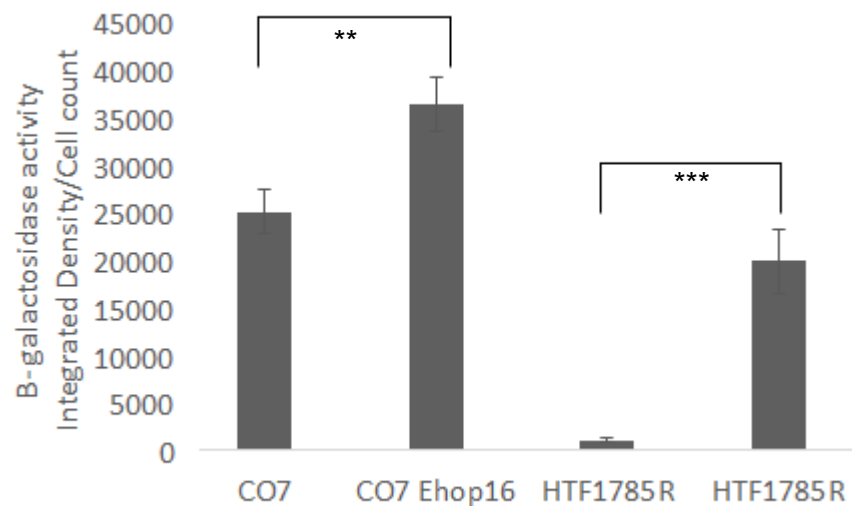
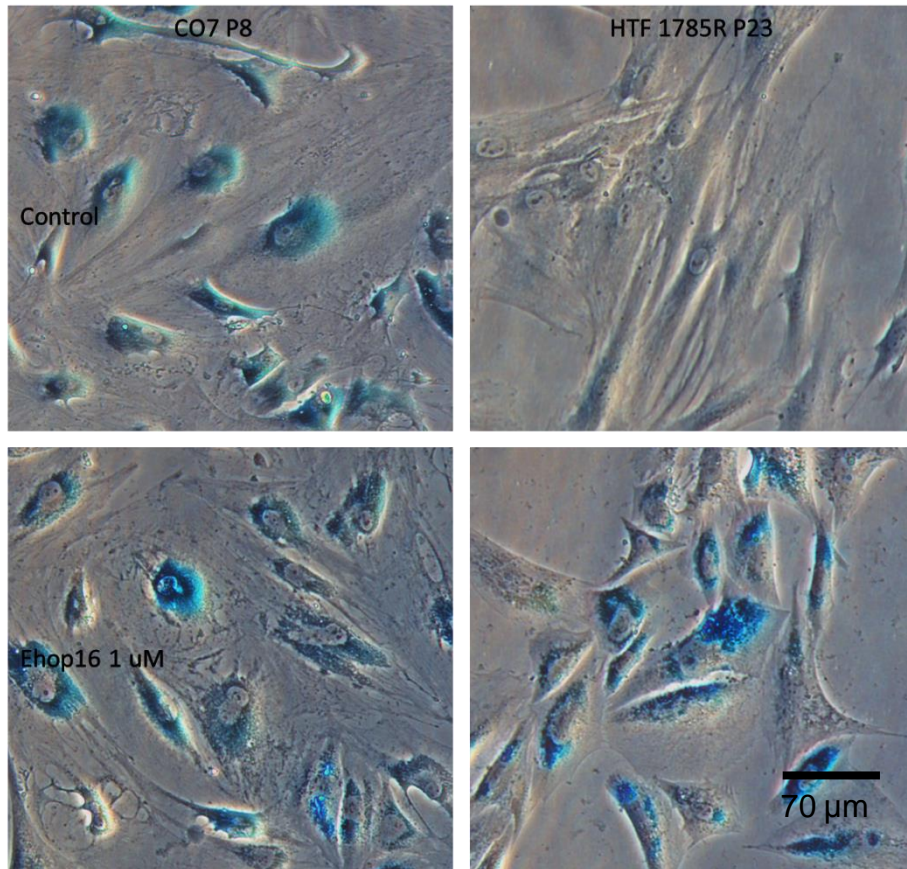


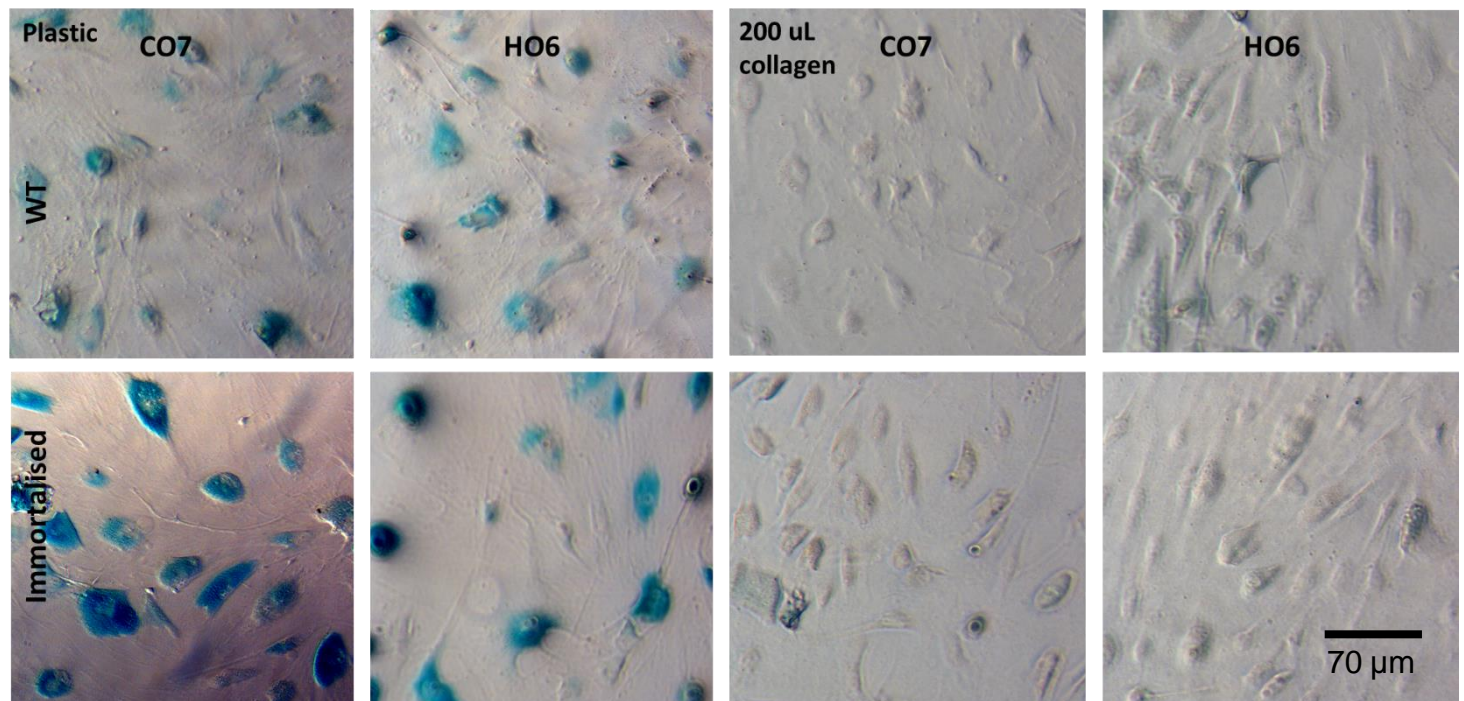
Figure 5. 11 Tenon fibroblasts display significantly lower β -galactosidase activity on rigid substrates than CO cells.

CO7 and HTF 1785R cells were cultured on plastic for 3 days with or without 1 μ M Ehop16 (a Vav GTPase inhibitor, fixed and stained for β -galactosidase activity. Signal intensity assessed with ImageJ. Data shown as mean integrated density per cell count \pm SEM, $n = 2$, ** $p < 0.01$, *** $p < 0.001$.

5.2.7 Immortalised orbital fibroblasts display senescence markers when cultured on plastic

Cell immortalisation is a process encountered in tumour growth, allowing cells to bypass senescence and proliferate indefinitely. Immortalisation can also be achieved for long-term use of cells and avoiding replicative senescence. Hypothetically, immortalised cells should not become senescent.

We used CO and HO cells transformed through SV40 viral transfection by Dr Bailly. We cultured transformed and WT CO and HO orbital fibroblasts on plastic for 3 days, fixed and stained for β -galactosidase activity. To our surprise, immortalised cells appeared not only senescent but also surpassed wild type cells in β -galactosidase activity. This is in line with previous experiments with immortalised MEF cells (not shown) which also exhibited positive β -galactosidase staining. In collagen gel cultured both transformed and wild type cells displayed little senescence, consistent with previous findings. However, Immortalised cells expressed significantly less p16INK4A protein while β -galactosidase staining in these cells is stronger.



A

B

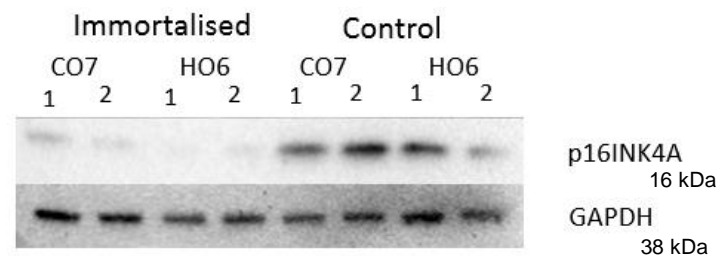
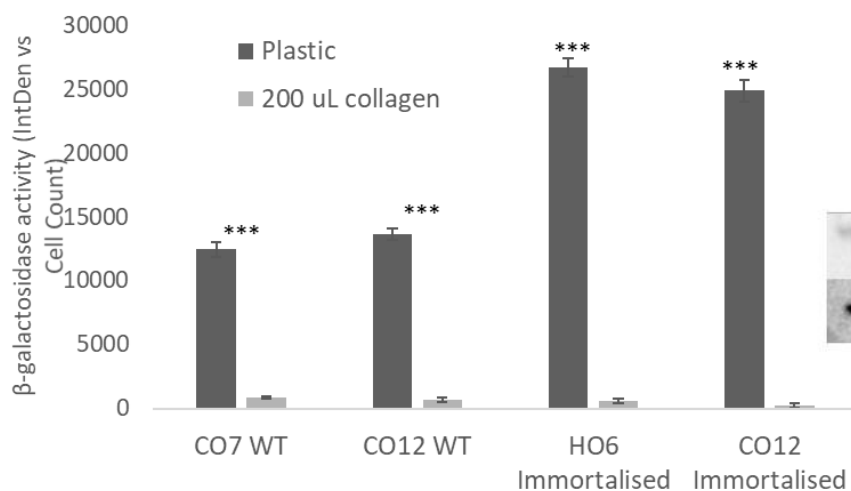


Figure 5.12. Cell immortalisation does not prevent substrate rigidity-associated senescence

(A) Immortalised CO and HO fibroblasts and plated them on plastic and 200 uL collagen gels for 3 days, fixed and stained for β -galactosidase activity. Transformed orbital fibroblasts exhibit significantly more ($p < 0.001$) β -galactosidase staining. Soft substrate culturing abolishes β -galactosidase staining, Data show as mean β -galactosidase activity \pm SEM, $n = 2$, *** $p < 0.001$. (B) p16INK4A expression is diminished in immortalised cells ($N = 2$, $n = 2$). Immortalised cells express little p16INK4A protein contrary to β -galactosidase staining.

5.3 Discussion

5.3.1 Orbital fibroblast proliferation is slower on stiff substrates

Findings available in the literature show that orbital fat possesses an elastic modulus of <1 kPa with increased stiffness in tissue isolated from GO patients (Yoo et al., 2011a). We were able to demonstrate that CO7 cells cultured on collagen-coated Cytosoft silicon gels proliferate faster and orbital fibroblasts divide the most when cultured on substrates with the rigidity of 0.5 and 0.2 kPa within the physiological range of orbital fat. We saw a similar trend when growing orbital fibroblasts on collagen gels, where thicker gels present lower gel surface stiffness (Buxboim et al., 2010). In this model we also observed increased proliferation in cells on thicker gels with HO6 cells growing faster than CO7. These findings indicate that the growth of orbital fibroblasts is hindered if cells are grown on stiffer substrates.

HO6 cells proliferated more at softer stiffness conditions. That can be explained by their similarity to MSCs, which have been demonstrated to proliferate faster on soft substrates and retain their stemness (Kureel et al., 2019). However, according to Kureel et al., “true” human MSCs reach peak proliferation rates when cultured at 5 kPa with softer and stiffer substrates yielding fewer cells. This claim is contradicted by multiple other sources; periodontal ligament mesenchymal stem cells (N. Liu et al., 2018) and bone marrow mesenchymal stem cells (M. Sun et al., 2018) increase proliferation with progressively stiffer substrates. This, however, could indicate that stem

cells grown in vitro prefer stiffness closer to their in vivo conditions. Orbital fibroblasts in our experiments also prefer stiffness closer to their native environment, which relative to most anatomic rigidity niches is very soft.

5.3.2 Stiff substrate orbital fibroblasts show senescence-associated β -galactosidase activity

We demonstrated that orbital fibroblasts produce more lipid droplets and proliferate faster in stiffness environments resembling that of orbital fat. Kureel et al. demonstrated that MSCs display senescent markers if cultured on stiff substrates. Furthermore, both age-related ECM remodelling (Waters et al., 2018) and fibrosis (Calhoun et al., 2016) contribute to replicative senescence while the link between ECM stiffening and senescence is poorly understood. We detected β -galactosidase activity in CO7 and HO6 fibroblasts at 40 kPa on bisAA/PAA-layered coverslips and at 8 and 50 kPa on Matrigen Softwell cultures. Stiffness conditions within the stiffness range of orbital fat didn't show any β -galactosidase activity. We also found that p16INK4A is present in CO7 cells at 64 kPa but not in lower stiffness cultures despite β -galactosidase staining visible at cultures grown on substrates as soft as 8 kPa. The biological function of p16INK4A is to cause a cell cycle arrest by binding cyclin-dependent kinases (Cdks) which in turn requires p16INK4A to be present in the cytoplasm (Alcorta et al., 1996). Our observations could indicate that cells grown on gels softer than 64 kPa can display β -galactosidase activity but still have not entered a cell cycle arrest. This idea fits with our previous observation of orbital fibroblasts proliferating increasingly faster on softer gels with the lowest observed rate of division at

64 kPa. Immunofluorescence staining for p16INK4A showed that in cells cultured on soft gels p16INK4A is absent from the cell nucleus while on glass coverslips p16INK4A co-localised with the nucleus while in both stiffness conditions the protein was clearly present in the cytoplasm. Cytoplasmic presence of p16 should indicate a cell cycle arrest, yet at these stiffness conditions, we observed a peak orbital fibroblast proliferation and no β -galactosidase staining. While p16INK4A has been regarded as a reliable senescence marker, more recent findings indicate that its role in senescence may be transient and its presence in senescent cells may also depend on the wild-type cell phenotype (Hernandez-Segura et al., 2017). p16INK4A presence in the nucleus in the context of senescence has not been documented before. In carcinoma cells, nuclear localisation of p16INK4A is associated with slower tumour growth and better patient survival, indicating that nuclear p16INK4A may slow down cell proliferation (Arifin et al., 2006). Together, our findings show that senescence markers are present in orbital fibroblasts cultured on stiffer substrates (and plastic) and indicate that replicative senescence can be caused by the altered mechanical environment. Cells which have entered full replicative senescence achieve a Senescence-associated secretory phenotype (SASP) where senescent cells release proinflammatory cytokines (W. J. Wang, Cai, & Chen, 2017). The next research step could explore if GO fibroblasts in stiff mechanical environments release SASP-specific chemical profile potentially contributing to GO progression.

Next, we investigated if fibroblasts with a predisposition to higher substrate rigidity exhibit β -galactosidase activity when grown on plastic. HTF1785R fibroblasts exhibited little β -galactosidase staining. When incubated with Ehop16, a Vav inhibitor, HTF1785R cells showed significant β -galactosidase activity. HTF in vivo resides at Young's modulus closer to that of orbital fibroblasts, plastic as a growth substrate is by multiple magnitudes stiffer. Lack of β -galactosidase staining in HTFs indicates that tenon fibroblasts are not as susceptible to stiffness- induced cellular senescence as orbital fibroblasts are. Vav proteins are a family of guanine exchange factor (GEF) proteins that regulate Rac protein activation (Bustelo, 2001). Vav proteins have not been associated with senescence while their downstream targets, the Rac family, have been shown to cause senescence in MEFs if their activity is above and below the baseline (Debidda, Williams, & Zheng, 2006a). The onset of senescence when inhibiting Vav and impairing Rac activation could indicate that Rac protein activity is important in preventing cell senescence and might be a factor in distinguishing which fibroblast phenotypes are sensitive to substrate-stiffness related replicative senescence. Further research is required to determine the role of Rac proteins in orbital fibroblast senescence.

5.3.3. SFK and PTPN22 downregulation reduces the β -galactosidase activity

We showed that both Fyn and Src are downregulated in cells grown on soft substrates. Src signalling axis has been demonstrated to be involved in senescence onset (Jung et al., 2019) and also as a positive regulator of

mTORc1, a senescence promoter (Vojtěchová et al., 2008). Neither Src or Fyn have been directly shown to be involved in replicative senescence onset. We show that both Fyn and Src knock-downs decreased β -galactosidase staining in orbital fibroblasts when cultured on plastic but when we downregulated the inhibitors of SFKs, PTPN22 and Csk we did not observe an increase or even a similar level to control. These results were further validated by orbital fibroblast incubation with LTV-1, a PTPN22 inhibitor showing a reduction in β -galactosidase activity. PTPN22 has not been shown to promote senescence, but a gain-of-function mutant of PTPN22 has been shown to accumulate in ageing T-cells indicating that increased PTPN22 activity could contribute to senescence (Rieck et al., 2007). Our results imply that in orbital fibroblasts PTPN22 promotes senescence through SFK independent means.

5.3.4. AMPK and mTORC1 regulate cellular senescence

Canonically, mTORc1 is established as a pro-growth, lipid and protein synthesis factor. Recently, mTORc1 has emerged as a senescence promoter, thought to activate senescence pathways as opposed to autophagy in starving or aged cells. Both AMPK and mTORc1 have been implicated in senescence regulation (Zhan et al., 2018). In our experiments, we were able to show that mTORc1 protein quantity is present in cells cultured on rigid substrates and plastic while nearly absent on soft substrate cells. AMPK, in contrast, had its activity and protein expression increased in soft substrate cultures. We investigated whether mTORc1 and AMPK activity contributes to senescence onset in orbital fibroblasts. Orbital

fibroblast treatment with rapamycin reduced cellular senescence on rigid substrates while incubation with MHY1485, a mTORc1 activator did not produce any statistically significant change. Orbital fibroblast treatment with salicylate, however, significantly decreased senescence in cells cultured on plastic. AMPK inhibition with dorsomorphin increased the mean staining intensity, which was not statistically significant ($p = 0.06$). Our findings confirm earlier results that AMPK and mTORc1 are involved in senescence regulation with substrate stiffness determining the activity of both. Relationship between AMPK and mTORc1 has been previously demonstrated in the context of senescence (Zhan et al., 2018b). mTORc1 regulation is subject to AMPK. We showed that induced AMPK activity reduces β -galactosidase activity even when orbital fibroblasts on plastic while a similar effect is seen with rapamycin treatment. AMPK induction with salicylate also removed p16INK4A protein expression in cells cultured on plastic (not shown), confirming the anti-senescent activity of AMPK. An anti-p16INK4A activity of AMPK has not been described previously. AMPK activity was increased in soft gel orbital fibroblast cultures. In the same cultures, mTORc1 protein expression was diminished. Our findings confirm AMPK and mTORc1 as important senescence regulators. Furthermore, earlier we showed that mTORc1 and AMPK activity also influences autophagy marker presence and lipid droplet production, a connection also established elsewhere (Hong Li et al., 2017; Yoon et al., 2015). Altogether our findings link these processes with AMPK and mTORc1 as the unifying factors behind them.

5.3.5 Immortalised cells enter senescence if cultured on rigid substrates

Cellular immortalisation is a functionally opposite process to replicative senescence with both processes regarded as mutually exclusive, replicating tumorigenesis, whose main characteristic is uncontrolled cellular proliferation (Fridman & Tainsky, 2008). We immortalised CO7 and HO6 fibroblasts assuming that it would abrogate replicative senescence on stiff substrates. Our findings contradicted this assumption showing that immortalised orbital fibroblasts not only are β -galactosidase staining sensitive but also surpass wild-type cells in signal intensity. However, immortalised cells displayed significantly little of p16INK4A compared to untreated controls on plastic, indicating that senescence in these cells may occur in a p16 independent manner. Another explanation, similar to our previous observations in CO7 fibroblasts grown on softer substrates (Figure 5.4 B), is that immortalised fibroblasts possibly may not enter a cell cycle arrest. However, due to incompatible mechanical stiffness, immortalised cells could enter a senescence-like state without p16INK4A protein expression. Immortalised CO7 and HO6 cells also proved to be much harder to cultivate than their WT counterparts due to extremely slow cell growth, uncharacteristic to immortalised cells making it possible that substrate rigidity may override immortalisation and prevent cells from proliferating.

5.4 Conclusion

We identified substrate stiffness as a major contributor to orbital fibroblast proliferation with rigid substrates slowing cell growth and forcing orbital fibroblasts to enter a senescence-like state. Moreover, we identified Src, Fyn and PTPN22 as potential regulators of mechanosensitive senescence. We also confirmed the role of AMPK and mTORc1 as major contributors to senescence while also linking their activity to our previous findings regarding fibrosis and lipid droplet production. Our findings may be important not only GO but other illnesses with fibrotic components, where senescence can impair the efficiency of therapies.

CHAPTER 6 DISCUSSION AND FUTURE DIRECTIONS

Graves' orbitopathy is an autoimmune disorder with debilitating consequences and a negative impact on patient's quality of life. Therapeutical options to treat GO are limited due to lack of knowledge of viable molecular targets and therefore limited development of pharmacological compounds to cure the disease. The majority of GO research focuses on inflammatory mechanisms that cause a phenotype shift in orbital fibroblasts to either adipocyte or myofibroblast-like cells, while knowledge of specific, promising molecular pathways to be targeted by drugs is underinvestigated.

This study aimed to investigate the involvement of Src family kinases in spontaneous lipid generation and contractility in orbital fibroblasts. We have demonstrated GO orbital fibroblasts spontaneously generate lipid droplets when cultured in 3D collagen matrices. With our own developed 3D contractility model, we showed that GO fibroblasts are more contractile than healthy controls (He Li et al., 2014). Both of these characteristics were decreased in cells treated with Src-family kinase inhibitors, a group of proteins involved in both adipogenesis, mechanotransduction and contractility. We found that downregulation of two kinases, Src and Fyn, already produces completely different outcomes concerning lipid droplet production and cause activity changes in cellular pathways regulating energy homeostasis, autophagy and lipid breakdown. SFKs radically

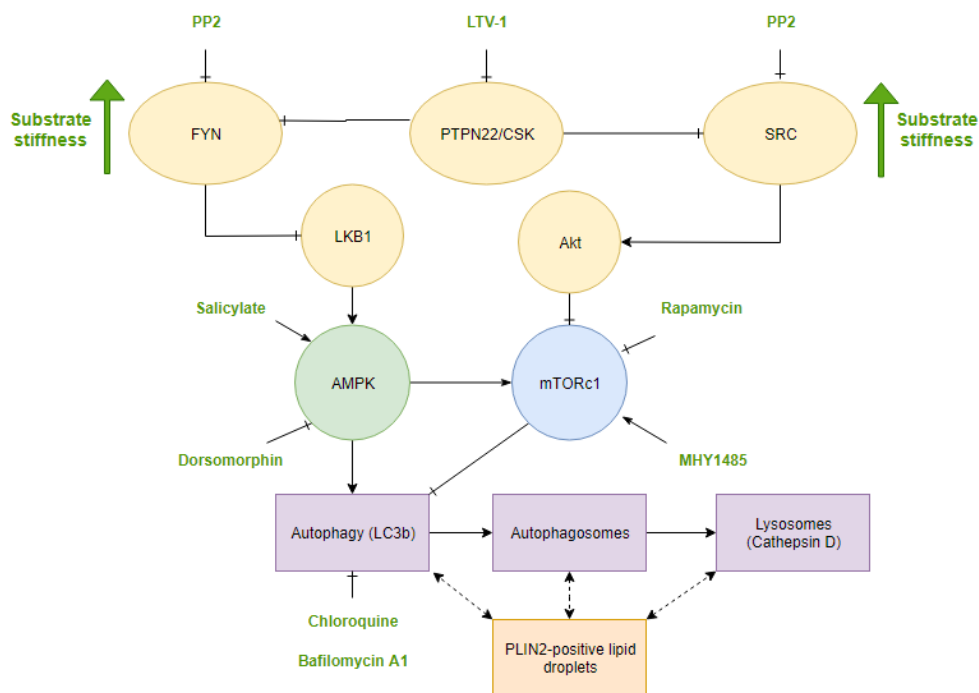


Figure 6. 1. Model of lipid droplet production

Src and Fyn activity is increased when cells are cultivated in rigid substrates which increases mTORc1 activity but blocks AMPK. When cells are cultured in 3D/soft substrates, Fyn and Src protein expression is decreased along with mTORc1 while AMPK activity increases. This prompts the onset of autophagy and production of autophagosomes filled with lipids, subsequently degraded in lysosomes. Co-localisation of PLIN2 with both autophagy and lysosomal markers indicates digestion of lipid droplets.

respond to softer mechanistic environments, shown to be less expressed in 3D cultures and cells cultured on softer substrates. The reason for this is not precisely known. Reduction in SFK protein expression might be caused by structural change in focal adhesions (Wozniak et al., 2004). We found that orbital fibroblasts, when cultured on soft substrates also spontaneously produce lipid droplets, previously observed in 3D, accompanied by reduction of SFKs, mTORc1 expression but increased AMPK activity. While our assumption is that mTORc1 protein expression is caused by loss of SFK

proteins, others have shown that mTORc1 inhibition causes a decrease in FAK phosphorylation (F. Y. Lee et al., 2017) and thus reduced FA assembly which also could mean that loss of mTORc1 activity leads to SFKs downregulation in soft matrix cultures. In soft-matrix cultured cells, we also detected an increase in autophagy marker expression, co-localising with most but not all lipid droplets. Upon further investigation, we observed some lipid droplet co-localisation with lysosomal markers and markers of lipid droplets. Lipid droplet production was disrupted in cells incubated with compounds that inhibit autophagy (Figure 6.1).

Our findings could have important implications in GO research revealing potential therapeutical targets in SFK and associate signalling pathways but also offering insights in lipid droplet production. Prevalent opinion in regards to lipid droplets in GO is that their build-up is due to activation of adipogenesis and a shift towards an adipocyte-like phenotype. We were able to demonstrate that GO orbital fibroblasts produce lipid droplets in 3D without increased expression of adipogenic markers and that substrate rigidity may have a major role in lipid droplet production.

6.1 Role of SRC family kinases in contractility and lipid droplet generation

Our lab has previously demonstrated that orbital fibroblasts are more contractile and generate lipid droplets in 3D cultures. Both of these effects are sensitive to SFK inhibition with PP2 (He Li et al., 2014). Src family kinases regulate cell attachment and focal adhesion formation (Playford &

Schaller, 2004b). Cell attachment dynamics have been demonstrated to differ in 3D, and different mechanistic environments significantly (Cukierman, Pankov, 2001). Involvement of Src in lipogenesis has been previously demonstrated in fibroblasts (Y. Sun et al., 2005) while Fyn involvement in cell contractility has been shown in renal and lung fibrosis (Fiore et al., 2015b; Seo et al., 2016). Fyn also has been shown to attenuate lipid breakdown in vitro and mice models (Woeller et al., 2015; Yamada et al., 2010).

We assessed Src and Fyn expression in control and GO cell lines. All GO cell lines had an increased amount of Fyn in comparison to control cells. Control cell lines, however, had a higher protein expression of Src, which was lower in all GO cells. Overall, Fyn expression was high in GO cells while low in control, while Src expression was the opposite. Overall lipid droplet production was higher in GO cells and could be attributed to the protein amount of both kinases. CO and HO cell lines also displayed different levels of Src activity, highest in CO cells. This potentially indicates that Src activity is impaired in HO cells.

We found that separate Src and Fyn downregulation causes diametrically opposite effects on lipid droplet production in control and GO orbital fibroblasts. Src knockdown significantly increased lipid droplet generation in 3D. Furthermore, lipid droplet production upon Src knock-down was also noticeable in 2D cultures on plastic. Src reduction also decreased GO fibroblasts contractility. We previously observed that overall HO cells have

a lower Src protein expression and activity. Increased lipid droplet production in Src knock-down cells could mean that Src is a limit factor in lipid droplet production.

In Src knock-down cell lysates, we also found reduced Akt and mTORc1 protein expression. This observation proved to be consistent with literature data where Src was shown to regulate mTORc1 protein expression.

Fyn knock-down abolished lipid droplet production in 3D while also decreased the contractility of control and GO fibroblasts. Cell lysates from Fyn knock-down cells showed increased AMPK activation explaining the absence of lipid droplets. In line with these findings, increased amounts of Fyn can partially explain why HO cells which are high in Fyn protein expression.

We also performed down-regulation of CSK and PTPN22 both negative regulators of SFKs. Here, we also observed a reduction of lipid droplets. Decreasing expression of negative regulators should fortify Src and Fyn activity. While Fyn activity appears to reduce lipid droplet breakdown, Src seems to block droplet formation, indicating Src activity is dominant over Fyn when negative regulators of both are diminished.

6.2 Mechanonsensitive lipid droplet production

Substrate rigidity is an important factor in cell growth and differentiation, promoting remodelling of the actin cytoskeleton and cell-ECM adhesion. We have demonstrated that GO orbital fibroblasts generate lipid droplets when

cultured in 3D; however, collagen matrices are significantly softer than plastic on which we cultured cell in standard cultures. We found that when both control and GO orbital fibroblasts are cultured on soft substrates, irrespective of the matrix composition, both cell lines generate lipid droplets. This demonstrates that 3D culturing is not the only factor causing spontaneous lipid droplet production. Furthermore, HO6 cells were less sensitive to increased substrate rigidity and retained their ability to generate lipid droplets while CO7 cells did not. This behaviour appears to be unique to orbital fibroblasts; lipid droplets were not present in dermal and Tenon's capsule fibroblasts under similar conditions. This opens a possibility that GO orbital fibroblasts generate more lipid droplets because of impaired mechanosensing ability that can also be attributed to lower Src protein levels. Src, Fyn and mTORc1 protein expression decreased with lower substrate rigidity while AMPK expression and activity increased under the same conditions. Lipid droplet generation was further increased when stimulating AMPK activity with salicylate and decreased when inhibiting with dorsomorphin. A decrease in lipid droplet production was seen in cells treated with mTORc1 activator. We assessed both soft-culture cell lysates and fixed cells for autophagy markers; LC3b expression was present in both assays, and a clear localisation with lipid droplets was seen. These findings indicate that the cytoplasmic lipid droplets are at least partially autophagosomes. We verified this hypothesis by disrupting the autophagic flux with appropriate inhibitors, and this resulted in significantly fewer lipid droplets. However, a significant amount of lipid droplets presented surface

markers (PLIN2) typical to lipid droplets. We stained the soft-culture cells for lysosomal markers and found that lipid droplet partially co-localise with lysosomes. Altogether, these findings indicate that lipid droplets occurring in orbital fibroblasts are actually a mixed population of lysosomal, autophagosomal and lipid droplet compartments. Lipid droplets have been shown to serve as an autophagy substrate which could explain the co-presence of autophagy and lysosomal markers with PLIN2 (Dong & Czaja, 2011). On rigid substrates, this phenomenon could be eliminated due to increased mTORc1 expression, and limited AMPK activity modulated by Fyn and Src. In relation to GO, it can be assumed that HO cells are less sensitive to their substrate and permissive to autophagy-related lipid droplet production.

While our findings shed more light on the nature of spontaneous lipid droplet formation in orbital fibroblasts, it still remains to be determined what cellular constituents are degraded during autophagy. Another possibility is that lipid droplets form soon after cells are put in 3D or on soft substrates only to become digested by autophagy and re-synthesised again, making lipid droplet generation a cyclic process. This assumption would explain co-localisation of autophagous, lysosomal and lipid droplet markers. Src and Fyn appear to “put breaks” on this process when cells are attached to rigid substrates by limiting AMPK activity and promoting the activity of mTORc1. In conclusion, we have demonstrated that SFK activity alters the dynamics of lipid droplet production, which previously has been attributed to adipogenesis and inflammatory response. Here, we have provided an

alternative explanation to lipid droplet production in GO orbital fibroblasts than can be linked to changes in mechanosensitivity or ECM rigidity. While these findings illustrate biological change in GO orbital fibroblasts, dependent on substrate stiffness, to fortify these findings soft orbital tissue from healthy donors and GO patients should be examined for AMPK activity and autophagy marker presence. While a potential link between autophagy and early stages of the disease has been proposed, investigation of autophagy markers expression and content in GO patient soft orbital tissue has not been investigated (Perez-Moreiras et al., 2018).

Our findings indicate that Fyn, Src, mTORc1 and AMPK as potential therapeutic targets to alleviate lipid droplet production in GO orbital fibroblasts. We were also able to demonstrate that disruption of autophagy limits lipid droplet production and opens up avenues for further therapeutic target exploration. Currently, developing therapies target more established GO pathogenesis pathways with teprotumumab, a IGF-1R inhibitor which recently has showed a significant reduction of proptosis in GO patients (Douglas et al., 2020). Another humanised monoclonal antibody, tocilizumab has been shown to reduce orbital soft tissue inflammation in GO patients by blocking the IL-6 receptor.

6.3 Mechanosensing-associated senescence

During assessing orbital fibroblast behaviour on substrates with different rigidity, we noticed that orbital fibroblasts on softer substrates proliferate much faster. Within 0.2 to 0.5 kPa range, orbital fibroblasts proliferated 6

times faster than when cultured on plastic (0.1 MPa). When staining the cells for β -galactosidase activity, we observed that cells cultured on plastic display almost no SA β -gal activity, while cells on plastic do. Furthermore, when cultured on substrates with rigidity higher than 0.5 kPa, SA β -gal activity was immediately detectable while p16, another senescence marker was present in cells cultured on plastic and at 64 kPa, indicating that orbital fibroblasts cultured in stiffness conditions outside their native rigidity range enter replicative senescence. However, p16INK4A was detected only at 64 kPa stiffness while β -galactosidase activity was observed at stiffnesses above 1 kPa. This might indicate that orbital fibroblasts slightly outside the physiological stiffness range may exhibit senescence-like properties but have not entered a cell cycle arrest. This notion is facilitated by increased cell proliferation at 2, 8 and 16 and 32 kPa compared to cells grown on plastic and at 64 kPa.

Knock-down of Fyn and Src reduced SA β -gal activity. Src has been previously shown to regulate senescence through Akt and mTORc1 pathways (Jung et al., 2019) while its activation can relieve chemically induced senescence (Vigneron, Roninson, Gamelin, & Coqueret, 2005) in cancer cells. Our findings put Src in a pro-senescence role.

Activation of AMPK with salicylate significantly reduced SA β -gal activity and p16 protein expression. While salicylate is established as an AMPK activator, its anti-senescent properties have thus far only been described in nematode plant models (Morris et al., 2000). mTORc1 has been shown to

increase cellular senescence, but its activity is blocked by AMPK (Zhan et al., 2018b). These findings could indicate that orbital fibroblasts, when cultured on substrates too rigid for optimum growth, enter replicative senescence, modulated by SFK activity. However, inhibition and knockdown of PTPN22 and Csk did not fortify senescence but also reduced it, indicating that the regulatory mechanisms of senescence onset may not lie with SFK/AMPK/mTORc1 regulation alone. Senescence was also abolished in cells incubated with ROCK and Vav inhibitors, indicating that the disruption of stress fibre formation, another consequence of cell exposure to rigid substrates, is deterministic to senescence. Contrary to our expectations, immortalisation of orbital fibroblasts increased cell senescence when cultured on plastic, indicating that rigid substrates can override cellular immortalisation.

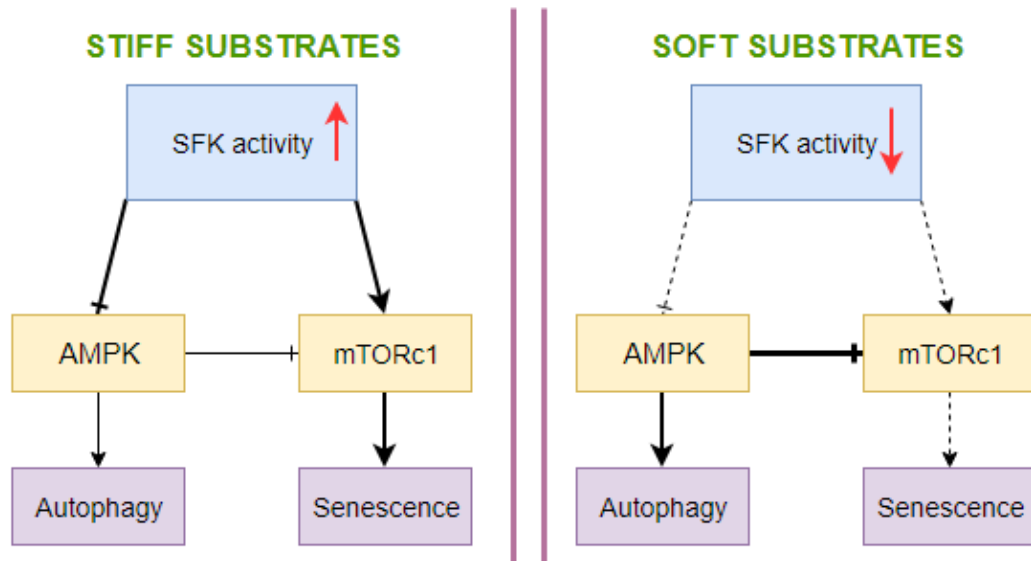


Figure 6. 2. Substrate stiffness regulates replicative senescence through SFKs

SFK activity is increased in orbital fibroblasts grown on stiff substrates. This can maintain mTORc1 activity and simultaneously suppress AMPK. Cell culture on soft matrices downregulates SFK activity. This may increase AMPK activity and limit mTORc1 protein expression and remove replicative senescence.

While increasing ECM stiffness has been associated with ageing (Mavrogenatou et al., 2019; Sprenger, Plymate, & Reed, 2010), rigidity-dependent SA β -gal activity has not been demonstrated before. Here, we characterised that replicative senescence occurs in orbital fibroblasts and can be alleviated when culturing cells on substrates with appropriate rigidity. Furthermore, we were able to show that SFK activity acts as a promoter of senescence via mTORc1/AMPK regulation when cells are cultured on rigid substrates. Attenuation of SFK, AMPK and mTORc1 activity could delay cellular ageing in tissue (Figure 6.2).

6. 4 Experimental limitations

We were able to demonstrate that orbital fibroblasts undergo spontaneous adipogenesis when cultured in 3D and on soft substrates with stiffness of soft orbital tissue. Furthermore, cultivation on soft matrices appears to downregulate mechanotransduction pathways through reduced Fyn/Src protein expression and AMPK/mTORc1 activity. Similar effects were observed by using corresponding inhibitors and activators. We showed that disrupting autophagy, lipid droplet production is reduced. To fortify these findings, investigation of GO patient and healthy patient soft orbital tissue could be beneficial; determining autophagy marker presence also comparing healthy vs GO tissue rigidity. In vivo Src and Fyn expression could be reconstituted in knock-down orbital fibroblasts to see if siRNA silencing effects on lipid droplet production are reversed.

Our soft substrate assays were able to show similar results in lipid droplet production, cell proliferation and senescence. However, none of these models could introduce a significant factor of GO progression; raised intraorbital pressure. The Bailly group has developed a model to mimic the effects of pressure by adding weights on top of 3D culture gels. However, combined with SFK knock-down treatments and inhibitors, this model proved to be highly toxic to the cells. To develop a fuller picture of SFK and autophagy relevance to spontaneous lipid droplet development, a gentler method of introducing pressure in this model should be found.

While β -galactosidase staining is widely used to assess cellular senescence, quantification of the staining signal may be dependent on other factors such as CO₂ enrichment or incubation time. To fortify our findings, parallel Western Blot experiments could be performed to test for β -galactosidase protein presence in cells. In experiments with immortalised CO and HO fibroblasts, cell cycle arrest proteins (p21 and other) could be checked by WB to explain the lack of growth.

6. 5 Concluding remarks

Our findings identify SFK Fyn and Src as potential targets in GO treatments, indicating that GO fibroblasts mechanosensitivity and substrate rigidity might play a crucial role in disease progression. We were able to demonstrate a new link in what causes spontaneous lipid droplet production in GO orbital fibroblasts, previously attributed to adipogenesis. Surprisingly, we discovered that orbital fibroblasts enter senescence on rigid substrates, which can be alleviated by SFK inhibition and culture on soft substrates. These findings open new research avenues in the prevention of GO progression and orbital tissue ageing.

7. BIBLIOGRAPHY

- Albiges-Rizo, C., Destaing, O., Fourcade, B., Planus, E., & Block, M. R. (2009). Actin machinery and mechanosensitivity in invadopodia, podosomes and focal adhesions. *Journal of Cell Science*, 122(17), 3037–3049. <https://doi.org/10.1242/jcs.052704>
- Alcorta, D. A., Xiong, Y., Phelps, D., Hannon, G., Beach, D., & Barrett, J. C. (1996). Involvement of the cyclin-dependent kinase inhibitor p16 (INK4a) in replicative senescence of normal human fibroblasts. *Proceedings of the National Academy of Sciences of the United States of America*, 93(24), 13742–13747. <https://doi.org/10.1073/pnas.93.24.13742>
- Alers, S., Löffler, A. S., Wesselborg, S., & Stork, B. (2012). Role of AMPK-mTOR-Ulk1/2 in the regulation of autophagy: cross talk, shortcuts, and feedbacks. *Molecular and Cellular Biology*, 32(1), 2–11. <https://doi.org/10.1128/MCB.06159-11>
- An Overview of the Cell Cycle - Molecular Biology of the Cell - NCBI Bookshelf. (n.d.). Retrieved May 27, 2020, from <https://www.ncbi.nlm.nih.gov/books/NBK26869/>
- Antonioli, E., Torres, N., Ferretti, M., de Azevedo Piccinato, C., & Sertie, A. L. (2019). Individual response to mTOR inhibition in delaying replicative senescence of mesenchymal stromal cells. *PLoS ONE*, 14(1). <https://doi.org/10.1371/journal.pone.0204784>
- Arifin, M. T., Hama, S., Kajiwar, Y., Sugiyama, K., Saito, T., Matsuura, S., ... Kurisu, K. (2006). Cytoplasmic, but not nuclear, p16 expression may signal poor prognosis in high-grade astrocytomas. *Journal of Neuro-Oncology*, 77(3), 273–277. <https://doi.org/10.1007/s11060-005-9037-5>
- Bahn, R. S. (2003, May 1). Clinical review 157 - Pathophysiology of Graves' ophthalmopathy: The cycle of disease. *Journal of Clinical Endocrinology and Metabolism*, Vol. 88, pp. 1939–1946. <https://doi.org/10.1210/jc.2002-030010>
- Bickel, P. E., Tansey, J. T., & Welte, M. A. (2009). PAT proteins, an ancient family of lipid droplet proteins that regulate cellular lipid stores. *Biochimica et Biophysica Acta*, 1791(6), 419–440. <https://doi.org/10.1016/j.bbailip.2009.04.002>
- Bingel, C., Koeneke, E., Ridinger, J., Bittmann, A., Sill, M., Peterziel, H., ... Oehme, I. (2017). Three-dimensional tumor cell growth stimulates autophagic flux and recapitulates chemotherapy resistance. *Cell Death & Disease*, 8(8), e3013. <https://doi.org/10.1038/cddis.2017.398>
- Blouin, C. M., Le Lay, S., Eberl, A., Köfeler, H. C., Guerrero, I. C., Klein, C., ... Dugail, I. (2010). Lipid droplet analysis in caveolin-deficient

- adipocytes: Alterations in surface phospholipid composition and maturation defects. *Journal of Lipid Research*, 51(5), 945–956. <https://doi.org/10.1194/jlr.M001016>
- Boggon, T. J., & Eck, M. J. (2004, October 18). Structure and regulation of Src family kinases. *Oncogene*, Vol. 23, pp. 7918–7927. <https://doi.org/10.1038/sj.onc.1208081>
- Bost, F., Aouadi, M., Caron, L., & Binétruy, B. (2005). The role of MAPKs in adipocyte differentiation and obesity. *Biochimie*, 87(1), 51–56. <https://doi.org/10.1016/J.BIOCHI.2004.10.018>
- Brandau, S., Bruderek, K., Hestermann, K., Görtz, G.-E., Horstmann, M., Mattheis, S., ... Berchner-Pfannschmidt, U. (2015a). Orbital Fibroblasts From Graves' Orbitopathy Patients Share Functional and Immunophenotypic Properties With Mesenchymal Stem/Stromal Cells. *Investigative Ophthalmology & Visual Science*, 56(11), 6549–6557. <https://doi.org/10.1167/iovs.15-16610>
- Brandau, S., Bruderek, K., Hestermann, K., Görtz, G.-E., Horstmann, M., Mattheis, S., ... Berchner-Pfannschmidt, U. (2015b). Orbital Fibroblasts From Graves' Orbitopathy Patients Share Functional and Immunophenotypic Properties With Mesenchymal Stem/Stromal Cells. *Investigative Ophthalmology & Visual Science*, 56(11), 6549. <https://doi.org/10.1167/iovs.15-16610>
- Burch, H. B., & Cooper, D. S. (2015). Management of Graves Disease. *JAMA*, 314(23), 2544. <https://doi.org/10.1001/jama.2015.16535>
- Burn, G. L., Svensson, L., Sanchez-Blanco, C., Saini, M., & Cope, A. P. (2011, December 1). Why is PTPN22 a good candidate susceptibility gene for autoimmune disease? *FEBS Letters*, Vol. 585, pp. 3689–3698. <https://doi.org/10.1016/j.febslet.2011.04.032>
- Bustelo, X. R. (2001, October 1). Vav proteins, adaptors and cell signaling. *Oncogene*, Vol. 20, pp. 6372–6381. <https://doi.org/10.1038/sj.onc.1204780>
- Buxboim, A., Rajagopal, K., Brown, A. E. X., & Discher, D. E. (2010). How deeply cells feel: methods for thin gels. *Journal of Physics: Condensed Matter*, 22(19), 194116. <https://doi.org/10.1088/0953-8984/22/19/194116>
- Cai, H., Dong, L. Q., & Liu, F. (2016). Recent Advances in Adipose mTOR Signaling and Function: Therapeutic Prospects. *Trends in Pharmacological Sciences*, 37(4), 303–317. <https://doi.org/10.1016/j.tips.2015.11.011>
- Calhoun, C., Shivshankar, P., Saker, M., Sloane, L. B., Livi, C. B., Sharp, Z. D., ... Jourdan Le Saux, C. (2016). Senescent Cells Contribute to the Physiological Remodeling of Aged Lungs. *Journals of Gerontology -*

Series A Biological Sciences and Medical Sciences, 71(2), 153–160.
<https://doi.org/10.1093/gerona/glu241>

- Caron-Lormier, G., & Berry, H. (2005). Amplification and oscillations in the FAK/Src kinase system during integrin signaling. *Journal of Theoretical Biology*, 232(2), 235–248. <https://doi.org/10.1016/J.JTBI.2004.08.010>
- Chang, M. Y., Huang, D. Y., Ho, F. M., Huang, K. C., & Lin, W. W. (2012). PKC-dependent human monocyte adhesion requires AMPK and Syk activation. *PLoS ONE*, 7(7). <https://doi.org/10.1371/journal.pone.0040999>
- Chen, R., Kim, O., Yang, J., Sato, K., Eisenmann, K. M., McCarthy, J., ... Qiu, Y. (2001a). Regulation of Akt/PKB activation by tyrosine phosphorylation. *The Journal of Biological Chemistry*, 276(34), 31858–31862. <https://doi.org/10.1074/jbc.C100271200>
- Chen, R., Kim, O., Yang, J., Sato, K., Eisenmann, K. M., McCarthy, J., ... Qiu, Y. (2001b). Regulation of Akt/PKB activation by tyrosine phosphorylation. *The Journal of Biological Chemistry*, 276(34), 31858–31862. <https://doi.org/10.1074/jbc.C100271200>
- Chen, W. C., Lin, H. H., & Tang, M. J. (2014). Regulation of proximal tubular cell differentiation and proliferation in primary culture by matrix stiffness and ECM components. *American Journal of Physiology - Renal Physiology*, 307(6), F695–F707. <https://doi.org/10.1152/ajprenal.00684.2013>
- Chen, Y., Zheng, Y., & Foster, D. A. (2003). Phospholipase D confers rapamycin resistance in human breast cancer cells. *Oncogene*, 22(25), 3937–3942. <https://doi.org/10.1038/sj.onc.1206565>
- Childs, B. G., Baker, D. J., Kirkland, J. L., Campisi, J., & Deursen, J. M. Van. (2014). *Embr0015-1139*. 15(11), 1139–1153. <https://doi.org/10.15252/embr.201439245>
- Choi, Y. J., Park, Y. J., Park, J. Y., Jeong, H. O., Kim, D. H., Ha, Y. M., ... Chung, H. Y. (2012). Inhibitory Effect of mTOR Activator MHY1485 on Autophagy: Suppression of Lysosomal Fusion. *PLoS ONE*, 7(8), e43418. <https://doi.org/10.1371/journal.pone.0043418>
- Clarke, F., Purvis, H. A., Sanchez-Blanco, C., Gutiérrez-Martinez, E., Cornish, G. H., Zamoyska, R., ... Cope, A. P. (2018a). The protein tyrosine phosphatase PTPN22 negatively regulates presentation of immune complex derived antigens. *Scientific Reports*, 8(1), 12692. <https://doi.org/10.1038/s41598-018-31179-x>
- Clarke, F., Purvis, H. A., Sanchez-Blanco, C., Gutiérrez-Martinez, E., Cornish, G. H., Zamoyska, R., ... Cope, A. P. (2018b). The protein tyrosine phosphatase PTPN22 negatively regulates presentation of immune complex derived antigens. *Scientific Reports*, 8(1).

<https://doi.org/10.1038/s41598-018-31179-x>

- Correia-Melo, C., Marques, F. D., Anderson, R., Hewitt, G., Hewitt, R., Cole, J., ... Passos, J. F. (2016). Mitochondria are required for pro-ageing features of the senescent phenotype. *The EMBO Journal*, 35(7), 724–742. <https://doi.org/10.15252/embj.201592862>
- Cross, V. L., Zheng, Y., Won Choi, N., Verbridge, S. S., Sutermaister, B. A., Bonassar, L. J., ... Stroock, A. D. (2010). Dense type I collagen matrices that support cellular remodeling and microfabrication for studies of tumor angiogenesis and vasculogenesis in vitro. *Biomaterials*, 31(33), 8596–8607. <https://doi.org/10.1016/j.biomaterials.2010.07.072>
- Cui, J., Bai, X. Y., Shi, S., Cui, S., Hong, Q., Cai, G., & Chen, X. (2012). Age-related changes in the function of autophagy in rat kidneys. *Age*, 34(2), 329–339. <https://doi.org/10.1007/s11357-011-9237-1>
- Cukierman, E., Pankov, R., Science, D. S., & 2001, undefined. (n.d.). Taking cell-matrix adhesions to the third dimension. *Science.Sciencemag.Org*. Retrieved from <https://science.sciencemag.org/content/294/5547/1708.short>
- Darby, I. A., & Hewitson, T. D. (2007). Fibroblast Differentiation in Wound Healing and Fibrosis. *International Review of Cytology*, Vol. 257, pp. 143–179. [https://doi.org/10.1016/S0074-7696\(07\)57004-X](https://doi.org/10.1016/S0074-7696(07)57004-X)
- Davies, T. F., Ando, T., Lin, R.-Y., Tomer, Y., & Latif, R. (2005). Thyrotropin receptor-associated diseases: from adenomata to Graves disease. *The Journal of Clinical Investigation*, 115(8), 1972–1983. <https://doi.org/10.1172/JCI26031>
- Debidda, M., Williams, D. A., & Zheng, Y. (2006a). Rac1 GTPase regulates cell genomic stability and senescence. *Journal of Biological Chemistry*, 281(50), 38519–38528. <https://doi.org/10.1074/jbc.M604607200>
- Debidda, M., Williams, D. A., & Zheng, Y. (2006b). *Rac1 regulates cellular senescence and cell cycle through reactive oxygen species and p53*. <https://doi.org/10.1074/jbc.M604607200>
- Desailloud, R., & Hober, D. (2009). Viruses and thyroiditis: An update. *Virology Journal*, Vol. 6. <https://doi.org/10.1186/1743-422X-6-5>
- Dik, W. A., Virakul, S., & van Steensel, L. (2016). Current perspectives on the role of orbital fibroblasts in the pathogenesis of Graves' ophthalmopathy. *Experimental Eye Research*, 142, 83–91. <https://doi.org/10.1016/j.exer.2015.02.007>
- Dong, H., & Czaja, M. J. (2011, June). Regulation of lipid droplets by autophagy. *Trends in Endocrinology and Metabolism*, Vol. 22, pp. 234–240. <https://doi.org/10.1016/j.tem.2011.02.003>

- Douglas, R. S., Kahaly, G. J., Patel, A., Sile, S., Thompson, E. H. Z., Perdok, R., ... Smith, T. J. (2020). Teprotumumab for the treatment of active thyroid eye disease. *New England Journal of Medicine*, 382(4), 341–352. <https://doi.org/10.1056/NEJMoa1910434>
- Douroudis, K., Prans, E., Haller, K., Nemvalts, V., Rajasalu, T., Tillmann, V., ... Uibo, R. (2008). Protein tyrosine phosphatase non-receptor type 22 gene variants at position 1858 are associated with type 1 and type 2 diabetes in Estonian population. *Tissue Antigens*, 72(5), 425–430. <https://doi.org/10.1111/j.1399-0039.2008.01115.x>
- Draman, M. S., Stechman, M., Scott-Coombes, D., Dayan, C. M., Rees, D. A., Ludgate, M., & Zhang, L. (2017). The role of thyrotropin receptor activation in adipogenesis and modulation of fat phenotype. *Frontiers in Endocrinology*, 8(APR). <https://doi.org/10.3389/fendo.2017.00083>
- Dulińska-Molak, I., Pasikowska, M., Pogoda, K., Lewandowska, M., Eris, I., & Lekka, M. (2014). Age-related changes in the mechanical properties of human fibroblasts and its prospective reversal after anti-wrinkle tripeptide treatment. *International Journal of Peptide Research and Therapeutics*, 20(1), 77–85. <https://doi.org/10.1007/s10989-013-9370-z>
- Dunlop, E. A., & Tee, A. R. (2013). The kinase triad, AMPK, mTORC1 and ULK1, maintains energy and nutrient homoeostasis. *Biochemical Society Transactions*, 41(4), 939–943. <https://doi.org/10.1042/BST20130030>
- Durand, C., Ambinder, R., Blankson, J., & Forman, S. (2012). HIV-1 and hematopoietic stem cell transplantation. *Biology of Blood and Marrow Transplantation : Journal of the American Society for Blood and Marrow Transplantation*, 18(1 Suppl), S172-6. <https://doi.org/10.1016/j.bbmt.2011.10.027>
- Duval, K., Grover, H., Han, L.-H., Mou, Y., Pegoraro, A. F., Fredberg, J., & Chen, Z. (2017). Modeling Physiological Events in 2D vs. 3D Cell Culture. *Physiology (Bethesda, Md.)*, 32(4), 266–277. <https://doi.org/10.1152/physiol.00036.2016>
- Fedetz, M., Matesanz, F., Caro-Maldonado, A., Smirnov, I. I., Chvorostinka, V. N., Moiseenko, T. A., & Alcina, A. (2006). The 1858T PTPN22 gene variant contributes to a genetic risk of type 1 diabetes in a Ukrainian population. *Tissue Antigens*, 67(5), 430–433. <https://doi.org/10.1111/j.1399-0039.2006.00591.x>
- Ferrari, S. M., Fallahi, P., Antonelli, A., & Benvenga, S. (2017, March 20). Environmental issues in thyroid diseases. *Frontiers in Endocrinology*, Vol. 8. <https://doi.org/10.3389/fendo.2017.00050>
- Fichter, N., Guthoff, R. F., & Schittkowski, M. P. (2012). Orbital decompression in thyroid eye disease. *ISRN Ophthalmology*, 2012,

739236. <https://doi.org/10.5402/2012/739236>

- Fiore, V. F., Strane, P. W., Bryksin, A. V, White, E. S., Hagood, J. S., & Barker, T. H. (2015a). Conformational coupling of integrin and Thy-1 regulates Fyn priming and fibroblast mechanotransduction. *The Journal of Cell Biology*, 211(1), 173–190. <https://doi.org/10.1083/jcb.201505007>
- Fiore, V. F., Strane, P. W., Bryksin, A. V, White, E. S., Hagood, J. S., & Barker, T. H. (2015b). Conformational coupling of integrin and Thy-1 regulates Fyn priming and fibroblast mechanotransduction. *The Journal of Cell Biology*, 211(1), 173–190. <https://doi.org/10.1083/jcb.201505007>
- Fiorillo, E., Orrú, V., Stanford, S. M., Liu, Y., Salek, M., Rapini, N., ... Bottini, N. (2010). Autoimmune-associated PTPN22 R620W variation reduces phosphorylation of lymphoid phosphatase on an inhibitory tyrosine residue. *The Journal of Biological Chemistry*, 285(34), 26506–26518. <https://doi.org/10.1074/jbc.M110.111104>
- Fridman, A. L., & Tainsky, M. A. (2008, October 9). Critical pathways in cellular senescence and immortalization revealed by gene expression profiling. *Oncogene*, Vol. 27, pp. 5975–5987. <https://doi.org/10.1038/onc.2008.213>
- Garrity, J. A., & Bahn, R. S. (2006). Pathogenesis of Graves Ophthalmopathy: Implications for Prediction, Prevention, and Treatment. *American Journal of Ophthalmology*, 142(1), 147-153.e2. <https://doi.org/10.1016/J.AJO.2006.02.047>
- Gruber, A., Cornaciu, I., Lass, A., Schweiger, M., Poeschl, M., Eder, C., ... Oberer, M. (2010). The N-terminal region of comparative gene identification-58 (CGI-58) is important for lipid droplet binding and activation of adipose triglyceride lipase. *Journal of Biological Chemistry*, 285(16), 12289–12298. <https://doi.org/10.1074/jbc.M109.064469>
- Guan, Y., Yang, X., Yang, W., Charbonneau, C., & Chen, Q. (2014). Mechanical activation of mammalian target of rapamycin pathway is required for cartilage development. *FASEB Journal : Official Publication of the Federation of American Societies for Experimental Biology*, 28(10), 4470–4481. <https://doi.org/10.1096/fj.14-252783>
- Hadjipanayi, E., Mudera, V., & Brown, R. A. (2009). Close dependence of fibroblast proliferation on collagen scaffold matrix stiffness. *Journal of Tissue Engineering and Regenerative Medicine*, 3(2), 77–84. <https://doi.org/10.1002/term.136>
- Hardie, D. G. (2014). AMP-activated protein kinase: A key regulator of energy balance with many roles in human disease. *Journal of Internal Medicine*. <https://doi.org/10.1111/joim.12268>

- Hawley, S. A., Fullerton, M. D., Ross, F. A., Schertzer, J. D., Chevtzoff, C., Walker, K. J., ... Hardie, D. G. (2012). The Ancient Drug Salicylate Directly Activates AMP-Activated Protein Kinase. *Science*, 336(6083), 918–922. <https://doi.org/10.1126/science.1215327>
- Hernandez-Segura, A., de Jong, T. V., Melov, S., Guryev, V., Campisi, J., & Demaria, M. (2017). Unmasking Transcriptional Heterogeneity in Senescent Cells. *Current Biology*, 27(17), 2652-2660.e4. <https://doi.org/10.1016/j.cub.2017.07.033>
- Herranz, N., & Gil, J. (2018, April 2). Mechanisms and functions of cellular senescence. *Journal of Clinical Investigation*, Vol. 128, pp. 1238–1246. <https://doi.org/10.1172/JCI95148>
- Herrera, J., Henke, C. A., & Bitterman, P. B. (2018, January 2). Extracellular matrix as a driver of progressive fibrosis. *Journal of Clinical Investigation*, Vol. 128, pp. 45–53. <https://doi.org/10.1172/JCI93557>
- Hillel, A. T., & Gelbard, A. (2015). Unleashing rapamycin in fibrosis. *Oncotarget*, Vol. 6, pp. 15722–15723. <https://doi.org/10.18632/oncotarget.4652>
- Hornberger, T. A. (2011). Mechanotransduction and the regulation of mTORC1 signaling in skeletal muscle. *International Journal of Biochemistry and Cell Biology*, Vol. 43, pp. 1267–1276. <https://doi.org/10.1016/j.biocel.2011.05.007>
- Huang, X., Wullschleger, S., Shpiro, N., McGuire, V. A., Sakamoto, K., Woods, Y. L., ... Alessi, D. R. (2008). Important role of the LKB1–AMPK pathway in suppressing tumorigenesis in PTEN-deficient mice. *Biochemical Journal*. <https://doi.org/10.1042/BJ20080557>
- Ingber, D. E. (2006). Cellular mechanotransduction: putting all the pieces together again. *The FASEB Journal*, 20(7), 811–827. <https://doi.org/10.1096/fj.05-5424rev>
- Ingle, E. (2008). Src family kinases: Regulation of their activities, levels and identification of new pathways. *Biochimica et Biophysica Acta (BBA) - Proteins and Proteomics*, 1784(1), 56–65. <https://doi.org/10.1016/J.BBAPAP.2007.08.012>
- Jääger, K., & Neuman, T. (2011). Human dermal fibroblasts exhibit delayed adipogenic differentiation compared with mesenchymal stem cells. *Stem Cells and Development*, 20(8), 1327–1336. <https://doi.org/10.1089/scd.2010.0258>
- Jaishy, B., & Abel, E. D. (2016). Lipids, lysosomes, and autophagy. *Journal of Lipid Research*, 57(9), 1619–1635. <https://doi.org/10.1194/jlr.R067520>
- Jiang, T., & Qiu, Y. (2003). Interaction between Src and a C-terminal proline-rich motif of Akt is required for Akt activation. *The Journal of*

- Biological Chemistry*, 278(18), 15789–15793.
<https://doi.org/10.1074/jbc.M212525200>
- Jung, S. H., Lee, M., Park, H. A., Lee, H. C., Kang, D., Hwang, H. J., ... Lee, J. S. (2019). Integrin $\alpha 6\beta 4$ -Src-AKT signaling induces cellular senescence by counteracting apoptosis in irradiated tumor cells and tissues. *Cell Death and Differentiation*, 26(2), 245–259.
<https://doi.org/10.1038/s41418-018-0114-7>
- Kang, H. T., Lee, K. B., Kim, S. Y., Choi, H. R., & Park, S. C. (2011). Autophagy Impairment Induces Premature Senescence in Primary Human Fibroblasts. *PLoS ONE*, 6(8), e23367.
<https://doi.org/10.1371/journal.pone.0023367>
- Kaushik, S., & Cuervo, A. M. (2016). AMPK-dependent phosphorylation of lipid droplet protein PLIN2 triggers its degradation by CMA. *Autophagy*, 12(2), 432–438. <https://doi.org/10.1080/15548627.2015.1124226>
- Kenific, C. M., Wittmann, T., & Debnath, J. (2016). Autophagy in adhesion and migration. *Journal of Cell Science*, Vol. 129, pp. 3685–3693.
<https://doi.org/10.1242/jcs.188490>
- Khong, J. J., McNab, A. A., Ebeling, P. R., Craig, J. E., & Selva, D. (2016). Pathogenesis of thyroid eye disease: Review and update on molecular mechanisms. *British Journal of Ophthalmology*.
<https://doi.org/10.1136/bjophthalmol-2015-307399>
- King, J. S., Veltman, D. M., & Insall, R. H. (2011). The induction of autophagy by mechanical stress. *Autophagy*, 7(12), 1490–1499.
<https://doi.org/10.4161/auto.7.12.17924>
- Koch, C. A., Anderson, D., Moran, M. F., Ellis, C., & Pawson, T. (1991). SH2 and SH3 domains: Elements that control interactions of cytoplasmic signaling proteins. *Science*, 252(5006), 668–674.
<https://doi.org/10.1126/science.1708916>
- Koegl, M., Zlatkine, P., Ley, S. C., Courtneidge, S. A., & Magee, A. I. (1994). Palmitoylation of multiple Src-family kinases at a homologous N-terminal motif. *Biochemical Journal*, 303(3), 749–753.
<https://doi.org/10.1042/bj3030749>
- Kozdon, K., Fitchett, C., Rose, G. E., Ezra, D. G., & Bailly, M. (2015). Mesenchymal Stem Cell-Like Properties of Orbital Fibroblasts in Graves' Orbitopathy. *Investigative Ophthalmology & Visual Science*, 56(10), 5743–5750. <https://doi.org/10.1167/iovs.15-16580>
- Krieger, C. C., Neumann, S., Place, R. F., Marcus-Samuels, B., & Gershengorn, M. C. (2015). Bidirectional TSH and IGF-1 Receptor Cross Talk Mediates Stimulation of Hyaluronan Secretion by Graves' Disease Immunoglobulins. *The Journal of Clinical Endocrinology & Metabolism*, 100(3), 1071–1077. <https://doi.org/10.1210/jc.2014-3566>

- Krieger, C. C., Place, R. F., Bevilacqua, C., Marcus-Samuels, B., Abel, B. S., Skarulis, M. C., ... Gershengorn, M. C. (2016). TSH/IGF-1 receptor cross talk in graves' ophthalmopathy pathogenesis. *Journal of Clinical Endocrinology and Metabolism*, 101(6), 2340–2347. <https://doi.org/10.1210/jc.2016-1315>
- Kumar, S., Coenen, M. J., Scherer, P. E., & Bahn, R. S. (2004). Evidence for enhanced adipogenesis in the orbits of patients with Graves' ophthalmopathy. *The Journal of Clinical Endocrinology and Metabolism*, 89(2), 930–935. <https://doi.org/10.1210/jc.2003-031427>
- Kurakazu, I., Akasaki, Y., Hayashida, M., Tsushima, H., Goto, N., Sueishi, T., ... Nakashima, Y. (2019). FOXO1 transcription factor regulates chondrogenic differentiation through transforming growth factor β 1 signaling. *Journal of Biological Chemistry*, 294(46), 17555–17569. <https://doi.org/10.1074/jbc.RA119.009409>
- Kureel, S. K., Mogha, P., Khadpekar, A., Kumar, V., Joshi, R., Das, S., ... Majumder, A. (2019). Soft substrate maintains proliferative and adipogenic differentiation potential of human mesenchymal stem cells on long-term expansion by delaying senescence. *Biology Open*, 8(4). <https://doi.org/10.1242/bio.039453>
- Kurz, D. J., Decary, S., Hong, Y., & Erusalimsky, J. D. (2000). Senescence-associated α -galactosidase reflects an increase in lysosomal mass during replicative ageing of human endothelial cells. *Journal of Cell Science*, 113(20), 3613–3622.
- Laplante, M., & Sabatini, D. M. (2009). An emerging role of mTOR in lipid biosynthesis. *Current Biology: CB*, 19(22), R1046-52. <https://doi.org/10.1016/j.cub.2009.09.058>
- Laplante, M., & Sabatini, D. M. (2013). Regulation of mTORC1 and its impact on gene expression at a glance. *Journal of Cell Science*, 126(Pt 8), 1713–1719. <https://doi.org/10.1242/jcs.125773>
- Latif, R., Morshed, S. A., Zaidi, M., & Davies, T. F. (2009). The thyroid-stimulating hormone receptor: impact of thyroid-stimulating hormone and thyroid-stimulating hormone receptor antibodies on multimerization, cleavage, and signaling. *Endocrinology and Metabolism Clinics of North America*, 38(2), 319–341, viii. <https://doi.org/10.1016/j.ecl.2009.01.006>
- Lawrence, J., & Nho, R. (2018, March 8). The role of the mammalian target of rapamycin (mTOR) in pulmonary fibrosis. *International Journal of Molecular Sciences*, Vol. 19. <https://doi.org/10.3390/ijms19030778>
- Lee, F.-Y., Zhen, Y.-Y., Yuen, C.-M., Fan, R., Chen, Y.-T., Sheu, J.-J., ... Yip, H.-K. (2017). The mTOR-FAK mechanotransduction signaling axis for focal adhesion maturation and cell proliferation. *American Journal of Translational Research*, 9(4), 1603–1617. Retrieved from

<http://www.ncbi.nlm.nih.gov/pubmed/28469768>

- Lee, F. Y., Zhen, Y. Y., Yuen, C. M., Fan, R., Chen, Y. T., Sheu, J. J., ... Yip, H. K. (2017). The mTOR-FAK mechanotransduction signaling axis for focal adhesion maturation and cell proliferation. *American Journal of Translational Research*, 9(4), 1603–1617.
- Levental, K. R., Yu, H., Kass, L., Lakins, J. N., Egeblad, M., Erler, J. T., ... Weaver, V. M. (2009). Matrix Crosslinking Forces Tumor Progression by Enhancing Integrin Signaling. *Cell*, 139(5), 891–906. <https://doi.org/10.1016/j.cell.2009.10.027>
- Li, He, Fitchett, C., Kozdon, K., Jayaram, H., Rose, G. E., Bailly, M., & Ezra, D. G. (2014). Independent Adipogenic and Contractile Properties of Fibroblasts in Graves' Orbitopathy: An In Vitro Model for the Evaluation of Treatments. *PLoS ONE*, 9(4), e95586. <https://doi.org/10.1371/journal.pone.0095586>
- Li, Hong, Yuan, Y., Zhang, Y., Zhang, X., Gao, L., & Xu, R. (2017). Icariin Inhibits AMPK-Dependent Autophagy and Adipogenesis in Adipocytes In vitro and in a Model of Graves' Orbitopathy In vivo. *Frontiers in Physiology*, 8, 45. <https://doi.org/10.3389/fphys.2017.00045>
- Li, L., Okura, M., & Imamoto, A. (2002). Focal Adhesions Require Catalytic Activity of Src Family Kinases To Mediate Integrin-Matrix Adhesion. *Molecular and Cellular Biology*, 22(4), 1203–1217. <https://doi.org/10.1128/mcb.22.4.1203-1217.2002>
- Li, W., Li, J., & Bao, J. (2012). Microautophagy: lesser-known self-eating. *Cellular and Molecular Life Sciences: CMLS*, 69(7), 1125–1136. <https://doi.org/10.1007/s00018-011-0865-5>
- Liang, Z., Li, T., Jiang, S., Xu, J., di, W., Yang, Z., ... Yang, Y. (2017, September 1). AMPK: A novel target for treating hepatic fibrosis. *Oncotarget*, Vol. 8, pp. 62780–62792. <https://doi.org/10.18632/oncotarget.19376>
- Liu, D. D., Han, C. C., Wan, H. F., He, F., Xu, H. Y., Wei, S. H., ... Xu, F. (2016). Effects of inhibiting PI3K-Akt-mTOR pathway on lipid metabolism homeostasis in goose primary hepatocytes. *Animal*, 10(08), 1319–1327. <https://doi.org/10.1017/S1751731116000380>
- Liu, N., Zhou, M., Zhang, Q., Yong, L., Zhang, T., Tian, T., ... Cai, X. (2018). Effect of substrate stiffness on proliferation and differentiation of periodontal ligament stem cells. *Cell Proliferation*, 51(5), e12478. <https://doi.org/10.1111/cpr.12478>
- Liu, X., Chhipa, R. R., Nakano, I., & Dasgupta, B. (2014). *The AMPK Inhibitor Compound C Is a Potent AMPK-Independent Antiglioma Agent*. <https://doi.org/10.1158/1535-7163.MCT-13-0579>
- Madsen, L., Petersen, R. K., & Kristiansen, K. (2005). Regulation of

- adipocyte differentiation and function by polyunsaturated fatty acids. *Biochimica et Biophysica Acta (BBA) - Molecular Basis of Disease*, 1740(2), 266–286. <https://doi.org/10.1016/J.BBADIS.2005.03.001>
- Maheshwari, R., & Weis, E. (2012). Thyroid associated orbitopathy. *Indian Journal of Ophthalmology*, 60(2), 87–93. <https://doi.org/10.4103/0301-4738.94048>
- Majd, S., Power, J. H. T., Chataway, T. K., & Grantham, H. J. M. (2018). A comparison of LKB1/AMPK/mTOR metabolic axis response to global ischaemia in brain, heart, liver and kidney in a rat model of cardiac arrest. *BMC Cell Biology*, 19(1), 7. <https://doi.org/10.1186/s12860-018-0159-y>
- Massey, A. C., Zhang, C., & Cuervo, A. M. (2006). Chaperone-mediated autophagy in aging and disease. *Current Topics in Developmental Biology*, 73, 205–235. [https://doi.org/10.1016/S0070-2153\(05\)73007-6](https://doi.org/10.1016/S0070-2153(05)73007-6)
- Mauthe, M., Orhon, I., Rocchi, C., Zhou, X., Luhr, M., Hijlkema, K.-J., ... Reggiori, F. (2018). Chloroquine inhibits autophagic flux by decreasing autophagosome-lysosome fusion. *Autophagy*, 14(8), 1435–1455. <https://doi.org/10.1080/15548627.2018.1474314>
- Mauvezin, C., & Neufeld, T. P. (2015). Bafilomycin A1 disrupts autophagic flux by inhibiting both V-ATPase-dependent acidification and Ca-P60A/SERCA-dependent autophagosome-lysosome fusion. *Autophagy*, 11(8), 1437–1438. <https://doi.org/10.1080/15548627.2015.1066957>
- Mavrogonatou, E., Pratsinis, H., Papadopoulou, A., Karamanos, N. K., & Kletsas, D. (2019, January 1). Extracellular matrix alterations in senescent cells and their significance in tissue homeostasis. *Matrix Biology*, Vol. 75–76, pp. 27–42. <https://doi.org/10.1016/j.matbio.2017.10.004>
- McHugh, D., & Gil, J. (2018, January 1). Senescence and aging: Causes, consequences, and therapeutic avenues. *Journal of Cell Biology*, Vol. 217, pp. 65–77. <https://doi.org/10.1083/jcb.201708092>
- McLeod, D. S. A., Caturegli, P., Cooper, D. S., Matos, P. G., & Hutfless, S. (2014). Variation in Rates of Autoimmune Thyroid Disease by Race/Ethnicity in US Military Personnel. *JAMA*, 311(15), 1563. <https://doi.org/10.1001/jama.2013.285606>
- Mester, T., Raychaudhuri, N., Gillespie, E. F., Chen, H., Smith, T. J., & Douglas, R. S. (2016). CD40 expression in fibrocytes is induced by TSH: Potential synergistic immune activation. *PLoS ONE*, 11(9). <https://doi.org/10.1371/journal.pone.0162994>
- Mizushima, N., & Yoshimori, T. (2007). How to Interpret LC3 Immunoblotting. *Autophagy*, 542(6). <https://doi.org/10.4161/auto.4600>

- Molina-Molina, M., Machahua-Huamani, C., Vicens-Zygmunt, V., Llatjós, R., Escobar, I., Sala-Llinas, E., ... Montes-Worboys, A. (2018). Anti-fibrotic effects of pirfenidone and rapamycin in primary IPF fibroblasts and human alveolar epithelial cells. *BMC Pulmonary Medicine*, 18(1). <https://doi.org/10.1186/s12890-018-0626-4>
- Morris, K., MacKerness, S. A., Page, T., John, C. F., Murphy, A. M., Carr, J. P., & Buchanan-Wollaston, V. (2000). Salicylic acid has a role in regulating gene expression during leaf senescence. *The Plant Journal : For Cell and Molecular Biology*, 23(5), 677–685. <https://doi.org/10.1046/j.1365-3113x.2000.00836.x>
- Morshed, S. A., & Davies, T. F. (2015). Graves' Disease Mechanisms: The Role of Stimulating, Blocking, and Cleavage Region TSH Receptor Antibodies. *Hormone and Metabolic Research*, 47(10), 727–734. <https://doi.org/10.1055/s-0035-1559633>
- Morshed, Syed A., Ando, T., Latif, R., & Davies, T. F. (2010). Neutral antibodies to the TSH receptor are present in Graves' disease and regulate selective signaling cascades. *Endocrinology*, 151(11), 5537–5549. <https://doi.org/10.1210/en.2010-0424>
- Moujaber, O., Fishbein, F., Omran, N., Liang, Y., Colmegna, I., Presley, J. F., & Stochaj, U. (2019). Cellular senescence is associated with reorganization of the microtubule cytoskeleton. *Cellular and Molecular Life Sciences : CMLS*, 76(6), 1169–1183. <https://doi.org/10.1007/s00018-018-2999-1>
- Mullen, C. A., Vaughan, T. J., Billiar, K. L., & McNamara, L. M. (2015). The effect of substrate stiffness, thickness, and cross-linking density on osteogenic cell behavior. *Biophysical Journal*, 108(7), 1604–1612. <https://doi.org/10.1016/j.bpj.2015.02.022>
- Niemelä, S., Miettinen, S., Sarkanen, J.-R., & Ashammakhi, N. (2008). Adipose Tissue and Adipocyte Differentiation: Molecular and Cellular Aspects and Tissue Engineering Applications. *Topics in Tissue Engineering. Volume 4*.
- O'Brien, A. J., Villani, L. A., Broadfield, L. A., Houde, V. P., Galic, S., Blandino, G., ... Steinberg, G. R. (2015). Salicylate activates AMPK and synergizes with metformin to reduce the survival of prostate and lung cancer cells *ex vivo* through inhibition of *de novo* lipogenesis. *Biochemical Journal*, 469(2), 177–187. <https://doi.org/10.1042/BJ20150122>
- Onal, G., Kutlu, O., Gozuacik, D., & Dokmeci Emre, S. (2017). Lipid Droplets in Health and Disease. *Lipids in Health and Disease*, 16(1), 128. <https://doi.org/10.1186/s12944-017-0521-7>
- Park, J. T., Kang, H. T., Park, C. H., Lee, Y. S., Cho, K. A., & Park, S. C. (2018). A crucial role of ROCK for alleviation of senescence-associated

- phenotype. *Experimental Gerontology*, 106, 8–15.
<https://doi.org/10.1016/j.exger.2018.02.012>
- Parkington, J. D., Siebert, A. P., LeBrasseur, N. K., & Fielding, R. A. (2003). Differential activation of mTOR signaling by contractile activity in skeletal muscle. *American Journal of Physiology-Regulatory, Integrative and Comparative Physiology*, 285(5), R1086–R1090.
<https://doi.org/10.1152/ajpregu.00324.2003>
- Pascual, G., Sullivan, A. L., Ogawa, S., Gamliel, A., Perissi, V., Rosenfeld, M. G., & Glass, C. K. (2007). Anti-inflammatory and antidiabetic roles of PPARgamma. *Novartis Foundation Symposium*, 286, 183–196; discussion 196–203. Retrieved from
<http://www.ncbi.nlm.nih.gov/pubmed/18269183>
- Paszek, M. J., Zahir, N., Johnson, K. R., Lakins, J. N., Rozenberg, G. I., Gefen, A., ... Weaver, V. M. (2005). Tensional homeostasis and the malignant phenotype. *Cancer Cell*, 8(3), 241–254.
<https://doi.org/10.1016/j.ccr.2005.08.010>
- Perez-Moreiras, J. V., Gomez-Reino, J. J., Maneiro, J. R., Perez-Pampin, E., Romo Lopez, A., Rodríguez Alvarez, F. M., ... Maiquez, M. P. (2018). Efficacy of Tocilizumab in Patients With Moderate-to-Severe Corticosteroid-Resistant Graves Orbitopathy: A Randomized Clinical Trial. *American Journal of Ophthalmology*, 195, 181–190.
<https://doi.org/10.1016/j.ajo.2018.07.038>
- Phillip, J. M., Aifuwa, I., Walston, J., & Wirtz, D. (2015). The Mechanobiology of Aging. *Annual Review of Biomedical Engineering*, 17(1), 113–141.
<https://doi.org/10.1146/annurev-bioeng-071114-040829>
- Piechota, M., Sunderland, P., Wysocka, A., Nalberczak, M., Sliwinska, M. A., Radwanska, K., & Sikora, E. (2016). Is senescence-associated β -galactosidase a marker of neuronal senescence? *Oncotarget*, 7(49), 81099–81109. <https://doi.org/10.18632/oncotarget.12752>
- Playford, M. P., & Schaller, M. D. (2004a). The interplay between Src and integrins in normal and tumor biology. *Oncogene*, 23(48), 7928–7946.
<https://doi.org/10.1038/sj.onc.1208080>
- Playford, M. P., & Schaller, M. D. (2004b, October 18). The interplay between Src and integrins in normal and tumor biology. *Oncogene*, Vol. 23, pp. 7928–7946. <https://doi.org/10.1038/sj.onc.1208080>
- Płoski, R., Szymański, K., & Bednarczuk, T. (2011). The Genetic Basis of Graves' Disease. *Current Genomics*, 12(8), 542.
<https://doi.org/10.2174/138920211798120772>
- Pomin, V. H., & Mulloy, B. (2018). *pharmaceuticals Editorial Glycosaminoglycans and Proteoglycans*.
<https://doi.org/10.3390/ph11010027>

- Rambold, A. S., Cohen, S., & Lippincott-Schwartz, J. (2015). Fatty acid trafficking in starved cells: Regulation by lipid droplet lipolysis, autophagy, and mitochondrial fusion dynamics. *Developmental Cell*, 32(6), 678–692. <https://doi.org/10.1016/j.devcel.2015.01.029>
- Resh, M. D. (1999, August 12). Fatty acylation of proteins: New insights into membrane targeting of myristoylated and palmitoylated proteins. *Biochimica et Biophysica Acta - Molecular Cell Research*, Vol. 1451, pp. 1–16. [https://doi.org/10.1016/S0167-4889\(99\)00075-0](https://doi.org/10.1016/S0167-4889(99)00075-0)
- Rieck, M., Arechiga, A., Onengut-Gumuscu, S., Greenbaum, C., Concannon, P., & Buckner, J. H. (2007). Genetic Variation in PTPN22 Corresponds to Altered Function of T and B Lymphocytes. *The Journal of Immunology*, 179(7), 4704–4710. <https://doi.org/10.4049/jimmunol.179.7.4704>
- Riedl, A., Schlederer, M., Pudelko, K., Stadler, M., Walter, S., Unterleuthner, D., ... Dolznig, H. (2017a). Comparison of cancer cells in 2D vs 3D culture reveals differences in AKT-mTOR-S6K signaling and drug responses. *Journal of Cell Science*, 130(1), 203–218. <https://doi.org/10.1242/jcs.188102>
- Riedl, A., Schlederer, M., Pudelko, K., Stadler, M., Walter, S., Unterleuthner, D., ... Dolznig, H. (2017b). Comparison of cancer cells in 2D vs 3D culture reveals differences in AKT-mTOR-S6K signaling and drug responses. *Journal of Cell Science*, 130(1), 203–218. <https://doi.org/10.1242/jcs.188102>
- Roskoski, R. (2004, November 26). Src protein-tyrosine kinase structure and regulation. *Biochemical and Biophysical Research Communications*, Vol. 324, pp. 1155–1164. <https://doi.org/10.1016/j.bbrc.2004.09.171>
- Roskoski, R. (2015). Src protein-tyrosine kinase structure, mechanism, and small molecule inhibitors. *Pharmacological Research*, 94, 9–25. <https://doi.org/10.1016/J.PHRS.2015.01.003>
- Ruiz-Ojeda, Méndez-Gutiérrez, Aguilera, & Plaza-Díaz. (2019). Extracellular Matrix Remodeling of Adipose Tissue in Obesity and Metabolic Diseases. *International Journal of Molecular Sciences*, 20(19), 4888. <https://doi.org/10.3390/ijms20194888>
- Salvi, A. M., & DeMali, K. A. (2018a). Mechanisms linking mechanotransduction and cell metabolism. *Current Opinion in Cell Biology*, 54, 114–120. <https://doi.org/10.1016/J.CEB.2018.05.004>
- Salvi, A. M., & DeMali, K. A. (2018b, October 1). Mechanisms linking mechanotransduction and cell metabolism. *Current Opinion in Cell Biology*, Vol. 54, pp. 114–120. <https://doi.org/10.1016/j.ceb.2018.05.004>

- Saxton, R. A., & Sabatini, D. M. (2017). mTOR Signaling in Growth, Metabolism, and Disease. *Cell*. <https://doi.org/10.1016/j.cell.2017.02.004>
- Schickel, J.-N., Kuhny, M., Baldo, A., Bannock, J. M., Massad, C., Wang, H., ... Meffre, E. (2016). PTPN22 inhibition resets defective human central B cell tolerance. *Science Immunology*, 1(1). <https://doi.org/10.1126/sciimmunol.aaf7153>
- Schmitt, R., & Melk, A. (2017, September 1). Molecular mechanisms of renal aging. *Kidney International*, Vol. 92, pp. 569–579. <https://doi.org/10.1016/j.kint.2017.02.036>
- Schweiger, M., Schreiber, R., Haemmerle, G., Lass, A., Fledelius, C., Jacobsen, P., ... Zimmermann, R. (2006). Adipose triglyceride lipase and hormone-sensitive lipase are the major enzymes in adipose tissue triacylglycerol catabolism. *The Journal of Biological Chemistry*, 281(52), 40236–40241. <https://doi.org/10.1074/jbc.M608048200>
- Sciarretta, S., Volpe, M., & Sadoshima, J. (2014, January 31). Mammalian target of rapamycin signaling in cardiac physiology and disease. *Circulation Research*, Vol. 114, pp. 549–564. <https://doi.org/10.1161/CIRCRESAHA.114.302022>
- Seo, H.-Y., Jeon, J.-H., Jung, Y.-A., Jung, G.-S., Lee, E. J., Choi, Y.-K., ... Lee, I.-K. (2016). Fyn deficiency attenuates renal fibrosis by inhibition of phospho-STAT3. *Kidney International*, 90(6), 1285–1297. <https://doi.org/10.1016/j.kint.2016.06.038>
- Shan, T., Zhang, P., Jiang, Q., Xiong, Y., Wang, Y., & Kuang, S. (2016). Adipocyte-specific deletion of mTOR inhibits adipose tissue development and causes insulin resistance in mice. *Diabetologia*, 59(9), 1995–2004. <https://doi.org/10.1007/s00125-016-4006-4>
- Shaw, R. J. (2009). LKB1 and AMP-activated protein kinase control of mTOR signalling and growth. *Acta Physiologica*, 196(1), 65–80. <https://doi.org/10.1111/j.1748-1716.2009.01972.x>
- Singh, R., Xiang, Y., Wang, Y., Baikati, K., Cuervo, A. M., Luu, Y. K., ... Czaja, M. J. (2009). Autophagy regulates adipose mass and differentiation in mice. *Journal of Clinical Investigation*, 119(11), 3329–3339. <https://doi.org/10.1172/JCI39228>
- Smart, E. J., Graf, G. A., McNiven, M. A., Sessa, W. C., Engelman, J. A., Scherer, P. E., ... Lisanti, M. P. (1999). Caveolins, liquid-ordered domains, and signal transduction. *Molecular and Cellular Biology*, 19(11), 7289–7304. <https://doi.org/10.1128/mcb.19.11.7289>
- Smith, T. J. (2015, March 26). TSH-receptor-expressing fibrocytes and thyroid-associated ophthalmopathy. *Nature Reviews Endocrinology*, Vol. 11, pp. 171–181. <https://doi.org/10.1038/nrendo.2014.226>

- Smith, T. J., Hegedüs, L., & Douglas, R. S. (2012, June). Role of insulin-like growth factor-1 (IGF-1) pathway in the pathogenesis of Graves' orbitopathy. *Best Practice and Research: Clinical Endocrinology and Metabolism*, Vol. 26, pp. 291–302. <https://doi.org/10.1016/j.beem.2011.10.002>
- Smith, T. J., & Hoa, N. (2004). Immunoglobulins from patients with graves' disease induce hyaluronan synthesis in their orbital fibroblasts through the self-antigen, insulin-like growth factor-I receptor. *Journal of Clinical Endocrinology and Metabolism*, 89(10), 5076–5080. <https://doi.org/10.1210/jc.2004-0716>
- Smith, T. J., Padovani-Claudio, D. A., Lu, Y., Raychaudhuri, N., Fernando, R., Atkins, S., ... Douglas, R. S. (2011). Fibroblasts expressing the thyrotropin receptor overarch thyroid and orbit in Graves' disease. *Journal of Clinical Endocrinology and Metabolism*, 96(12), 3827–3837. <https://doi.org/10.1210/jc.2011-1249>
- Smith, T. J., Tsai, C. C., Shih, M.-J., Tsui, S., Chen, B., Han, R., ... Gianoukakis, A. G. (2008). Unique attributes of orbital fibroblasts and global alterations in IGF-1 receptor signaling could explain thyroid-associated ophthalmopathy. *Thyroid : Official Journal of the American Thyroid Association*, 18(9), 983–988. <https://doi.org/10.1089/thy.2007.0404>
- Solon, J., Levental, I., Sengupta, K., Georges, P. C., & Janmey, P. A. (2007). Fibroblast adaptation and stiffness matching to soft elastic substrates. *Biophysical Journal*, 93(12), 4453–4461. <https://doi.org/10.1529/biophysj.106.101386>
- Spandl, J., White, D. J., Peychl, J., & Thiele, C. (2009). Live Cell Multicolor Imaging of Lipid Droplets with a New Dye, LD540. *Traffic*, 10(11), 1579–1584. <https://doi.org/10.1111/j.1600-0854.2009.00980.x>
- Sprenger, C. C., Plymate, S. R., & Reed, M. J. (2010, December 15). Aging-related alterations in the extracellular matrix modulate the microenvironment and influence tumor progression. *International Journal of Cancer*, Vol. 127, pp. 2739–2748. <https://doi.org/10.1002/ijc.25615>
- Starkey, K., Heufelder, A., Baker, G., Joba, W., Evans, M., Davies, S., & Ludgate, M. (2003). Peroxisome proliferator-activated receptor- γ in thyroid eye disease: Contraindication for thiazolidinedione use? *Journal of Clinical Endocrinology and Metabolism*, 88(1), 55–59. <https://doi.org/10.1210/jc.2002-020987>
- Sun, M., Chi, G., Li, P., Lv, S., Xu, J., Xu, Z., ... Li, Y. (2018). Effects of matrix stiffness on the morphology, adhesion, proliferation and osteogenic differentiation of mesenchymal stem cells. *International Journal of Medical Sciences*, 15(3), 257–268. <https://doi.org/10.7150/ijms.21620>

- Sun, Y., Ma, Y. C., Huang, J., Chen, K. Y., McGarrigle, D. K., & Huang, X. Y. (2005). Requirement of Src-family tyrosine kinases in fat accumulation. *Biochemistry*, 44(44), 14455–14462. <https://doi.org/10.1021/bi0509090>
- Suzuki, K., Yamamoto, T., Usui, T., Suzuki, K., Heldin, P., & Yamashita, H. (2003). Expression of hyaluronan synthase in intraocular proliferative diseases: Regulation of expression in human vascular endothelial cells by transforming growth factor- β . *Japanese Journal of Ophthalmology*, 47(6), 557–564. <https://doi.org/10.1016/j.jjo.2003.09.001>
- Tan, P., Wang, Y. J., Li, S., Wang, Y., He, J. Y., Chen, Y. Y., ... Liu, Y. S. (2016). The PI3K/Akt/mTOR pathway regulates the replicative senescence of human VSMCs. *Molecular and Cellular Biochemistry*, 422(1–2). <https://doi.org/10.1007/s11010-016-2796-9>
- Tansey, J. T., Sztalryd, C., Gruia-Gray, J., Roush, D. L., Zee, J. V, Gavrilova, O., ... Londos, C. (2001). Perilipin ablation results in a lean mouse with aberrant adipocyte lipolysis, enhanced leptin production, and resistance to diet-induced obesity. *Proceedings of the National Academy of Sciences of the United States of America*, 98(11), 6494–6499. <https://doi.org/10.1073/pnas.101042998>
- Tontonoz, P., & Spiegelman, B. M. (2008). Fat and Beyond: The Diverse Biology of PPAR γ . *Annual Review of Biochemistry*, 77(1), 289–312. <https://doi.org/10.1146/annurev.biochem.77.061307.091829>
- Tse, J. R., & Engler, A. J. (2010). Preparation of hydrogel substrates with tunable mechanical properties. *Current Protocols in Cell Biology*. <https://doi.org/10.1002/0471143030.cb1016s47>
- Ulbricht, A., Eppler, F. J., Tapia, V. E., Van Der Ven, P. F. M., Hampe, N., Hersch, N., ... Rg Hö Hfeld, J. (2013). Report Cellular Mechanotransduction Relies on Tension-Induced and Chaperone-Assisted Autophagy. *Current Biology*, 23, 430–435. <https://doi.org/10.1016/j.cub.2013.01.064>
- Usui, M., Uno, M., & Nishida, E. (2016). Src family kinases suppress differentiation of brown adipocytes and browning of white adipocytes. *Genes to Cells*, 21(4), 302–310. <https://doi.org/10.1111/gtc.12340>
- Van Zeijl, C. J. J., Fliers, E., Van Koppen, C. J., Surovtseva, O. V., De Gooyer, M. E., Mourits, M. P., ... Boelen, A. (2011). Thyrotropin receptor-stimulating Graves' disease immunoglobulins induce hyaluronan synthesis by differentiated orbital fibroblasts from patients with Graves' ophthalmopathy not only via cyclic adenosine monophosphate signaling pathways. *Thyroid*, 21(2), 169–176. <https://doi.org/10.1089/thy.2010.0123>
- Vigneron, A., Roninson, I. B., Gamelin, E., & Coqueret, O. (2005). Src inhibits adriamycin-induced senescence and G2 checkpoint arrest by

- blocking the induction of p21waf1. *Cancer Research*, 65(19), 8927–8935. <https://doi.org/10.1158/0008-5472.CAN-05-0461>
- Vitiello, E., Moreau, P., Nunes, V., Mettouchi, A., Maiato, H., Ferreira, J. G., ... Balland, M. (2019). Acto-myosin force organization modulates centriole separation and PLK4 recruitment to ensure centriole fidelity. *Nature Communications*, 10(1). <https://doi.org/10.1038/s41467-018-07965-6>
- Vivar, R., Humeres, C., Muñoz, C., Boza, P., Bolivar, S., Tapia, F., ... Diaz-Araya, G. (2016). FoxO1 mediates TGF-beta1-dependent cardiac myofibroblast differentiation. *Biochimica et Biophysica Acta - Molecular Cell Research*, 1863(1), 128–138. <https://doi.org/10.1016/j.bbamcr.2015.10.019>
- Vojtechová, M., Turecková, J., Kucerová, D., Šloncová, E., Vachtenheim, J., & Tuháčková, Z. (2008). Regulation of mTORC1 signaling by Src kinase activity is Akt1-independent in RSV-transformed cells. *Neoplasia (New York, N.Y.)*, 10(2), 99–107. Retrieved from <http://www.ncbi.nlm.nih.gov/pubmed/18283331>
- Vojtěchová, M., Turečková, J., Kučerová, D., Šloncová, E., Vachtenheim, J., & Tuháčková, Z. (2008). Regulation of mTORC1 Signaling by Src Kinase Activity Is Akt1-Independent in RSV-Transformed Cells. *Neoplasia*, 10(2), 99–107. <https://doi.org/10.1593/NEO.07905>
- Wakelkamp, I. M. M. J., Bakker, O., Baldeschi, L., Wiersinga, W. M., & Prummel, M. F. (2003). TSH-R expression and cytokine profile in orbital tissue of active vs. inactive Graves' ophthalmopathy patients. *Clinical Endocrinology*, 58(3), 280–287. <https://doi.org/10.1046/j.1365-2265.2003.01708.x>
- Wang, C., Zhang, X., Teng, Z., Zhang, T., & Li, Y. (2014). Downregulation of PI3K/Akt/mTOR signaling pathway in curcumin-induced autophagy in APP/PS1 double transgenic mice. *European Journal of Pharmacology*, 740, 312–320. <https://doi.org/10.1016/j.ejphar.2014.06.051>
- Wang, W. J., Cai, G. Y., & Chen, X. M. (2017). Cellular senescence, senescence-associated secretory phenotype, and chronic kidney disease. *Oncotarget*, Vol. 8, pp. 64520–64533. <https://doi.org/10.18632/oncotarget.17327>
- Wang, Y. K., Wang, Y. H., Wang, C. Z., Sung, J. M., Chiu, W. T., Lin, S. H., ... Tang, M. J. (2003). Rigidity of collagen fibrils controls collagen gel-induced down-regulation of focal adhesion complex proteins mediated by $\alpha 2\beta 1$ integrin. *Journal of Biological Chemistry*, 278(24), 21886–21892. <https://doi.org/10.1074/jbc.M300092200>
- Waters, D. W., Blokland, K. E. C., Pathinayake, P. S., Burgess, J. K., Mutsaers, S. E., Prele, C. M., ... Knight, D. A. (2018, August 1).

- Fibroblast senescence in the pathology of idiopathic pulmonary fibrosis. *American Journal of Physiology - Lung Cellular and Molecular Physiology*, Vol. 315, pp. L162–L172. <https://doi.org/10.1152/ajplung.00037.2018>
- Weichhart, T. (2018). mTOR as Regulator of Lifespan, Aging, and Cellular Senescence: A Mini-Review. *Gerontology*, 64(2), 127–134. <https://doi.org/10.1159/000484629>
- Welte, M. A. (2007). Proteins under new management: lipid droplets deliver. *Trends in Cell Biology*, 17(8), 363–369. <https://doi.org/10.1016/j.tcb.2007.06.004>
- White, E. S., Atrasz, R. G., Hu, B., Phan, S. H., Stambolic, V., Mak, T. W., ... Toews, G. B. (2006). Negative Regulation of Myofibroblast Differentiation by PTEN (Phosphatase and Tensin Homolog Deleted on Chromosome 10). *American Journal of Respiratory and Critical Care Medicine*, 173(1), 112–121. <https://doi.org/10.1164/rccm.200507-1058OC>
- Woeller, C. F., O'Loughlin, C. W., Pollock, S. J., Thatcher, T. H., Feldon, S. E., & Phipps, R. P. (2015). Thy1 (CD90) controls adipogenesis by regulating activity of the Src family kinase, Fyn. *The FASEB Journal*, 29(3), 920–931. <https://doi.org/10.1096/fj.14-257121>
- Woodcock, H., Peace, S., Nanthakumar, C., Maher, T., Mercer, P., & Chambers, R. (2015, September). *mTOR signalling is an essential pathway for TGF- β 1 induced collagen synthesis*. PA935. <https://doi.org/10.1183/13993003.congress-2015.pa935>
- Woodcock, H. V., Eley, J. D., Guillotin, D., Platé, M., Nanthakumar, C. B., Martufi, M., ... Chambers, R. C. (2019). The mTORC1/4E-BP1 axis represents a critical signaling node during fibrogenesis. *Nature Communications*, 10(1). <https://doi.org/10.1038/s41467-018-07858-8>
- Wozniak, M. A., Desai, R., Solski, P. A., Der, C. J., & Keely, P. J. (2003). ROCK-generated contractility regulates breast epithelial cell differentiation in response to the physical properties of a three-dimensional collagen matrix. *The Journal of Cell Biology*, 163(3), 583–595. <https://doi.org/10.1083/jcb.200305010>
- Wozniak, M. A., Modzelewska, K., Kwong, L., & Keely, P. J. (2004). Focal adhesion regulation of cell behavior. *Biochimica et Biophysica Acta (BBA) - Molecular Cell Research*, 1692(2–3), 103–119. <https://doi.org/10.1016/J.BBAMCR.2004.04.007>
- Wynn, T. A., & Ramalingam, T. R. (2012). Mechanisms of fibrosis: therapeutic translation for fibrotic disease. *Nature Medicine*, 18(7), 1028–1040. <https://doi.org/10.1038/nm.2807>
- Xie, J., Bao, M., Bruekers, S. M. C., & Huck, W. T. S. (2017). Collagen Gels

- with Different Fibrillar Microarchitectures Elicit Different Cellular Responses. *ACS Applied Materials & Interfaces*, 9(23), 19630–19637. <https://doi.org/10.1021/acsami.7b03883>
- Yamada, E., Okada, S., Bastie, C. C., Vatish, M., Nakajima, Y., Shibusawa, R., ... Yamada, M. (2016). Fyn phosphorylates AMPK to inhibit AMPK activity and AMP-dependent activation of autophagy. *Oncotarget*, 7(46), 74612–74629. <https://doi.org/10.18632/oncotarget.11916>
- Yamada, E., Pessin, J. E., Kurland, I. J., Schwartz, G. J., & Bastie, C. C. (2010). Fyn-Dependent Regulation of Energy Expenditure and Body Weight Is Mediated by Tyrosine Phosphorylation of LKB1. *Cell Metabolism*, 11(2), 113–124. <https://doi.org/10.1016/j.cmet.2009.12.010>
- Yang, H., Galea, A., Sytnyk, V., & Crossley, M. (2012). Controlling the size of lipid droplets: lipid and protein factors. *Current Opinion in Cell Biology*, 24(4), 509–516. <https://doi.org/10.1016/j.ceb.2012.05.012>
- Yang, I.-H., Rose, G. E., Ezra, D. G., & Bailly, M. (2019). Macrophages promote a profibrotic phenotype in orbital fibroblasts through increased hyaluronic acid production and cell contractility. *Scientific Reports*, 9(1), 9622. <https://doi.org/10.1038/s41598-019-46075-1>
- Yeung, T., Georges, P. C., Flanagan, L. A., Marg, B., Ortiz, M., Funaki, M., ... Janmey, P. A. (2005). Effects of substrate stiffness on cell morphology, cytoskeletal structure, and adhesion. *Cell Motility and the Cytoskeleton*, 60(1), 24–34. <https://doi.org/10.1002/cm.20041>
- Yoo, L., Reed, J., Shin, A., Kung, J., Gimzewski, J. K., Poukens, V., ... Demer, J. L. (2011a). Characterization of ocular tissues using microindentation and hertzian viscoelastic models. *Investigative Ophthalmology & Visual Science*, 52(6), 3475–3482. <https://doi.org/10.1167/iovs.10-6867>
- Yoo, L., Reed, J., Shin, A., Kung, J., Gimzewski, J. K., Poukens, V., ... Demer, J. L. (2011b). Characterization of ocular tissues using microindentation and Hertzian viscoelastic models. *Investigative Ophthalmology and Visual Science*, 52(6), 3475–3482. <https://doi.org/10.1167/iovs.10-6867>
- Yoon, J. S., Lee, H. J., Chae, M. K., & Lee, E. J. (2015). Autophagy is Involved in the Initiation and Progression of Graves' Orbitopathy. *Thyroid*, 25(4), 445–454. <https://doi.org/10.1089/thy.2014.0300>
- Yu, W., Bozza, P. T., Tzizik, D. M., Gray, J. P., Cassara, J., Dvorak, A. M., & Weller, P. F. (1998). Co-compartmentalization of MAP kinases and cytosolic phospholipase A2 at cytoplasmic arachidonate-rich lipid bodies. *The American Journal of Pathology*, 152(3), 759–769. Retrieved from <http://www.ncbi.nlm.nih.gov/pubmed/9502418>

- Yu, W., Cassara, J., & Weller, P. F. (2000). Phosphatidylinositide 3-kinase localizes to cytoplasmic lipid bodies in human polymorphonuclear leukocytes and other myeloid-derived cells. *Blood*, 95(3), 1078–1085. Retrieved from <http://www.ncbi.nlm.nih.gov/pubmed/10648425>
- Yun, Y. R., Won, J. E., Jeon, E., Lee, S., Kang, W., Jo, H., ... Kim, H. W. (2010). Fibroblast growth factors: Biology, function, and application for tissue regeneration. *Journal of Tissue Engineering*, Vol. 1, pp. 1–18. <https://doi.org/10.4061/2010/218142>
- Zaffagnini, G., & Martens, S. (2016). Mechanisms of Selective Autophagy. *Journal of Molecular Biology*, 428(9Part A), 1714. <https://doi.org/10.1016/J.JMB.2016.02.004>
- Zhan, J. K., Wang, Y. J., Li, S., Wang, Y., Tan, P., He, J. Y., ... Liu, Y. S. (2018a). AMPK/TSC2/mTOR pathway regulates replicative senescence of human vascular smooth muscle cells. *Experimental and Therapeutic Medicine*, 16(6), 4853–4858. <https://doi.org/10.3892/etm.2018.6767>
- Zhan, J. K., Wang, Y. J., Li, S., Wang, Y., Tan, P., He, J. Y., ... Liu, Y. S. (2018b). AMPK/TSC2/mTOR pathway regulates replicative senescence of human vascular smooth muscle cells. *Experimental and Therapeutic Medicine*, 16(6), 4853–4858. <https://doi.org/10.3892/etm.2018.6767>
- Zhang-Nunes, S. X., Dang, S., Garneau, H. C., Hwang, C., Isaacs, D., Chang, S. H., & Goldberg, R. (2015). Characterization and outcomes of repeat orbital decompression for thyroid-associated orbitopathy. *Orbit*, 34(2), 57–65. <https://doi.org/10.3109/01676830.2014.949784>
- Zhang, C., Zhang, X., Ma, L., Peng, F., Huang, J., & Han, H. (2012). Thalidomide inhibits adipogenesis of orbital fibroblasts in Graves' ophthalmopathy. *Endocrine*, 41(2), 248–255. <https://doi.org/10.1007/s12020-012-9600-8>
- Zhang, H., Stallock, J. P., Ng, J. C., Reinhard, C., & Neufeld, T. P. (2000). Regulation of cellular growth by the Drosophila target of rapamycin dTOR. *Genes and Development*, 14(21), 2712–2724. <https://doi.org/10.1101/gad.835000>
- Zhang, L., Baker, G., Janus, D., Paddon, C. A., Fuhrer, D., & Ludgate, M. (2006). Biological effects of thyrotropin receptor activation on human orbital preadipocytes. *Investigative Ophthalmology and Visual Science*, 47(12), 5197–5203. <https://doi.org/10.1167/iov.06-0596>
- Zhang, S., Wang, Y., Cui, L., Deng, Y., Xu, S., Yu, J., ... Liu, P. (2016). Morphologically and Functionally Distinct Lipid Droplet Subpopulations. *Scientific Reports*, 6. <https://doi.org/10.1038/srep29539>
- Zhang, Y., Goldman, S., Baerga, R., Zhao, Y., Komatsu, M., & Jin, S.

- (2009). Adipose-specific deletion of autophagy-related gene 7 (atg7) in mice reveals a role in adipogenesis. *Proceedings of the National Academy of Sciences of the United States of America*, 106(47), 19860–19865. <https://doi.org/10.1073/pnas.0906048106>
- Zhao, S., Chen, C., Wang, S., Ji, F., & Xie, Y. (2016). MHY1485 activates mTOR and protects osteoblasts from dexamethasone. *Biochemical and Biophysical Research Communications*, 481(3–4), 212–218. <https://doi.org/10.1016/j.bbrc.2016.10.104>
- Zhebrun, D., Kudryashova, Y., Babenko, A., Maslyansky, A., Kunitskaya, N., Popcova, D., ... Shlyakhto, E. (2011). Association of PTPN22 1858T/T genotype with type 1 diabetes, Graves' disease but not with rheumatoid arthritis in Russian population. *Aging*, 3(4), 368–373. <https://doi.org/10.18632/aging.100305>
- Zimmermann, R., Haemmerle, G., Schoiswohl, G., Birner-gruenberger, R., Riederer, M., Lass, A., ... Eisenhaber, F. (2004). Fat Mobilization in Adipose Tissue Is Promoted by Adipose Triglyceride Lipase Fat Mobilization in Adipose Tissue Is Promoted by Adipose Triglyceride Lipase. *Science*, 306(2004), 1383–1386. <https://doi.org/10.1126/science.1100747>
- Zindy, F., Quelle, D., Roussel, M., Oncogene, C. S., & 1997, undefined. (n.d.). Expression of the p16INK4a tumor suppressor versus other INK4 family members during mouse development and aging. *Nature.Com*. Retrieved from <https://www.nature.com/articles/1201178>